

Utah State University

DigitalCommons@USU

---

All Graduate Theses and Dissertations

Graduate Studies

---

8-2019

## Numerical Analysis and Spanwise Shape Optimization for Finite Wings of Arbitrary Aspect Ratio

Joshua D. Hodson  
*Utah State University*

Follow this and additional works at: <https://digitalcommons.usu.edu/etd>

---

### Recommended Citation

Hodson, Joshua D., "Numerical Analysis and Spanwise Shape Optimization for Finite Wings of Arbitrary Aspect Ratio" (2019). *All Graduate Theses and Dissertations*. 7574.  
<https://digitalcommons.usu.edu/etd/7574>

This Dissertation is brought to you for free and open access by the Graduate Studies at DigitalCommons@USU. It has been accepted for inclusion in All Graduate Theses and Dissertations by an authorized administrator of DigitalCommons@USU. For more information, please contact [digitalcommons@usu.edu](mailto:digitalcommons@usu.edu).



NUMERICAL ANALYSIS AND SPANWISE SHAPE OPTIMIZATION  
FOR FINITE WINGS OF ARBITRARY ASPECT RATIO

By

Joshua D. Hodson

A dissertation submitted in partial fulfillment  
of the requirements for the degree

of

DOCTOR OF PHILOSOPHY

In

Mechanical Engineering

Approved:

---

Douglas F. Hunsaker, Ph.D.  
Major Professor

---

Geordie Richards, Ph.D.  
Committee Member

---

Robert E. Spall, Ph.D.  
Major Professor

---

James J. Joo, Ph.D.  
Committee Member

---

Barton L. Smith, Ph.D.  
Committee Member

---

Richard S. Inouye, Ph.D.  
Vice Provost for Graduate Studies

UTAH STATE UNIVERSITY  
Logan, Utah

2019

Copyright © 2019 by Joshua D. Hodson

All Rights Reserved

*Dedicated to my father*

*Lee James Hodson*

*1939-2018*

## ABSTRACT

Numerical Analysis and Spanwise Shape Optimization  
for Finite Wings of Arbitrary Aspect Ratio

by

Joshua D. Hodson, Doctor of Philosophy

Utah State University, 2019

Major Professors: Dr. Douglas Hunsaker and Dr. Robert Spall

Department: Mechanical and Aerospace Engineering

Improvements to the current state of the art in wing shape optimization for morphing wing applications are presented, with a focus on low-fidelity analysis methods for preliminary design. An existing aerodynamic analysis tool based on lifting line theory is the foundation upon which this work builds, and several software development efforts are presented that enhance the capabilities of this tool relative to wing shape optimization. An automatic differentiation tool is integrated with the aerodynamic analysis tool to facilitate accurate and efficient derivative calculations for gradient-based optimization. A light-weight optimization framework written in Python is presented that is capable of efficiently searching the design space using popular gradient-based optimization techniques and parallelization of independent objective function evaluations. Several example optimization problems are presented using this toolset, and a method for visualizing the design space of morphing wings using this toolset is also presented and discussed.

The morphing wing application of primary interest to the current work, the Variable Camber Compliant Wing developed at the United States Air Force Research Laboratory, has an aspect ratio that falls below the acceptable range of aspect ratios for lifting line theory analysis. This has led to the development of a new method for applying lifting line theory to low-aspect-ratio lifting surfaces. A thorough review of Prandtl's classical lifting line theory is first presented, followed by several low-aspect-ratio proposals from the slender wing theory of Jones to the lifting surface theories of Birnbaum, Blenk, and others. A new formulation for slender wing theory is presented that provides new insights into the appropriate limits for a formulation capable of spanning the entire range of aspect ratios from slender to infinite. A new empirical relation is

proposed that satisfies the limits at both extremes and agrees well with high-order inviscid panel code results. A method is then presented for implementing this empirical relation in both analytical and numerical lifting line algorithms. A comparison of results computed using this method to experimental results for the Variable Camber Compliant Wing is also given.

(327 pages)

## PUBLIC ABSTRACT

Numerical Analysis and Spanwise Shape Optimization  
for Finite Wings of Arbitrary Aspect Ratio

by

Joshua D. Hodson, Doctor of Philosophy

Utah State University, 2019

Major Professors: Dr. Douglas Hunsaker and Dr. Robert Spall

Department: Mechanical and Aerospace Engineering

This work focuses on the development of efficient methods for wing shape optimization for morphing wing technologies. Existing wing shape optimization processes typically rely on computational fluid dynamics tools for aerodynamic analysis, but the computational cost of these tools makes optimization of all but the most basic problems intractable. In this work, we present a set of tools that can be used to efficiently explore the design spaces of morphing wings without reducing the fidelity of the results significantly. Specifically, this work discusses automatic differentiation of an aerodynamic analysis tool based on lifting line theory, a light-weight gradient-based optimization framework that provides a parallel function evaluation capability not found in similar frameworks, and a modification to the lifting line equations that makes the analysis method and optimization process suitable to wings of arbitrary aspect ratio. The toolset discussed is applied to several wing shape optimization problems. Additionally, a method for visualizing the design space of a morphing wing using this toolset is presented. As a result of this work, a light-weight wing shape optimization method is available for analysis of morphing wing designs that reduces the computational cost by several orders of magnitude over traditional methods without significantly reducing the accuracy of the results.

## ACKNOWLEDGMENTS

I have had several mentors throughout the course of this research, and I would like to express my gratitude to each for helping me along in this journey: to Dr. Hope Forsmann at the Idaho National Laboratory for her guidance and expertise in nuclear reactor thermal hydraulics and the Fortran programming language, to Dr. James Joo at the U.S. Air Force Research Laboratory for his help in understanding morphing wing systems and their role in the future of aerospace systems, and to Drs. Stephen Whitmore and Warren Phillips at Utah State University for helping me realize my passion for aerospace. Also to Dalon Work and Tyson Etherington for their advice, encouragement, and friendship.

Three professors in particular have had an exceptional impact on my education. First, Dr. Robert Spall, who has been guide and mentor to me from my first day as a freshman undergraduate student to my last day as a PhD candidate 20 years later, and who first introduced me to the worlds of computational fluid dynamics, aerodynamics, and high performance computing. I wish him all the best as he sets sail this summer. Second, Dr. Barton Smith, who has been a mentor for nearly as long and who reminds me that there is a real world outside my numerical simulations, without which my numerical simulations would have no meaning. I also want to thank Dr. Smith for connecting me with the RELAP5-3D team at Idaho National Laboratory. Finally, Dr. Douglas Hunsaker, who among all his other responsibilities as a new faculty member at USU gave me a majority share of his time and resources. I am forever indebted to these three men for their mentorship and commitment to my success.

I would like to thank my wife Megan and my kids Wesley, Abigail, Preston, and Aliya, for supporting me on a daily basis as I furthered my education. They have each made sacrifices so that I could pursue my goal of earning a doctoral degree, and I thank them for sticking by me throughout it all. I also want to thank my mother for her continual words of encouragement, which on a few occasions came at times when I was ready to quit but gave me the boost I needed to forge ahead; and my father for his examples of hard work and perseverance that have motivated me to test the limits of my abilities and always strive to do my best.

I would also like to thank those organizations that provided financial support for this work. Portions of this research have been funded under a grant from the Office of Naval Research Sea-Based Aviation Program (grant no. N00014-16-1-2074) and fellowships from the Department of Energy Nuclear Energy University



Program, the U.S. Air Force Research Laboratory's Summer Faculty Fellowship Program, and the USU School of Graduate Studies Dissertation Fellowship Program.

Finally, I thank my Heavenly Father for His guidance and sustainment throughout the course of this work. I acknowledge His hand in this and all things.

Joshua D. Hodson

## CONTENTS

	Page
ABSTRACT .....	iv
PUBLIC ABSTRACT .....	vi
ACKNOWLEDGMENTS .....	vii
LIST OF TABLES .....	xiii
LIST OF FIGURES .....	xiv
LIST OF ACRONYMS .....	xvii
NOMENCLATURE .....	xviii
1 INTRODUCTION .....	1
2 DUAL NUMBER AUTOMATIC DIFFERENTIATION FOR WING SHAPE OPTIMIZATION .....	4
2.1 Introduction .....	4
2.2 Derivative Calculation Methods .....	5
2.2.1 Symbolic Differentiation .....	5
2.2.2 Finite Differencing .....	9
2.2.3 Automatic Differentiation .....	11
2.2.4 Discussion .....	14
2.3 Methods and Tools for Forward-Mode Automatic Differentiation .....	15
2.4 Dual Number Automatic Differentiation .....	17
2.4.1 Dual Number Theory .....	18
2.4.2 The Dual Number Data Type .....	19
2.4.3 Integration with Fortran Algorithms .....	20
2.4.4 Special Considerations when Integrating DNAD with Existing Fortran Algorithms .....	23
2.5 Automatic Differentiation of a 1D Scalar Transport Equation Solver .....	26
2.5.1 Mathematical Model .....	26
2.5.2 Numerical Model .....	28
2.5.3 Automatic Differentiation of the 1D Scalar Transport Problem using DNAD .....	29
2.5.4 Results and Discussion .....	30

2.6	Automatic Differentiation of MachUp .....	36
2.6.1	The MachUp Numerical Lifting Line Solver .....	37
2.6.2	Modifications to the MachUp Source Code .....	39
2.6.3	Results and Discussion .....	41
3	WING SHAPE OPTIMIZATION USING A NUMERICAL LIFTING LINE ALGORITHM AND DUAL NUMBER AUTOMATIC DIFFERENTIATION.....	46
3.1	Introduction .....	46
3.2	Optix.....	47
3.2.1	Optimization Method.....	47
3.2.2	Code Structure .....	48
3.2.3	Parallel Execution of Independent Function Evaluations .....	49
3.2.4	Linear and Quadratic Line Searching .....	49
3.2.5	Limitations.....	50
3.3	Wing Shape Optimization in Inviscid Flow .....	51
3.3.1	Optimized Planform Shapes for Minimum Induced Drag .....	52
3.3.2	Optimized Geometric Twist Distributions for Minimum Induced Drag .....	54
3.3.3	Optimized Aerodynamic Twist Distributions for Minimum Induced Drag .....	56
3.4	Wing Shape Optimization for Viscous Flow .....	58
3.4.1	Optimized Planform Shapes for Minimum Total Drag .....	60
3.4.2	Optimized Geometric Twist Distributions for Minimum Total Drag .....	61
3.4.3	Optimized Aerodynamic Twist Distributions for Minimum Total Drag .....	63
3.5	Visualization of the Design Space for Wing Shape Optimization.....	64
4	ANALYTICAL LIFTING LINE METHOD FOR WINGS OF ARBITRARY ASPECT RATIO .....	68
4.1	Introduction .....	68
4.2	Lift Generated by a Finite Wing .....	69
4.3	Classical Lifting Line Theory.....	70
4.4	Slender Wing Theory .....	77
4.5	Lifting Surface Theory .....	81

4.6	A Unifying Formulation of Lifting Line, Slender Wing, and Lifting Surface Methods.....	82
4.7	Results and Discussion .....	92
5	NUMERICAL LIFTING LINE METHOD FOR WINGS OF ARBITRARY ASPECT RATIO .....	103
5.1	Introduction .....	103
5.2	The Phillips and Snyder Numerical Lifting Line Method .....	104
5.3	Modifications to the Numerical Lifting Line Method for Wings of Arbitrary Aspect Ratio .....	108
5.4	Results and Discussion .....	110
6	SUMMARY AND CONCLUSIONS.....	124
	REFERENCES .....	127
	APPENDICES.....	137
A	MODIFIED DNAD SOURCE CODE .....	138
B	ONE-DIMENSIONAL SCALAR TRANSPORT SOLVER IN FORTRAN.....	168
B.1	User Interface .....	168
B.2	Physics Module .....	169
B.3	I/O Module .....	172
C	SUMMARY OF CODE CHANGES TO APPENDIX B FOR DNAD INTEGRATION.....	181
C.1	Changes to adpsolver Module .....	181
C.2	Changes to adpio Module .....	181
D	SUMMARY OF CODE CHANGES TO MACHUP FOR DNAD INTEGRATION .....	185
D.1	Changes to loads_m Module .....	185
D.2	Changes to plane_m Module .....	185
D.3	Changes to special_functions_m Module .....	191
D.4	Changes to view_m Module .....	195
D.5	Changes to wing_m Module .....	196
D.6	Changes to airfoil_m Module .....	198
D.7	Changes to atmosphere_m Module .....	198
D.8	Changes to dataset_m Module .....	199
D.9	Changes to math_m Module .....	199

D.10	Changes to <code>section_m</code> Module .....	200
D.11	Changes to <code>myjson_m</code> Module .....	201
E	EXAMPLE MACHUP INPUT FILES.....	209
E.1	Example JSON-Formatted Input File .....	209
E.2	Example Parameter File for a NACA 2412 Airfoil in Inviscid Incompressible Flow .....	209
E.3	Example Profile File for a NACA 2412 Airfoil .....	210
F	OPTIX SOURCE CODE .....	211
G	INPUT FILES AND PYTHON SCRIPTS FOR WING SHAPE OPTIMIZATION .....	225
G.1	Main Optimization Execution Script .....	225
G.2	Objective Function ( <code>obj_fcn.evaluate</code> ) .....	226
G.3	Objective Function with Gradient Calculations ( <code>obj_fcn.evaluate_with_gradient</code> ) .....	228
G.4	Helper Function for Extracting Variable Names ( <code>get_list_of_vars</code> ) .....	230
G.5	Main MachUp Input File .....	230
H	AERODYNAMIC CALCULATIONS USING PANAIR .....	233
I	MACHUP FUNCTIONS FOR WRITING PANAIR INPUT FILES .....	239
J	EXAMPLE PANAIR INPUT FILE .....	245
K	PRALINES SOURCE CODE .....	250
K.1	Pralines Main Program ( <code>main.f90</code> ) .....	250
K.2	Interface Module ( <code>liftinglineinterface.f90</code> ) .....	250
K.3	Planform Class Module ( <code>class_Planform.f90</code> ) .....	262
K.4	Module of Setter Functions ( <code>liftinglinesetters.f90</code> ) .....	268
K.5	Solver Module ( <code>liftinglinesolver.f90</code> ) .....	276
K.6	Output Module ( <code>liftinglineoutput.f90</code> ) .....	284
K.7	Matrix Solver Module ( <code>matrix.f90</code> ) .....	292
K.8	Utilities Module ( <code>utilities.f90</code> ) .....	293
L	PROOF OF EQUATION (5.2.5) .....	300
M	TABULATED PROPERTIES OF THE NACA X410 FAMILY OF AIRFOILS .....	302
	CURRICULUM VITAE .....	306

## LIST OF TABLES

Table	Page
2.1	Methods for Declaring Floating-Point Variables in Fortran .....26
3.1	Aerodynamic coefficients for the NACA X412 family of airfoils in inviscid flow .....52
3.2	Minimum induced drag results for untwisted wings with optimized planforms .....53
3.3	Minimum induced drag results for geometric-twist-optimized rectangular wings.....55
3.4	Minimum induced drag results for aerodynamic-twist-optimized rectangular wings .....58
3.5	Aerodynamic coefficients for the NACA X412 family of airfoils in viscous, incompressible flow at a Reynolds number of $Re = 10^6$ ..... 59
3.6	Drag coefficients for initial rectangular wing and baseline elliptic wing in viscous flow. ....60
3.7	Minimum total drag results for untwisted wings with optimized planforms.....60
3.8	Minimum total drag results for geometric-twist-optimized rectangular wings. ....62
3.9	Drag components for geometric-twist-optimized rectangular wing with 11 control points. ....62
3.10	Minimum total drag results for aerodynamic-twist-optimized rectangular wings. ....63
3.11	Drag components for aerodynamic-twist-optimized rectangular wing with 11 control points.....63
4.1	Summary of limits for $R_1$ and $R_2$ .....92
4.2	Comparison of methods for calculating the wing lift slope of a finite elliptic wing .....93
4.3	Comparison of resistance values $R_1$ from methods for calculating the wing lift slope of a finite elliptic wing .....94
4.4	Comparison of resistance values $R_2$ from methods for calculating the wing lift slope of a finite elliptic wing .....95
M.1	Airfoil Coefficient Data for the NACA 2410 Airfoil.....302
M.2	Airfoil Coefficient Data for the NACA 4410 Airfoil .....303
M.3	Airfoil Coefficient Data for the NACA 6410 Airfoil.....304
M.4	Airfoil Coefficient Data for the NACA 8410 Airfoil.....305

## LIST OF FIGURES

Figure	Page
2.1	An example of forward-mode AD using the function $f(x_1, x_2) = x_1 \sin(x_2)$ ..... 12
2.2	An example of reverse-mode AD using the function $f(x_1, x_2) = x_1 \sin(x_2)$ ..... 13
2.3	Header lines added to a Fortran module to include DNAD capabilities. .... 21
2.4	Example source code, compiler commands, and code execution (a) before and (b) after DNAD integration. Differences are highlighted in bold..... 22
2.5	Example source code for customizing output of dual number objects. .... 23
2.6	Example of inconsistent data types used in a common block in different program units. .... 25
2.7	Example input file for the Fortran program given in Appendix B. .... 29
2.8	Closed-form and numerical solutions to the 1D transport equation. .... 31
2.9	Percent error in numerical solution at $x = 0.75$ for various grid resolutions. .... 31
2.10	Comparison of $\partial\phi/\partial u$ computed using DNAD and Eq. (2.5.8). .... 32
2.11	Comparison of $\partial\phi/\partial\Gamma$ computed using DNAD and Eq. (2.5.9)..... 32
2.12	Comparison of $\partial\phi/\partial C$ computed using DNAD and Eq. (2.5.10). .... 33
2.13	Comparison of errors in $\partial\phi/\partial u$ computed using DNAD and finite differencing. .... 34
2.14	Comparison of errors in $\partial\phi/\partial\Gamma$ computed using DNAD and finite differencing..... 34
2.15	Comparison of errors in $\partial\phi/\partial C$ computed using DNAD and finite differencing. .... 35
2.16	Run-time benchmarks for the adpsolver code using DNAD and finite differencing. .... 36
2.17	Percent error in lift and drag coefficients for various grid densities relative to the solution computed using $n = 1280$ nodes per semispan. .... 41
2.18	Comparison of errors in $\partial C_L/\partial\alpha$ using DNAD and finite differencing relative to the DNAD solution computed using 1280 nodes per semispan. .... 42
2.19	Comparison of errors in $\partial C_{D_i}/\partial\alpha$ using DNAD and finite differencing relative to the DNAD solution computed using 1280 nodes per semispan. .... 42
2.20	Run-time benchmarks for MachUp using DNAD and finite differencing. .... 44
3.1	Optimized planforms for minimum induced drag. .... 54
3.2	Optimized geometric twist distributions for minimum induced drag..... 56

3.3	Optimized aerodynamic twist distributions for minimum induced drag. ....	58
3.4	Optimized planforms for minimum total drag. ....	61
3.5	Optimized geometric twist distributions for minimum total drag. ....	62
3.6	Optimized aerodynamic twist distributions for minimum total drag. ....	64
3.7	Contours of (a) induced and (b) parasitic drag for finite wing sections. Results are included for rectangular wings with $A = 8$ , $C_L = 0.5$ , and optimized aerodynamic twist for variable $N$ . ....	65
4.1	Discrete system of overlapping horseshoe vortices on a finite wing. ....	71
4.2	Velocity induced at point $P$ by a semi-infinite vortex filament. ....	72
4.3	Comparison of lift slope calculation methods applied to a finite elliptic wing ....	96
4.4	Comparison of lift slope calculation methods applied to a finite rectangular wing ....	97
4.5	Comparison of lift slope calculation methods applied to a tapered wing with $R_T = 0.75$ ....	97
4.6	Comparison of spanwise lift coefficient distributions for elliptic wings. ....	99
4.7	Comparison of spanwise lift distributions for elliptic wings. ....	99
4.8	Comparison of spanwise lift distributions for rectangular wings. ....	100
4.9	Comparison of spanwise lift distributions for tapered wings with $R_T = 0.75$ . ....	100
4.10	Sample calculations of the aspect ratio efficiency factor using Pralines and Panair. ....	101
5.1	Discrete system of side-by-side horseshoe vortices on a finite wing. ....	104
5.2	Velocity induced at point $P$ by an arbitrary vortex segment $\overline{OR}$ . ....	105
5.3	Comparison of wing lift slope calculations for finite elliptic wings. ....	108
5.4	Comparison of analytical and numerical calculations for wing lift slope of elliptic wings. ....	110
5.5	Comparison of spanwise lift distributions for elliptic wings. ....	111
5.6	Comparison of spanwise lift distributions for rectangular wings. ....	112
5.7	Comparison of spanwise lift distributions for tapered wings with $R_T = 0.75$ . ....	112
5.8	Sample calculations of the aspect ratio efficiency factor using MachUp and Panair. ....	113
5.9	Comparison of numerical and experimental lift coefficients for the CAD-0 test. ....	114
5.10	Comparison of numerical and experimental lift coefficients for the CAD-2 test. ....	115
5.11	Comparison of numerical and experimental lift coefficients for the CAD-8 test. ....	115



5.12	Comparison of numerical and experimental lift coefficients for the VCCW-2 test. ....	117
5.13	Comparison of numerical and experimental lift coefficients for the VCCW-8 test. ....	117
5.14	Comparison of numerical and experimental lift coefficients for the VCCW-CU test.....	118
5.15	Comparison of numerical and experimental lift coefficients for the VCCW-CD test.....	118
5.16	Comparison of numerical and experimental lift coefficients for the VCCW-LW test. ....	119
5.17	Comparison of numerical and experimental drag coefficients for the CAD-0 test. ....	119
5.18	Comparison of numerical and experimental drag coefficients for the CAD-2 test. ....	120
5.19	Comparison of numerical and experimental drag coefficients for the CAD-8 test. ....	120
5.20	Comparison of numerical and experimental drag coefficients for the VCCW-2 test.....	121
5.21	Comparison of numerical and experimental drag coefficients for the VCCW-8 test.....	122
5.22	Comparison of numerical and experimental drag coefficients for the VCCW-CU test. ....	122
5.23	Comparison of numerical and experimental drag coefficients for the VCCW-CD test. ....	123
5.24	Comparison of numerical and experimental drag coefficients for the VCCW-LW test.....	123
H.1	Lift distribution with a $20 \times 20$ mesh for an elliptic wing with $A = 4$ and $\bar{t}_{\max} = 4\%$ . ....	234
H.2	Lift distributions as a function of average chord length with an $80 \times 80$ mesh for an elliptic wing with $A = 4$ and $\bar{t}_{\max} = 4\%$ .....	235
H.3	Mesh refinement and extrapolated results computed for an elliptic wing with $A = 4$ and $\bar{t}_{\max} = 4\%$ . ....	237
H.4	Lift coefficient results computed for elliptic wings of different airfoil thicknesses with $A = 4$ and extrapolated results for $\bar{t}_{\max} = 0\%$ ..	237
H.5	Comparison of wing lift coefficients for wings with straight quarter-chord and straight mid-chord.....	238
H.6	Comparison of spanwise lift coefficients for wings with straight quarter-chord and straight mid-chord.....	238

## LIST OF ACRONYMS

AD	Automatic Differentiation
AFRL	Air Force Research Laboratory
AVX	Advanced Vector Extensions
BFGS	Quasi-Newton optimization method of Broyden, Fletcher, Goldfarb, and Shanno
CCSA	Conservative Convex Separable Approximation
CFD	Computational Fluid Dynamics
DNAD	Dual Number Automatic Differentiation
DOE	Design of Experiments
JSON	JavaScript Object Notation
NACA	National Advisory Committee for Aeronautics
OO	Operator Overloading
RMS	Root-Mean-Square
SCT	Source Code Transformation
SIMD	Single Instruction, Multiple Data
SSE	Streaming SIMD Extensions
STL	Stereolithography file format
VCCW	Variable Camber Compliant Wing
VWT	Vertical Wind Tunnel

## NOMENCLATURE

$A$	Aspect ratio of a finite wing
$a$	Wing lift slope
$a_0$	Section lift slope
$b$	Wingspan
$C$	Source term proportionality constant
$c$	Chord length
$\bar{c}$	Average chord length
$C_D$	Total wing drag coefficient ( $C_{D_i} + C_{D_p}$ )
$c_d$	Total section drag coefficient ( $c_{d_i} + c_{d_p}$ )
$c_{d_0}$ , $c_{d_1}$ , $c_{d_2}$	Constant, linear, and quadratic terms in section parasitic drag equation
$C_{D_i}$	Wing induced drag coefficient
$c_{d_i}$	Section induced drag coefficient
$C_{D_p}$	Wing parasitic drag coefficient
$c_{d_p}$	Section parasitic drag coefficient
$C_L$	Wing lift coefficient
$c_l$	Section lift coefficient
$c_r$	Section resultant aerodynamic force coefficient
$e_A$	Aspect ratio efficiency factor
$e_s$	Span efficiency factor
$f, g$	Arbitrary functions
$\mathbf{f}$	Vector function response of a fluid system in a coupled multiphysics problem
$\mathbf{H}$	Hessian matrix
$h$	Infinitesimal perturbation parameter
$\mathbf{I}$	Identity matrix
$\mathbf{J}$	Jacobian of a subsystem in a couple multiphysics problem

$\mathfrak{J}$	Global Jacobian of a coupled multiphysics problem
$L$	Wing lift force
$l$	Section lift force
$m'$	Additional apparent mass
$n$	Number of iterations in an iterative solution process; also the grid size in a discretized model
$N$	Number of independent variables in an arbitrary function; also the length of a gradient vector
$\mathcal{O}$	Order of accuracy operator
$p$	Arbitrary performance function
$R_1, R_2, R_{\text{tot}}$	Resistance values in a parallel circuit
$R_e$	Effective downwash resistance value
$R_i$	Induced downwash resistance value
$R_T$	Taper ratio
$Re_c$	Reynolds number based on chord length
$S_w$	Planform area
$\mathbf{s}$	Vector function response of a structural system in a coupled multiphysics problem
$u, v, w$	Cartesian velocity components
$\mathbf{u}_n, \mathbf{u}_a$	Unit vectors in the normal and axial directions, respectively
$V_\infty$	Freestream velocity
$w$	Downwash; also intermediate variable used in automatic differentiation
$w_e$	Effective downwash
$w_i$	Induced downwash
$x, y, z$	Cartesian coordinates; also chordwise, spanwise, and normal coordinates, respectively
$x$	Arbitrary independent variable
$\bar{z}_{c_{\text{max}}}$	Percent maximum camber
$\alpha$	Section angle of attack
$\alpha_e$	Effective angle of attack

$\alpha_i$	Induced angle of attack
$\alpha_{L0}$	Zero-lift angle of attack
$\alpha_{\text{wing}}$	Wing geometric angle of attack
$\Gamma$	Diffusivity; also vortex strength
$\Delta$	Finite perturbation of an arbitrary parameter (e.g. $\Delta x$ )
$\Delta\alpha_{\text{geometric}}$	Change in local angle of attack due to geometric twist
$\Delta\alpha_{\text{aerodynamic}}$	Change in local angle of attack due to aerodynamic twist
$\zeta, \eta, \theta$	Change of variables
$\rho_{\infty}$	Freestream density
$\phi$	Scalar field quantity
$\Omega_{\text{max}}$	Maximum twist value of a finite wing
$\nabla$	Gradient operator

## 1 INTRODUCTION

Aerodynamic shape optimization is an important step in the design process of modern aircraft. This step allows designers to tailor the aerodynamic features of an aircraft to meet a specific set of mission requirements in the most effective way possible. Optimization can be performed early in the design process to identify what features of a design are most important and toward the end of the design process to refine certain aspects of the design based on mission requirements. In many cases, high-fidelity Computational Fluid Dynamics (CFD) analyses are used as the objective functions in these optimization analyses (for example, see Refs. [1–4]). While CFD analyses provide significant insight into the specific flow characteristics of a design, they come at a relatively high cost due to the complex computational meshes and substantial computing resources required. This is especially true for optimization studies in which many cases must be run to evaluate performance changes with respect to design variables. As a result, CFD is not always the best solution for early-stage optimization when insights into trends and interactions between design parameters are more important than highly-accurate performance characteristics.

The computational challenge of using full CFD simulations for aerodynamic optimization are compounded when the application is a morphing wing. In an effort to improve aircraft efficiency through all phases of flight, several morphing-wing technologies are currently in development (for example, see Refs. [5–8]). In order to take full advantage of the benefits provided by morphing-wing technologies, performance characteristics and control derivatives for the wing in multiple morphed configurations must be readily available. Due to the large number of possible configurations for a morphing wing with even just a few degrees of freedom, the efficiency of aerodynamic and structural computations is a prodigious concern.

Several alternatives to full CFD simulations are available for wing optimization. The first practical method dates back to the early 20th century when Lanchester [9] and Prandtl [10,11] developed what is known today as classical lifting line theory. While this was the first mathematical model able to predict lift distributions over a 3D wing with reasonable accuracy, the original formulation is restricted to analyses of a single finite wing with a straight quarter-chord and moderate-to-high aspect ratio in an incompressible, inviscid flow. This method has been used to minimize induced drag [12,13] and maximize lift [14] of various wing planforms.

Low-fidelity methods such as the vortex lattice method and vortex panel method represent another alternative. These potential flow methods are widely used in industry and academia, and their development can be found in common aerodynamic textbooks. For a well-cited overview of these methods, see Katz and Plotkin [15]. These methods can be used to predict lift, induced drag, and pressure distributions over complex geometries but are generally unable to account for viscous effects and airfoil thickness.

A more recent development in aerodynamic analysis is a modern numerical lifting line method presented by Phillips and Snyder [16]. This method is similar to classical lifting line theory but uses the more general 3D vortex lifting law. The numerical formulation allows for the analysis of a system of interacting lifting surfaces with arbitrary camber, twist, sweep, and dihedral. It can also account for viscous effects through the use of 2D airfoil section coefficients. This model should not be confused with the vortex lattice method when a single element is used in the chordwise direction. Although the placement of the horseshoe vortices is similar in both methods, the fundamental equations are significantly different. For example, the vortex lattice method with a single chordwise element places a control point at the three-quarter-chord position and closes the formulation by requiring the normal velocity relative to the local camber line at the control point to be zero. On the other hand, the numerical lifting line method of Phillips and Snyder [16] uses the 2D section lift produced by the local airfoil section to calculate the 3D vortex lift of the finite wing. The latter approach is the numerical equivalent to the analytical approach taken by Prandtl [10,11].

It is worth noting that numerical methods for solving the lifting line equation from classical lifting line theory have been presented by McCormick [17] and Anderson et al. [18]. These methods show accurate results for wings below stall, but they neglect the downwash produced by the bound vorticity and are therefore limited in application to isolated straight wings without sweep or dihedral.

In this work, the numerical lifting line method of Phillips and Snyder [16] has been used as a foundation upon which a system is built for analyzing and optimizing morphing wings. We begin in Chapter 2 with a presentation of methods for computing derivatives and a demonstration of the process of automatic differentiation (AD) in a numerical lifting line algorithm. In Chapter 3 we discuss the development of an optimization framework for aerodynamic analysis and apply the derivative calculations from Chapter 2 to several wing shape optimization problems. We also demonstrate a method for using lifting line calculations to visualize the design space of morphing wings, which can assist in understanding and improving the wing

shape optimization process and results. Chapter 4 presents a detailed overview of classical lifting line theory along with a discussion of its limitations relative to aspect ratio. We discuss the works of several researchers directed at improving predictions for low-aspect-ratio wings and present several new analytical developments that extend the validity of classical lifting line theory to wings of arbitrary aspect ratio. Chapter 5 presents a method for implementing the results of Chapter 4 in the numerical lifting line method of Phillips and Snyder [16], and concludes with a comparison of numerical results to experimental data for a low-aspect-ratio morphing wing.



## 2 DUAL NUMBER AUTOMATIC DIFFERENTIATION FOR WING SHAPE OPTIMIZATION

### 2.1 Introduction

The focus of this chapter is to present an implementation for accurately and efficiently computing derivatives within an aerodynamic analysis tool for the purpose of facilitating gradient-based wing shape optimization. Derivative calculations are an important consideration in any gradient-based optimization study. The gradient of the objective – a vector of partial derivatives of the objective with respect to the design variables – is used to determine the appropriate direction and magnitude for changes in the design variables in order to find a minimum (or maximum) in the objective. Constrained optimization algorithms usually require the calculation of the gradient for each constrained variable as well. The ability of gradient-based optimization algorithms to accurately and efficiently converge upon a local extremum is strongly influenced by the accuracy and efficiency of the derivative calculations upon which they rely. For many gradient-based optimization problems, the calculation of derivatives is often the costliest step in the optimization cycle (see Martins [19]), thus special care must be taken in obtaining these derivatives.

Fortunately, derivatives are important to many fields of application beyond optimization and therefore have a long history of research which can be drawn upon. The first formal presentations of derivatives are traditionally credited to Isaac Newton and Gottfried Leibniz in the late 17<sup>th</sup> century, though the fundamental concept of a derivative appeared much earlier (see Simmons [20]). Numerical analysis methods such as the finite difference (see Courant et al. [21]) and finite element (see Hrennikoff [22] and Courant [23]) methods arose from the need to solve sophisticated problems for which solutions could not be obtained through the methods of analytical calculus. The elliptic and hyperbolic partial differential equations used to describe boundary value and initial value problems are examples of these. For an examination of the history of the finite difference and finite element methods, see Thomée [24].

With the advent of modern computers came a new method for computing derivatives. Wengert [25] presented a technique for the “computation of numerical values of derivatives without developing analytical expressions for the derivatives.” Wengert’s method formed the foundation for what is now known as automatic (or algorithmic) differentiation (AD). Numerous publications exist on the subject, covering topics that range from theoretical research to software development to implementation in practical analysis applications. See, for example, Griewank and Walther [26], Rall [27], and Corliss et al. [28]. A wide variety

of open-source software tools for implementing AD methods in analysis software have been published, and numerous engineering software packages include AD capabilities. For a recent review of theoretical AD methods, see Martins and Hwang [29]. For a recent comparison of AD software tools for various languages, see Šrajer et al. [30].

In this chapter we apply a specific implementation of AD to MachUp, an open-source aerodynamics analysis tool based on the numerical lifting line method of Phillips and Snyder [16]. We do this to better facilitate accurate and efficient gradient calculations for wing shape optimization and other gradient-based optimization problems in which MachUp is used as the objective function. We begin with a general overview of the gradient calculation methods described above – namely, symbolic differentiation, finite differencing, and AD. We then proceed with a description of Dual Number Automatic Differentiation (DNAD), an open-source implementation of forward-mode AD in Fortran (see Yu and Blair [31] and Spall and Yu [32]). We discuss modifications to DNAD that were made to improve the flexibility and ease of integrating the tool with Fortran codes. A simple example is given illustrating the implementation process, and important considerations when implementing DNAD in existing Fortran codes are discussed. Finally, we present the process used to implement DNAD in MachUp.

## 2.2 Derivative Calculation Methods

Methods used for computing derivatives can be divided into three general categories as discussed in Sec. 2.1 – namely, symbolic differentiation, finite differencing, and AD. The three categories are presented here, and considerations for their use are discussed.

### 2.2.1 Symbolic Differentiation

Given our understanding of differential calculus, the most obvious method for computing derivatives is direct symbolic differentiation of the objective function. This involves application of the definition of the derivative as given in any elementary calculus textbook, namely

$$\frac{\partial f}{\partial x} = \lim_{h \rightarrow 0} \frac{f(x+h) - f(x)}{h} \quad (2.2.1)$$

where  $f$  is the objective function,  $x$  is the independent variable, and  $h$  is a perturbation parameter. Through symbolic differentiation, we obtain an explicit analytical equation for the derivative of a function which can be evaluated independent of the original function and is accurate to infinite precision. Algebraic manipulation

of the derivative formula can be performed to express the formula in its simplest form. From a computational perspective, the “simplest form” is that which requires the fewest mathematical operations to evaluate. Thus, symbolic differentiation represents the most accurate and the most efficient method available for derivative computations.

For simple functions such as those found in elementary calculus textbooks, there are no disadvantages to using symbolic differentiation for derivative computations. On the other extreme, direct symbolic differentiation of practical engineering problems is rarely feasible. For example, consider a coupled multiphysics model in which fluid and structural analyses are performed iteratively to determine the response of a system. Results from one analysis are used to update the boundary conditions of the other analysis between iterations, and the number of iterations performed is controlled through the evaluation of residuals in the fluid and structural responses of the system. Expressing this function as a single formula that can be differentiated symbolically would require accumulating each mathematical operation in the process into a single expression. Since the number of iterations – and therefore the number of mathematical operations to be evaluated – is variable, the exact expression cannot be known *a priori*.

Even in the situation described above, it may still be possible to obtain symbolic derivatives of the objective function if the problem can be broken into smaller sub-functions for which symbolic derivatives are available. This approach uses the chain rule of differentiation to propagate derivative information through each sub-function evaluation. For each sub-function evaluation, the Jacobian matrix – which contains the partial derivatives of all function outputs with respect to each variable input – must be evaluated and stored. These Jacobian matrices can then be chained together to compute the gradient of the final objective function with respect to each original input.

To continue the coupled multiphysics example described above, let  $p$  be a single-value function that represents the performance of the coupled multiphysics system. Also, let  $\mathbf{x} = (\mathbf{x}_f, \mathbf{x}_s)$  be the complete set of inputs required for the coupled multiphysics model, where  $\mathbf{x}_f = (x_{f_1}, x_{f_2}, \dots, x_{f_l})$  is the set of  $l$  inputs required for the fluid analysis and  $\mathbf{x}_s = (x_{s_1}, x_{s_2}, \dots, x_{s_m})$  is the set of  $m$  inputs required for the structural analysis. Then  $p = p(\mathbf{x}) = p(\mathbf{x}_f, \mathbf{x}_s)$ . The problem at hand is then to determine  $\nabla p$ , where

$$\nabla p = \frac{\partial p}{\partial \mathbf{x}} = \left( \frac{\partial p}{\partial \mathbf{x}_f}, \frac{\partial p}{\partial \mathbf{x}_s} \right) = \left( \frac{\partial p}{\partial x_{f_1}}, \frac{\partial p}{\partial x_{f_2}}, \dots, \frac{\partial p}{\partial x_{f_1}}, \frac{\partial p}{\partial x_{s_1}}, \frac{\partial p}{\partial x_{s_2}}, \dots, \frac{\partial p}{\partial x_{s_m}} \right) \quad (2.2.2)$$

Now, let  $\mathbf{f}$  and  $\mathbf{s}$  be vector functions that represent the responses of the fluid and structural models, respectively. Then  $\mathbf{f} = \mathbf{f}(\mathbf{x}_f, \mathbf{s})$  and  $\mathbf{s} = \mathbf{s}(\mathbf{x}_s, \mathbf{f})$ . If  $\mathbf{f}$  is symbolically differentiable with respect to the input vectors  $\mathbf{x}_f$  and  $\mathbf{s}$ , then the Jacobian of  $\mathbf{f}$

$$\mathbf{J}_f = \begin{bmatrix} \frac{\partial \mathbf{f}}{\partial \mathbf{x}_f} & \frac{\partial \mathbf{f}}{\partial \mathbf{s}} \end{bmatrix} \quad (2.2.3)$$

can be determined analytically. Likewise, if  $\mathbf{s}$  is symbolically differentiable with respect to the input vectors  $\mathbf{x}_s$  and  $\mathbf{f}$ , then the Jacobian of  $\mathbf{s}$

$$\mathbf{J}_s = \begin{bmatrix} \frac{\partial \mathbf{s}}{\partial \mathbf{x}_s} & \frac{\partial \mathbf{s}}{\partial \mathbf{f}} \end{bmatrix} \quad (2.2.4)$$

can also be determined analytically. Equations (2.2.3) and (2.2.4) can be used to assemble a global Jacobian  $\mathfrak{J}$ , which contains a row and column for each element in the  $\mathbf{x}_f$ ,  $\mathbf{x}_s$ ,  $\mathbf{f}$ , and  $\mathbf{s}$  vectors. In general, this global Jacobian has the form

$$\mathfrak{J} = \begin{bmatrix} \frac{\partial \mathbf{x}_f}{\partial \mathbf{x}_f} & \frac{\partial \mathbf{x}_f}{\partial \mathbf{x}_s} & \frac{\partial \mathbf{x}_f}{\partial \mathbf{f}} & \frac{\partial \mathbf{x}_f}{\partial \mathbf{s}} \\ \frac{\partial \mathbf{x}_s}{\partial \mathbf{x}_f} & \frac{\partial \mathbf{x}_s}{\partial \mathbf{x}_s} & \frac{\partial \mathbf{x}_s}{\partial \mathbf{f}} & \frac{\partial \mathbf{x}_s}{\partial \mathbf{s}} \\ \frac{\partial \mathbf{f}}{\partial \mathbf{x}_f} & \frac{\partial \mathbf{f}}{\partial \mathbf{x}_s} & \frac{\partial \mathbf{f}}{\partial \mathbf{f}} & \frac{\partial \mathbf{f}}{\partial \mathbf{s}} \\ \frac{\partial \mathbf{s}}{\partial \mathbf{x}_f} & \frac{\partial \mathbf{s}}{\partial \mathbf{x}_s} & \frac{\partial \mathbf{s}}{\partial \mathbf{f}} & \frac{\partial \mathbf{s}}{\partial \mathbf{s}} \end{bmatrix} \quad (2.2.5)$$

where each term in Eq. (2.2.5) is a submatrix itself.

If we evaluate the fluid model first, we must provide an initial guess for the structural response, namely  $\mathbf{s}_0$ . Then  $\mathbf{f}_1 = \mathbf{f}(\mathbf{x}_f, \mathbf{s}_0)$  and the global Jacobian for this step is

$$\mathfrak{J}_{f_1} = \begin{bmatrix} \mathbf{I} & \mathbf{0} & \mathbf{0} & \mathbf{0} \\ \mathbf{0} & \mathbf{I} & \mathbf{0} & \mathbf{0} \\ \frac{\partial \mathbf{f}_1}{\partial \mathbf{x}_f} & \mathbf{0} & \mathbf{0} & \frac{\partial \mathbf{f}_1}{\partial \mathbf{s}_0} \\ \mathbf{0} & \mathbf{0} & \mathbf{0} & \mathbf{I} \end{bmatrix} \quad (2.2.6)$$

More generally, the global Jacobian for the  $i$ th evaluation of the fluid model can be written as

$$\mathfrak{J}_{f_i} = \begin{bmatrix} \mathbf{I} & \mathbf{0} & \mathbf{0} & \mathbf{0} \\ \mathbf{0} & \mathbf{I} & \mathbf{0} & \mathbf{0} \\ \frac{\partial \mathbf{f}_i}{\partial \mathbf{x}_f} & \mathbf{0} & \mathbf{0} & \frac{\partial \mathbf{f}_i}{\partial \mathbf{s}_{i-1}} \\ \mathbf{0} & \mathbf{0} & \mathbf{0} & \mathbf{I} \end{bmatrix} \quad (2.2.7)$$

Note that the third diagonal entry in Eqs. (2.2.6) and (2.2.7) is  $\mathbf{0}$  as opposed to the identity matrix. This is because  $\mathbf{f}$  is the dependent variable in the fluid model, so that the  $\mathbf{f}$  in the numerators is one iteration ahead of the  $\mathbf{f}$  in the denominators and we have  $\partial \mathbf{f}_i / \partial \mathbf{f}_{i-1} = \mathbf{0}$  for the third diagonal entry.

The structural model is evaluated using results from the fluid model as input, so that the global Jacobian for the structural evaluation is

$$\mathfrak{J}_{s_i} = \begin{bmatrix} \mathbf{I} & \mathbf{0} & \mathbf{0} & \mathbf{0} \\ \mathbf{0} & \mathbf{I} & \mathbf{0} & \mathbf{0} \\ \mathbf{0} & \mathbf{0} & \mathbf{I} & \mathbf{0} \\ \mathbf{0} & \frac{\partial \mathbf{s}_i}{\partial \mathbf{x}_s} & \frac{\partial \mathbf{s}_i}{\partial \mathbf{f}_i} & \mathbf{0} \end{bmatrix} \quad (2.2.8)$$

Similar to the global Jacobian for the fluid model, the fourth diagonal entry in Eq. (2.2.8) is  $\mathbf{0}$  because  $\mathbf{s}$  is the dependent variable here. Then the  $\mathbf{s}$  in the numerator is one iteration ahead of the  $\mathbf{s}$  in the denominator and we have  $\partial \mathbf{s}_i / \partial \mathbf{s}_{i-1} = \mathbf{0}$  for the fourth diagonal entry.

The global Jacobian for the entire coupled solution is found by chaining the global Jacobians, Eqs. (2.2.7) and (2.2.8), over each iteration. A coupled solution evaluated for  $n$  iterations will have a global Jacobian given by

$$\mathfrak{J}_n = \prod_{i=1}^n \mathfrak{J}_{s_i} \mathfrak{J}_{f_i} \quad (2.2.9)$$

Equation (2.2.2) can now be written as

$$\nabla p = \left[ \frac{\partial p}{\partial \mathbf{x}_f} \quad \frac{\partial p}{\partial \mathbf{x}_s} \quad \frac{\partial p}{\partial \mathbf{f}_n} \quad \frac{\partial p}{\partial \mathbf{s}_n} \right] \mathfrak{J}_n \quad (2.2.10)$$

While it would be tedious to symbolically evaluate Eq. (2.2.9) by hand, computer algebra systems can readily perform the evaluations and produce a symbolic formula for the evaluation of  $\nabla p$  over  $n$  iterations. However, this symbolic formula may be of little use in practice as it is dependent on the number of iterations performed.

A more practical use of the methodology presented here is to evaluate the global Jacobians numerically during each step in the solution process and propagate a single aggregate Jacobian through each iteration. This approach results in numerical derivatives as opposed to symbolic expressions for the derivatives, but no additional assumptions or approximations are made in their evaluation.

An important distinction must here be made regarding the symbolic derivatives produced using this method compared to the derivatives that would be obtained from symbolically differentiating the governing mathematical model. While the derivatives discussed here are computed using symbolic derivatives of the individual analysis components, they are exact in terms of the numerical model and not the underlying mathematical model upon which the numerical algorithm is based. For further discussion on the implications of numerical modeling error in regard to derivative calculations, see Pakalapati et al. [33] and Sec. 2.4.4.

One potential benefit of using this method is that it can provide a measurement for the level of convergence in an iterative process such as the one described above. In our example, the last column of submatrices in the  $i$ th global Jacobian contains the derivatives of fluid and structural responses  $\mathbf{f}_i$  and  $\mathbf{s}_i$  with respect to the initial guess  $\mathbf{s}_0$ . As the solution approaches convergence, the responses should become independent of the initial guess, so that these derivatives should tend toward zero. Examining the magnitudes of these derivatives may offer insight into the level of convergence achieved at each iteration.

In summary, symbolic differentiation provides the most accurate and computationally efficient method of calculating derivatives. Unfortunately, symbolic derivatives are not readily available for most practical engineering problems. In some cases, the problem can be broken into smaller, symbolically differentiable components and the partial derivatives of the complete problem can be found through application of the chain rule of differentiation, either numerically or symbolically, without any loss in accuracy.

### 2.2.2 *Finite Differencing*

In 1928, Courant et al. [21] proposed a method for converting partial differential equations into simple algebraic functions by replacing the partial differentials with quotient approximations. Of particular interest to the authors were the boundary value and eigenvalue problems for elliptic differential equations and the initial value problem for hyperbolic and parabolic differential equations, for which there are few known analytical solutions and none of practical interest. Their development is general enough that it can readily be

applied to other problems requiring the calculation of derivatives, and different formulations for the quotient approximations allow for variable levels of accuracy and complexity.

The simplest example of a finite difference approximation can be taken directly from the definition of the derivative given in Eq. (2.2.1). Removing the limit and replacing the infinitesimal perturbation parameter  $h$  with a finite step size  $\Delta x$  gives

$$\frac{\partial f}{\partial x} = \frac{f(x + \Delta x) - f(x)}{\Delta x} + \mathcal{O}(\Delta x) \quad (2.2.11)$$

which is the first-order-accurate forward difference formula. The first-order-accurate backward difference formula is similar but perturbed by  $-\Delta x$ , specifically

$$\frac{\partial f}{\partial x} = \frac{f(x) - f(x - \Delta x)}{\Delta x} + \mathcal{O}(\Delta x) \quad (2.2.12)$$

The second-order-accurate central difference formula is found by perturbing the functions in both positive and negative directions, which gives

$$\frac{\partial f}{\partial x} = \frac{f(x + \Delta x) - f(x - \Delta x)}{2\Delta x} + \mathcal{O}(\Delta x^2) \quad (2.2.13)$$

This approach can be applied iteratively to obtain derivatives of higher order as well. For example, an approximation to the second derivative of  $f$  can be found by first finding approximations for  $\partial f / \partial x$  from Eq. (2.2.13) centered at  $x + \Delta x / 2$  and  $x - \Delta x / 2$  using a perturbation of  $\Delta x / 2$ , and then using these derivative approximations as the perturbed function values in Eq. (2.2.13). This gives

$$\frac{\partial^2 f}{\partial x^2}(x) = \frac{\frac{\partial f}{\partial x}\left(x + \frac{\Delta x}{2}\right) - \frac{\partial f}{\partial x}\left(x - \frac{\Delta x}{2}\right)}{\Delta x} + \mathcal{O}(\Delta x^2) = \frac{f(x + \Delta x) - 2f(x) + f(x - \Delta x)}{\Delta x^2} + \mathcal{O}(\Delta x^2) \quad (2.2.14)$$

Many other finite difference approximations are available. Other methods for deriving these formulas also exist. For example, Taylor series expansions of the function  $f$  can be used to obtain Eqs. (2.2.11)-(2.2.14) and many other finite difference formulas. In fact, the orders of accuracy listed in these equations were determined using Taylor series expansion. For more finite difference formulas and the methods used to derive them, see LeVeque [34].

While the finite difference method was originally developed specifically as a tool for solving partial differential equations, it can be used anytime the derivative of a function is needed and an approximation is

acceptable. In general, the finite difference method can readily be applied to any numerical algorithm without the need to make internal modifications to the algorithm. This is done simply by running the algorithm multiple times at perturbed states and then applying the appropriate finite difference equation to the results. Because of this, the finite difference method is the most versatile derivative-approximation method available.

It is also the least accurate and least efficient method, however. All of the methods discussed here are limited in accuracy by machine precision and numerical modeling error; but the finite difference method is subject to truncation error as well. The finite difference method is also less efficient than other methods because full evaluations of the objective function are required for each perturbed function value in the finite difference formula. A function with  $N$  input variables would need to be evaluated  $N + 1$  times to obtain a first-order-accurate approximation of its gradient vector using Eqs. (2.2.11) or (2.2.12), or  $2N$  times for a second-order-accurate approximation using Eq. (2.2.13).

### 2.2.3 Automatic Differentiation

As mentioned previously, AD is a method of numerically computing partial derivatives of an algorithm, accurate to machine precision, without the need to express the partial derivative symbolically. There are several different approaches to AD, but all stem from the same basic idea that every numerical algorithm can be broken down into a series of fundamental mathematical operations. If each mathematical operation in an algorithm is differentiable, then the entire algorithm can be differentiated through sequential applications of the chain rule of differentiation. This concept is quite similar to the example discussed in Sec. 2.2.1, but applied at a much finer level.

The different approaches to AD can be classified into two main groups. The first group, called forward-mode AD, performs derivative calculations in concert with the primary function evaluation. The chain rule of differentiation is used to propagate derivative calculations from one mathematical operation to the next, so that the derivatives of intermediate variables with respect to the independent variables are computed alongside the calculation of the intermediate variables themselves. This is the form of AD that was first developed by Wengert [25].

An example of forward-mode AD is given in Figure 2.1. The primary function  $f(x_1, x_2) = x_1 \sin(x_2)$  is evaluated as shown, moving from top to bottom. An intermediate variable  $w_i$  is produced by each mathematical operation, and the derivatives of each intermediate variable with respect to the two independent



variables are computed alongside the function values. Substitution using the definitions given, shown at the bottom of Figure 2.1, confirms that numerical results calculated using this process are consistent with the exact symbolic partial derivatives of the function.

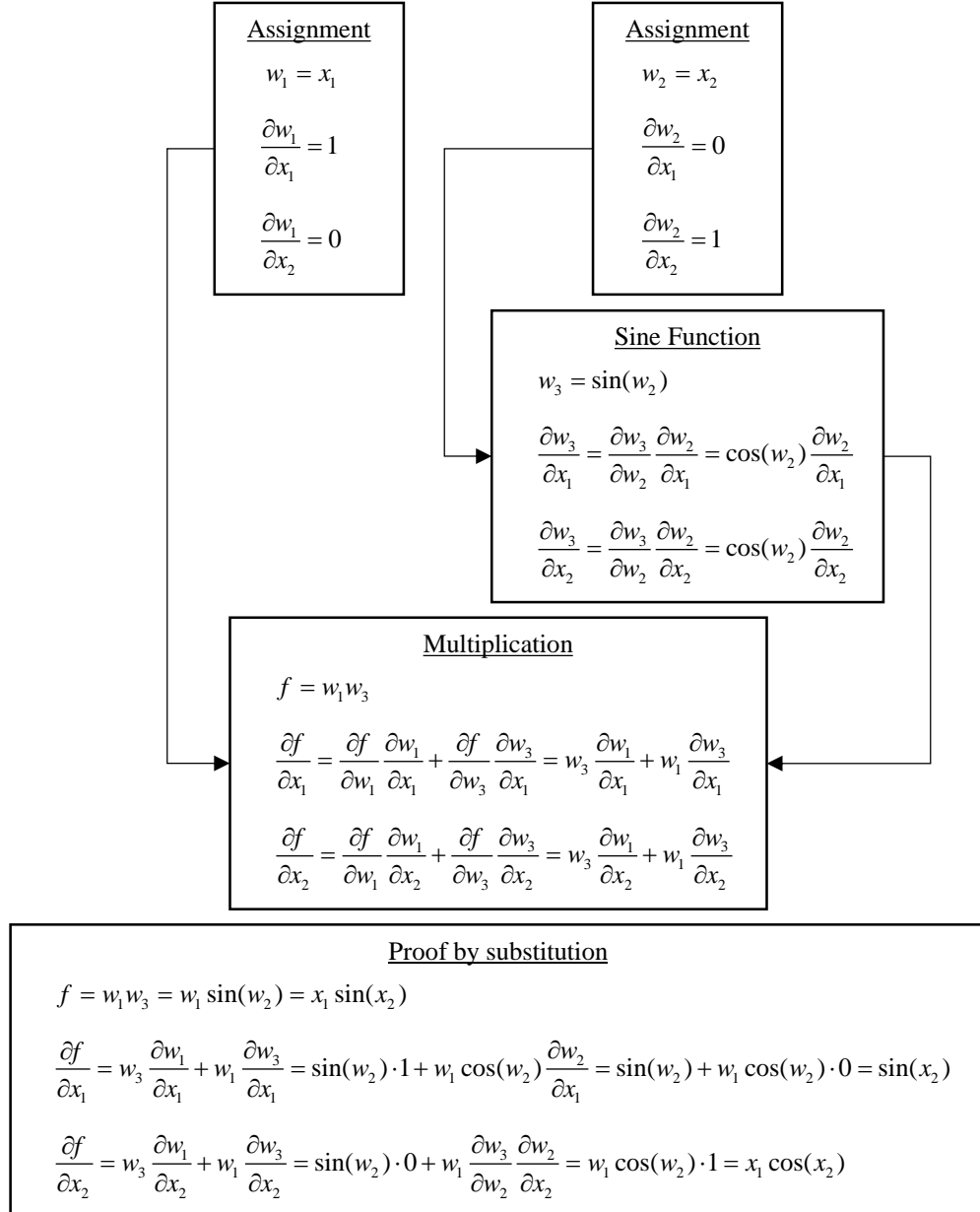


**Figure 2.1** An example of forward-mode AD using the function  $f(x_1, x_2) = x_1 \sin(x_2)$ .

An example of reverse-mode AD is given in Figure 2.2, again using the function  $f(x_1, x_2) = x_1 \sin(x_2)$ . The function evaluation proceeds as normal, but each partial derivative evaluation listed represents an addition to the computational graph. Once the function evaluation has been completed, the computational graph is traversed in reverse-order to produce the partial derivatives given in the right-hand box of Figure 2.2.

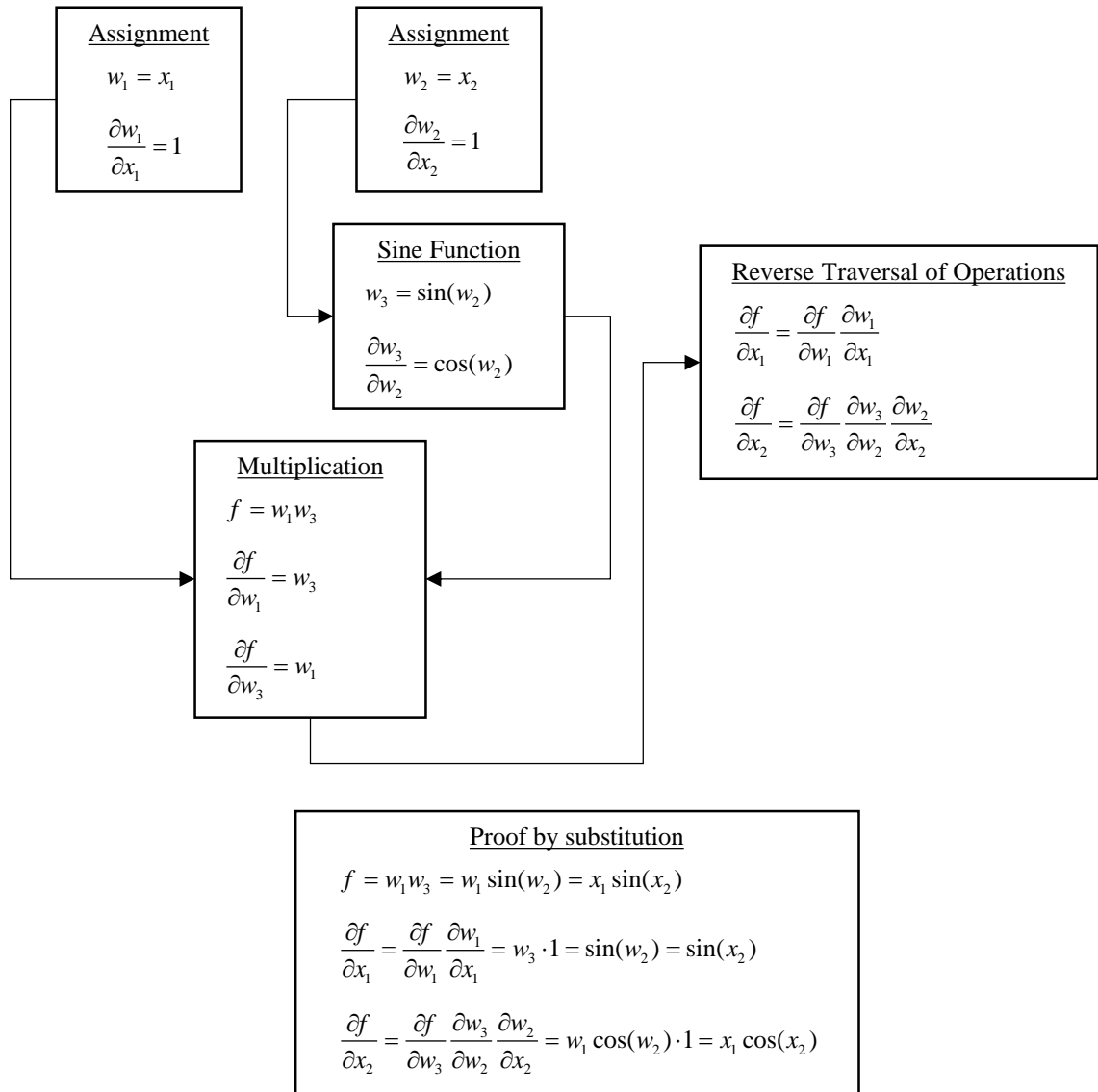


Figure 2.2 An example of reverse-mode AD using the function  $f(x_1, x_2) = x_1 \sin(x_2)$ .

Figures 2.1 and 2.2 were given to illustrate the overall processes of the respective methods, but many details are hidden so that a comprehensive comparison of the two methods cannot be made based on these examples alone. Fewer computations are required to arrive at the partial derivative solutions given in Figure 2.2 than were required to arrive at the same solution in Figure 2.1. This is only true, however, because the number of design variables (2) is larger than the number of output variables (1). In general, the complexity of the derivative calculations using forward-mode AD scales according to the number of design variables in the problem, while the complexity of the derivative calculations using reverse-mode AD scales according to the number of output variables for which gradients are needed.

Also not apparent from the examples illustrated in Figures 2.1 and 2.2 are the memory requirements for each method. Forward-mode AD algorithms must store the intermediate partial derivatives at each step in the solution process, so they require more memory than either symbolic differentiation or the finite difference method. Reverse-mode AD algorithms must store the entire computational graph, however, so that their memory requirements are considerably larger.

The effort required to implement the different modes in code is also not illustrated. In general, forward-mode AD is considered easier to implement and less intrusive to the original source code than reverse-mode AD. This is because, in reverse-mode AD, additional coding is required to build, manage, and traverse the computational graph. Additionally, each output variable for which derivatives are needed must be handled individually with existing reverse-mode AD methods, while forward-mode AD methods can be applied in such a way that a single version of the source code can compute derivatives of any output variable with respect to any input variable. This will be demonstrated later in this chapter. The reader is referred to the literature (see, for example, Refs. [26–28]) for more detailed discussions on the two AD methods.

#### 2.2.4 Discussion

The purpose of the present chapter is to facilitate accurate and efficient derivative calculations within MachUp, as discussed in the introduction. Symbolic differentiation of the algorithm is infeasible due to the complexity of the nonlinear system of equations which form the basis of the numerical lifting line algorithm implemented by MachUp. Finite differencing introduces truncation error into the derivative calculations and is less efficient than AD methods. For these reasons, the author has selected AD for implementation in MachUp.

Of the available AD methods, reverse-mode AD is considered more efficient than forward-mode AD when the number of design variables is larger than the number of dependent variables. This is likely to be the case for any wing shape optimization problem in which MachUp is used to evaluate the objective function, but this advantage is expected to be small because of the limited number of inputs required to define even complex wing geometries in MachUp. The memory advantages of forward-mode AD are also not important to this effort because the memory requirements for most typical MachUp simulations are several orders of magnitude less than the available memory on most modern machines. The primary concerns in deciding between forward-mode and reverse-mode AD for the current work, then, are the amount of effort required for implementation in the existing source code and the flexibility of the resulting code in computing derivatives of various output variables with respect to various input variables. As discussed in Sec. 2.2.3, forward-mode AD holds advantages over reverse-mode AD in both respects.

### **2.3 Methods and Tools for Forward-Mode Automatic Differentiation**

Two methods exist for implementing forward-mode AD in source code, namely source code transformation (SCT) and operator-overloading (OO). SCT is done by scanning the existing source code, identifying all floating-point variables and mathematical operations, adding additional variable declarations for the storage of partial derivative values, and adding additional lines of code for the computation of partial derivative values anytime a mathematical operation is performed. While to perform this process manually would be tedious at best, several algorithms have been developed to perform SCT automatically for a variety of programming languages. See, for example, Refs. [35–39]. SCT is possible in all programming languages, but tools for performing SCT are quite complex. Because the derivative computations appear explicitly in the differentiated source code, the resulting source code can be quite large when compared to the original undifferentiated code, and different source code is obtained depending on which input variables are made available for differentiation. As a result, several versions of the source code must be maintained in order to allow for any flexibility in the derivative calculations, which has negative implications regarding version control.

OO methods rely on the use of a custom data type with specifically-defined behavior for mathematical operations. The custom data type contains storage for a single floating-point variable and its derivative with respect to one or more independent variables. Any time a mathematical operator is applied to an instance of

this custom data type, code is executed to evaluate both the mathematical operation and its analytical partial derivative(s) automatically. Not all programming languages support the polymorphic features required for implementing AD through OO, but most common languages used for scientific and engineering applications do (e.g. Fortran, Matlab, C++, Python, R, and Java).

As with SCT, several tools are available for implementing OO in existing source code, but implementations are quite varied in both functionality and ease-of-use. One common method for implementing OO, because of its overall simplicity, is the complex step method proposed by Lyness [40]. This method replaces all floating-point variables in an algorithm with the built-in complex data type that is standard in most modern programming languages. The independent variable with respect to which derivatives are desired is given an initial assignment that includes a small imaginary perturbation. Calculations for the algorithm then proceed under the normal rules of complex mathematics, assuming all operators in the algorithm are defined for complex numbers. Outputs of the algorithm will then contain the normal function value in the real part of the complex number and the first derivative of the function, multiplied by the small perturbation used, in the imaginary part of the complex number. To illustrate this method, consider a Taylor series expansion of the arbitrary function  $f(x)$  using the perturbation  $ih$ ,

$$f(x + ih) = f(x) + ih \frac{\partial f}{\partial x}(x) - \frac{h^2}{2!} \frac{\partial^2 f}{\partial x^2}(x) - \frac{ih^3}{3!} \frac{\partial^3 f}{\partial x^3}(x) + \dots \quad (2.3.1)$$

Isolating the real part of Eq. (2.3.1) and solving for  $f(x)$  gives

$$f(x) = \text{Re}[f(x + ih)] + \frac{h^2}{2!} \frac{\partial^2 f}{\partial x^2}(x) - \dots \quad (2.3.2)$$

so that  $\text{Re}[f(x + ih)]$  gives an approximation to the function  $f(x)$  that is second-order accurate in  $h$ .

Isolating the imaginary part of Eq. (2.3.1) and solving for the first derivative gives

$$\frac{\partial f}{\partial x} = \frac{\text{Im}[f(x + ih)]}{h} + \frac{h^2}{3!} \frac{\partial^3 f}{\partial x^3}(x) + \dots \quad (2.3.3)$$

so that  $\text{Im}[f(x + ih)]/h$  gives an approximation to the first derivative of  $f$  with respect to  $x$  that is also second-order accurate in  $h$ . On finite-precision machines, careful selection of the size of the perturbation parameter  $h$  can potentially eliminate the truncation errors in both Eqs. (2.3.2) and (2.3.3). See Martins et al.

[41] for a more detailed discussion on the complex step method and considerations for eliminating the truncation errors when using this method.

While the complex step method is relatively simple to implement and does not require the construction of a custom data type, it has several drawbacks that discourage its use over other OO methods. Martins et al. [41] showed a Fortran implementation of the complex step method to be significantly less efficient than even finite difference methods with only marginal improvement in accuracy. Also, the requirement for a perturbation step size introduces the potential for additional truncation error in the results that would not be incurred with a full OO implementation. Finally, the restriction to a complex number data type limits the number of independent variables with respect to which partial derivatives can be obtained to one per simulation.

Several full OO implementations of forward-mode AD have been developed for a variety of programming languages. Fortran implementations include ADF95 (see Straka [42]), AUTO\_DERIV (see Stamatiadis et al. [43]), COSY INFINITY (see Berz et al. [44]), AD01 (see Pryce and Reid [45]), and DNAD (see Yu and Blair [31]). Of these, DNAD has been selected for use in this work. Several considerations were weighed in comparing these tools, including licensing, extensibility, level of complexity in the interface, and runtime performance. A thorough discussion of DNAD is given in the remainder of this chapter, including a presentation of dual number theory upon which DNAD is based, an examination of the algorithm, and the process of integrating DNAD with MachUp. For details on the other software packages listed, the reader is referred to Refs. [42–45].

## 2.4 Dual Number Automatic Differentiation

DNAD is essentially a derived data type that implements the rules of dual number theory programmatically, which can then be used in computational software to perform dual number calculations. In this section, we shall first present an overview of what dual number theory is. We shall then describe how this theory is implemented as a data type in DNAD. Finally, we shall discuss the process of integrating this derived data type into Fortran source code for automatic differentiation of an algorithm.

### 2.4.1 Dual Number Theory

The theory of dual numbers was first introduced by Clifford [46] for the purpose of describing biquaternions. It has since found application in several areas including the calculation of derivatives. Dual numbers extend the real number space by adjoining a nilpotent unit  $\varepsilon$ , which has the property

$$\varepsilon^n = \begin{cases} 1, & n = 1 \\ 0, & n \neq 1 \end{cases} \quad (2.4.1)$$

This is similar to how complex numbers extend the real number space using the imaginary unit  $i$ , but the differences in properties between the nilpotent unit and the imaginary unit result in distinct behavior between the two number sets. A dual number  $d$  can be written as

$$d = a + b\varepsilon \quad (2.4.2)$$

where  $a$  is the real component and  $b$  is the dual component of the dual number. A Taylor series expansion of the dual number perturbed about the real component by the dual unit  $\varepsilon$  gives

$$f(a + \varepsilon) = f(a) + f'(a)\varepsilon + f''(a)\frac{\varepsilon^2}{2!} + \dots \quad (2.4.3)$$

or, applying the definition of the nilpotent unit given in Eq. (2.4.1),

$$f(a + \varepsilon) = f(a) + f'(a)\varepsilon \quad (2.4.4)$$

From Eq. (2.4.4) we see that the real component of  $f(a + \varepsilon)$  gives the function value  $f(a)$  and the dual component gives the first derivative of the function,  $f'(a)$ . Note that Eq. (2.4.4) is not a truncation of Eq. (2.4.3), so that the function value and its derivative obtained in this manner are exact.

Now consider two functions  $f$  and  $g$  represented as dual numbers  $d_1 = f + f'\varepsilon$  and  $d_2 = g + g'\varepsilon$ . The product of these two dual numbers is

$$d_1 d_2 = (f + f'\varepsilon)(g + g'\varepsilon) = fg + (fg' + gf')\varepsilon + f'g'\varepsilon^2 = fg + (fg' + gf')\varepsilon \quad (2.4.5)$$

which gives the correct values for the function and its derivative as the real and dual components, respectively. Similarly, the quotient of these two dual numbers is

$$\frac{d_1}{d_2} = \frac{f + f'\varepsilon}{g + g'\varepsilon} \quad (2.4.6)$$

Multiplying top and bottom by the dual conjugate of the denominator,  $g - g'\varepsilon$ , gives

$$\frac{d_1}{d_2} = \frac{fg + (f'g - fg')\varepsilon - f'g'\varepsilon^2}{g^2 - g'\varepsilon^2} = \frac{f}{g} + \frac{f'g - fg'}{g^2}\varepsilon \quad (2.4.7)$$

which again gives the correct values for the function and its derivative as the real and dual components, respectively.

The dual number of a trigonometric function can be determined using another Taylor series expansion. For example, the function  $f = \sin(x)$  can be expressed as a dual number as

$$d_3 = f(x + \varepsilon) = \sin(x) + \cos(x)x'\varepsilon - \sin(x)\frac{x''}{2!}\varepsilon^2 - \dots \quad (2.4.8)$$

so that the real part –  $\sin(x)$  – gives the original function and the dual part –  $\cos(x)x'$  – gives the correct derivative. All other terms are zero by definition of the nilpotent unit.

This exercise can be repeated for all other continuously differentiable mathematical operations with consistent results. Additionally, the chain rule of differentiation allows multiple operations to be chained together to produce accurate expressions for the function and its derivative for functions of arbitrary complexity.

Retention of higher-order terms in  $\varepsilon$  allows for higher-order derivatives to be calculated in like manner to the first-order derivatives illustrated above. For an example of how dual numbers can be applied to compute second-order derivatives, see Fike and Alonso [47]. Only first-order derivatives will be treated in this work. However, future effort may extend DNAD to facilitate higher-order derivatives. This would facilitate accurate and efficient calculations of Hessian matrices, which can then be used to improve the performance of some gradient-based optimization algorithms.

#### 2.4.2 The Dual Number Data Type

The dual number theory described in Sec. 2.4.1 has been implemented in Fortran by Yu and Blair [31] using a derived data type with operator overloading. The derived data type consists of a single floating-point variable that stores the primary function value, an array of floating-point values of arbitrary length containing any number of partial derivative values, and a series of overloaded operator functions defining the mechanics of dual number algebra. The DNAD source code is provided in Appendix A.

The source code given in Appendix A contains several modifications from the original version published by Yu and Blair. These modifications have been made in an effort to make the software more flexible and



easier to use. In the original version, variables for precision and the length of the derivative vectors were defined explicitly in the source code. These definitions have been removed. Floating-point precision is now controlled through options specified at compile-time. For example, the DNAD module can be compiled for double-precision floating-point algebra using the `-fdefault-real-8` flag in the gfortran compiler or the `-r8` flag in the Intel Fortran compiler. Similarly, the length of the derivative vector can be specified using preprocessor directives. For example, a derivative vector length of 3 is defined by specifying `-Dndv=3` when invoking the preprocessor. By making these modifications, the floating-point precision and derivative vector length are now contained in the DNAD programming interface as opposed to being explicitly contained in the DNAD source code. Additionally, the source code has been reorganized and is now contained within a single source file. This is simply for convenience when compiling the module and linking it with Fortran algorithms. Note that the use of preprocessor directives requires that the preprocessor be invoked before the source code can be compiled. This is usually done when invoking the compiler by specifying a preprocessor flag (e.g. `-cpp` when using gfortran or `-fpp` when using the Intel Fortran compiler) or by capitalizing the file extension (e.g. `*.F` or `*.F90` as opposed to `*.f` or `*.f90`).

Several additional operators have been added to the programming interface, including the intrinsic Fortran `tan`, `dtan`, `atan`, `atan2`, and `maxloc` functions. The `abs` operator overload has been modified to prevent excessive not-a-number (NaN) occurrences in the derivative values when the primary value is constant with respect to any of the independent variables. These changes make the DNAD module more versatile in its application to existing Fortran algorithms.

#### 2.4.3 *Integration with Fortran Algorithms*

A streamlined process for integrating DNAD with Fortran algorithms has been developed. Most source files can be modified simply by adding the lines of code shown in Figure 2.3 to the beginning of the file. When other modifications to the source file are necessary, e.g. when logic must be added to handle input and/or output of the additional data contained in the dual number type, these modifications can also be contained inside compiler directives so that the normal behavior of the code can be retained when the DNAD module is not included in the compiling process.

```

#ifdef dnad
    use dnadmod
#define real type(dual)
#endif

```

**Figure 2.3 Header lines added to a Fortran module to include DNAD capabilities.**

In some situations, the programmer may need to exclude specific floating-point variables from conversion to dual numbers. For example, a named constant (usually defined with the `parameter` keyword) cannot be converted directly to a dual number because Fortran does not allow for implicit type conversion to derived data types. A simple trick has been successfully applied in these cases which takes advantage of the fact that the algorithms used to parse the preprocessor directives are case-sensitive, while the Fortran compiler itself is case-insensitive. Therefore, the commands shown in Figure 2.3 will only convert variables declared as `real` to `type(dual)`. Variables declared as uppercase `REAL` will remain unchanged.

As a simple example, consider the Fortran source code contained in the top box of Figure 2.4(a). This code prompts the user for a value for the radius (`r`) of a circle, which it then uses to compute the area of the circle. The compiler command used to generate an executable from this source code, using the open-source `gfortran` compiler, is given in the middle box of Figure 2.4(a). A single execution of the resulting executable is illustrated in the bottom box, where the user has specified a radius of 5.

In comparison, the modified source code to generate an executable capable of automatic differentiation using DNAD is shown in the top box of Figure 2.4(b). Only two changes have been made to the original code: the addition of four header lines from Figure 2.3 to include the DNAD module in the executable, and the change to uppercase `REAL` for the declaration of the parameter `pi`. The command needed to compile this code, given in the middle box of Figure 2.4(b), now specifies the DNAD source code file and defines the length of the derivative vectors. The `-Ddnad` option tells the preprocessor to execute the commands contained inside the `#ifdef` preprocessor directive at the top of the `Circle` program. Also note that the name of the source code file has been changed to use a capital “F” in the extension so that the preprocessor is automatically invoked. Execution of the resulting executable, shown in the bottom box of Figure 2.4(b), is again slightly different from that shown in the bottom box of Figure 2.4(a). In addition to specifying the radius of the circle, the user must also specify the partial derivative of the radius with respect to the

<pre> program Circle      implicit none      real, parameter :: pi=3.1416     real :: r, a      write(*,*) "Enter a radius: "     read(*,*) r     a = pi * r**2     write(*,*) "Area = ", a end program Circle </pre>	<pre> program Circle <b>#ifdef dnad</b>     <b>use dnadmod</b> <b>#define real type(dual)</b> <b>#endif</b>     implicit none      <b>REAL</b>, parameter :: pi=3.1416     real :: r, a      write(*,*) "Enter a radius: "     read(*,*) r     a = pi * r**2     write(*,*) "Area = ", a end program Circle </pre>
gfortran Circle.f90	gfortran -Ddnad -Dndv=1 dnad.F90 Circle.F90
<pre> ./a.out Enter a radius 5 Area = 78.5400009 </pre>	<pre> ./a.out Enter a radius 5 1 Area = 78.5400009 31.4159985 </pre>
a)	b)

**Figure 2.4 Example source code, compiler commands, and code execution (a) before and (b) after DNAD integration. Differences are highlighted in bold.**

independent variable of interest. In this case, the independent variable of interest is the radius, so that  $\partial r / \partial r = 1$ . In addition to outputting the area, the code has automatically output the derivative vector because a free-formatted output command was used. If different formatting is desired for the output, preprocessor directives can be used to customize the output. An example of this based on the CircleArea program is given in Figure 2.5.

Using the source code given in Figure 2.4(b) with the compiler command given in Figure 2.4(a) will produce an executable identical to the executable produced from the unmodified code. Thus, for this simple program, the same source code can now be used to generate both normal and differentiated versions of the software. It shall be shown later that this same result can be achieved for even complex algorithms. The simplification to a single source code for both normal and differentiated versions of the software is a significant advantage over other AD tools where separate source code repositories must be maintained.

```

program Circle
...
#ifdef dnad
    write(*,*) "Area = ", a
#else
    write(*, ' (A, F12.7) ') "Area = ", a%x
    write(*, ' (A, F12.7) ') "dA/dr = ", a%dx
#endif
end program Circle

```

**Figure 2.5** Example source code for customizing output of dual number objects.

#### 2.4.4 *Special Considerations when Integrating DNAD with Existing Fortran Algorithms*

Throughout the course of this work, several items have been identified that require special care in order to correctly implement DNAD with an existing Fortran code. Most of these items, with the exception of the first, relate to specific components of the Fortran programming language. Most of these components have been deprecated since the release of the Fortran 90 language standard and are generally discouraged from use in new source code. The abundance of legacy Fortran analysis codes that were written to language standards prior to Fortran 90, however, motivates the enumeration of these items.

The first item of note is the definition of “exact” when used to describe derivatives computed using AD. Most numerical algorithms use approximate methods – for example, interpolation methods, iterative root-finding methods, and finite volume and finite differencing approximations – to implement a mathematical model in code. Pakalapati et al. [33] noted that the derivatives computed using AD are derived directly from the numerical algorithm and have no knowledge of the underlying mathematical model from which the numerical algorithm was derived. As such, the derivatives are only exact in relation to the numerical model, and even then only to the limit of machine precision. The practice of referring to derivatives computed using AD as “exact” stems from the absence of truncation error in their calculations. However, it is important to keep in mind that derivative calculations computed using AD are still susceptible to mathematical modeling error, numerical modeling error, and round-off error.

The next item of concern for DNAD integration is the use of fixed-form source code. Prior to the Fortran 90 standard, all lines of Fortran code were required to conform to a set of fixed form rules. Fixed form source code is restricted to 72 characters per line of code, and the first six characters of each line are reserved. Continuation lines can be used to divide longer statements across multiple lines, but individual lines

exceeding 72 characters in length are automatically truncated by the compiler. When preprocessor directives are used to modify fixed form source code (such as when `real` variable declarations are replaced with `type(dual)` – an increase of six characters – using the preprocessor directives listed in Figure 2.3), the resulting lines of code must conform to this same limit or be truncated.

With the publication of the Fortran 90 language standard, free form source code formatting was introduced which allows for up to 132 characters per line of code and removes the special reservation of the first six characters on each line. This added flexibility reduces the likelihood that modifying the source code through the preprocessor directives given in Figure 2.3 will cause inadvertent truncation of the source code. However, the possibility still exists. For fixed form source code, the code must be checked for any lines containing floating-point variable declarations that exceed 65 characters in width. For free form source code, these declaration lines cannot exceed 125 characters in width. Any lines exceeding these limits must be shortened or divided into multiple lines.

Another hurdle to the implementation of DNAD in Fortran codes is the use of the `common` statement to share information between program units. When data types of variables in a `common` statement are consistent between program units, the conversion of floating-point variables from `real` to `type(dual)` should work seamlessly. However, it is possible for the memory space assigned to a `common` statement to be declared as one data type in one program unit and a different data type in another program unit. This can lead to data misalignment when the data types of variables in the common block are changed. The code given in Figure 2.6 illustrates this problem. The same common block is declared in two separate subroutines but with inconsistent data types. The common block `cb`, when the two subroutines are compiled using a double-precision compiler flag (e.g. `-fdefault-real-8` for the gfortran compiler or `-r8` for the Intel Fortran compiler), will have a size of 8 bytes. However, if the DNAD header from Figure 2.3 is included and the subroutines are recompiled, the size of the common block `cb` in subroutine `sub1` will be  $8(N + 1)$ , where  $N$  is the length of the derivative vector. This is incompatible with the size of the common block in subroutine `sub2` and will generate a compiler error. Even worse, if the name is omitted from the common block declarations so that the blank common block is used, the code will compile successfully but the character string `c` in subroutine `sub2` will only align with the first eight bytes of the dual number `x` in subroutine `sub1`. Any additional variables included in the common block will then be misaligned in the executable.

```

subroutine sub1
  implicit none
  real :: x
  common /cb/ x ...
end subroutine sub1

subroutine sub2
  implicit none
  character(len=8) :: c
  common /cb/ c ...
end subroutine sub2

```

**Figure 2.6** Example of inconsistent data types used in a common block in different program units.

A similar problem is encountered when codes use the equivalence statement to associate two variables within a program unit to the same memory location. Again, if a floating-point variable is associated with a non-floating-point variable in this manner, conversion to dual numbers will result in data misalignment and a potential bug in the resulting executable.

Both the common and equivalence statements have been deprecated in favor of modern replacements that, when used properly, ensure correct alignment of the underlying bit data and enforce consistency between program units automatically. New code development should use modules in place of common blocks and transfer statements in place of equivalence statements. When common and equivalence statements are encountered in legacy codes, the statements may need to be updated to their modern counterparts before successful differentiation of the codes can be achieved with the DNAD module.

Next we discuss concerns with using the Fortran data statement. The data statement is used to initialize variables to specific values at the beginning of a program unit. It is the recommended way for initializing large arrays of floating-point values prior to calculations and is therefore quite common in scientific and engineering applications. Unfortunately, custom constructors cannot be invoked implicitly within the Fortran programming language, so conversion of variables from real to type(dual) will also require a change to any data statements involving those variables. These changes can be wrapped inside preprocessor directives, but care must be taken to ensure consistency between initial values in both branches of the control.

The last concern to be discussed in this section is the multitude of ways in which floating-point variables can be declared in Fortran programs. Table 2.1 provides a summary of the different statements that can be used to declare floating-point variables. In this work the author has recommended using lowercase real for

variables, uppercase REAL for constant parameters, and controlling precision through compiler options. However, all the options listed in Table 2.1 are valid statements and may be encountered in codes developed without DNAD in mind. Some codes may include several of the forms listed in Table 2.1. In order to correctly differentiate an algorithm via DNAD, all forms used in the code need to be accounted for in the conversion. This can be done by adding additional `#define` directives to the header lines given in Figure 2.3 or by modifying all floating-point variable declarations in the source code to use a single, consistent format.

**Table 2.1 Methods for Declaring Floating-Point Variables in Fortran**

Declaration	Description
<code>real</code>	Single-precision
<code>double precision</code>	Double-precision
<code>real*N</code>	$N$ -byte floating-point value, where $N$ is an integer
<code>real(kind=p)</code>	Floating-point value of kind $p$ , where $p$ is a kind value returned from the <code>selected_real_kind</code> function

## 2.5 Automatic Differentiation of a 1D Scalar Transport Equation Solver

In this section DNAD is applied to a 1D scalar transport equation solver implemented in Fortran. We begin with a description of the mathematical model for 1D transport of a scalar quantity which includes advection, diffusion, and production terms. We then describe the method used to implement this model numerically. Next, we discuss changes needed to obtain partial derivatives via the DNAD module. Finally, we present results computed using this model and comparisons with alternative methods for derivative calculations.

### 2.5.1 Mathematical Model

The Fortran algorithm is based on the mathematical model presented by Pakalapati et al. [33] and was written specifically for the purpose of demonstrating differentiation of a fluid dynamics algorithm using DNAD. The governing equation,

$$u \frac{\partial \phi}{\partial x} = \Gamma \frac{\partial^2 \phi}{\partial x^2} + C \phi \quad (2.5.1)$$

describes the 1D transport of a scalar field quantity  $\phi$  due to advection, diffusion, and production, where  $x$  is the spatial coordinate,  $u$  is the velocity,  $\Gamma$  is the diffusivity, and  $C$  is a proportionality constant such that the source term is directly proportional to the local concentration  $\phi$ .

Two boundary conditions are required to close Eq. (2.5.1). For certain boundary conditions, a closed-form solution can be obtained which will aid in evaluating the accuracy of derivatives computed using DNAD. A closed-form solution to Eq. (2.5.1) with boundary conditions  $\phi(0) = 1$  and  $\phi(1) = 0$  is given by Pakalapati et al. [33] as

$$\phi(x) = \frac{e^{\lambda^-} e^{\lambda^+ x} - e^{\lambda^+} e^{\lambda^- x}}{e^{\lambda^-} - e^{\lambda^+}} \quad (2.5.2)$$

where

$$\lambda^\pm = \frac{u \pm \sqrt{u^2 - 4\Gamma C}}{2\Gamma} \quad (2.5.3)$$

when  $u^2 - 4\Gamma C > 0$ .

We desire the derivatives of the scalar field function  $\phi$  with respect to the  $x$  coordinates and the three proportionality constants  $u$ ,  $\Gamma$ , and  $C$ . Symbolic differentiation of Eq. (2.5.2) with respect to  $\lambda^\pm$  gives

$$\frac{\partial \phi}{\partial \lambda^\pm} = \pm \frac{e^{\lambda^+} e^{\lambda^-} (e^{\lambda^+ x} - e^{\lambda^- x}) + x e^{\lambda^\mp} e^{\lambda^\pm x} (e^{\lambda^-} - e^{\lambda^+})}{(e^{\lambda^-} - e^{\lambda^+})^2} \quad (2.5.4)$$

Differentiation of  $\lambda^\pm$  with respect to the three proportionality constants gives

$$\frac{\partial \lambda^\pm}{\partial u} = \pm \frac{\lambda^\pm}{\sqrt{u^2 - 4\Gamma C}} \quad (2.5.5)$$

$$\frac{\partial \lambda^\pm}{\partial \Gamma} = \pm \frac{C - u\lambda^\pm}{\Gamma \sqrt{u^2 - 4\Gamma C}} \quad (2.5.6)$$

$$\frac{\partial \lambda^\pm}{\partial C} = \mp \frac{1}{\sqrt{u^2 - 4\Gamma C}} \quad (2.5.7)$$

From the chain rule of differentiation, the partial derivatives of  $\phi$  with respect to the three proportionality constants are

$$\frac{\partial \phi}{\partial u} = \frac{\partial \phi}{\partial \lambda^+} \frac{\partial \lambda^+}{\partial u} + \frac{\partial \phi}{\partial \lambda^-} \frac{\partial \lambda^-}{\partial u} \quad (2.5.8)$$



$$\frac{\partial \phi}{\partial \Gamma} = \frac{\partial \phi}{\partial \lambda^+} \frac{\partial \lambda^+}{\partial \Gamma} + \frac{\partial \phi}{\partial \lambda^-} \frac{\partial \lambda^-}{\partial \Gamma} \quad (2.5.9)$$

$$\frac{\partial \phi}{\partial C} = \frac{\partial \phi}{\partial \lambda^+} \frac{\partial \lambda^+}{\partial C} + \frac{\partial \phi}{\partial \lambda^-} \frac{\partial \lambda^-}{\partial C} \quad (2.5.10)$$

### 2.5.2 Numerical Model

The 1D transport problem can be solved numerically by discretizing the domain and applying finite difference approximations such as those discussed in Sec. 2.2.2 to the derivative terms in Eq. (2.5.1). For example, we can use the first-order-accurate backward difference formula given by Eq. (2.2.12) to approximate  $\partial \phi / \partial x$  in the advection term and the second-order-accurate central difference formula given by Eq. (2.2.14) to approximate  $\partial^2 \phi / \partial x^2$  in the diffusion term. This gives

$$a_w \phi_{i-1} + a_p \phi_i + a_e \phi_{i+1} = 0 \quad (2.5.11)$$

where

$$a_w = \begin{cases} \frac{\Gamma}{\Delta x^2} - \frac{u}{2\Delta x} & u \geq 0 \\ \frac{\Gamma}{\Delta x^2} & u < 0 \end{cases} \quad (2.5.12)$$

$$a_e = \begin{cases} \frac{\Gamma}{\Delta x^2} & u \geq 0 \\ \frac{\Gamma}{\Delta x^2} + \frac{u}{2\Delta x} & u < 0 \end{cases} \quad (2.5.13)$$

$$a_p = -(a_w + a_e + C) \quad (2.5.14)$$

Equation (2.5.11) is a tridiagonal system of linear equations that can be solved implicitly using, for example, the Thomas Algorithm (see Thomas [48]).

A basic Fortran implementation of the solution procedure described above is given in Appendix B. This implementation uses a card-style input format for specifying the boundary conditions and proportionality constants, as well as the number of grid points to use in the domain discretization. An example input file is given in Figure 2.7. Upon completion, the program generates a comma-delimited ASCII text file containing the solution of  $\phi$  at each discretized  $x$ -coordinate. For comparison, the closed-form solution given by Eq. (2.5.2) has also been included in the Fortran code and can be solved by changing the solver method to

```

*job, name=adpsolver_example
*bc, phi0=1.0, phi1=0.0
*props, u=1.0, gamma=0.1, c=-1.0
*grid, npts=41
*solver, method=implicit

```

**Figure 2.7** Example input file for the Fortran program given in Appendix B.

analytical. Closed-form partial derivatives based on Eqs. (2.5.8)-(2.5.10) can then be calculated by adding a `derivatives` parameter to the solver card and setting its value to `yes`. Note that the closed-form solution is only valid when the boundary conditions are  $\phi(0) = 1$  and  $\phi(1) = 0$ , and the `derivatives` parameter is only used when the solver method is set to `analytical`.

### 2.5.3 Automatic Differentiation of the 1D Scalar Transport Problem using DNAD

The process outlined in Sec. 2.4.3 was used to differentiate the 1D scalar transport problem via the DNAD module. Code modifications are summarized in Appendix C. No modifications to the main program unit were required because no floating-point variables are declared in this unit. Conversion of floating-point variables from `real` to `type(dual)` in the `adpsolver` and `adpio` modules was facilitated using the preprocessor directives given in Figure 2.3. No other modifications to the `adpsolver` module were needed. Several additional modifications were needed in the `adpio` module, however, in order to properly handle options for requesting derivatives in the input file and to include the derivative calculations in the output file.

First, three new static variables were declared in the `adpio` module to store information relative to the partial derivatives requested by the user. This is necessary in order to ensure that the derivative vectors are not overrun by too many partial derivative requests and to ensure that the derivative information is properly written to the output file.

Next, an additional case was added to the `parseCard` function so that a `*dnad` card can be processed, and an additional function (`setDNADField`) was added to process this card. The `*dnad` card is used to enumerate specific inputs with respect to which partial derivatives are to be computed. Available options supported by the `setDNADField` function include derivatives with respect to  $u$ ,  $\Gamma$ , and  $C$ . An example card requesting derivatives with respect to all three of these variables is

```
*dnad, dv=u, dv=gamma, dv=c
```

The boundary conditions  $\phi(0)$  and  $\phi(1)$  are the only other floating-point inputs to this code. Support for derivatives with respect to these variables could easily be added with just a few more lines of code to the `setDNADField` function.

A minor change was made to the type declaration of the `stringToReal` function (line 342 in the original code). The `real` keyword was changed to all-caps (`REAL`) so that the return type of this function would not be converted to `type(dual)` by the preprocessor. This ensures that only a single floating-point value is parsed when processing the text for a parameter value, and only the primary variable value (not the partial derivative values) is modified by the function assignment.

The last set of changes made to the `adpio` module was to add an alternative version of the `writeData` function that includes statements for writing out the results with automatic derivatives. The `writeData` function that is included when the code is compiled is controlled by placing the two functions inside an `#ifndef dnad` preprocessor directive. This complete separation of code for the undifferentiated and differentiated versions of the algorithm allows for flexibility in how the derivative information is output to the results file without affecting the original format.

Preprocessor directives were used around each of the modifications described above, so that inclusion of the DNAD module in the compiled executable can be controlled entirely through preprocessor options specified at compile-time. Adding the `-Ddnad` and `-Dndv=<#>` options to the compiler command will activate the DNAD module and enable automatic differentiation within the resulting executable, while omitting these options from the compiler command will produce the same executable as would be generated by the original code contained in Appendix B.

#### 2.5.4 Results and Discussion

Figure 2.8 compares numerical results of the 1D scalar transport problem described above using three different grid resolutions to the closed-form solution given by Eq. (2.5.2). For  $x < 0.5$  the closed-form curve is relatively linear and the numerical results are in good agreement. For larger  $x$  values, the curve becomes more nonlinear and the accuracy of the numerical results is reduced. However, refinement of the grid demonstrates convergence of the numerical results toward the closed-form solution. Figure 2.9 shows the

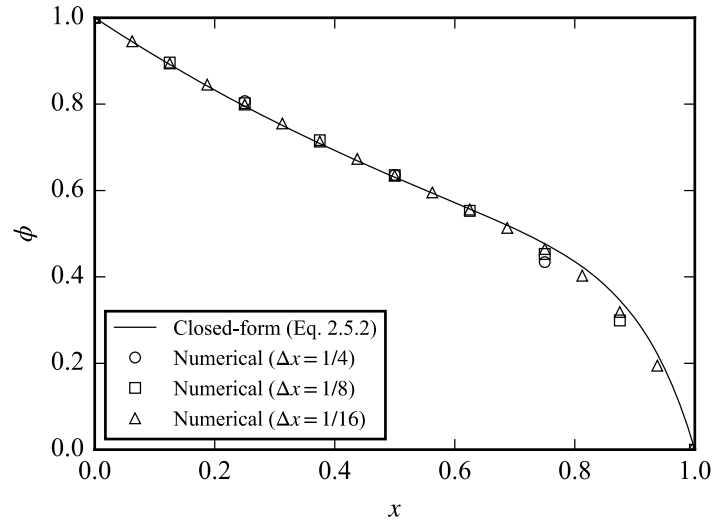


**Figure 2.8 Closed-form and numerical solutions to the 1D transport equation.**

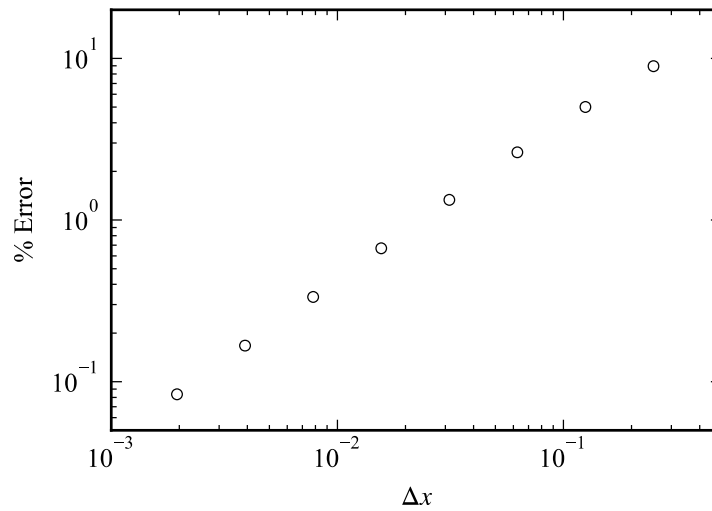


**Figure 2.9 Percent error in numerical solution at  $x = 0.75$  for various grid resolutions.**

percent error of the solution at  $x = 0.75$  for several grid sizes on a log-log plot. The slope of the data indicates the algorithm has a first-order convergence rate. This convergence rate corresponds with the order of the backward difference formula – see Eq. (2.2.12) – that was used in developing the numerical model.

Figures 2.10-2.12 provide a comparison of partial derivative results computed using both the DNAD module and the closed-form solutions given by Eqs. (2.5.8)-(2.5.10). Also included are DNAD-computed

derivatives of Eq. (2.5.2). The DNAD-computed derivatives of Eq. (2.5.2) match Eqs. (2.5.8)-(2.5.10) to machine precision, confirming that these results are the numerical equivalent of symbolic differentiation of the governing equation. The DNAD-computed derivatives of the numerical model are not as accurate, and the error is shown to be inversely proportional to the step size  $\Delta x$  used in the analysis.

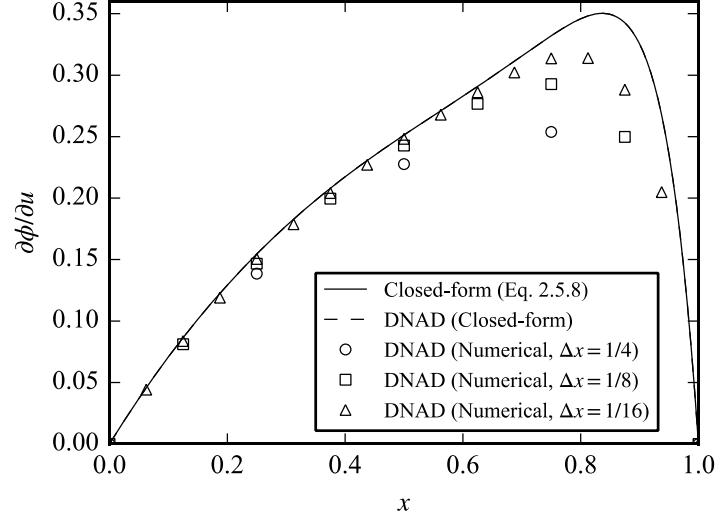


**Figure 2.10** Comparison of  $\partial\phi/\partial u$  computed using DNAD and Eq. (2.5.8).

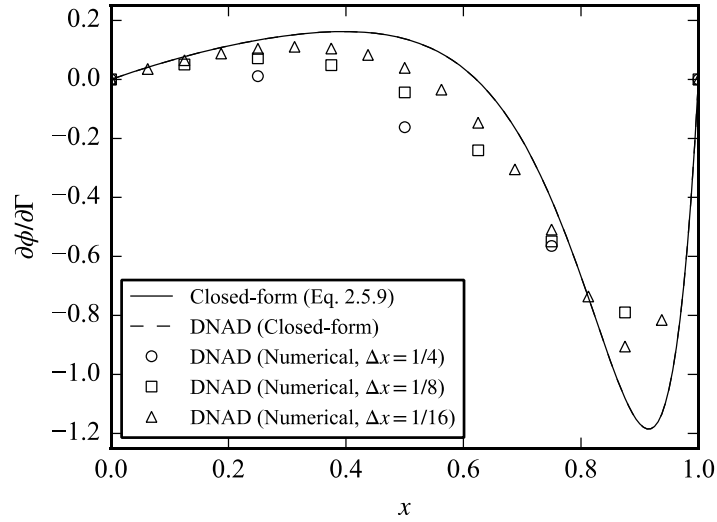


**Figure 2.11** Comparison of  $\partial\phi/\partial\Gamma$  computed using DNAD and Eq. (2.5.9).

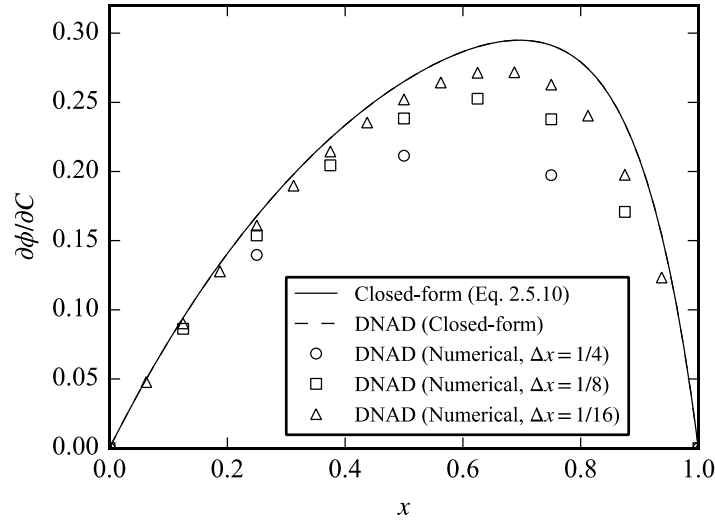


**Figure 2.12 Comparison of  $\partial\phi/\partial C$  computed using DNAD and Eq. (2.5.10).**

Figures 2.13-2.15 compare the root-mean-square (RMS) errors of the DNAD calculations with RMS errors in corresponding solutions computed using finite difference methods. In general, all of the methods exhibit a first-order convergence rate, and for coarse grids ( $\Delta x > 10^{-2}$ ) there is little difference in the RMS error values between the different methods. There are lower limits in  $\Delta x \Delta x$ , however, below which the finite difference methods no longer converge or even begin to diverge. These limits depend on the finite differencing method used and the finite differencing step size (e.g.  $\Delta u$ ,  $\Delta \Gamma$ , or  $\Delta C$ ) used. DNAD derivatives do not have this limit and will continue toward the exact solution with decreasing  $\Delta x$  at the same approximate convergence rate as  $\phi$  until reaching the accuracy of machine precision.

Some of the finite difference solutions shown in Figures 2.14 and 2.15 have smaller RMS errors than the corresponding DNAD solutions for a given  $\Delta x$ . In each of these cases, the truncation error due to discretization of the governing equation is in the opposite direction as the truncation error due to discretization of the partial derivative, so that the two error sources partially cancel, lowering the overall RMS error. The reductions in error are small and only occur at particular combinations of  $\Delta x$  and the finite differencing step size ( $\Delta \Gamma$  or  $\Delta C$ ), so that taking advantage of this situation during a typical analysis would be impractical.

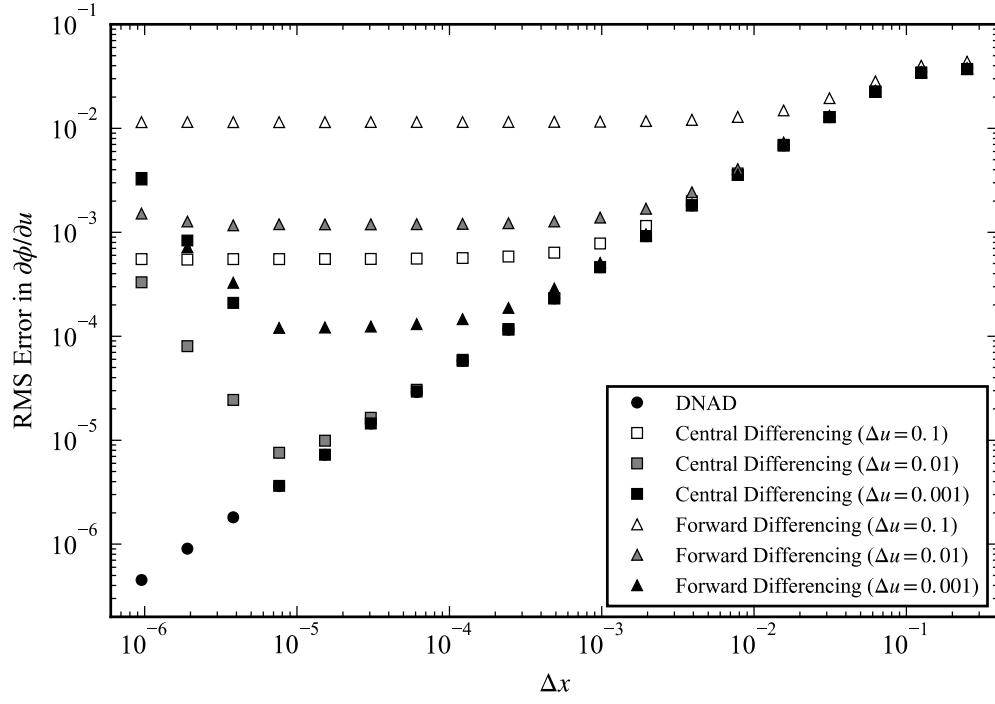


Figure 2.13 Comparison of errors in  $\partial\phi/\partial u$  computed using DNAD and finite differencing.

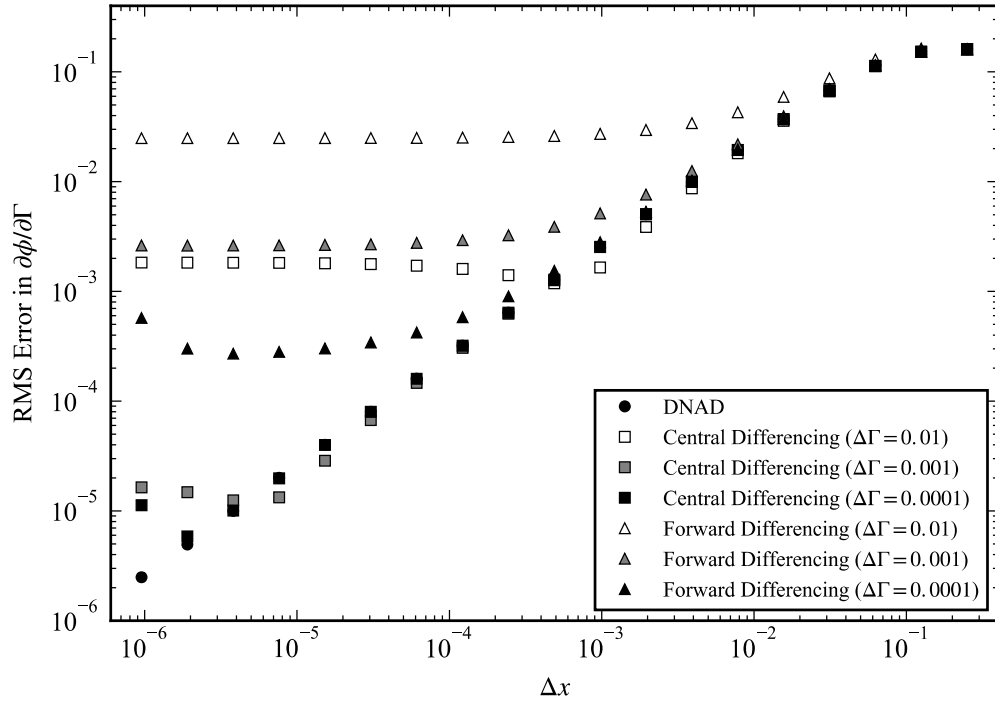
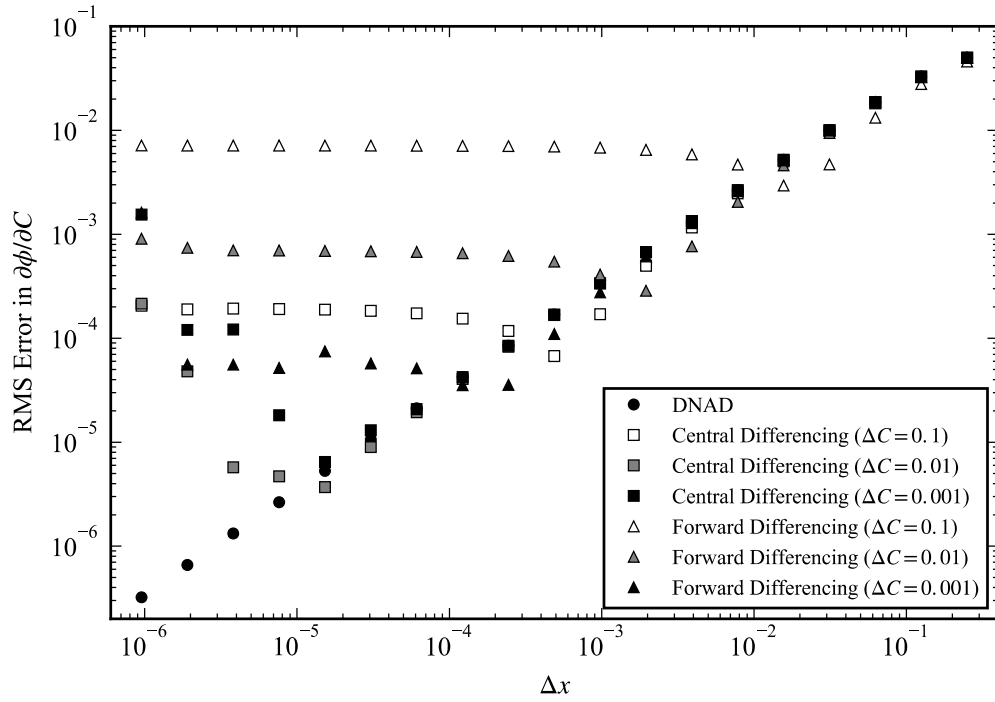


Figure 2.14 Comparison of errors in  $\partial\phi/\partial\Gamma$  computed using DNAD and finite differencing.



**Figure 2.15 Comparison of errors in  $\partial\phi/\partial C$  computed using DNAD and finite differencing.**

Time benchmarks for the adpsolver code were collected using a standard desktop computer running Windows 10 Enterprise 64-bit with a third-generation Intel Core i7-3770 3.4 GHz processor, 16 GB of 1600 MHz DDR3 RAM, and a 1 TB 7200 RPM Serial ATA internal hard drive. The adpsolver code was compiled using version 6.3.0 of the GNU Fortran compiler.

The example input file given in Figure 2.7 was used as a baseline input file for all of the timed analyses, except that the number of grid points was changed and a `*dnad` card was added for the benchmarking analyses of the differentiated code. Figure 2.16 shows timing results for the differentiated code normalized by the time required to execute the undifferentiated code. Also included for comparison are the normalized times that would be required to compute the same derivatives using first-order forward differencing (Eq. (2.2.11)) and second-order central differencing (Eq. (2.2.13)).

The results presented here demonstrate that using DNAD can improve the accuracy and run-time efficiency of derivative calculations over finite differencing methods. The run-time cost using the DNAD



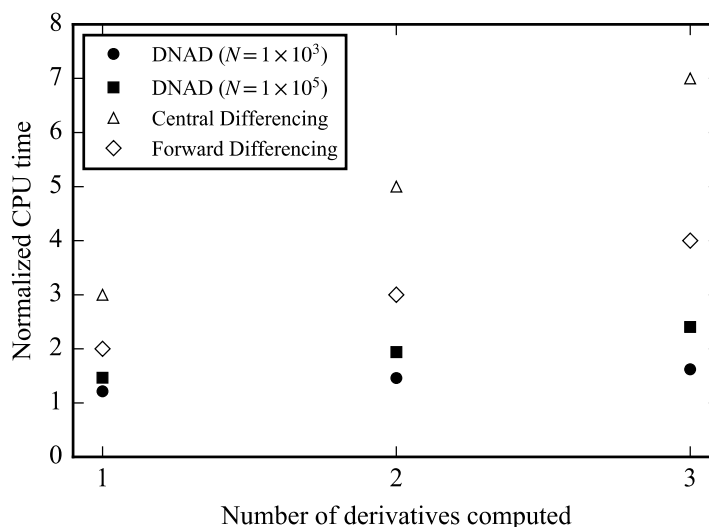


**Figure 2.16 Run-time benchmarks for the adpsolver code using DNAD and finite differencing.**

module is dependent on mesh size, though this dependency is small. For each of the data sets shown in Figure 2.16, the run-time cost increases almost linearly with the number of derivatives computed. The additional cost of each derivative computed using DNAD is less than half the cost of the primary function if a mesh size of  $N = 10^5$  is used and less than one-fourth the cost of the primary function if a mesh size of  $N = 10^3$  is used. Source code changes required to differentiate the adpsolver code using DNAD were minimal and mostly confined to I/O operations. The effort required to implement these changes was comparable to the effort required to find the appropriate perturbation step sizes for computing the derivatives using finite differencing. This is a relatively simple code with fewer than one thousand lines of code, however, so these same conclusions may not apply to more complicated software with larger code bases.

## 2.6 Automatic Differentiation of MachUp

In this section we discuss automatic differentiation of the numerical lifting line code MachUp using DNAD. This code was written without DNAD in mind, but it presents an ideal application for DNAD since relatively few inputs are required for an analysis and the results generated by MachUp are of value to wing design problems. The MachUp source code is developed and maintained by the USU Aero Lab\* and is

---

\* <http://aero.go.usu.edu>

available for download from github\*. The entire source code is not included in this work, but Appendix D contains the modifications that were made for this effort. We begin this section with a discussion of the MachUp software. Next we discuss in detail the modifications that were made to the MachUp source code in order to enable automatic differentiation via DNAD. Finally, we demonstrate the accuracy and efficiency of the resulting derivative calculations through a limited set of results and performance measurements.

### 2.6.1 *The MachUp Numerical Lifting Line Solver*

MachUp is an open-source aerodynamics analysis tool for evaluating the performance characteristics of systems of finite wings. It is written in modern, object-oriented Fortran and interfaces with web applications and other software packages through human-readable input and output files. The core algorithm in MachUp is based on the numerical lifting line method of Phillips and Snyder [16]. Although rooted in potential flow theory, this method has the ability to include viscous effects in the analysis. It can be used to model multi-wing systems and wings with sweep and dihedral. The algorithm equates the 3D vortex theory of lift to the 2D section lift at discrete control points located along the quarter-chord of a wing to solve for the bound vorticity strength at these locations. This development produces a nonlinear system of equations that must be solved iteratively. A linear approximation is used as an initial guess, and Newton's method is applied to update the solution until changes in the calculated vortex strengths between iterations fall below a user-specified threshold. The algorithm has been used for a number of wing design studies, including studies of propeller-wing interactions [49] and ground effect [50].

The MachUp source code is organized into several modules which contain the data structures for different components of the analysis. For example, a `plane_t` object stores all of the data and methods needed to define and solve the system of horseshoe vortices for the complete model, including an array of `wing_t` objects that define the geometry for each individual lifting surface. Further, each `wing_t` object contains an array of `section_t` objects that each define the 2D airfoil section properties at one control point on the wing.

Input to MachUp is handled through ASCII text files that use the JavaScript Object Notation (JSON) format for data structures. This data-interchange format is often used in web applications and can easily

---

\* <https://github.com/usuaero/machup>

interface with other common engineering tools such as Matlab and Python. In addition, these input files are human-readable and can be created and edited in any standard text editor. The JSON data structures are handled within MachUp through an open-source JSON parsing tool available on Github\* and also included within the MachUp source code. A sample MachUp input file is shown in Appendix E. The input file defines a single wing with an aspect ratio of 8; an elliptic chord distribution; no sweep, dihedral, or geometric twist; and a uniform cross-section with properties corresponding approximately to those of a NACA 2412 airfoil in inviscid, incompressible flow. The airfoil properties and profile are defined in separate files that reside within the specified airfoil database folder. An example of these property and profile files for the NACA 2412 airfoil is given in Appendix E.

Commands to be executed are specified under the “run” record in the JSON input file. The example file in Appendix E lists multiple commands, all of which can be performed with a single execution of the software. The first command, “targetc1”, solves the complete lifting line algorithm multiple times using Newton’s method to adjust the angle of attack until the specified lift coefficient is achieved. The “forces” command generates a JSON output file that contains the aerodynamic performance coefficients calculated by the lifting line algorithm. The “distributions” command generates a comma-separated values (CSV) file that contains aerodynamic results for each wing section in the model. Finally, the “stl” command generates a stereolithography (STL) file that contains a geometric representation of the model for visualization. Note that any of the “run” commands listed can be temporarily disabled by setting the “run” parameter for that command to 0.

Viscous effects can be included in a MachUp analysis by specifying viscous properties for the 2D airfoils used in the analysis. For example, a 2D potential flow solution for flow around a NACA 2412 airfoil gives a zero-lift angle of attack of approximately  $\alpha_{L0} = -0.0380$  rad and a section lift slope of approximately  $a_0 = 6.86/\text{rad}$ , but 2D viscous flow solutions give somewhat different values. XFOIL (see Refs. [51,52]) predicts a zero-lift angle of attack of approximately  $\alpha_{L0} = -0.0372$  rad and a section lift slope of approximately  $a_0 = 6.26/\text{rad}$  for a NACA 2412 airfoil in viscous flow at a Reynolds number of  $\text{Re} = 1\text{E}6$ .

---

\* <https://github.com/jacobwilliams/json-fortran>

Similarly, the zero-lift moment coefficient and moment slope of an airfoil will also be different between inviscid and viscous flows and, for viscous flows, will depend on Reynolds number. Section parasitic drag is estimated in MachUp using the relation

$$c_{d_p} = c_{d_0} + c_{d_1} c_l + c_{d_2} c_l^2 \quad (2.6.1)$$

where the coefficients  $c_{d_0}$ ,  $c_{d_1}$ , and  $c_{d_2}$  must be determined using a viscous analysis tool such as XFOIL or from experimental data. These coefficients are identically zero by definition for inviscid flows. MachUp sums the individual section parasitic drag components computed from Eq. (2.6.1) about the aircraft center of gravity to evaluate global viscous forces and moments as described by Phillips [53].

The example input file in Appendix E contains other parameters not discussed here, and still other parameters are supported by MachUp that have not been included in the example. A comprehensive description of each available parameter is beyond the scope of this work. The reader is instead referred to the MachUp documentation and source code available on Github.

### 2.6.2 Modifications to the MachUp Source Code

The original and modified lines of code required for DNAD integration in MachUp have been listed in Appendix D. Two of the MachUp source files – `main.f90` and `json.f90` – were left unmodified. A few other files – `airfoil.f90`, `dataset.f90`, and `section.f90` – required only the addition of the preprocessor directives from Figure 2.3.

After adding the preprocessor directives from Figure 2.3, several compiler errors were encountered due to improper handling of data type conversions between `real` and `type(dual)`. These compiler errors were resolved by manually inspecting the source code and ensuring that floating point variables were properly declared as either `real` or `REAL` as discussed in Sec. 2.4.3.

All of the remaining code changes dealt directly with I/O functions of the program. An intermediate layer between the third-party JSON interface and the computational portion of the MachUp source code already existed prior to DNAD integration (see `myjson.f90`), but was not fully implemented. Several lines of code still called directly into the `json_m` module, so that variables declared as `type(dual)` were not properly processed. These errors were resolved by completing the implementation of the `myjson_m` module and adding some additional functions specifically for handling variables of `type(dual)`. The preprocessor directive for

converting all real variable declarations to `type(dual)` was not added to the `myjson_m` module (as was done with the other modules) so that functions for handling input and output of both data types are included in the compiled executable. Fortran interfaces were defined at the beginning of the `myjson_m` module so that the appropriate I/O function is called based on the type declarations of the arguments passed to the function. As with other DNAD-specific changes, the functions and interfaces for handling variables of `type(dual)` were enclosed in preprocessor directives so that they are only included in the compiled executable when the DNAD module is activated.

DNAD implementation in the manner described here affords some very significant advantages over other automatic differentiation methods. Because all JSON-specific I/O operations are processed through the `myjson_m` module, no variable-specific code is needed to make a floating-point variable available for derivative calculations. Instead, derivatives with respect to any floating-point variable contained in the JSON input file can be computed simply by converting the single value in the JSON input file to a two-value array. For example, consider again the example JSON input file given in Appendix E. The angle of attack and sideslip angle are specified under the “condition” keyword:

```
"condition": { "alpha": 0, "beta": 0 }
```

Derivatives with respect to angle of attack can be computed simply by replacing the above line with the following:

```
"condition": { "alpha": [0, 1], "beta": 0 }
```

Note, however, that angle of attack is specified in the input file in units of degrees, so that partial derivatives of output quantities will have units of  $\text{deg}^{-1}$ . Partial derivatives of lift coefficient, pitching moment coefficient, and other aerodynamic performance coefficients with respect to angle of attack are typically reported in units of  $\text{rad}^{-1}$ . This conversion can be performed after the analysis, but it can be handled more conveniently by specifying the operating conditions as:

```
"condition": { "alpha": [0, 57.2957795131], "beta": 0 }
```

so that, by nature of the chain rule of differentiation, all partial derivatives output by the code will have units of  $\text{rad}^{-1}$ .

The JSON output file, written upon successful execution of the MachUp “forces” command, also takes advantage of the `myjson_m` module so that partial derivative information is automatically written for all

variables of type(dual). As with the input file, no variable-specific code modifications were needed to enable output of partial derivative information, so that the partial derivative information is available for all variables written to a JSON output file automatically.

### 2.6.3 Results and Discussion

The order of convergence of MachUp can be estimated by considering how the solution changes as the number of nodes is increased. For this analysis, we use an elliptic wing with a straight quarter-chord, an average chord of 1, an aspect ratio of 8, a uniform cross-section with a section lift slope of  $2\pi$ , and no geometric or aerodynamic twist. The wing is operating at an angle of attack of  $\alpha = 1^\circ$ . Figure 2.17 shows the magnitude of the percent difference between the lift and drag computed for several grid densities relative to that computed using  $n = 1280$ , where  $n$  is the mesh size (i.e. number of nodes per semispan). The plot reveals an approximately second-order convergence rate for both lift and induced drag.

An elliptic wing with the same parameters described above was also used to evaluate the accuracy of derivative calculations. Derivatives of lift and drag with respect to angle of attack were evaluated using the DNAD module, forward differencing (Eq. (2.2.11)), and central differencing (Eq. (2.2.13)). Percent errors were computed relative to the DNAD solution using a grid size of 1280 nodes per semispan. Results are plotted in Figures 2.18 and 2.19.

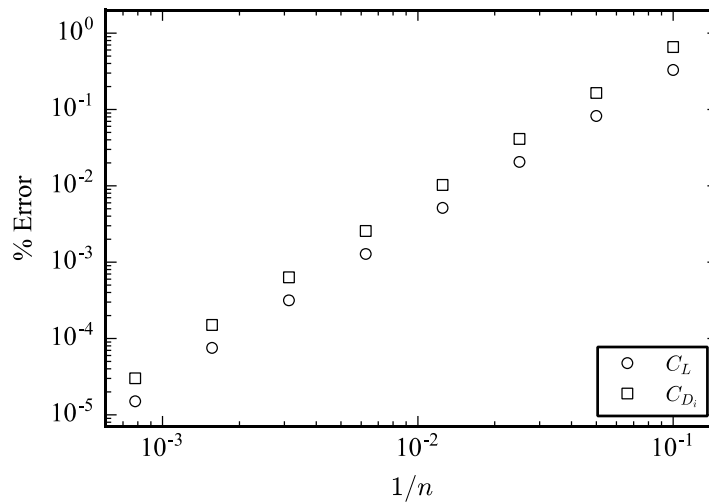


**Figure 2.17** Percent error in lift and drag coefficients for various grid densities relative to the solution computed using  $n = 1280$  nodes per semispan.

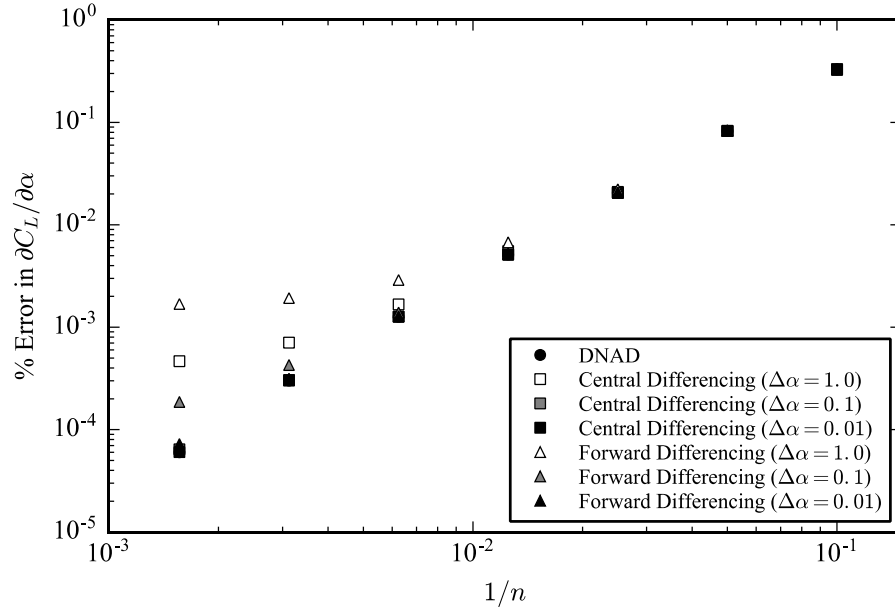


Figure 2.18 Comparison of errors in  $\partial C_L / \partial \alpha$  using DNAD and finite differencing relative to the DNAD solution computed using 1280 nodes per semispan.

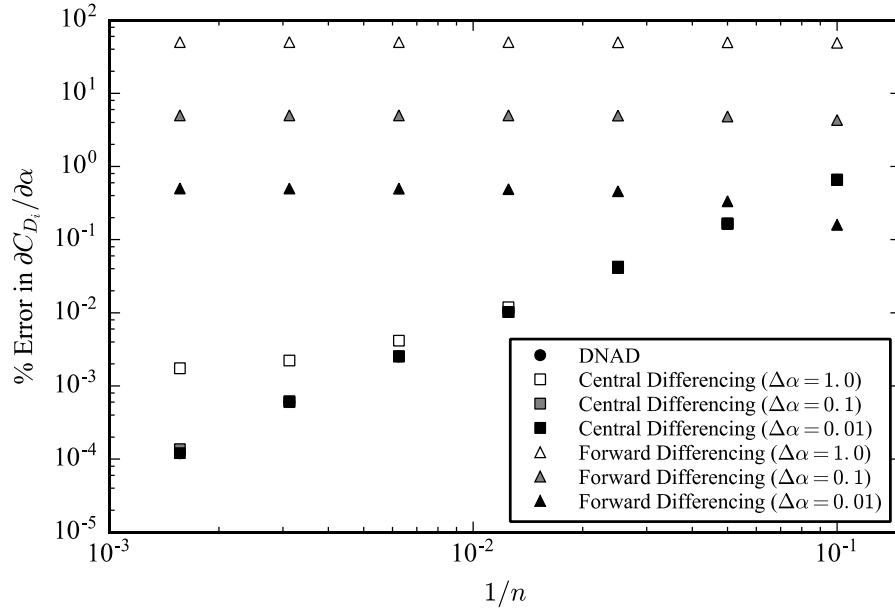


Figure 2.19 Comparison of errors in  $\partial C_{D_t} / \partial \alpha$  using DNAD and finite differencing relative to the DNAD solution computed using 1280 nodes per semispan.

Derivatives of lift with respect to angle of attack computed using DNAD and the two finite difference formulas are nearly indistinguishable for grid sizes below 100 nodes per semispan or when a perturbation step size of  $\Delta\alpha = 0.01$  is used. This is because the lift is nearly linear in angle of attack so that the finite difference approximations are able to closely represent the function. On the other hand, the behavior of induced drag is approximately quadratic in angle of attack. The forward difference method (Eq. (2.2.11)) does a relatively poor job of predicting  $\partial C_{D_i} / \partial\alpha$ , while the central difference method (Eq. (2.2.13)) is still nearly as accurate as the DNAD calculations, especially for small  $\Delta\alpha$ . There seems to be little advantage in terms of accuracy to using DNAD over the second-order central difference method in these calculations when an appropriate step size is used. However, determination of an appropriate step size is still an added requirement to the finite difference method, and other derivative calculations whose primary functions are neither linear nor quadratic may not be satisfactorily represented by either finite difference method. DNAD calculations are not limited by either of these issues.

Classical lifting line theory [10,11] provides closed-form solutions to the partial derivatives of lift and induced drag with respect to angle of attack, namely

$$\frac{\partial C_L}{\partial\alpha} = a = \frac{a_0}{1 + a_0 / \pi A} \quad (2.6.2)$$

$$\frac{\partial C_{D_i}}{\partial\alpha} = \frac{2C_L}{\pi A} \frac{\partial C_L}{\partial\alpha} \quad (2.6.3)$$

While the numerical lifting line algorithm implemented in MachUp is closely related to this theory, results for  $\partial C_L / \partial\alpha$  and  $\partial C_{D_i} / \partial\alpha$  computed with MachUp do not converge exactly to the solutions given by Eqs. (2.6.2) and (2.6.3). This is because Prandtl [10,11] aligned the trailing wake with the chord line of the wing in his derivation, while Phillips and Snyder [16] aligned the trailing wake with the freestream. This change in formulation results in a difference of less than 0.002% in both  $\partial C_L / \partial\alpha$  and  $\partial C_{D_i} / \partial\alpha$  between the results of Eqs. (2.6.2) and (2.6.3) and those of MachUp with a grid size of 1280 nodes per semispan. This difference is why the percent errors plotted in Figures 2.18 and 2.19 must be computed relative to the fine-grid MachUp results and not the closed-form solutions.

As with the adpsolver code, time benchmarks for MachUp were collected using a standard desktop computer running Windows 10 Enterprise 64-bit with a third-generation Intel Core i7-3770 3.4 GHz



processor, 16 GB of 1600 MHz DDR3 RAM, and a 1 TB 7200 RPM Serial ATA internal hard drive. The MachUp code was compiled using version 6.3.0 of the GNU Fortran compiler.

The example input file given in Appendix E was used as a baseline input file for all of the benchmarking analyses, except that the “targetc1” and “st1” commands were disabled and DNAD calculations were requested by changing selected floating point inputs to 2-value lists and compiling the code using the appropriate DNAD preprocessor commands. Also, two different grid sizes were used: 40 and 80 nodes per semispan. Figure 2.20 shows timing results for the differentiated code normalized by the time required to execute the undifferentiated code. Also included for comparison are the normalized times that would be required to compute the same derivatives using first-order forward differencing (Eq. (2.2.11)) and second-order central differencing (Eq. (2.2.13)).

The performance of MachUp with DNAD integration is shown to be highly dependent on the number of nodes per semispan ( $n$ ) used in the simulation. This is because, for small  $n$ , the majority of execution time is spent on problem setup and I/O operations which are not heavily influenced by the DNAD module. As grid size increases, the percentage of execution time spent on computations such as  $LU$  decomposition and forward and backward substitution also increases, so that the performance impact of the DNAD module is more heavily felt.

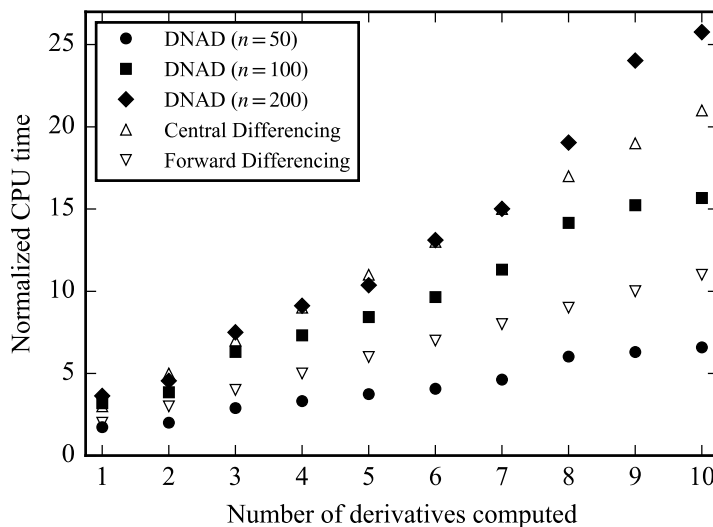


**Figure 2.20** Run-time benchmarks for MachUp using DNAD and finite differencing.

We note disproportionately large increases in the DNAD execution times shown in Figure 2.20 when going from 2 derivatives to 3 and from 7 to 8. This has been attributed to single instruction, multiple data (SIMD) vectorization capabilities of the hardware. Vectorization extensions such as Streaming SIMD Extensions (SSE) and Advanced Vector Extensions (AVX) use SIMD registers to process a single instruction on multiple data more efficiently than if the instruction was processed on each piece of data individually. The size of the SIMD registers sets limitations on how many pieces of data can be processed with a single vectorized instruction, so that behavior such as that seen in Figure 2.20 when going from 2 derivatives to 3 and from 7 to 8 is expected.

As a result of the above observations, the answer to whether DNAD calculations are more advantageous than finite difference methods depends on the size of the model and the purpose of the analysis. If the entire model has fewer than 400 nodes and fewer than 8 design variables for which derivatives are required, DNAD presents an appealing solution in terms of both runtime efficiency and accuracy. For larger models and problem setups with 8 or more design variables, the finite differencing approach may be satisfactory. For problems with less than 400 nodes and 8 or more design variables, a reverse-mode AD method may be the most efficient option, but integration of a reverse-mode AD tool and verification of this is beyond the scope of the current work.

### 3 WING SHAPE OPTIMIZATION USING A NUMERICAL LIFTING LINE ALGORITHM AND DUAL NUMBER AUTOMATIC DIFFERENTIATION

#### 3.1 Introduction

Aerodynamic shape optimization is the process of designing the outer mold line (OML) of an aerodynamic structure such that specific aerodynamic performance requirements are met in the most efficient manner possible. As mentioned in Chapter 1, CFD analyses can be used to generate high-fidelity aerodynamic performance predictions, but the computational cost of CFD makes it ill-suited for use as the objective function in aerodynamic shape optimization problems. Lyu et al. [4] states that visualization of design spaces for these types of problems is not possible with current CFD capabilities and hardware limitations. This leads aerodynamicists to consider lower-fidelity aerodynamic tools that trade accuracy for runtime efficiency. This approach can be especially useful early in the design process when insights into trends and interactions between design parameters are more important than highly-accurate performance characteristics.

One such tool is MachUp, an implementation of the numerical lifting line method of Phillips and Snyder [16]. This tool was discussed in Sec. 2.6, where a method for automatic differentiation of the software was presented. In this chapter, we discuss the use of MachUp as the objective function in an aerodynamic shape optimization problem. Note that the modified version of MachUp discussed in Sec. 2.6, which uses DNAD for derivative calculations, is used here. We first present Optix, an open-source optimization framework being developed in the Utah State University AeroLab and available through the groups Github page\*. The version of the code considered in this work is included in Appendix F. We then present solutions to several inviscid wing shape optimization problems that were computed using MachUp and Optix, and compare the results to known analytical solutions developed using classical lifting line theory [10,11]. Similar wing shape optimization problems using viscous airfoil properties are then presented. Finally, we present and discuss a wing design contour plot that was generated using MachUp and serves to visualize the complete design space for the viscous wing shape optimization problems discussed previously.

---

\* <https://github.com/usuaero/optix>

### 3.2 Optix

Optix is an open-source, gradient-based optimization framework written in Python. It has the capability of solving a wide range of nonlinear optimization problems and offers some unique features that set it apart from similar optimization frameworks. Because Optix is written entirely in Python, it is easy to interface with and can readily be extended and customized to fit a particular problem. Optix is also cross-platform and highly portable. It can be run on any machine where Python is available, and NumPy (see Oliphant [54]) is the only package dependency outside of the Python Standard Library. Any combination of software available on the host machine can be executed within the objective function, so that the objective function – typically the most computationally expensive part of an optimization analysis – can be written in a high-performance computing language such as Fortran or C++. The following subsections highlight the key features of Optix.

#### 3.2.1 Optimization Method

Optix implements the BFGS method of Broyden [55], Fletcher [56], Goldfarb [57], and Shanno [58]. This is a quasi-Newton method that uses historical calculations of the objective function and its gradient to approximate a Hessian matrix, which in turn is used to estimate a search direction. According to Nocedal and Wright [59] the BFGS method is among the most popular quasi-Newton methods. It has been implemented in several scientific computing packages that offer gradient-based optimization utilities, including the GNU Scientific Library, MATLAB, R, and SciPy.

At the beginning of the BFGS algorithm, the objective function and its gradient at the initial design point are calculated and the Hessian matrix is initialized to the identity matrix (i.e.  $[\mathbf{H}]_0 = [\mathbf{I}]$ ) so that the first search direction corresponds to the direction of steepest descent. A line search is then performed to find the local minimum in the search direction. The design point is then updated to this location, and a new gradient vector is calculated. The BFGS algorithm then determines an updated Hessian matrix  $[\mathbf{H}]_{k+1}$  from the previous Hessian matrix  $[\mathbf{H}]_k$  according to

$$[\mathbf{H}]_{k+1} = [\mathbf{H}]_k + \frac{\left[1 + \left(\{\gamma\}[\mathbf{H}]_k\{\gamma\}^T\right)\right] \{\delta\mathbf{x}\}^T \{\delta\mathbf{x}\}}{\{\delta\mathbf{x}\}\{\gamma\}^T} - \frac{\{\delta\mathbf{x}\}^T \{\gamma\}[\mathbf{H}]_k + [\mathbf{H}]_k\{\gamma\}^T \{\delta\mathbf{x}\}}{\{\delta\mathbf{x}\}\{\gamma\}^T} \quad (3.2.1)$$

where

$$\{\delta\mathbf{x}\} = \{\mathbf{x}\}_{k+1} - \{\mathbf{x}\}_k \quad (3.2.2)$$

$$\{\gamma\} = \{\nabla \mathbf{f}\}_{k+1} - \{\nabla \mathbf{f}\}_k \quad (3.2.3)$$

are the changes in the design point and gradient vector, respectively, between the current and previous iterations. The direction of the next line search is then given by

$$\{\mathbf{s}\}_{k+1} = -[\mathbf{H}]_{k+1} \{\nabla \mathbf{f}\} \quad (3.2.4)$$

This algorithm is repeated until either of two exit criteria are met: 1) the curvature condition proposed by Wolfe [60,61] is no longer satisfied, or 2) the change in the objective function between iterations falls below a user-specified threshold. Once one of these conditions is satisfied, the Hessian matrix is reset to the identity matrix, and the entire process begins again using the last minimum as the initial design point. The optimization process is complete when one of the two exit criteria are met on an iteration where the Hessian matrix is equal to the identity matrix. The current value of the objective function and the corresponding design point are then returned to the calling function as the final results of the optimization process.

### 3.2.2 Code Structure

Optix is composed of two object classes and several utility functions. The source code for these classes and functions are listed in Appendix F. The first object class handles execution of the user-specified objective function. The objective function is a Python function provided by the user that must accept as arguments the current design point and a case identifier, and it must return the value of the objective function evaluated at the current design point. A second function can be provided to evaluate gradients of the objective function, but this is not required. If specified, the gradient function must accept the same arguments as the objective function. It must return both the value of the objective function and the gradient vector at the specified design point. If this function is not specified, Optix evaluates the primary objective function multiple times with perturbed design points and uses a second-order central differencing algorithm – see Eq. (2.2.13) – to approximate the gradient of the objective function.

The second object class contained in the Optix source code is used for controlling the optimization algorithm. The number of design variables, their names, and their initial values are specified through an instance of this class. In addition, line search settings, parameters for the exit criteria, and whether to use the linear or quadratic line search algorithms (explained later in Sec. 3.2.4) are set here. A helper function is also provided through which the user can specify a JSON file from which to load these optimizer settings.

The `optimize` function orchestrates the entire optimization process. It accepts one instance each of the two object classes described above and returns the optimized objective function value and corresponding design point upon completion. The `optimize` function relies on the Python NumPy package for efficient matrix computations.

### 3.2.3 *Parallel Execution of Independent Function Evaluations*

Optix uses the `multiprocessing` module (part of the Standard Python Library) to execute independent evaluations of the objective function simultaneously. For example, each function evaluation within the line search is independent of all other line search evaluations, so the separate function evaluations can be divided among available processors and run simultaneously. In addition, if finite differencing is used to approximate the gradient vector, these function evaluations can also be executed in parallel. One gradient evaluation using the second-order central differencing formula given in Eq. (2.2.13) requires  $2N+1$  function evaluations, where  $N$  is the number of active design variables in the optimization analysis. Running these evaluations in parallel can significantly reduce the total optimization time when even just a few design variables are active.

### 3.2.4 *Linear and Quadratic Line Searching*

As mentioned previously, Optix relies on line searching methods to locate the local minimum in a given search direction. Two types of line searching algorithms exist in the literature, namely exact and inexact methods. Exact methods typically require some *a priori* knowledge of the design space to be searched and are restricted in application to only specific problem types. For example, the conjugate gradient method of Hestenes and Stiefel [62] requires the design space to be composed of a system of linear equations whose matrix is symmetric and positive-definite. While exact line searching algorithms are typically quite efficient when applied to the correct types of problems, restrictions to specific problem types make them ill-suited for a general optimization framework such as Optix.

Inexact line searching algorithms use approximation methods to estimate the minimum in a given search direction, and then rely on the optimization algorithm to narrow in on the design space minimum through successive updates to the gradient vector and Hessian matrix. Two popular inexact algorithms are the backtracking algorithms of Goldstein [63] and Armijo [64], which attempt to overshoot the minimum of the objective function and then successively reduce the step size until the minimum is sufficiently bounded.

Optix provides two backtracking algorithms of relative simplicity: a linear and a quadratic algorithm. The linear algorithm evaluates the objective function at multiple design points in the search direction. Evaluations continue at increasingly larger distances from the initial design point until an increase in the objective function is obtained, at which point the algorithm fits a parabola through the last three design points evaluated. The next design point is placed at the parabola's vertex.

The quadratic algorithm evaluates the objective function at a user-specified number of equally-spaced design points along the search direction and fits a parabola to the results. If the minimum of the parabola is within a user-specified threshold of any one of the design points evaluated, or if a minimum does not exist (i.e. the parabola reduces to a straight line or is concave), the design point corresponding to the minimum objective function value is returned to the BFGS algorithm. If neither of these conditions are met, a new set of design points is selected with one of them located at the parabola's vertex, and the objective function is reevaluated at these new locations. For convex problems, the quadratic line searching algorithm can significantly reduce the total optimization time from that required for the linear algorithm.

### 3.2.5 *Limitations*

One limitation of Optix over other similar optimization frameworks is the lack of built-in methods for applying bounds and constraints. Constraints can still be enforced using penalty function methods (for example, see Smith and Coit [65]), but more efficient and robust methods exist. Some example methods include the method of Lagrange multipliers for problems having only equality constraints, the simplex method for linear programming problems, and the ellipsoid method for quadratic programming problems. Explanations of these methods can be found in any introductory textbook on gradient-based optimization (for example, see Griva et al. [66]). However, it should be noted that each method is only suited to a specific subset of constrained optimization problems, whereas the penalty function method can be applied universally to all constrained optimization problems.

Another limitation of Optix is its inability to distinguish between local minima and the global minimum of a design space. For optimization problems that involve complex design spaces with multiple local minima, results returned by Optix may depend on the initial design point provided to the optimizer. This is a common shortfall of gradient-based optimization methods, but there are some algorithms – e.g. the conservative convex separable approximation (CCSA) methods presented by Svanberg [67] – that have overcome this

limitation. Locatelli and Schoen [68] present a thorough overview of globally-convergent optimization methods. The BFGS method implemented in Optix is not globally convergent. However, a simple design of experiments (DOE) approach can be used to improve the likelihood of finding the global minimum of a design space. The DOE approach systematically selects multiple design points distributed throughout the design space and uses each point to initiate a complete gradient-based optimization analysis. The collective results from this set of analyses does not guarantee discovery of the global minimum within the design space but simply improves the likelihood of finding it. The level of complexity of the design space will determine the number of simulations needed to provide adequate coverage of the design space. The computational cost of this approach can be significant since each analysis is a full optimization analysis, but the separate analyses are completely independent and can be run simultaneously given adequate computational resources. In the sample analyses that follow, the objective functions are convex so the locally-convergent BFGS method is satisfactory for this work.

### 3.3 Wing Shape Optimization in Inviscid Flow

Optix and MachUp have been used to solve several wing shape optimization problems for which closed-form solutions are available. Results from these simulations are presented and discussed here. Each simulation began with the same initial wing model – namely a spanwise-symmetric, untwisted, rectangular wing with an aspect ratio of  $A = 8$  and a section lift slope of  $a_0 = 6.8806 \text{ rad}^{-1}$  – operating at a wing lift coefficient of  $C_L = 0.5$ . Control points (locations where the optimizer is allowed to vary geometric and aerodynamic properties of the wing) were spaced uniformly along one semispan of the wing. The other semispan was automatically updated so that the wing remained symmetric. All simulations used a grid density of 100 nodes per semispan. The main MachUp input file and Python code used for these simulations are given in Appendix G.

The aerodynamic properties of the airfoils used in these analyses are shown in Table 3.1 and correspond to the NACA 4-digit X412 family of airfoils with percent maximum cambers,  $\bar{z}_{c_{\max}}$ , ranging from 0% to 8%. The data were generated using an inviscid panel code. The induced drag for the initial rectangular model at a lift coefficient of  $C_L = 0.5$  was calculated to be  $C_{D_i} = 1.0554 \times 10^{-2}$ .



**Table 3.1 Aerodynamic coefficients for the NACA X412 family of airfoils in inviscid flow**

Airfoil	$\alpha_{L0}$ (rad)	$a_0$ (rad <sup>-1</sup> )
NACA 0012	0.0000	6.8806
NACA 2412	-0.0380	6.8583
NACA 4412	-0.0761	6.8369
NACA 6412	-0.1141	6.8165
NACA 8412	-0.1519	6.7973

Prandtl [10,11] showed analytically that, for a finite wing of given aspect ratio, the induced drag is minimized by an elliptic lift distribution according to the relation

$$l = \frac{4L}{\pi b} \sqrt{1 - (2y/b)^2} \quad (3.3.1)$$

where  $L$  is the total lift generated by the wing,  $y$  is the spanwise coordinate measured from the root of the wing, and  $b$  is the wingspan. In nondimensional form, Eq. (3.3.1) becomes

$$c_l = \frac{4b}{\pi A} \frac{C_L}{c} \sqrt{1 - (2y/b)^2} \quad (3.3.2)$$

where  $c$  is the local chord and  $A$  is the aspect ratio determined by the wingspan  $b$  and the planform area  $S_w$  according to the relationship

$$A \equiv \frac{b^2}{S_w} \quad (3.3.3)$$

The induced drag generated by a wing having this lift distribution is given by

$$C_{D_i} = \frac{C_L^2}{\pi A} \quad (3.3.4)$$

For example, a wing having an elliptic lift distribution, an aspect ratio of  $A = 8$ , and a wing lift coefficient of  $C_L = 0.5$  will have an induced drag coefficient of  $C_{D_i} = 9.9472 \times 10^{-3}$ , which is about 6% less than the rectangular planform mentioned above. This result is used for comparison in the following inviscid optimization analyses.

### 3.3.1 Optimized Planform Shapes for Minimum Induced Drag

Prandtl [10,11] proposed achieving the elliptic lift distribution by using an elliptic planform, i.e. a chord distribution prescribed by

$$c = \frac{4b}{\pi A} \sqrt{1 - (2y/b)^2} \quad (3.3.5)$$

and no geometric or aerodynamic twist. For this planform, the section lift coefficient specified by Eq. (3.3.2) reduces to a constant value equal to the wing lift coefficient. Here we present a numerical optimization solution to this problem. To solve for the optimized planform shape numerically, control points were spaced uniformly along one semispan of the wing and the optimizer was configured to adjust the local chord length at each control point except the wing tip. The chord length at the wing tip was constrained such that an aspect ratio of  $A = 8$  was maintained, thus making the degrees of freedom for this problem one less than the number of control points  $N$ . A linear interpolation scheme was used to define the section chord at spanwise locations between control points. The gradient of the induced drag coefficient was calculated internally with MachUp using the DNAD module discussed in Chapter 2.

The planform shape was optimized using 2, 3, 6, and 11 control points. Results are summarized in Table 3.2. When  $N = 2$ , the planform corresponds to a tapered wing with a taper ratio of approximately  $R_r = 0.366$  and produces 1.121% more induced drag than the elliptic planform. Adding a third control point reduces this percentage by almost a fourth. As the number of control points is increased, the induced drag for the optimized solution converges toward that of an elliptic planform at the expense of increasing planform complexity and computational cost.

Figure 3.1 compares the final planform design of each optimization simulation to the initial rectangular planform and an elliptic planform of the same aspect ratio. The optimized solutions appear to converge toward the elliptic planform as the number of degrees of freedom increases. In each case, the maximum deviation from the elliptic planform occurs at the wing tip where the curvature is highest and the section lift coefficient and contribution to induced drag are smallest.

**Table 3.2 Minimum induced drag results for untwisted wings with optimized planforms**

Case	BFGS Iterations	$C_{D_i}$	Difference from Eq. (3.3.4)
Rectangular	—	0.010554	6.099%
$N = 2$	5	0.010059	1.121%
$N = 3$	9	0.009977	0.297%
$N = 6$	18	0.009952	0.051%
$N = 11$	38	0.009949	0.014%
Elliptic	—	0.009947	—

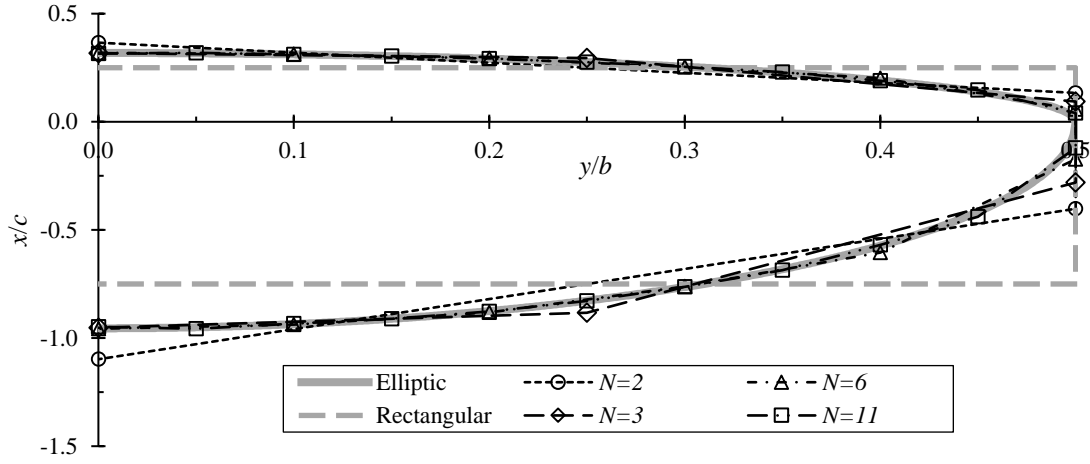


**Figure 3.1 Optimized planforms for minimum induced drag.**

### 3.3.2 Optimized Geometric Twist Distributions for Minimum Induced Drag

In 2004, Phillips [69] extended the analytical solutions of Prandtl [10,11] and showed that the minimum induced drag produced by a finite wing with an elliptic planform and no twist can also be achieved by a finite wing of arbitrary planform by prescribing the total twist as a function of spanwise location. For a generic wing with no sweep and no dihedral, Phillips [69] showed that the optimum twist distribution as a function of spanwise location is given by

$$(\alpha - \alpha_{L0})_{\text{root}} - (\alpha - \alpha_{L0}) = \Omega_{\text{max}} \left( 1 - \sqrt{1 - (2y/b)^2} \right) \quad (3.3.6)$$

where the angles  $\alpha$  and  $\alpha_{L0}$  represent local section values. The maximum twist  $\Omega_{\text{max}}$  is related to the lift coefficient according to

$$\Omega_{\text{max}} = \frac{4bC_L}{\pi A a_0 c_{\text{root}}} \quad (3.3.7)$$

and occurs at the wing tips ( $y = \pm b/2$ ). For a rectangular wing with uniform camber (i.e. no aerodynamic twist),  $\alpha_{L0} = (\alpha_{L0})_{\text{root}}$  so that Eq. (3.3.6) reduces to

$$\Delta \alpha_{\text{geometric}} = \Omega_{\text{max}} \left( 1 - \sqrt{1 - (2y/b)^2} \right) \quad (3.3.8)$$

where

$$\Delta\alpha_{\text{geometric}} \equiv \alpha_{\text{root}} - \alpha \quad (3.3.9)$$

Equation (3.3.8) describes an elliptic geometric twist distribution analogous to the elliptic chord distribution given by Eq. (3.3.5). Note that, by definition, the geometric twist at the root is zero. For the present optimization analyses, the root angle of attack  $\alpha_{\text{root}}$  was determined such that a lift coefficient of  $C_L = 0.5$  was maintained. The amount of twist at each control point other than the wing root was controlled by the optimizer, so that the degrees of freedom were again one less than the number of control points  $N$ .

The optimization problem was again solved numerically with 2, 3, 6, and 11 control points. The wing design was constrained to a rectangular planform with a uniform NACA 0012 cross section. Results are summarized in Table 3.3. We again see that the induced drag converged toward that of an elliptic lift distribution as the number of control points was increased. Comparing the results in Table 3.3 to those in Table 3.2 for equal  $N$ , optimizing the geometric twist distribution is slightly more efficient than optimizing the chord distribution in terms of both the number of BFGS iterations required and the aerodynamic performance of the optimized wings.

Figure 3.2 compares the geometric twist distribution determined by each optimization analysis to that prescribed by Eq. (3.3.8). We again see that the optimization solutions converge toward the expected solution as the number of control points increases, and the largest deviation from the geometric twist distribution prescribed by Eq. (3.3.8) occurs at the wing tip in each case.

**Table 3.3 Minimum induced drag results for geometric-twist-optimized rectangular wings**

Case	BFGS Iterations	$C_{D_i}$	Difference from Eq. (3.3.4)
Rectangular	—	0.010554	6.099%
$N = 2$	4	0.010026	0.793%
$N = 3$	7	0.009960	0.124%
$N = 6$	13	0.009948	0.009%
$N = 11$	24	0.009947	0.001%
Elliptic	—	0.009947	—

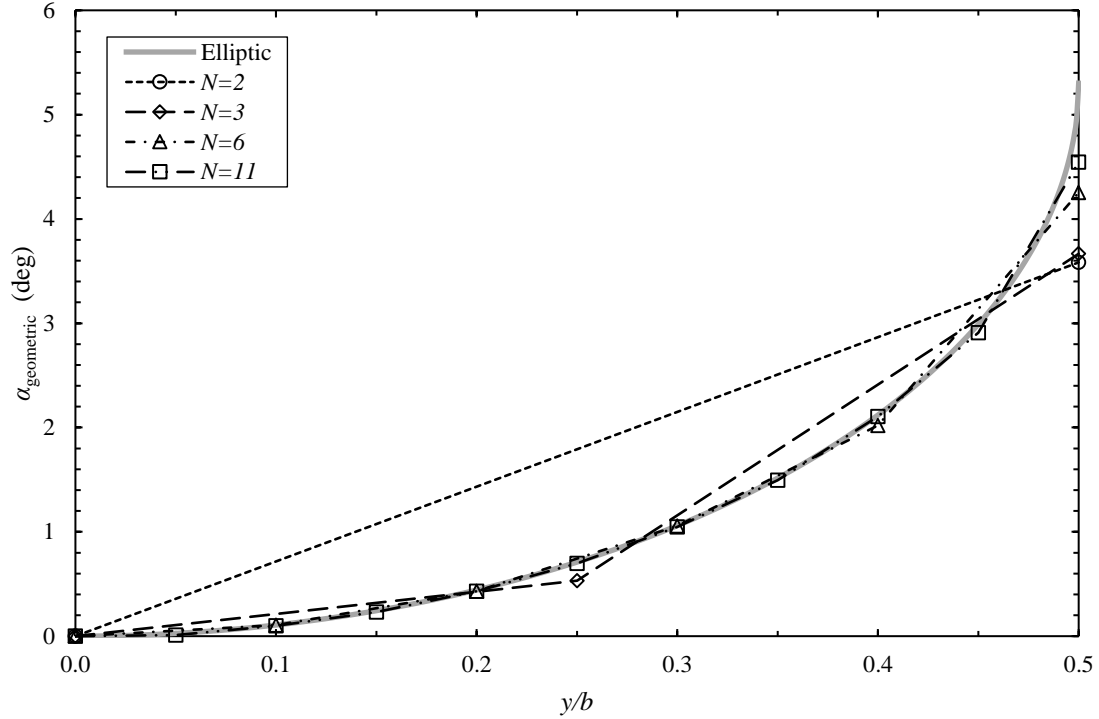


**Figure 3.2 Optimized geometric twist distributions for minimum induced drag.**

### 3.3.3 Optimized Aerodynamic Twist Distributions for Minimum Induced Drag

In the previous section, the geometric twist distribution of a finite rectangular wing with no aerodynamic twist was optimized for minimum induced drag. Similar results can be obtained by setting the geometric twist to zero and instead optimizing the spanwise aerodynamic twist of the wing. In this section, we present a method for optimizing the spanwise aerodynamic twist of a wing by allowing the optimizer to select from a family of airfoils of varying amounts of camber. For the analyses presented here, airfoil selection was restricted to the NACA X412 airfoils with maximum camber values ranging from 0% to 8% of the chord. Airfoil properties from Table 3.1 were used, and properties for airfoils in the specified camber range but not explicitly listed in Table 3.1 were determined by linear interpolation.

The section lift slopes of the NACA X412 airfoils listed in Table 3.1 vary slightly. Because of this variation, Eq. (3.3.7) cannot be applied directly without introducing some error into the analytical solution. Since the standard deviation of the section lift slopes listed in Table 3.1 is less than half a percent, the average

section lift slope from this family of airfoils can be used in Eq. (3.3.7) with negligible effect on the results, and we can use the approximation  $\alpha \approx \alpha_{\text{root}}$  in Eq. (3.3.6) such that

$$\Delta\alpha_{\text{aerodynamic}} \approx \Omega'_{\text{max}} \left( 1 - \sqrt{1 - (2y/b)^2} \right) \quad (3.3.10)$$

where

$$\Delta\alpha_{\text{aerodynamic}} \equiv \alpha_{L0} - (\alpha_{L0})_{\text{root}} \quad (3.3.11)$$

$$\Omega'_{\text{max}} = \frac{4bC_L}{\pi A(a_0)_{\text{avg}} c_{\text{root}}} \quad (3.3.12)$$

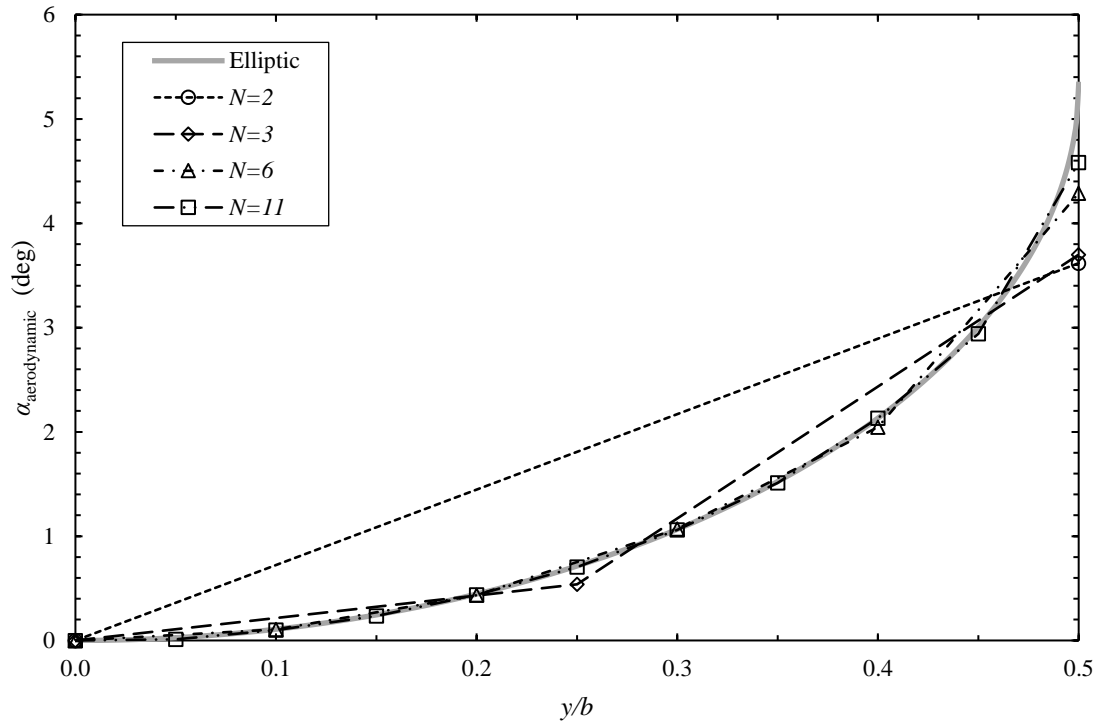
and the prime indicates an approximation due to the use of the average section lift slope. Optimization analyses with families of airfoils having a large standard deviation in section lift slope will not produce an aerodynamic twist distribution consistent with Eq. (3.3.10). However, the section lift distribution of the final optimized solution should still be consistent with Eqs. (3.3.1) and (3.3.2).

Because Eq. (3.3.10) specifies only a difference between the section zero-lift angles of attack and does not specify their absolute magnitude, an additional constraint is needed to isolate a single optimal solution. In the results that follow, the airfoil section at the wing tip was set to a NACA 2412 airfoil. The optimizer was configured to control the airfoil definition at all other control points by specifying the percent maximum camber  $\bar{z}_{c_{\text{max}}}$ , which MachUp then used to determine the airfoil properties at each control point via linear interpolation of the data in Table 3.1.

The resulting optimal designs for 2, 3, 6, and 11 control points are summarized in Table 3.4. The corresponding aerodynamic twist distributions are shown in Figure 3.3. Induced drag results are almost identical to those obtained for optimized geometric twist. The number of BFGS iterations required to obtain the optimized solutions were also comparable between the two sets of analyses in all cases except  $N = 11$ . For  $N = 11$ , about 2.5 times fewer iterations were required to find the optimal geometric twist distribution as were required to find the optimal aerodynamic twist distribution. This is because the percent maximum camber value of the third control point from the root was almost exactly 4% in the latter case. Since linear interpolation is used to determine the airfoil properties, derivatives are discontinuous at the interpolation nodes. This led to some confusion in the optimization algorithm regarding the appropriate search direction.

**Table 3.4 Minimum induced drag results for aerodynamic-twist-optimized rectangular wings**

Case	BFGS Iterations	$C_{D_i}$	Difference from Eq. (3.3.4)
Rectangular	—	0.010554	6.099%
$N = 2$	5	0.010026	0.792%
$N = 3$	7	0.009960	0.124%
$N = 6$	15	0.009948	0.009%
$N = 11$	61	0.009947	0.001%
Elliptic	—	0.009947	—

**Figure 3.3 Optimized aerodynamic twist distributions for minimum induced drag.**

### 3.4 Wing Shape Optimization for Viscous Flow

While the optimization analyses presented in Sec. 3.3 are beneficial from an academic perspective due to the existence of known closed-form solutions, they have limited practical application due to their neglect of viscous effects. As described in Sec. 2.6.1, viscous effects can be included within a MachUp analysis by using viscous airfoil data that includes estimates of the section parasitic drag coefficients  $c_{d_0}$ ,  $c_{d_1}$ , and  $c_{d_2}$  from Eq. (2.6.1). Estimates of these parasitic drag coefficients, the zero-lift angle of attack, and the section

lift slope are listed in Table 3.5 for the NACA X412 family of airfoils in viscous, incompressible flow at a Reynolds number of  $Re = 10^6$ . These coefficients were determined using XFOIL (see Refs. [51,52]).

For the inviscid optimization problems presented in Sec. 3.3, closed-form solutions were available for comparison with the optimized results produced by Optix. For the viscous optimization problems of this section, no closed-form solutions exist. An untwisted elliptic wing with an aspect ratio of  $A = 8$ , uniform camber, and no sweep or dihedral will be used as a baseline model for comparisons. An optimization analysis was performed to determine the optimum airfoil section (selected from the NACA X412 family of airfoils) to achieve minimum total drag for this baseline elliptic wing operating at a lift coefficient of  $C_L = 0.5$ . The optimum airfoil section selected by the optimizer has a maximum camber of  $\bar{z}_{c_{\max}} = 3.59\%$ .

The setup for the optimization cases presented in this section was similar to that of the inviscid cases of Sec. 3.3 with one important difference. The airfoil specified at the tip section had negligible effect on the induced drag results of the foregoing analyses, and therefore was selected arbitrarily in each analysis. However, this is not the case for the viscous analyses presented in this section. In each case here, an additional degree of freedom was needed to allow the optimizer to specify the airfoil at the tip section (and therefore the entire wing for wings of uniform cross-section). As a result, the degrees of freedom were equal to the number of control points for each viscous analysis. The initial rectangular wing design used to start each viscous analysis was identical to that used in the corresponding inviscid analyses except that the airfoil section at each control point was initialized to the airfoil section of the baseline elliptic wing, i.e.  $\bar{z}_{c_{\max}} = 3.59\%$ . The drag results for this initial rectangular wing and the baseline elliptic wing in viscous flow are summarized in Table 3.6.

**Table 3.5 Aerodynamic coefficients for the NACA X412 family of airfoils in viscous, incompressible flow at a Reynolds number of  $Re = 10^6$ .**

Airfoil	$\alpha_{L0}$ (rad)	$a_0$ (rad <sup>-1</sup> )	$c_{d_0}$	$c_{d_1}$	$c_{d_2}$
NACA 0012	0.00000	6.4194	0.00562	0.00000	0.00804
NACA 2412	-0.03720	6.2639	0.00612	-0.00362	0.00827
NACA 4412	-0.07536	6.1093	0.00780	-0.00753	0.00829
NACA 6412	-0.11176	6.0833	0.01091	-0.01067	0.00739
NACA 8412	-0.15006	5.9184	0.01556	-0.01556	0.00821



**Table 3.6 Drag coefficients for initial rectangular wing and baseline elliptic wing in viscous flow.**

Component	Initial Rectangular Wing	Baseline Elliptic Wing	Percent Difference
$C_{D_i}$	0.010643	0.009952	6.94%
$C_{D_p}$	0.006149	0.006085	1.06%
$C_D$	0.016792	0.016037	4.71%

### 3.4.1 Optimized Planform Shapes for Minimum Total Drag

Here we present the planform shapes that correspond to minimum total drag, including viscous effects, as determined by Optix and MachUp for 2, 3, 6, and 11 control points. Total drag results for these cases are summarized in Table 3.7. The viscous cases generally required more BFGS iterations than their inviscid counterparts listed in Table 3.2. The one exception to this is  $N = 11$ , where the viscous case required four fewer BFGS iterations than the inviscid case, a reduction in computational cost of about 10%. In all four cases, the airfoil section selected by the optimizer matched that selected for the baseline elliptic wing to within 0.01% maximum camber.

The planform designs produced by the optimizer are plotted in Figure 3.4 and are nearly indistinguishable from those shown in Figure 3.1. Indeed, the chord lengths at each control point differ between the two cases by less than 1% of the average chord. These slight differences became smaller as the number of control points increased, and we therefore conclude that the optimum planform design for an untwisted wing is essentially the same in both viscous and inviscid flows and has the elliptic spanwise chord distribution defined by Eq. (3.3.5).

**Table 3.7 Minimum total drag results for untwisted wings with optimized planforms.**

Case	BFGS Iterations	$C_D$	Difference from Baseline Elliptic Wing
Rectangular	—	0.016792	4.710%
$N = 2$	11	0.016182	0.907%
$N = 3$	13	0.016078	0.256%
$N = 6$	21	0.016045	0.048%
$N = 11$	34	0.016039	0.014%
Elliptic	—	0.016037	—

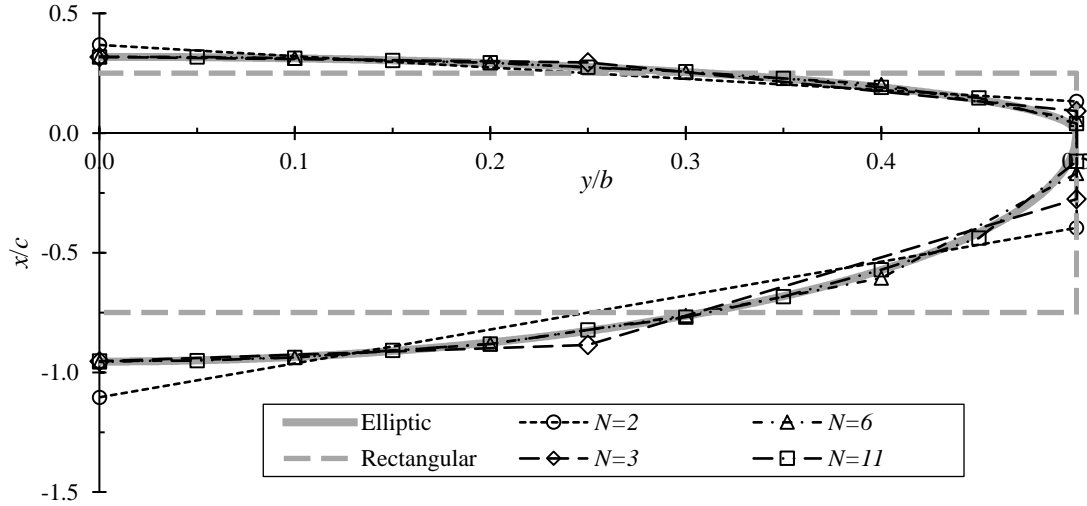


**Figure 3.4 Optimized planforms for minimum total drag.**

We note one issue in how viscous effects have been included in these analyses. The viscous airfoil coefficients included in Table 3.5 correspond to a Reynolds number based on chord length of  $Re = 10^6$ . In the optimized planform analyses, however, the chord length is a function of spanwise location and so, therefore, is the Reynolds number. In fact, the spanwise Reynolds numbers for the elliptic planform vary from  $1.27 \times 10^6$  at the root to 0 at the tip. Adjustments to the airfoil coefficients due to these variations in Reynolds number were not attempted during the analyses presented here. This issue does not affect the inviscid optimization cases presented previously, nor does it affect the following optimization cases in which the chord length is held constant.

### 3.4.2 Optimized Geometric Twist Distributions for Minimum Total Drag

Table 3.8 summarizes the results for optimized geometric twist distributions to minimize total drag on a rectangular wing with uniform cross section. In each case the drag was more than 1% higher than the baseline elliptic solution. This increased drag came almost entirely from parasitic drag, as shown in Table 3.9 for the case of  $N = 11$ .

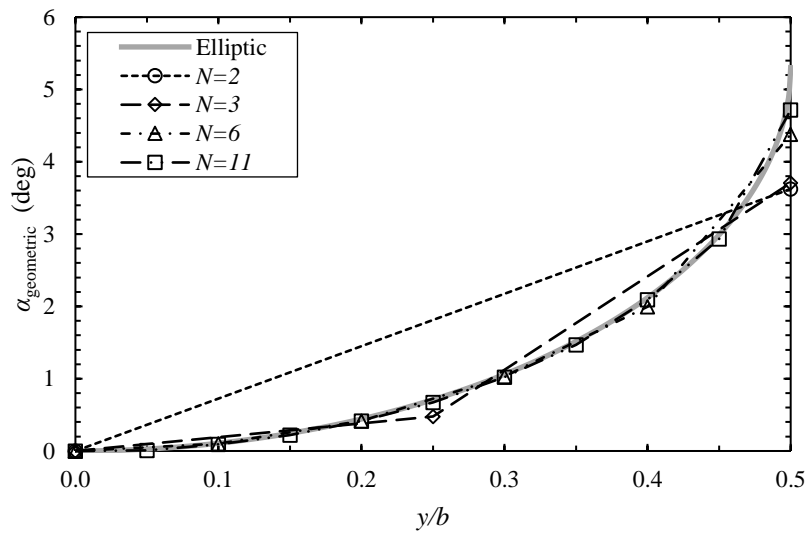
**Table 3.8** Minimum total drag results for geometric-twist-optimized rectangular wings.

Case	BFGS Iterations	$C_D$	Difference from Baseline Elliptic Wing
Rectangular	—	0.016792	4.710%
$N = 2$	6	0.016284	1.537%
$N = 3$	10	0.016213	1.099%
$N = 6$	18	0.016200	1.014%
$N = 11$	29	0.016199	1.008%
Elliptic	—	0.016037	—

**Table 3.9** Drag components for geometric-twist-optimized rectangular wing with 11 control points.

Component	Value	Difference from Baseline Elliptic Wing
$C_{D_i}$	0.009959	0.065%
$C_{D_p}$	0.006240	2.549%
$C_D$	0.016199	1.008%

Again, the airfoil section selected by the optimizer for each case matched that selected for the baseline elliptic wing to within 0.01% maximum camber. The optimized geometric twist distributions are plotted in Figure 3.5. For each case, the geometric twist angle selected at each control point differed from the corresponding value for minimum induced drag (see Figure 3.2) by less than 0.06 deg. The only exceptions

**Figure 3.5** Optimized geometric twist distributions for minimum total drag.

to this were at the wing tip for  $N = 6$  and  $N = 11$ , where the slope of the twist distribution curve is large and the influence on wing drag is small.

### 3.4.3 Optimized Aerodynamic Twist Distributions for Minimum Total Drag

Optimized aerodynamic twist distributions for minimizing total drag are summarized in Table 3.10. Values here are lower than those for the corresponding optimized geometric twist cases, but not as low as those for the optimized planform cases. The parasitic drag component is still the largest contributor to the increase in drag above the baseline elliptic wing result, as shown in Table 3.11 for the case of  $N = 11$ .

Optimized aerodynamic twist distributions are plotted in Figure 3.6. Noticeable differences between these data and the inviscid data presented in Figure 3.3, especially around  $y/b = 0.25$ , indicate that the optimized aerodynamic twist distribution for minimum total drag does not converge to the elliptic distribution described by Eq. (3.3.10) as the number of control points increases. This is primarily due to the differences in the parasitic drag equation coefficients of the airfoils in the NACA X412 family. Essentially, the optimizer is favoring an increase in induced drag in these profiles to achieve a more substantial decrease in parasitic drag.

**Table 3.10 Minimum total drag results for aerodynamic-twist-optimized rectangular wings.**

Case	BFGS Iterations	$C_D$	Difference from Baseline Elliptic Wing
Rectangular	—	0.016792	4.710%
$N = 2$	13	0.016203	1.033%
$N = 3$	20	0.016107	0.435%
$N = 6$	46	0.016095	0.362%
$N = 11$	122	0.016093	0.351%
Elliptic	—	0.016037	—

**Table 3.11 Drag components for aerodynamic-twist-optimized rectangular wing with 11 control points.**

Component	Value	Difference from Baseline Elliptic Wing
$C_{D_i}$	0.009962	0.103%
$C_{D_p}$	0.006131	0.755%
$C_D$	0.016093	0.351%

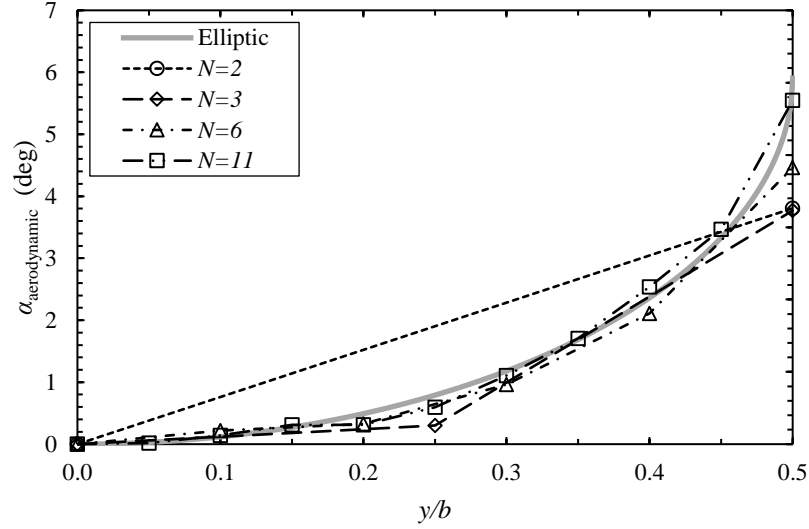


**Figure 3.6 Optimized aerodynamic twist distributions for minimum total drag.**

### 3.5 Visualization of the Design Space for Wing Shape Optimization

Let us here consider the aerodynamic-performance design space within which airfoil sections of a finite wing must operate. The total drag produced by any section of an airfoil wing is the sum of the section induced and parasitic drags. The section induced drag is a function of the section lift and induced angle of attack  $\alpha_i$  as given by

$$c_{d_i} = c_l \sin(\alpha_i) \quad (3.5.1)$$

The section parasitic drag is a function of the section lift coefficient and parasitic drag coefficients  $c_{d_0}$ ,  $c_{d_1}$ , and  $c_{d_2}$  from Eq. (2.6.1). The section lift coefficient is, in turn, a function of the section angle of attack  $\alpha$ , the section lift slope  $a_0$ , and the section zero-lift angle of attack  $\alpha_{L0}$  according to

$$c_l = a_0(\alpha - \alpha_{L0}) \quad (3.5.2)$$

Note that the local angle of attack  $\alpha$  is a function of the wing angle of attack  $\alpha_{\text{wing}}$ , the local induced angle of attack  $\alpha_i$ , and the local geometric twist  $\Delta\alpha_{\text{geometric}}$  according to

$$\alpha = \alpha_{\text{wing}} + \alpha_i - \Delta\alpha_{\text{geometric}} \quad (3.5.3)$$

The relationships described above have been used to generate the contour plots shown in Figure 3.7. Although these contour plots do not follow the traditional approach to visualizing drag as a function of lift or angle of attack, great care has been taken to construct this figure in a manner that portrays the key relationships when considering the additional dimensions of variable airfoils and wing geometries. Visualizing the data in this format can provide significant insights into the intricacies of wing shape optimization.

Figure 3.7(a) presents contours of section induced drag as a function of section induced angle of attack and section lift coefficient, and it is independent of airfoil section. Figure 3.7(b) presents contours of section parasitic drag as a function of section angle of attack and section lift coefficient, and it is specific to the NACA X412 family of airfoils defined in Table 3.5. Figure 3.7(b) uses the same linear interpolation scheme implemented in MachUp for determining lift and parasitic drag coefficients for airfoils intermediate to those listed in Table 3.5. First-order discontinuities in the contour lines are artifacts of this interpolation scheme.

The locus of minimum parasitic drag values for each section lift coefficient has been plotted as a solid line in Figure 3.7(b) and indicates the airfoil section that provides the minimum parasitic drag for a given lift coefficient. The locus of minimum parasitic drag values is first-order discontinuous for the same reason as the contour lines. Using a higher-order interpolation scheme or refining the airfoil data by adding additional airfoils will lead to more realistic contour lines and a smoother locus of minimum parasitic drag values.

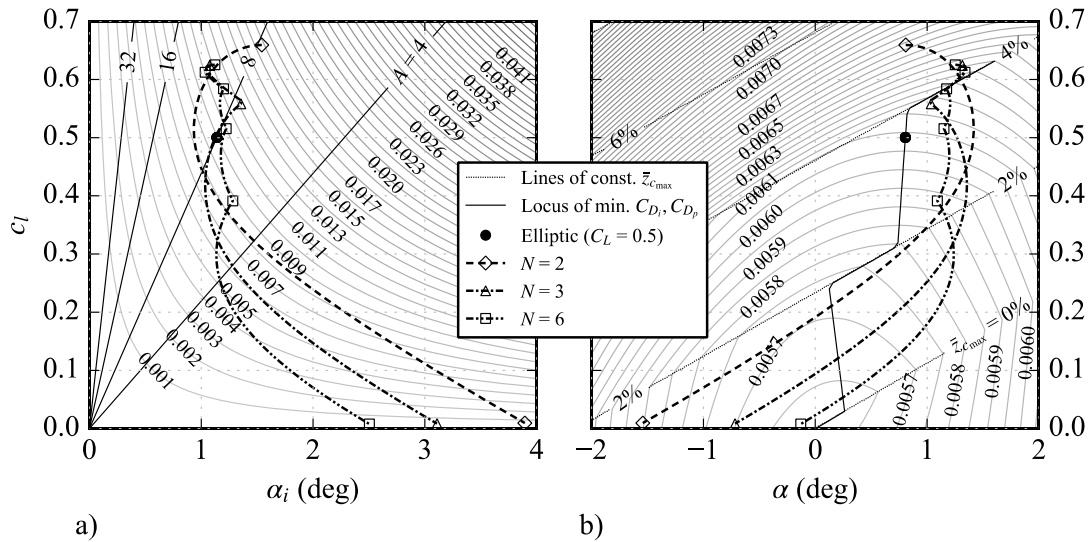


**Figure 3.7** Contours of (a) induced and (b) parasitic drag for finite wing sections. Results are included for rectangular wings with  $A = 8$ ,  $C_L = 0.5$ , and optimized aerodynamic twist for variable  $N$ .

Unlike the locus of minimum parasitic drag values, the corresponding locus of minimum induced drag values is a function of aspect ratio. For an untwisted elliptic wing, downwash is uniform and all sections of the wing experience the same induced angle of attack and, therefore, the same section lift coefficient. Thus  $c_l = C_L$  and  $c_{d_i} = C_{D_i}$  along the entire wingspan. Using these substitutions in Eq. (3.3.4), we can then combine Eqs. (3.3.4) and (3.5.1) to yield

$$c_l = \pi A \sin(\alpha_i) \quad (3.5.4)$$

Equation (3.5.4) has been plotted in Figure 3.7(a) for a selection of aspect ratios.

Now consider again the untwisted elliptic wing. Downwash is uniform for this wing, and therefore every section along the wingspan operates at the same angle of attack, induced angle of attack, and lift coefficient. The data for every section along the wingspan therefore collapses to a single point on each of the contour plots in Figure 3.7. This point is shown for an untwisted elliptic wing with an aspect ratio of  $A = 8$  and uniform camber of  $\bar{z}_{c_{max}} = 3.59\%$ , operating at a lift coefficient of  $C_L = 0.5$ .

Prandtl [10,11] showed analytically that an untwisted elliptic wing produces the least amount of induced drag possible for a given aspect ratio and lift coefficient, and Phillips [69] extended this work to show that the same minimum in induced drag can be achieved by a rectangular wing having an elliptic twist distribution. This can be seen visually in Figure 3.7(a). Because the relationship between lift and induced drag is approximately linear for small angles (see Eq. (3.5.1)), any two wings whose sections all lie along the same line of constant  $\alpha_i$  and integrate to the same lift coefficient will also integrate to the same induced drag coefficient.

The relationship between lift and parasitic drag is nonlinear and strongly dependent on the characteristics of the airfoils selected, so that designs which produce minimum induced drag may not necessarily produce minimum parasitic drag. It is the job of an optimizer, then, to balance these two competing objectives in order to find a design that represents the minimum total drag for a given design space and given constraints.

The patterned lines with symbols in Figure 3.7 represent data from the optimization cases of Sec. 3.4.3 – that is, optimized aerodynamic twist distributions for minimum total drag produced by a rectangular wing of aspect ratio  $A = 8$  with no geometric twist and operating at a lift coefficient of  $C_L = 0.5$ . The symbols indicate the aerodynamic state at each control point. The connecting lines represent the distribution of

aerodynamic states at spanwise locations between control points. Note that, for a given wing, changing the camber at one control point will affect the downwash along the entire wingspan, adjusting the location of all other control points for that wing and the shape of the lines connecting them. This is also true of changes in geometric twist and chord in designs where those parameters are allowed to vary. There is no mechanism whereby the optimizer can adjust the aerodynamic state of one control point without affecting the aerodynamic state of every section along the wingspan.

The data for a rectangular wing with no geometric twist and an elliptic aerodynamic twist distribution – see Eq. (3.3.10) – would form a vertical line on both contour plots in Figure 3.7. This would minimize induced drag but not parasitic drag. A rectangular wing with a twist and camber distribution such that the data for each section of the wing lie somewhere along the locus of minimum parasitic drag would minimize parasitic drag but not induced drag. In an optimization analysis, the optimizer must find a solution that represents the best possible balance between these two competing objectives, with the added restriction of a limited number of control points.

The ability to visualize this design space and understand the balancing act between the two components of drag is significant. Several rudimentary implications of the data portrayed in Figure 3.7 have been discussed here. More detailed studies of this plot and similar plots based on other families of airfoils may provide additional insights that can aid in our understanding of the design space of finite wings. This level of insight is impossible to gain from traditional approaches to aerodynamic shape optimization that rely on high-fidelity CFD simulations to evaluate the objective function (see Lyu et al. [4]). By limiting the section profiles of the wing to a family of airfoils with known aerodynamic properties, the optimization method presented here reduces the number of design variables and the complexity of the numerical solution by several orders of magnitude. Additionally, this approach allows us to generate drag contours of the design space in order to more fully understand the optimized distributions arrived at through numerical optimization. For applications that lie within the assumptions of lifting line theory, the benefits are realized without a significant reduction in accuracy. For applications that lie outside the limits of these assumptions, this method should be applied with caution but may still be useful in providing qualitative insights to the design space and optimization problem of the specific application.



## 4 ANALYTICAL LIFTING LINE METHOD FOR WINGS OF ARBITRARY ASPECT RATIO

### 4.1 Introduction

In 1918, Prandtl [10,11] published his landmark paper on what is known today as classical lifting line theory. This groundbreaking innovation was the first practical method for analyzing flow over a finite three-dimensional wing. From this theory, Prandtl was able to show that the most efficient wing design in terms of minimizing induced drag is one which produces an elliptic spanwise lift distribution. This finding led to the distinctive elliptic planform design of the famous British Supermarine Spitfire, which is considered one of the most strategically important fighter aircraft of World War II. Many other valuable insights to aircraft design and performance have been gleaned from this theory in the one hundred years since its publication.

Despite its successes, classical lifting line theory is not without limitations. For example, it was originally formulated for wings with no sweep or dihedral, and it quickly became clear that Prandtl's theory did not adequately account for the effects of aspect ratio for aspect ratios below about 4 (for example, see Birnbaum [70] and Blenk [71]). However, by building upon the solid foundation laid by Prandtl, researchers have been able to produce methods for overcoming one or more of the early limitations of classical lifting line theory. One method, published in 2000 by Phillips and Snyder [16], accounts for sweep and dihedral in the wing and provides a method for integrating viscous effects into the solution. Another method, known as lifting surface theory (see Multhopp (1938) [72]), extends the applicable range of aspect ratios to less than 1. Küchemann [73] provides an elegant formulation of lifting surface theory which recasts it in such a way that the concepts of lifting surface theory can be readily applied to classical lifting line theory. The current work seeks to combine the efforts of Phillips and Snyder [16] and Küchemann [73] into a single method that incorporates the advantages of both methods. In essence, we seek to use Küchemann's development to modify the numerical lifting line algorithm of Phillips and Snyder so that its range of validity extends to slender wings as well as high-aspect ratio wings.

In this chapter, a rigorous development of classical lifting line theory is presented, along with some important observations regarding elliptic wings that arose from direct application of classical lifting line theory. The equations for slender wing theory and lifting surface theory are also developed. Several observations are made in comparing these theories with classical lifting line theory, and a modified equation for slender wing theory is proposed. Several empirical equations are discussed and compared for modifying

classical lifting line theory to bring it into closer agreement with results from lifting surface theory and a high-order panel method. A generalized formulation of lifting line theory is presented that allows us to more easily compare the various modifications that have been presented in the literature. Finally, a new equation is proposed that provides a reasonable balance between simplicity and accuracy for wings of arbitrary aspect ratio and planform shape.

## 4.2 Lift Generated by a Finite Wing

We begin with a statement of the most basic equation which we are trying to solve – that of lift generated by a finite wing. From classical airfoil theory, the lift generated by a 2D airfoil is related to the angle of attack by the approximation

$$c_l = a_0 (\alpha - \alpha_{L0}) \quad (4.2.1)$$

where small angles have been assumed for both  $\alpha$  and  $\alpha_{L0}$ . This equation works well for 2D airfoils (i.e. wings of infinite span), but quickly breaks down when we move to 3D wings of finite span. At the wing tips of a finite wing, nothing separates the airflow below the wing from the airflow above the wing. The pressure difference across the wing causes some of the higher-pressure air below the wing to escape around the wingtip and into the lower-pressure region above the wing. As a result, the airflow below the wing will have a slight outward motion (from root to tip), while the airflow above the wing will have a slight inward motion (from tip to root). This effect is more exaggerated at the wingtips but is present along the entire span of a finite wing.

The circulation of air around the wingtips, as just described, generates a sheet of vorticity immediately behind the trailing edge of the wing. The energy that goes into generating this vortex sheet reduces the effectiveness of the wing in generating lift, and Eq. (4.2.1) no longer holds. Empirically, we can modify Eq. (4.2.1) by defining two new angles: the “effective” angle of attack,  $\alpha_e$ , and the “induced” angle of attack,  $\alpha_i$ . These angles are defined such that

$$\alpha_e = (\alpha - \alpha_{L0}) - \alpha_i \quad (4.2.2)$$

and Eq. (4.2.1) becomes

$$c_l = a_0 \alpha_e \quad (4.2.3)$$

To determine the total lift generated by a finite wing, we take the area-weighted average of the lift coefficients at each spanwise location by integrating Eq. (4.2.3) over the wingspan,

$$C_L = \frac{1}{S_w} \int_{y=-b/2}^{b/2} c_l c dy = \frac{1}{S_w} \int_{y=-b/2}^{b/2} a_0 \alpha_e c dy \quad (4.2.4)$$

In doing so, we have relied upon an assumption that was first made by Prandtl [10,11] in his original development of classical lifting line theory – that is, that the spanwise sections of a finite wing behave the same as a 2D airfoil section operating at the same angle of attack. While Prandtl offered no mathematical justification for this assumption, it has proven to be quite reliable through a century of application.

The trick now, and the focus of this chapter, is to determine an expression for  $\alpha_e$  such that Eq. (4.2.4) is accurate for finite wings ranging in aspect ratio from slender to infinite. Several researchers, beginning with Prandtl [10,11], have presented methods for determining an appropriate expression for  $\alpha_e$  under various assumptions. Those of greatest interest to the present work are classical lifting line theory, slender wing theory, and lifting surface theory. Each, in turn, shall here be presented and discussed.

### 4.3 Classical Lifting Line Theory

Consider a flat or uniformly cambered wing of finite span in an infinite potential flow field. The boundary condition for this flow field requires that the flow is everywhere tangent to the wing surface such that

$$\frac{w}{V_\infty} = -\frac{dz}{dx} = \alpha - \alpha_{L0} \quad (4.3.1)$$

where we have applied the small angle approximation  $\tan(\alpha - \alpha_{L0}) \approx \alpha - \alpha_{L0}$ . Note that we have defined the downwash  $w$  to be positive for positive angle of attack, so that positive downwash acts in the direction of the  $-z$  axis.

Prandtl proposed satisfying this boundary condition by representing the wing as a series of horseshoe vortices, each horseshoe vortex consisting of a single spanwise vortex segment aligned with the quarter-chord of the wing and two semi-infinite vortex segments extending chordwise downstream, as shown in Figure 4.1. In the limit as the number of horseshoe vortices goes to infinity, the streamwise vortex segments form a continuous vortex sheet trailing behind the wing. It is this vortex sheet that is responsible for the reduced

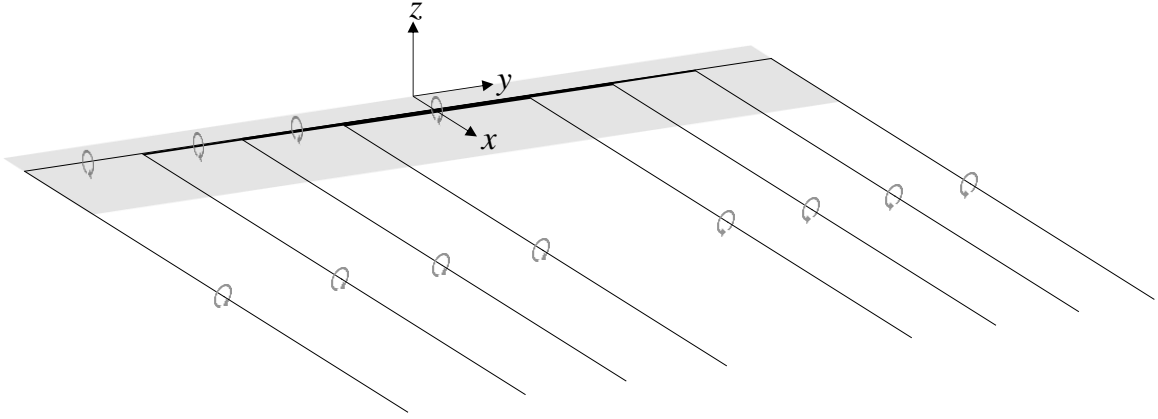


**Figure 4.1 Discrete system of overlapping horseshoe vortices on a finite wing.**

effectiveness of the wing as was explained earlier. The spanwise vortex segments, on the other hand, generate a force on the surrounding fluid that is equal in magnitude but opposite in direction to the lift force experienced by the wing. This is the “lifting line” from which Prandtl’s theory derives its name.

It is important to note here that each horseshoe vortex is a continuous vortex filament that must abide by the vortex theorems of Helmholtz [74] – namely, that the filament cannot end in a fluid (so that the trailing vortex segments must be semi-infinite), and that the circulation strength of the vortex filament cannot vary along its length. Therefore, the strength of each spanwise vortex segment must be equal to that of the two trailing vortex segments to which it is attached, and the direction of circulation must be unchanged along the entire filament (as shown in Figure 4.1).

The problem is now to determine the continuous distribution of vortex strengths  $\Gamma(y)$  such that the boundary condition of Eq. (4.3.1) is satisfied. To facilitate this, we first decompose  $w$  into two components,  $w_e$  and  $w_i$ , such that

$$w = w_e + w_i \quad (4.3.2)$$

where  $w_e$ , or the “effective downwash,” is the downwash due to the spanwise vortex segments; and  $w_i$ , or the “induced downwash,” is the downwash due to the trailing vortex sheet. Again, both components of downwash are considered positive in the  $-z$  direction. Note that by dividing Eq. (4.3.2) by  $V_\infty$ , applying the

small angle approximation, and rearranging, we arrive at Eq. (4.2.2), so that both are equivalent statements of the boundary condition.

Consider the semi-infinite vortex filament shown in Figure 4.2. The origin  $O$  and the arbitrary point  $P$  lie on the same plane perpendicular to the vortex filament, with the vector  $\mathbf{h}$  pointing from  $O$  to  $P$ . From the Biot-Savart law (see Sec. 5.2 of Anderson [75]), the differential velocity vector  $d\mathbf{V}$  induced at point  $P$  due to the differential vortex element of length  $d\mathbf{l}$  located at point  $Q$  is given by

$$d\mathbf{V} = \frac{\Gamma}{4\pi} \frac{d\mathbf{l} \times \mathbf{r}}{r^3} \quad (4.3.3)$$

where  $\mathbf{r}$  is the vector pointing from  $Q$  to  $P$ . The total velocity induced at point  $P$  by the entire vortex filament is then

$$\mathbf{V} = \int d\mathbf{V} = \int_0^\infty \frac{\Gamma}{4\pi} \frac{d\mathbf{l} \times \mathbf{r}}{r^3} \quad (4.3.4)$$

By inspection, the length from  $O$  to  $Q$  is  $h/\tan(\theta)$  so that

$$dl = -\frac{h}{\sin^2(\theta)} d\theta \quad (4.3.5)$$

and the magnitudes of the vectors  $\mathbf{r}$  and  $\mathbf{h}$  are related by

$$r = h/\sin \theta \quad (4.3.6)$$

Using Eqs. (4.3.5) and (4.3.6) in Eq. (4.3.4) and taking the magnitude, we get

$$V = \frac{\Gamma}{4\pi} \int_{\pi/2}^{\pi} \frac{\sin \theta}{h} d\theta = \frac{\Gamma}{4\pi h} \quad (4.3.7)$$

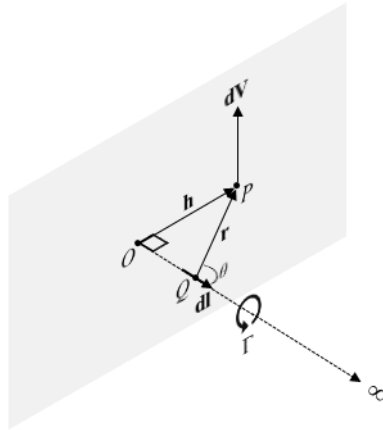


**Figure 4.2** Velocity induced at point  $P$  by a semi-infinite vortex filament.

The direction of  $V$  is given by the cross product of the vectors  $\overline{OQ}$  and  $\overline{OP}$ .

Now consider the trailing vortex sheet proposed by Prandtl, consisting of an infinite number of differential semi-infinite vortex filaments originating at the quarter chord line and extending in the direction of the chord. By analogy to Eq. (4.3.7), the differential induced downwash at a point  $y$  along the quarter chord by a differential slice of this vortex sheet located at  $y = \eta$  is

$$dw_i(y) = \frac{d\Gamma(\eta)}{4\pi(y-\eta)} \quad (4.3.8)$$

The total induced downwash due to the trailing vortex sheet is then the integral of Eq. (4.3.8) over the wingspan

$$w_i(y) = \frac{1}{4\pi} \int_{\eta=-b/2}^{b/2} \frac{d\Gamma(\eta)/d\eta}{y-\eta} d\eta \quad (4.3.9)$$

The effective downwash  $w_e(y)$  cannot be determined in the same manner, i.e. using the potential flow equations of a vortex filament, because the locations at which we are interested in determining the velocity lie along the axis of the spanwise vortex segments where the velocity is singular. Prandtl therefore turned to an alternative means for computing the effective downwash – namely, the two-dimensional Kutta-Joukowski theorem. At this point, Prandtl injects his hypothesis that each spanwise section of a finite wing could be modeled as a two-dimensional airfoil subject to the same circulation. The spanwise section lift is then, by the Kutta-Joukowski theorem,

$$l(y) = \rho_\infty V_\infty \Gamma(y) \quad (4.3.10)$$

and from classical airfoil theory we have

$$l(y) = \frac{1}{2} \rho_\infty V_\infty^2 c(y) c_l(y) = \frac{1}{2} \rho_\infty V_\infty^2 c(y) a_0 \alpha_e(y) \quad (4.3.11)$$

Equating the right-hand sides of Eqs. (4.3.10) and (4.3.11) and solving for  $\alpha_e$  gives

$$\alpha_e(y) = \frac{2\Gamma(y)}{V_\infty a_0 c(y)} \quad (4.3.12)$$

so that the effective downwash becomes

$$w_e(y) = V_\infty \alpha_e(y) = \frac{2\Gamma(y)}{a_0 c(y)} \quad (4.3.13)$$

Substituting the right-hand sides of Eqs. (4.3.9) and (4.3.13) into Eq. (4.3.2) and substituting that result in for the total downwash in Eq. (4.3.1) gives

$$\frac{2\Gamma(y)}{V_\infty a_0 c(y)} + \frac{1}{4\pi V_\infty} \int_{\eta=-b/2}^{b/2} \frac{d\Gamma(\eta)/d\eta}{y-\eta} d\eta = \alpha - \alpha_{L0} \quad (4.3.14)$$

which is the fundamental equation of Prandtl's classical lifting line theory. The only unknown in Eq. (4.3.14) is the circulation distribution  $\Gamma(y)$ , all other variables being parameters of either the wing geometry or the operating conditions. Solution methods to this equation are not directly relevant to the current discussion; the reader is instead referred to Anderson [75] and Phillips [53].

One important solution to Eq. (4.3.14) is the elliptic circulation distribution given by

$$\Gamma(y) = \Gamma_0 \sqrt{1 - \left(\frac{2y}{b}\right)^2} \quad (4.3.15)$$

Besides being the most efficient circulation distribution in terms of minimizing induced drag, it conveniently results in uniform induced downwash across the entire wingspan. We can see this by inserting the derivative of Eq. (4.3.15) with respect to  $y$  into Eq. (4.3.9) and evaluating. The substitution gives

$$(w_i)_{\text{elliptic}} = -\frac{\Gamma_0}{\pi b^2} \int_{\eta=-b/2}^{b/2} \frac{\eta}{y-\eta} \left[1 - \left(\frac{2\eta}{b}\right)^2\right]^{-1/2} d\eta \quad (4.3.16)$$

A convenient method for solving this integral is to use the change of variables  $y = -\frac{b}{2} \cos(\theta_0)$  and  $\eta = -\frac{b}{2} \cos(\theta)$ , which gives

$$(w_i)_{\text{elliptic}} = \frac{\Gamma_0}{2\pi b} \int_{\theta=0}^{\pi} \frac{\cos(\theta)}{\cos(\theta) - \cos(\theta_0)} d\theta \quad (4.3.17)$$

Eq. (4.3.17) can be evaluated from (see Karamcheti [76])

$$\int_0^\pi \frac{\cos(n\theta)}{\cos(\theta) - \cos(\theta_0)} d\theta = \frac{\pi \sin(n\theta_0)}{\sin(\theta_0)} \quad (4.3.18)$$

By inspection we see that  $n=1$  so that

$$(w_i)_{\text{elliptic}} = \frac{\Gamma_0}{2b} \quad (4.3.19)$$

Consider a flat or uniformly-cambered wing with the elliptic circulation distribution given by Eq. (4.3.15). Eq. (4.3.19) states that the induced downwash is uniform along the wingspan, and therefore by Eq.

(4.3.2) the effective downwash must also be uniform. Substituting the circulation distribution, Eq. (4.3.15), into Eq. (4.3.13) gives

$$(w_e)_{\text{elliptic}} = \frac{2}{a_0 c(y)} \Gamma_0 \sqrt{1 - \left(\frac{2y}{b}\right)^2} \quad (4.3.20)$$

which (assuming  $a_0$  to be constant over the wingspan) can only be constant if the chord distribution is also elliptic, i.e.

$$c_{\text{elliptic}} = c_0 \sqrt{1 - \left(\frac{2y}{b}\right)^2} = \frac{4\bar{c}}{\pi} \sqrt{1 - \left(\frac{2y}{b}\right)^2} \quad (4.3.21)$$

so that Eq. (4.3.20) becomes

$$(w_e)_{\text{elliptic}} = \frac{\pi \Gamma_0}{2a_0 \bar{c}} \quad (4.3.22)$$

Substituting the right-hand sides of Eqs. (4.3.19) and (4.3.22) into Eq. (4.3.2) and solving for  $\Gamma_0$ , we get

$$\Gamma_0 = 2wb \left( \frac{a_0}{a_0 + \pi A} \right) \quad (4.3.23)$$

where  $A = b^2/S_w = b/\bar{c}$  is the aspect ratio of the wing. Using this result in Eqs. (4.3.19) and (4.3.22) gives

$$w_i = \frac{w}{1 + (\pi A)/a_0} \quad (4.3.24)$$

$$w_e = \frac{w}{1 + a_0/(\pi A)} \quad (4.3.25)$$

respectively; or, by Eq. (4.3.1),

$$\alpha_i = \frac{\alpha - \alpha_{L0}}{1 + (\pi A)/a_0} \quad (4.3.26)$$

$$\alpha_e = \frac{\alpha - \alpha_{L0}}{1 + a_0/(\pi A)} \quad (4.3.27)$$

We can now use Eq. (4.3.27) in Eq. (4.2.4) to solve for the total lift coefficient of the wing. The chord is the only variable that is a function of  $y$ , and the integral of the chord over the wingspan gives the planform area  $S_w$ . Then Eq. (4.2.4) evaluates to

$$C_L = a_0 \alpha_e = \frac{a_0}{1 + a_0/(\pi A)} (\alpha - \alpha_{L0}) \quad (4.3.28)$$



and the effective wing lift slope becomes

$$a = \frac{a_0}{1 + a_0 / (\pi A)} \quad (4.3.29)$$

Equation (4.3.28) gives the lift coefficient of a finite elliptic wing according to Prandtl's classical lifting line theory. Note that in developing this equation we have assumed  $a_0$ ,  $\alpha$ , and  $\alpha_{L0}$  are all constant along the wingspan. This led to the requirement that the chord distribution be elliptic according to Eq. (4.3.21). In reality, the same circulation distribution specified in Eq. (4.3.15) can be achieved through an unlimited number of wing configurations in which the twist ( $\alpha$ ), camber ( $\alpha_{L0}$ ), thickness ( $a_0$ ), and chord are all potential functions of  $y$ . In any case, Eq. (4.3.10) still holds so that an elliptic circulation distribution will always produce an elliptic lift distribution. The implications these alternative wing designs have on drag were considered in detail in Chapter 3.

We can now also compute the induced drag generated on the wing by the trailing vortex sheet. This drag is not due to viscous effects (recall that everything we have considered so far is based on inviscid potential flow), but instead is due to the change in local angle of attack resulting from the induced downwash  $w_i$ . By definition, lift is the component of the aerodynamic force that is normal to the freestream, and drag is the component tangent to the freestream. The section lift coefficient given by Eq. (4.2.3) is therefore not actually lift relative to the wing but the total resultant aerodynamic force coefficient,  $c_r$ , generated by the wing section and acting at an angle  $\alpha_i$  to the direction of lift. However, applying the small angle approximation we get

$$c_l = c_r \cos(\alpha_i) \approx c_r \quad (4.3.30)$$

so that Eq. (4.2.3) still holds to a good approximation. The induced drag coefficient is given by

$$c_{d_i} = c_r \sin(\alpha_i) \approx c_r \alpha_i \quad (4.3.31)$$

and the total induced drag is then the area-weighted average of Eq. (4.3.31) similar to Eq. (4.2.4). Evaluating this integral with the definitions for the induced and effective angles of attack from Eqs. (4.3.26) and (4.3.27) gives

$$\alpha_i = \frac{C_L}{\pi A} \quad (4.3.32)$$

$$C_{D_i} = \frac{C_L^2}{\pi A} \quad (4.3.33)$$

which is the well-known solution first given by Prandtl [10,11].

Equation (4.3.33) was developed under the assumption that the wing has an elliptic lift distribution, which Prandtl [10,11] showed produces the minimum induced drag for a wing of given aspect ratio and lift. A span efficiency factor ( $e_s$ ) can be used to adjust Eq. (4.3.33) for other lift distributions. See Phillips [53]. Equation (4.3.33) is then

$$C_{D_i} = \frac{C_L^2}{\pi A e_s} \quad (4.3.34)$$

where  $e_s = 1$  for any wing with an elliptic lift distribution and  $e_s < 1$  for all other lift distributions.

#### 4.4 Slender Wing Theory

The limitations of classical lifting line theory with respect to aspect ratio were recognized shortly after its publication. Prandtl's model was based on the assumption that the chordwise vorticity distribution at every section of a finite wing is the same as that predicted by classical airfoil theory for a two-dimensional wing. This assumption is only strictly true for wings of infinite aspect ratio. For finite wings, the chordwise vorticity distribution is a function of spanwise location. Deviations from the predictions of classical airfoil theory become more pronounced as aspect ratio is reduced, especially at spanwise sections near the wing tips.

In considering the lower limit of aspect ratio, the works of Munk [77], Bollay [78], and Jones [79] provide analytical relationships for the aerodynamic characteristics of finite wings in the limit as  $A \rightarrow 0$ . Their results form the basis of slender wing theory. Here we present a modified formulation of classical lifting line theory based on their results, which is only valid for small aspect ratios ( $A < 1$ ).

In order to develop a formulation for slender wing theory similar to Eq. (4.3.14), we must first consider several important results obtained through the development of slender wing theory. Munk [77] demonstrated that flow in planes perpendicular to the x-axis of a slender body can be viewed as two-dimensional, and he introduced the concept of an "additional apparent mass,"  $m'$ , that represents the mass of fluid displaced by each chordwise section of the wing as the wing moves into the flow. Jones [79] extended this concept to develop relations for the lift generated by an uncambered slender delta wing. He used Munk's relation for the additional apparent mass,

$$m' = \rho \frac{\pi b^2}{4} dx \quad (4.4.1)$$

which is equivalent to the mass of fluid within a cylindrical volume of diameter  $b$  and length  $dx$ . The momentum imparted to the wing at each chordwise section must balance the momentum imparted to the additional apparent mass of fluid at that chordwise section, so that the lift force on the wing becomes

$$l(x) = V\alpha \frac{dm'}{dt} \quad (4.4.2)$$

The time derivative of the additional apparent mass is given by

$$\frac{dm'}{dt} = \frac{dm'}{dx} \frac{dx}{dt} = \left( \rho \frac{\pi b}{2} \frac{db}{dx} dx \right) V \quad (4.4.3)$$

so that the lift becomes

$$l(x) = \frac{1}{2} \rho V^2 \pi \alpha b \frac{db}{dx} dx \quad (4.4.4)$$

and the lift coefficient becomes

$$c_l(x) = \pi \alpha \frac{db}{dx} \quad (4.4.5)$$

The total lift coefficient generated by the delta wing is then given by integration, as in Eq. (4.2.4), but this time we are integrating over the chord. We get

$$C_L = \frac{1}{S_w} \int_0^c c_l(x) b dx = \frac{\pi \alpha}{2} \frac{b_{\max}^2}{S_w} = \frac{\pi A}{2} \alpha \quad (4.4.6)$$

since, for any delta wing,  $b = 0$  at  $x = 0$  and  $b = b_{\max}$  at  $x = c$ . This gives for the lift slope of a slender delta wing

$$a = \frac{\pi A}{2} \quad (4.4.7)$$

which is the well-known result from Jones [79].

Jones then made three observations critical to our current development. The first is that, in order to satisfy the Kutta condition, only sections of increasing span (i.e.  $db/dx > 0$ ) can generate lift, so that the use of  $b_{\max}$  in Eq. (4.4.6) is general for any planform regardless of the chordwise location at which  $b_{\max}$  actually occurs. The second, which Jones demonstrated through a development of the surface potential, is that the spanwise lift distribution of a slender wing is elliptical and independent of chord distribution. The third observation, which also came about through Jones' development of the surface potential, is that the vorticity distribution

of a slender wing is concentrated at the leading edge of the wing, so that the aerodynamic center is also located at the leading edge. We expect these observations to be true for any viable formulation of the slender wing problem.

We now proceed to cast Eq. (4.3.14) in terms of these findings. First we consider the system of horseshoe vortices that must be used to represent a slender wing. In Figure 4.1, the system of horseshoe vortices from classical lifting line theory is shown with the lifting line located at the quarter-chord of the wing, which corresponds to the aerodynamic center for wings of infinite span. Jones [79] demonstrated that the aerodynamic center of a slender wing is located at the leading edge of the wing. Küchemann [73] therefore proposed moving the lifting line from the quarter-chord to the leading edge when evaluating slender wings, and – to represent the infinite chord-to-span ratio of slender wings – placing the leading edge of the wing at  $x = -\infty$ .

With this modified system of horseshoe vortices, the only change needed to Eqs. (4.3.4) and (4.3.7) is the lower limit of integration, so that Eq. (4.3.8) becomes

$$dw_i(y) = \frac{d\Gamma(\eta)}{2\pi(y-\eta)} \quad (4.4.8)$$

and the induced downwash becomes

$$w_i(y) = \frac{1}{2\pi} \int_{\eta=-b/2}^{b/2} \frac{d\Gamma(\eta)/d\eta}{y-\eta} d\eta \quad (4.4.9)$$

Next we consider the effective downwash generated by slender wings. Küchemann [73] states – and it is obvious from Eq. (4.4.6) that he is correct – that  $C_L \rightarrow 0$  as  $A \rightarrow 0$ , so that the effective downwash must also go to zero. Thus  $w_e \ll w_i$  by Eq. (4.3.2) and we can write, to a good approximation,

$$\frac{1}{2\pi V_\infty} \int_{\eta=-b/2}^{b/2} \frac{d\Gamma(\eta)/d\eta}{y-\eta} d\eta = \alpha - \alpha_{L0} \quad (4.4.10)$$

There is only one possible solution to Eq. (4.4.10), namely

$$\Gamma(y) = wb \sqrt{1 - \left(\frac{2y}{b}\right)^2} \quad (4.4.11)$$

which is both elliptic and independent of chord distribution in agreement with the observations of Jones [79] stated earlier. Note that Eq. (4.4.11) differs by a factor of 2 from the elliptic circulation distribution given by

Eqs. (4.3.15) and (4.3.23) in the limit as  $A \rightarrow 0$ . The lift can now be found by integrating Eq. (4.3.10) over the span. In nondimensional form we get

$$C_L = \frac{2}{V_\infty S_w} \int_{-b/2}^{b/2} \rho V_\infty \Gamma(y) dy = \frac{\pi A}{2} (\alpha - \alpha_{L0}) \quad (4.4.12)$$

which agrees exactly with the lift slope predicted by Jones [79], Eq. (4.4.7).

Previous works on slender wing theory have ended at this point, and we are left with Eq. (4.4.10) as our lifting line theory equivalent of slender wing theory. However, there is one additional step we can take due to the knowledge that our circulation distribution is elliptic according to Eq. (4.4.11). Recall that the induced and effective downwashes produced by a high-aspect-ratio wing with elliptic circulation, Eqs. (4.3.24) and (4.3.25) respectively, are constant over the span. Since our slender wing solution is forced to an elliptic circulation distribution, we conjecture that the two components of downwash are constant in this case as well. Then from Eq. (4.2.4) and (4.4.12) we have

$$C_L = a_0 \alpha_e = \frac{\pi A}{2} (\alpha - \alpha_{L0}) \quad (4.4.13)$$

Solving for  $\alpha_e$  and multiplying by  $V_\infty$ , we get

$$w_e = \frac{\pi A}{2a_0} w \quad (4.4.14)$$

Solving Eq. (4.4.11) for  $w$  and substituting, we get

$$w_e = \frac{2\Gamma}{a_0 \left[ \frac{4\bar{c}}{\pi} \sqrt{1 - \left( \frac{2y}{b} \right)^2} \right]} \quad (4.4.15)$$

which is identical to Eq. (4.3.13) except that the actual spanwise chord distribution has been replaced by the elliptic chord distribution of Eq. (4.3.21). Thus for elliptic wings, Eqs. (4.3.13) and (4.4.15) are equivalent. This again agrees with the observations of Jones [79] stated earlier, specifically that the results for a slender wing are independent of chord distribution.

By Eqs. (4.4.9) and (4.4.15) we now have for our slender wing lifting line equation

$$\frac{2\Gamma}{V_\infty a_0 \left[ \frac{4\bar{c}}{\pi} \sqrt{1 - \left( \frac{2y}{b} \right)^2} \right]} + \frac{1}{2\pi V_\infty} \int_{\eta=-b/2}^{b/2} \frac{d\Gamma(\eta)/d\eta}{y-\eta} d\eta = \alpha - \alpha_{L0} \quad (4.4.16)$$

Eq. (4.4.16) is a more complete statement of slender wing theory than has been presented previously. Results computed using Eq. (4.4.16) are nearly identical to those computed using the slender wing theory of Jones [79] for aspect ratios less than about 1, which is typically considered the upper limit for slender wing theory. Inclusion of the effective downwash term, however, offers important insights as we look to combine slender wing theory and classical lifting line theory into a single theory applicable for all aspect ratios. We shall refer to this formulation hereinafter as the “modified slender wing equation.”

#### 4.5 Lifting Surface Theory

Early efforts to extend the concepts of lifting line theory to wings of low aspect ratio began with the works of Birnbaum [70] and Blenk [71] and developed into what is known today as lifting surface theory. Blenk [71] was able to show good results for aspect ratios down to about 1 by replacing the single lifting line in Prandtl’s formulation with a chordwise distribution of lifting lines, thus forming a lifting surface. His overall formulation, however, was limited to a single finite wing of rectangular planform in inviscid, incompressible flow. He attributed the error for aspect ratios less than one to nonlinear effects that could not be accounted for in his linear formulation.

Zimmerman [80,81] and Winter [82] performed experimental studies on low-aspect-ratio wings. They attributed the divergence between their results and lifting surface theory to stalling phenomena that could not be treated with inviscid theoretical methods. Bollay [78] later developed analytical solutions for a flat rectangular plate in which he attributed the phenomena seen by the aforementioned experimenters to the finite angle at which the trailing vortices leave the plate.

The only purely analytical solution of lifting surface theory currently available in the literature is that of Hauptman and Miloh [83]. By assuming an elliptic planform with a straight midchord, they derived the acceleration potential (see Prandtl [84]) in terms of ellipsoidal harmonics and applied this to a linearized formulation of lifting surface theory. The result was a set of closed-form equations for spanwise lift as a function of aspect ratio. While Hauptman and Miloh [83] state that these equations “are exact within the realm of the linear theory,” the equations are too cumbersome to apply practically as they involve evaluation of the complete elliptic integral of the second kind (see Hauptman and Miloh [85], Smith [86], and Laitone [87]) and, for spanwise distributions, evaluation of infinite summations that do not readily converge.

Using numerical calculations from lifting surface theory, several authors have proposed empirical and semi-empirical expressions for the lift slope of low-aspect-ratio wings. Some of the more interesting proposals come from Jones [88], Helmbold [89], Van Dyke [90], Germain [91], Kida and Miyai [92], and Laitone [87]; but there are many others. Unfortunately, none of these provide spanwise lift distributions in their developments, but only provide equations for the total lift coefficient produced by a wing as a function of aspect ratio. Küchemann [73], on the other hand, presents a very elegant method for correcting the two components of downwash in classical lifting line theory, Eq. (4.3.14), which does allow for the calculation of spanwise lift distributions. He facilitates this by assuming that the effects of aspect ratio are uniform over the span, which is obviously not true near the wing tips, but Küchemann [73] observes that “the error cannot be serious, however, as the lift falls to zero there.”

#### 4.6 A Unifying Formulation of Lifting Line, Slender Wing, and Lifting Surface Methods

Without considering spanwise lift distributions (since most of the methods mentioned above lack sufficient development to facilitate consideration of such), we shall here present a unifying formulation of the three theories described above for calculating the wing lift coefficients. All the methods presented here consider only an elliptic planform in their development. Most consider a straight quarter-chord line while some – namely Hauptman and Miloh [83] and Küchemann [73] – consider a straight mid-chord. Panair results given in Figure H.6 of Appendix H show little difference between the two, so we shall not attempt any correction to the methods based on where the straight chord line is located.

In general, the lift coefficient of a finite wing has already been given as

$$C_L = \frac{1}{S_w} \int_{y=-b/2}^{b/2} c_l c(y) dy = \frac{1}{S_w} \int_{y=-b/2}^{b/2} a_0 \alpha_e c(y) dy \quad (4.2.4)$$

where

$$\alpha_e = (\alpha - \alpha_{L0}) - \alpha_i \quad (4.2.2)$$

For an elliptic wing, the effective and induced angles of attack predicted by classical lifting line theory are constant over the wingspan and Eq. (4.2.4) becomes

$$C_L = a_0 \alpha_e = a_0 (\alpha - \alpha_{L0} - \alpha_i) \quad (4.6.1)$$

The induced angle of attack is related to the lift coefficient according to Eq. (4.3.32),

$$\alpha_i = \frac{C_L}{\pi A} \quad (4.3.32)$$

and by definition the effective wing lift slope is related to the lift coefficient according to

$$C_L = a(\alpha - \alpha_{L0}) \quad (4.6.2)$$

Using Eqs. (4.3.32) and (4.6.2) in Eq. (4.6.1) and solving for  $a$  we get

$$a_{\text{classical}} = \left( \frac{1}{a_0} + \frac{1}{\pi A} \right)^{-1} \quad (4.6.3)$$

where we have designated this coefficient with the subscript “classical” to indicate it is the effective lift slope predicted by classical lifting line theory. This equation is strikingly similar to that commonly used to determine the total resistance in a circuit of two parallel resistors, namely

$$R_{\text{tot}} = \left( \frac{1}{R_1} + \frac{1}{R_2} \right)^{-1} \quad (4.6.4)$$

where, by analogy,  $a_0$  is the resistance of the first resistor and  $C_L/\alpha_i = \pi A$  is the resistance of the second.

We shall use this analogy in comparing the equations of Refs. [10,73,79,83,88–91] by casting the wing lift slope given by each method in the form of Eq. (4.6.4) and comparing the values of  $R_1$  and  $R_2$ .

Additionally, we also wish to consider the limits of  $a$  for the two bounding conditions. From Eq. (4.6.3) we get

$$\lim_{A \rightarrow \infty} a_{\text{classical}} = a_0 \quad (4.6.5)$$

which is the exact value predicted by classical airfoil theory, and

$$\lim_{A \rightarrow 0} a_{\text{classical}} = \pi A \quad (4.6.6)$$

which is twice the value predicted by slender wing theory, Eq. (4.4.7).

From slender wing theory, Jones [79] gives

$$a_{\text{slender}} = \frac{\pi A}{2} \quad (4.6.7)$$

By comparison to Eq. (4.6.4),  $R_1 = \infty$  and  $R_2 = \pi A/2$ , and the trivial bounding limits are

$$\lim_{A \rightarrow \infty} a_{\text{slender}} = \lim_{A \rightarrow 0} a_{\text{slender}} = \frac{\pi A}{2} \quad (4.6.8)$$

The modified slender wing equation – Eq. (4.4.16) – gives for the wing lift slope



$$a_{\text{modified\_slender}} = \left( \frac{1}{a_0} + \frac{2}{\pi A} \right)^{-1} \quad (4.6.9)$$

which has the limits

$$\lim_{A \rightarrow \infty} a_{\text{modified\_slender}} = a_0 \quad (4.6.10)$$

$$\lim_{A \rightarrow 0} a_{\text{modified\_slender}} = \frac{\pi A}{2} \quad (4.6.11)$$

Now let us consider some of the other proposals that attempt to bridge the gap between the two bounding theories. Helmbold [89] proposed

$$a_{\text{Helmbold}} = \frac{a_0}{\sqrt{1 + \frac{a_0^2}{(\pi A)^2}} + \frac{a_0}{\pi A}} \quad (4.6.12)$$

which, when recast in the form of Eq. (4.6.4), gives

$$a_{\text{Helmbold}} = \left( \sqrt{\frac{1}{a_0^2} + \frac{1}{(\pi A)^2}} + \frac{1}{\pi A} \right)^{-1} \quad (4.6.13)$$

Helmbold's equation is especially remarkable because it is quite elegant compared to the other proposals and gives the correct limits for both the upper and lower bounds of aspect ratio, namely

$$\lim_{A \rightarrow \infty} a_{\text{Helmbold}} = a_0 \quad (4.6.14)$$

$$\lim_{A \rightarrow 0} a_{\text{Helmbold}} = \frac{\pi A}{2} \quad (4.6.15)$$

It was also proposed much earlier than most of the other methods considered here, including Jones' slender wing theory [79].

Before publishing his paper on slender wing theory, Jones [88] used potential flow theory to show that the ratio of velocity around the edge of an infinite elliptic wing to that around the edge of a finite wing is equal to the ratio of parameters  $E$  for the wings, where  $E$  is itself a ratio of the semiperimeter to the span. The parameter  $E$  for an infinite wing is 1 so that the ratio of velocities becomes  $1/E$ . Jones then proposed adjusting the wing lift coefficient according to the relation

$$a_{\text{Jones}} = a_0 \frac{A}{EA + a_0/\pi} \quad (4.6.16)$$

or, in the form of Eq. (4.6.4)

$$a_{\text{Jones}} = \left[ \frac{E}{a_0} + \frac{1}{\pi A} \right]^{-1} \quad (4.6.17)$$

This equation has the upper and lower limits of

$$\lim_{A \rightarrow \infty} a_{\text{Jones}} = a_0 \quad (4.6.18)$$

$$\lim_{A \rightarrow 0} a_{\text{Jones}} = \frac{\pi a_0 A}{\pi + a_0} \quad (4.6.19)$$

Van Dyke [90] approached this problem as a singular perturbation problem in which the span and chord are primary and secondary characteristic dimensions, respectively. He presented a third-order approximation to the lift slope equation as

$$a_{\text{VanDyke}} = \frac{a_0}{1 + \frac{a_0}{\pi A} + \left( \frac{2a_0}{\pi^2 A} \right)^2 \left[ \ln(\pi A) - \frac{9}{8} \right]} \quad (4.6.20)$$

Recast in the form of Eq. (4.6.4), Eq. (4.6.20) becomes

$$a_{\text{VanDyke}} = \left\{ \frac{1}{a_0} + \frac{1 + \frac{4a_0}{\pi^3 A} \left[ \ln(\pi A) - \frac{9}{8} \right]}{\pi A} \right\}^{-1} \quad (4.6.21)$$

with upper and lower limits of

$$\lim_{A \rightarrow \infty} a_{\text{VanDyke}} = a_0 \quad (4.6.22)$$

$$\lim_{A \rightarrow 0} a_{\text{VanDyke}} = \frac{\pi^4 A^2}{4a_0 \ln(\pi A)} \quad (4.6.23)$$

Van Dyke's equation provides reasonable accuracy for aspect ratios above about 2, but fails to converge to the correct limit as  $A \rightarrow 0$ . Even worse, it has an asymptote at about  $A = 0.4749$  and approaches the lower limit from the wrong direction. Germain [91] presented a modified version of Van Dyke's equation which somewhat alleviated these concerns. Germain's original equation perpetuated an error introduced by Van Dyke, which Van Dyke later corrected [93] to give

$$a_{\text{Germain}} = \frac{a_0}{1 + \frac{a_0}{\pi A} + \frac{4a_0^2}{(\pi A)^2} \left[ \ln(1 + \pi e^{-9/8} A) \right]} \quad (4.6.24)$$

which can be rearranged as

$$a_{\text{Germain}} = \left( \frac{1}{a_0} + \frac{1 + \frac{4a_0}{\pi^3 A} \left[ \ln(1 + \pi e^{-9/8} A) \right]}{\pi A} \right)^{-1} \quad (4.6.25)$$

This equation eliminates the asymptote found in Van Dyke's equation, and the lower limit

$$\lim_{A \rightarrow 0} a_{\text{Germain}} = \frac{\pi^2 A}{\pi + 8e^{-9/8}} \approx 1.72A \quad (4.6.26)$$

comes within about 10% of that predicted by slender wing theory.

Hauptman and Miloh [83] have provided closed-form expressions for the wing lift slope based on the acceleration potential of an ellipse (see Prandtl [84]) and a linearized formulation of lifting surface theory.

Their derivation resulted in a piecewise formulation, namely

$$a_{\text{Hauptman\&Miloh}} = \begin{cases} \frac{4k}{1 + \frac{E^2(h)}{1 + (k^2/h) \ln(1/k + h/k)}}, & k = \frac{\pi A}{4} \leq 1 \\ \frac{4}{k + \frac{E^2(h)}{k + \sin^{-1}(h)/h}}, & k = \frac{4}{\pi A} \leq 1 \end{cases} \quad (4.6.27)$$

where  $h$  is the eccentricity of the ellipse,  $k = \sqrt{1-h^2}$ , and  $E(h)$  is the complete elliptic integral of the second kind. Note that, by definition, the eccentricity of an ellipse is always real and between the limits of 0 and 1, i.e.  $0 \leq h \leq 1$ . Also note that Eq. (4.6.27) was taken from Laitone [87], as it corrects a typo in the original paper of Hauptman and Miloh [83]. Rearranging Eq. (4.6.27) gives

$$a = \begin{cases} \left[ \frac{E^2(h)}{\pi A + (4k^3/h) \ln(1/k + h/k)} + \frac{1}{\pi A} \right]^{-1}, & k = \frac{\pi A}{4} \leq 1 \\ \left[ \frac{E^2(h)}{4(k + \sin^{-1}(h)/h)} + \frac{1}{\pi A} \right]^{-1}, & k = \frac{4}{\pi A} \leq 1 \end{cases} \quad (4.6.28)$$

This function approaches the correct limits for both slender and infinite wings, namely

$$\lim_{A \rightarrow \infty} a_{\text{Hauptman\&Miloh}} = 2\pi \quad (4.6.29)$$

$$\lim_{A \rightarrow 0} a_{\text{Hauptman\&Miloh}} = \frac{\pi A}{2} \quad (4.6.30)$$

However, the section lift slope  $a_0$  does not appear explicitly in Eq. (4.6.27) due to the method by which it was derived, and it is unclear how to correct this equation for section lift slopes other than  $2\pi$ .

The last equation that we shall consider from the literature is that of Küchemann [73]. Küchemann uses the flat plate distribution of Birnbaum [70] to demonstrate that classical lifting line theory can actually be considered a lifting surface theory. Birnbaum [70] showed that the pressure distribution over a flat infinite plate at angle of attack is given by

$$\Delta C_p(x) = -\frac{2C}{V_\infty} \left( \frac{1-x/c}{x/c} \right)^{1/2} \quad (4.6.31)$$

which can similarly be expressed as a continuous sheet of vorticity  $\gamma_x(x)$  through the Kutta-Joukowski law, where the coefficient  $C$  must be determined. The section lift is given by

$$c_l = -\frac{1}{c} \int_0^c \Delta C_p dx \quad (4.6.32)$$

Inserting Eq. (4.6.31) into Eq. (4.6.32) and performing the integration gives

$$c_l = \frac{\pi}{V_\infty} C \quad (4.6.33)$$

or, rearranging,

$$C = \frac{V_\infty}{\pi} c_l \quad (4.6.34)$$

The effective downwash can now be determined by applying the Biot-Savart Law,

$$w_e = -\frac{1}{4\pi c} \int_0^c \int_0^c \Delta C_p(x') \frac{dx'}{x-x'} dx = \frac{C}{2} \quad (4.6.35)$$

Combining Eqs. (4.6.34) and (4.6.35), we get

$$c_l = 2\pi\alpha_e \quad (4.6.36)$$

which gives the section lift slope of a thin airfoil. This demonstrates that using a section lift slope of  $a_0 = 2\pi$  in classical lifting line theory is equivalent to a lifting surface theory with the chordwise pressure distribution of Eq. (4.6.31). Other pressure distributions will result in a different section lift slope, so that the chordwise pressure distribution of any section can be incorporated into classical lifting line theory through the use of an appropriate section lift slope.

Küchemann [73] then showed that a slightly modified pressure distribution,

$$\Delta C_p(x) = -\frac{2C}{V_\infty} \left( \frac{1-x/c}{x/c} \right) \quad (4.6.37)$$

can be used to obtain the slender wing results of Jones [79] in a similar manner. The obvious parallels between Eqs. (4.6.31) and (4.6.37) led Küchemann [73] to propose a more general distribution, namely

$$\Delta C_p(x) = -\frac{2C}{V_\infty} \left( \frac{1-x/c}{x/c} \right)^n \quad (4.6.38)$$

where the parameter  $n$  can be defined such that a smooth transition occurs between the chordwise distributions of Eqs. (4.6.31) and (4.6.37). Using Eq. (4.6.38) in Eq. (4.6.32) and performing the integration gives

$$C = \frac{V_\infty}{2} \frac{\sin \pi n}{\pi n} c_l \quad (4.6.39)$$

Applying the Biot-Savart Law, Eq. (4.6.35), gives

$$c_l = \frac{4\pi n}{1 - \pi n \cot \pi n} \alpha_e \quad (4.6.40)$$

The coefficient in front of  $\alpha_e$  can be interpreted as the “effective” section lift slope. Note that, for added generality,  $2\pi$  in the numerator can be replaced with  $a_0$ .

The only known requirements on  $n$  are that it must go to 1 in the limit  $A \rightarrow 0$  and it must go to  $1/2$  in the limit  $A \rightarrow \infty$ . On this basis Küchemann [73] proposed, somewhat arbitrarily, to use

$$n = 1 - \frac{1}{2} \left[ 1 + \left( \frac{a_0}{\pi A} \right)^2 \right]^{-1/4} \quad (4.6.41)$$

Noting the similarities between Eqs. (4.3.9) and (4.4.9), Küchemann [73] then proposed multiplying the induced downwash term by the same parameter  $n$ . The result was an expression similar to Eqs. (4.3.14) and (4.4.16), from classical lifting line theory and slender wing theory respectively, but general enough to be applied over the whole range of aspect ratio,

$$\frac{2\Gamma(y)}{V_\infty a_0 c(y)} \left( \frac{1 - \pi n \cot(\pi n)}{2n} \right) + \frac{n}{2\pi V_\infty} \int_{\eta=-b/2}^{b/2} \frac{d\Gamma(\eta)/d\eta}{y-\eta} d\eta = \alpha - \alpha_{L0} \quad (4.6.42)$$

By assuming an elliptic lift distribution and following the same methodology as was used to arrive at Eq. (4.3.29), the wing lift slope resulting from this equation can be determined. It is

$$a_{\text{Küchemann}} = \frac{2na_0}{1 - \pi n \cot(\pi n) + \frac{4n^2 a_0}{\pi A}} \quad (4.6.43)$$

or, recast in the form of Eq. (4.6.4),

$$a_{\text{Küchemann}} = \left[ \frac{1 - \pi n \cot(\pi n)}{2na_0} + \frac{2n}{\pi A} \right]^{-1} \quad (4.6.44)$$

The limits of this equation are

$$\lim_{A \rightarrow \infty} a_{\text{Küchemann}} = a_0 \quad (4.6.45)$$

$$\lim_{A \rightarrow 0} a_{\text{Küchemann}} = \frac{\pi A}{2} \quad (4.6.46)$$

What is significant here is that Küchemann [73] has provided us with a mechanism whereby any formulation cast in the form of Eq. (4.6.4), with definitions for  $R_1$  and  $R_2$ , can be directly implemented in the more general lifting line equation

$$\frac{2\Gamma(y)}{V_\infty a_0 c(y)} \left( \frac{a_0}{R_1} \right) + \frac{1}{4\pi V_\infty} \left( \frac{\pi A}{R_2} \right) \int_{\eta=-b/2}^{b/2} \frac{d\Gamma(\eta)/d\eta}{y-\eta} d\eta = \alpha - \alpha_{L0} \quad (4.6.47)$$

This equation can be solved in the same manner as Eq. (4.3.14).

Let us consider again the elliptic circulation distribution given by Eq. (4.3.15), namely

$$\Gamma(y) = \Gamma_0 \sqrt{1 - \left( \frac{2y}{b} \right)^2} \quad (4.3.15)$$

but this time applied to the general lifting line equation, Eq. (4.6.47). The induced downwash is given by

$$(w_i)_{\text{elliptic}} = \frac{1}{4\pi} \left( \frac{\pi A}{R_2} \right) \int_{\eta=-b/2}^{b/2} \frac{d\Gamma(\eta)/d\eta}{y-\eta} d\eta = -\frac{\Gamma_0}{\pi b^2} \left( \frac{\pi A}{R_2} \right) \int_{\eta=-b/2}^{b/2} \frac{\eta}{y-\eta} \left[ 1 - \left( \frac{2\eta}{b} \right)^2 \right]^{-1/2} d\eta \quad (4.6.48)$$

which, following the same solution procedure as before (see Eqs. (4.3.17) and (4.3.18)), reduces to

$$(w_i)_{\text{elliptic}} = \frac{\Gamma_0}{2b} \left( \frac{\pi A}{R_2} \right) \quad (4.6.49)$$

The effective downwash, following the same reasoning as was given with Eqs. (4.3.20)-(4.3.22), is then

$$(w_e)_{\text{elliptic}} = \frac{\pi \Gamma_0}{2a_0 c} \left( \frac{a_0}{R_1} \right) \quad (4.6.50)$$

In applying the elliptic chord distribution from Eq. (4.3.21) here, we have relied on the assumptions that both  $a_0$  and  $R_1$  are constant over the wingspan. Substituting the right hand sides of Eqs. (4.6.49) and (4.6.50) into Eq. (4.3.2) and solving for  $\Gamma_0$ , we get

$$\Gamma_0 = \frac{2wb}{\pi A} \left( \frac{1}{R_1} + \frac{1}{R_2} \right) \quad (4.6.51)$$

Substitution of Eq. (4.6.51) into Eqs. (4.6.49) and (4.6.50) now gives

$$w_i = \frac{w}{1 + R_2/R_1} \quad (4.6.52)$$

$$w_e = \frac{w}{1 + R_1/R_2} \quad (4.6.53)$$

respectively; or, by Eq. (4.3.1),

$$\alpha_i = \frac{\alpha - \alpha_{L0}}{1 + R_2/R_1} \quad (4.6.54)$$

$$\alpha_e = \frac{\alpha - \alpha_{L0}}{1 + R_1/R_2} \quad (4.6.55)$$

The total lift coefficient of the wing is found by integrating Eq. (4.2.4) over the wingspan with the effective angle of attack given by Eq. (4.6.55). This gives

$$C_L = a_0 \alpha_e = \frac{a_0}{1 + R_1/R_2} (\alpha - \alpha_{L0}) \quad (4.6.56)$$

and the effective wing lift slope becomes

$$a = \frac{a_0}{1 + R_1/R_2} \quad (4.6.57)$$

Equation (4.6.56) can be rewritten in terms of induced angle of attack as

$$C_L = a_0 \alpha_i \left( \frac{R_2}{R_1} \right) \quad (4.6.58)$$

so that the drag coefficient is now

$$C_{D_i} = \frac{C_L^2}{a_0} \left( \frac{R_1}{R_2} \right) \quad (4.6.59)$$

in contrast to Eq. (4.3.33). Note that Eqs. (4.6.58) and (4.6.59) reduce to Eqs. (4.3.32) and (4.3.33) when the resistance values from classical lifting line theory – see Eq. (4.6.3) – are used. Similar relations can be obtained for the lift and drag coefficients based on the other low-aspect-ratio formulations discussed above.

We can derive an aspect ratio efficiency factor similar to the span efficiency factor discussed in Sec. 4.3 by direct comparison of Eqs. (4.6.59) and (4.3.34). The aspect ratio efficiency factor,  $e_A$ , is then

$$e_A = \frac{a_0 R_2}{\pi A R_1} \quad (4.6.60)$$

Note, however, that this efficiency factor only considers the effects of aspect ratio and does not account for deviations from the elliptic lift distribution. It is therefore not a replacement of the span efficiency factor so that our generalized induced drag equation becomes

$$C_{D_i} = \frac{C_L^2}{\pi A e_s e_A} \quad (4.6.61)$$

where  $e_A \rightarrow 1$  as  $A \rightarrow \infty$  (from classical lifting line theory) and  $e_A \rightarrow 1/2$  as  $A \rightarrow 0$  (from the modified slender wing equation). The span efficiency factor  $e_s$  has the same properties as in Eq. (4.3.34).

While all of the formulations discussed above were developed specifically for untwisted elliptic wings, Eq. (4.6.47) allows us to consider these same relations for other planforms and twist distributions, under the assumption that the effects of aspect ratio are unchanged for these other configurations. We have also assumed in the development of Eq. (4.6.47) that the effects of aspect ratio are felt equally along the wingspan. This last assumption could be removed, however, by allowing  $R_1$  and  $R_2$  to be functions of spanwise location. Doing so, however, would affect the result of the integration so that Eq. (4.6.57) could no longer be used to find the effective wing lift slope  $a$ . In this case a comprehensive solution of Eq. (4.6.47), either analytical or numerical, would be required.

Comparing Eq. (4.6.47) with Eqs. (4.3.14) and (4.4.16) gives the exact values for  $R_1$  and  $R_2$  in the limits as  $A \rightarrow \infty$  and  $A \rightarrow 0$ . These values are summarized in Table 4.1. Note that by Eq. (4.3.21),  $R_1 = \text{const} = a_0$  for an elliptic wing. While the modified slender wing equation and the equations of Helmbold [89], Hauptman and Miloh [83] (assuming a section lift slope of  $a_0 = 2\pi$ ), and Küchemann [73] have the correct limits for wing lift slope, none of them match all of the limits given in Table 4.1 for  $R_1$  and  $R_2$ .



**Table 4.1 Summary of limits for  $R_1$  and  $R_2$** 

Parameter	$\lim_{A \rightarrow \infty}$	$\lim_{A \rightarrow 0}$
$R_1$	$a_0$	$a_0 \frac{4\bar{c}}{\pi c(y)} \sqrt{1 - \left(\frac{2y}{b}\right)^2}$
$R_2$	$\pi A$	$\frac{\pi A}{2}$

It is a simple matter to conceive of other possible forms for  $R_1$  and  $R_2$  than have already been presented.

An alternative equation is here proposed by the author which is both simple and accurate, though developed empirically. It is given in the form of Eq. (4.6.4) as

$$a_{Hodson} = \left\{ \frac{1}{a_0} + \frac{1}{A \left[ \pi - \tan^{-1} \left( \frac{2a_0}{\pi A} \right) \right]} \right\}^{-1} \quad (4.6.62)$$

which gives

$$R_1 = a_0 \quad (4.6.63)$$

$$R_2 = A \left[ \pi - \tan^{-1} \left( \frac{2a_0}{\pi A} \right) \right] \quad (4.6.64)$$

For an elliptic wing, this equation meets all four limit requirements from Table 4.1.

#### 4.7 Results and Discussion

Table 4.2 provides a summary of the equations discussed in the previous section, which includes the values for wing lift slope predicted by these equations in the upper and lower limits of aspect ratio. Tables 4.3 and 4.4 summarize the resistance values to be used in Eqs. (4.6.4) and (4.6.47) for each of the methods considered, including their respective limiting values. While the modified slender wing equation and the equations of Helmbold [89], Hauptman and Miloh [83] (assuming a section lift slope of  $a_0 = 2\pi$ ), and Küchemann [73] have the correct limits for wing lift slope, none of them match all of the limits given in Table 4.1 for  $R_1$  and  $R_2$ . Only Eq. (4.6.62) achieves all the correct limits from Table 4.1. We note, however, that Küchemann [73] does match all the correct limits if the lower limits are taken from Jones' [79] slender wing theory given by Eq. (4.4.12) as opposed to the modified slender wing equation given by Eq. (4.4.16).

**Table 4.2 Comparison of methods for calculating the wing lift slope of a finite elliptic wing**

Method	Equation	Wing Lift Slope ( $a$ )	$\lim_{A \rightarrow \infty} a$	$\lim_{A \rightarrow 0} a$
Classical lifting line theory [10,11]	Eq. (4.6.3)	$a_{\text{classical}} = [1/a_0 + 1/(\pi A)]^{-1}$	$a_0$	$\pi A$
Slender wing theory [79]	Eq. (4.6.7)	$a_{\text{slender}} = \pi A/2$	$\pi A/2$	$\pi A/2$
Modified slender wing equation	Eq. (4.6.9)	$a_{\text{modified\_slender}} = [1/a_0 + 2/(\pi A)]^{-1}$	$a_0$	$\pi A/2$
Helmbold [89]	Eq. (4.6.12)	$a_{\text{Helmbold}} = \frac{a_0}{\sqrt{1 + a_0^2/(\pi A)^2} + a_0/\pi A}$	$a_0$	$\pi A/2$
Jones [88]	Eq. (4.6.16)	$a_{\text{Jones}} = a_0 \frac{A}{EA + a_0/\pi}$	$a_0$	$\frac{\pi a_0 A}{\pi + a_0}$
Van Dyke [90]	Eq. (4.6.20)	$a_{\text{VanDyke}} = \frac{a_0}{1 + a_0/\pi A + [2a_0/(\pi^2 A)]^2 [\ln(\pi A) - \frac{9}{8}]}$	$a_0$	$\frac{\pi^4 A^2}{4a_0 \ln(\pi A)}$
Germain [91]	Eq. (4.6.24)	$a_{\text{Germain}} = \frac{a_0}{1 + \frac{a_0}{\pi A} + \frac{4a_0^2}{(\pi A)^2} [\ln(1 + \pi e^{-9/8} A)]}$	$a_0$	$\frac{\pi^2 A}{\pi + 8e^{-9/8}}$
Hauptman & Miloh [83]	Eq. (4.6.27)	$a_{\text{Hauptman\&Miloh}} = \begin{cases} \frac{4k}{1 + \frac{E^2(h)}{1 + (k^2/h) \ln(1/k + h/k)}}, & k = \frac{\pi A}{4} \leq 1 \\ \frac{4}{k + \frac{E^2(h)}{k + \sin^{-1}(h)/h}}, & k = \frac{4}{\pi A} \leq 1 \end{cases}$	$2\pi$	$\pi A/2$
Küchemann [73]	Eq. (4.6.43)	$a_{\text{Küchemann}} = \frac{2na_0}{1 - \pi n \cot(\pi n) + 4n^2 a_0/(\pi A)}, n = 1 - \frac{1}{2} \left[ 1 + \left( \frac{a_0}{\pi A} \right)^2 \right]^{-1/4}$	$a_0$	$\pi A/2$
Hodson	Eq. (4.6.62)	$a_{\text{Hodson}} = \left\{ 1/a_0 + 1/A \left[ \pi - \tan^{-1} \left( \frac{2a_0}{\pi A} \right) \right] \right\}^{-1}$	$a_0$	$\pi A/2$

**Table 4.3 Comparison of resistance values  $R_l$  from methods for calculating the wing lift slope of a finite elliptic wing**

Method	Equation	$R_l$	$\lim_{A \rightarrow \infty} R_l$	$\lim_{A \rightarrow 0} R_l$
Classical lifting line theory [10,11]	Eq. (4.6.3)	$a_0$	$a_0$	$a_0$
Slender wing theory [79]	Eq. (4.6.7)	$\infty$	$\infty$	$\infty$
Modified slender wing equation	Eq. (4.6.9)	$a_0$	$a_0$	$a_0$
Helmbold [89]	Eq. (4.6.13)	$\left[ \frac{1}{a_0^2} + \frac{1}{(\pi A)^2} \right]^{-1/2}$	$a_0$	$\pi A$
Jones [88]	Eq. (4.6.17)	$a_0/E$	$a_0$	$a_0 A$
Van Dyke [90]	Eq. (4.6.21)	$a_0$	$a_0$	$a_0$
Germain [91]	Eq. (4.6.25)	$a_0$	$a_0$	$a_0$
Hauptman & Miloh [83]	Eq. (4.6.28)	$\frac{\pi A + (4k^3/h) \ln(1/k + h/k)}{E^2(h)}, \quad k = \frac{\pi A}{4} \leq 1$ $\frac{4(k + \sin^{-1}(h)/h)}{E^2(h)}, \quad k = \frac{4}{\pi A} \leq 1$	$2\pi$	$\pi A$
Küchemann [73]	Eq. (4.6.44)	$\frac{2na_0}{1 - \pi n \cot(\pi n)}, \quad n = 1 - \frac{1}{2} \left[ 1 + \left( \frac{a_0}{\pi A} \right)^2 \right]^{-1/4}$	$a_0$	0
Hodson	Eq. (4.6.62)	$a_0$	$a_0$	$a_0$

**Table 4.4** Comparison of resistance values  $R_2$  from methods for calculating the wing lift slope of a finite elliptic wing

Method	Equation	$R_2$	$\lim_{A \rightarrow \infty} R_2$	$\lim_{A \rightarrow 0} R_2$
Classical lifting line theory [10,11]	Eq. (4.6.3)	$\pi A$	$\pi A$	$\pi A$
Slender wing theory [79]	Eq. (4.6.7)	$\pi A/2$	$\pi A/2$	$\pi A/2$
Modified slender wing equation	Eq. (4.6.9)	$\pi A/2$	$\pi A/2$	$\pi A/2$
Helmbold [89]	Eq. (4.6.13)	$\pi A$	$\pi A$	$\pi A$
Jones [88]	Eq. (4.6.17)	$\pi A$	$\pi A$	$\pi A$
Van Dyke [90]	Eq. (4.6.21)	$\frac{\pi A}{1 + \frac{4a_0}{\pi^3 A} \left[ \ln(\pi A) - \frac{9}{8} \right]}$	$\pi A$	$\frac{\pi^4 A^2}{4a_0 \ln(\pi A)}$
Germain [91]	Eq. (4.6.25)	$\frac{\pi A}{1 + \frac{4a_0}{\pi^3 A} \ln(1 + \pi e^{-9/8} A)}$	$\pi A$	$\frac{\pi^2 A}{\pi + 8e^{-9/8}}$
Hauptman & Miloh [83]	Eq. (4.6.28)	$\pi A$	$\pi A$	$\pi A$
Küchemann [73]	Eq. (4.6.44)	$\frac{\pi A}{2n}$	$\pi A$	$\pi A/2$
Hodson	Eq. (4.6.62)	$A \left[ \pi - \tan^{-1} \left( \frac{2a_0}{\pi A} \right) \right]$	$\pi A$	$\pi A/2$

Figure 4.3 compares the wing lift slope calculations from classical lifting line theory, slender wing theory, the modified slender wing equation, Helmbold [89], Küchemann [73], Hauptman and Miloh [83], and the current author with numerical lifting surface results from Kinner [94], Krienes [95], Jordan [96], and Medan [97]. Also included are high-order panel method results computed by the author using Panair [98–100] and described in Appendix H. In these calculations we have modeled an elliptic wing with a uniform, symmetric cross section having a section lift slope of  $a_0 = 2\pi$ .

While the equations of Helmbold [89] and Küchemann [73] show reasonable agreement with the numerical results presented in Figure 4.3, the equations of Hauptman and Miloh [83] and the present author perform better. However, Eq. (4.6.27) from Hauptman and Miloh [83] is a piecewise formulation that requires a solution of the complete elliptic integral of the second kind. These additional complexities in Eq. (4.6.27) make Eq. (4.6.62) a more reasonable choice for any practical applications of the solution method discussed herein.

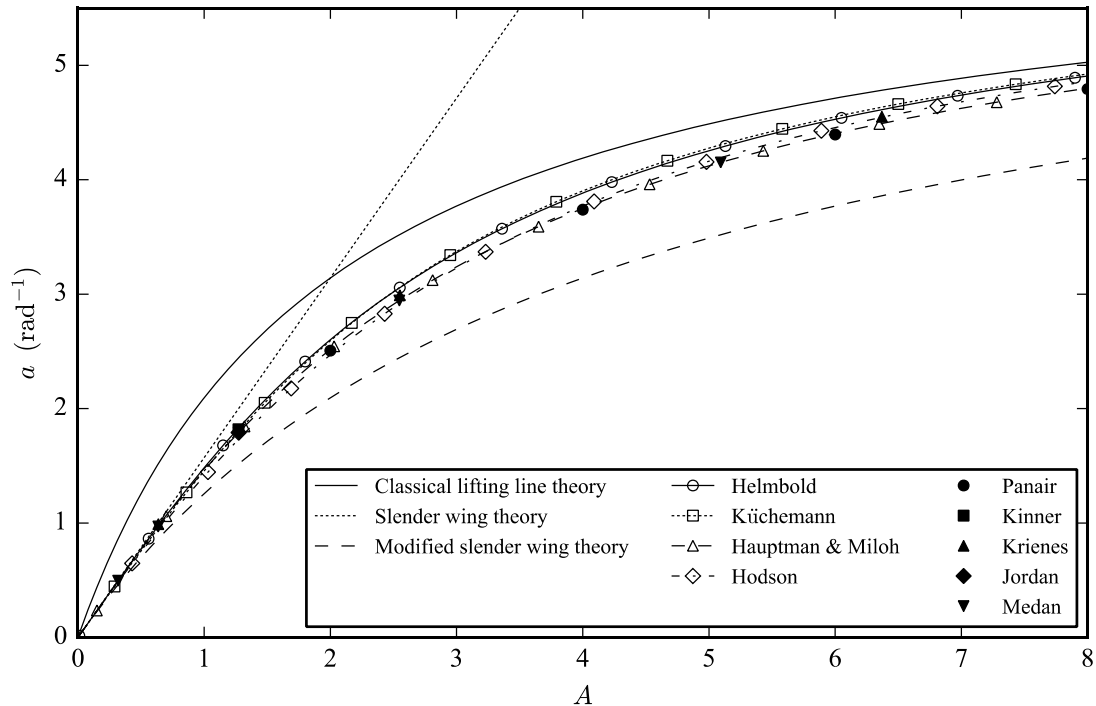


**Figure 4.3 Comparison of lift slope calculation methods applied to a finite elliptic wing**

It is necessary to remember that the equations presented above and summarized in Table 4.2 have been developed specifically for wings of elliptic planform according to Eq. (4.3.21). For arbitrary planforms, the correct value of  $R_l$  must be dependent on spanwise location at low aspect ratio, and the rate at which  $R_l$  transitions between the upper and lower limits cannot be determined from a study of elliptic planforms. Since most wing designs are not elliptic, it is of interest to the present study to consider the validity of the proposed equations to other planform designs. Figures 4.4 and 4.5 provide comparisons of solutions to Eq. (4.6.47) for rectangular and tapered planforms using the resistance values from classical lifting line theory, the modified slender wing equation, and Eqs. (4.6.63)-(4.6.64). Results computed using Panair are also included. Solutions

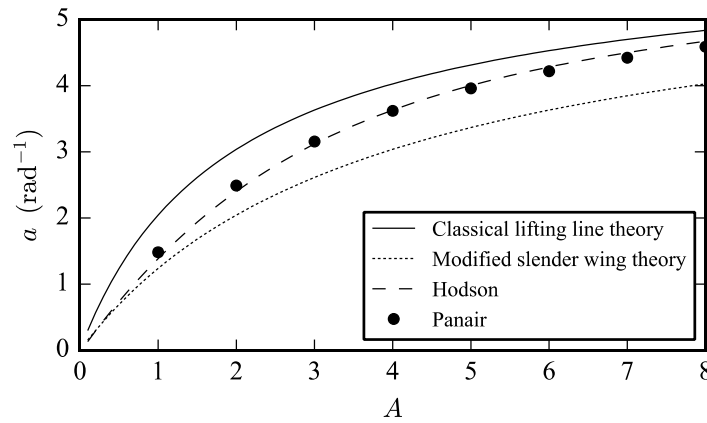


**Figure 4.4 Comparison of lift slope calculation methods applied to a finite rectangular wing**

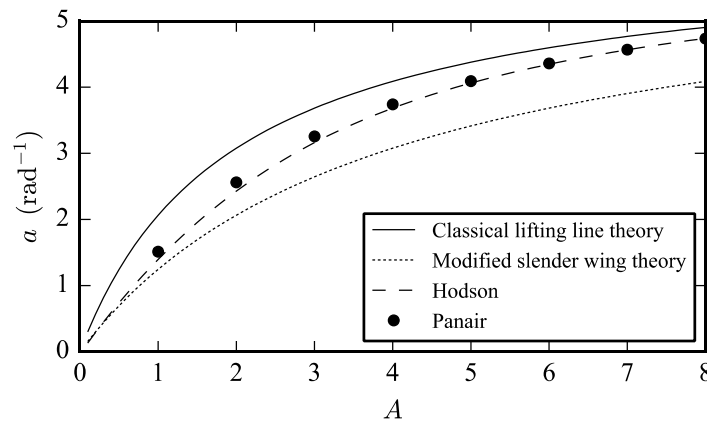


**Figure 4.5 Comparison of lift slope calculation methods applied to a tapered wing with  $R_T = 0.75$**

to Eq. (4.6.47) were obtained using Pralines,<sup>\*</sup> an open-source Fortran code developed by the author. This code is based on the solution procedure presented by Phillips [53], in which Eq. (4.6.47) is approximated as a truncated Fourier sine series. The source code is given in Appendix K.

Despite having been developed specifically for elliptic planforms, the proposed equation shows excellent agreement with the Panair results for the rectangular and tapered planforms considered. It outperforms classical lifting line theory over the full range of aspect ratios for both rectangular and tapered cases.

At this point we have only considered predictions of the total wing lift slope of a finite wing without regard to the spanwise lift distribution. In fact the development presented here has assumed that the influence of aspect ratio beyond that already captured in classical lifting line theory is felt uniformly along the wingspan. Pralines can be used to scrutinize this assumption. For an elliptic wing, Eq. (4.6.47) predicts an elliptic lift distribution (i.e. a constant section lift coefficient), regardless of the resistance values used. This is shown and compared to Panair results in Figure 4.6 for a selection of aspect ratios. The results computed using Eqs. (4.6.63) and (4.6.64) in Eq. (4.6.47) show good agreement with Panair results for  $y/b < 0.4$  regardless of aspect ratio. As expected, larger discrepancies are seen at the wing tips. However, the magnitudes of the discrepancies shown in Figure 4.6 can be misleading since they are scaled by the inverse of the chord length and the chord length goes to zero at the wing tip. Figure 4.7 shows the same data but with the spanwise lift coefficients multiplied by the local chord ratio  $c/\bar{c}$ , which more accurately reflects the relative influence of each spanwise value on the overall wing lift coefficient. From Figure 4.7 we see that the results computed using Eqs. (4.6.63) and (4.6.64) provide excellent agreement with the Panair results over the entire wingspan. There is a slight outward shift of lift when compared to the Panair results, but overall this shift is small – less than half a percent of the total lift generated by the wing.

Figures 4.8 and 4.9 compare lifting line theory and Panair results for rectangular and tapered planforms. The lift coefficients have again been scaled by the local chord ratio  $c/\bar{c}$ , as in Figure 4.7, to better visualize the influence of the spanwise values on the overall lift generated by the wing. The lifting line results based on the resistance values given by Eqs. (4.6.63) and (4.6.64) again do an excellent job of matching the Panair results, though the discrepancies are slightly larger for rectangular and tapered wings than for elliptic wings.

---

<sup>\*</sup> <https://github.com/joddlehod/pralines>

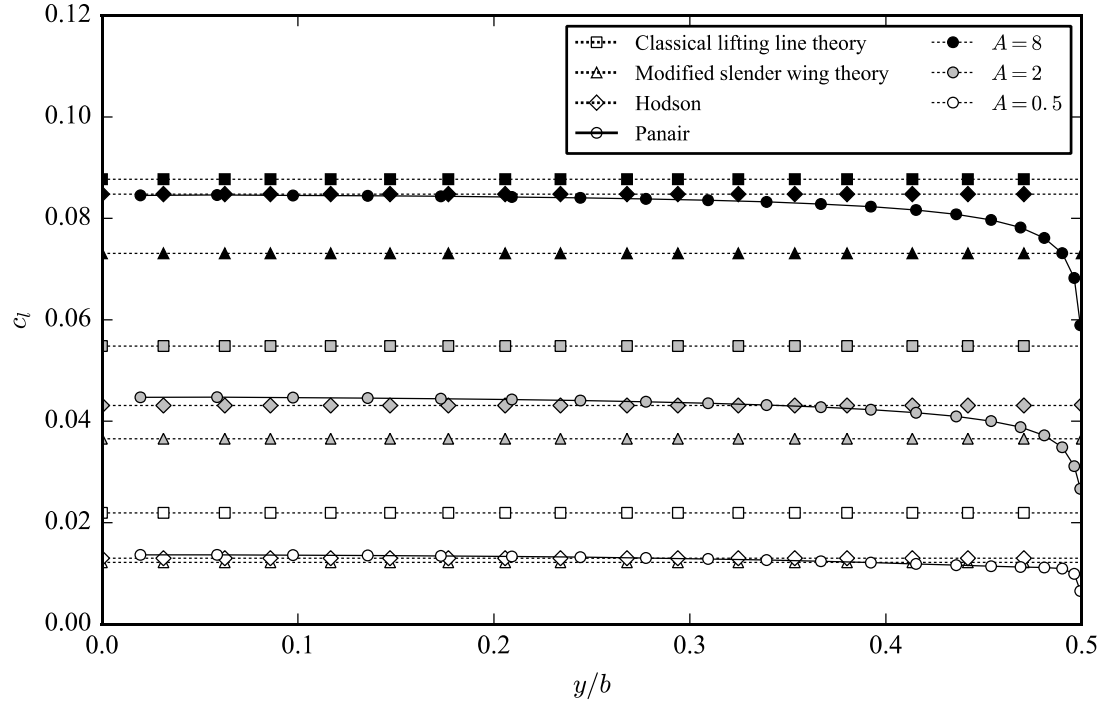


Figure 4.6 Comparison of spanwise lift coefficient distributions for elliptic wings.

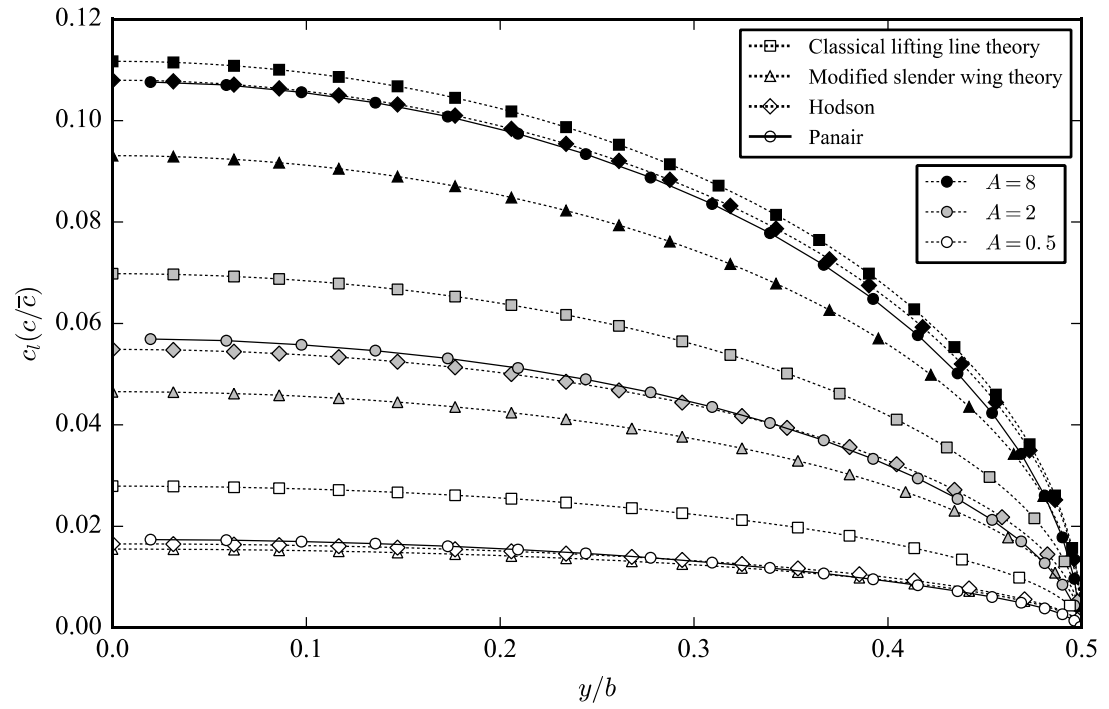


Figure 4.7 Comparison of spanwise lift distributions for elliptic wings.



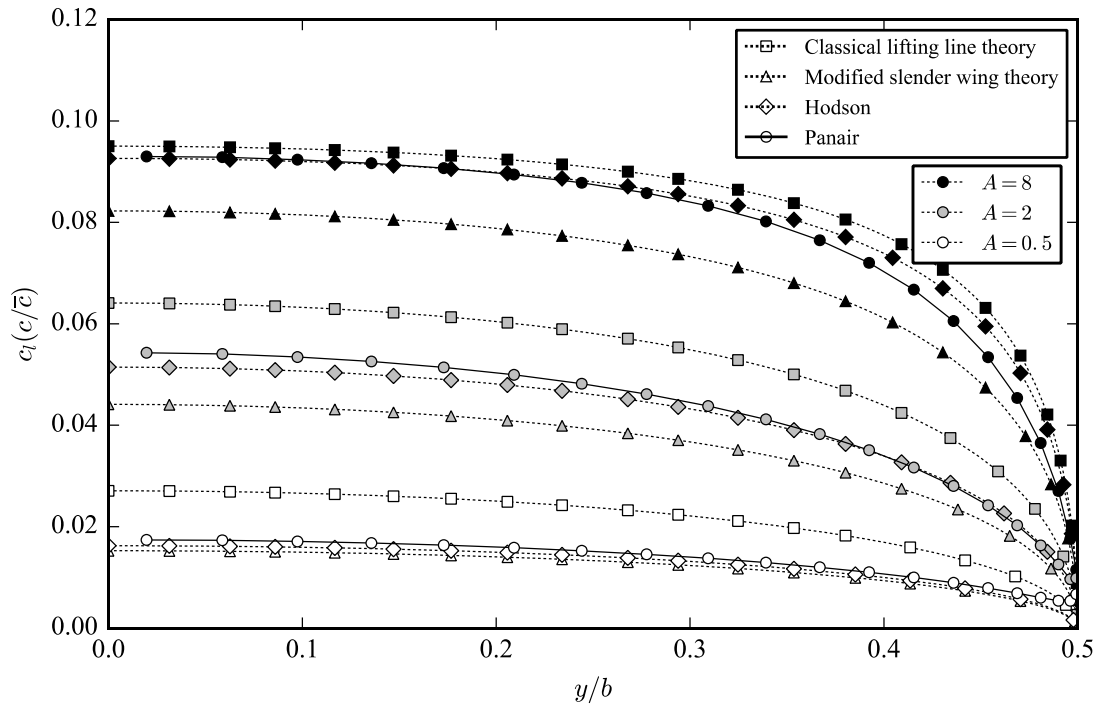


Figure 4.8 Comparison of spanwise lift distributions for rectangular wings.

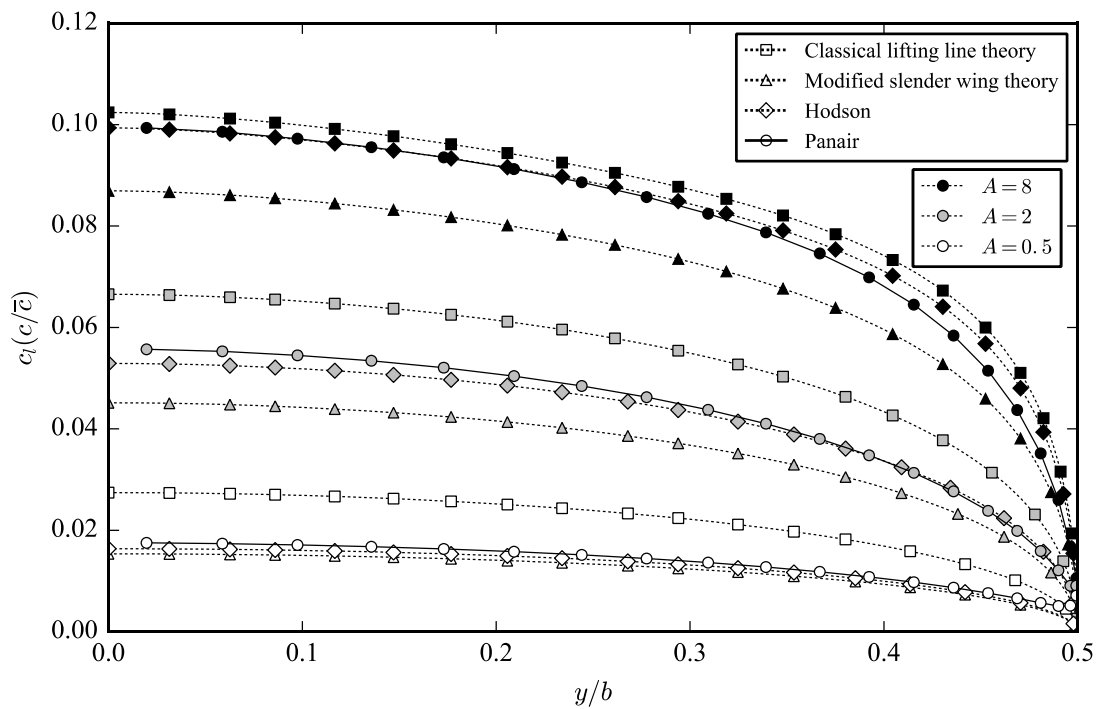
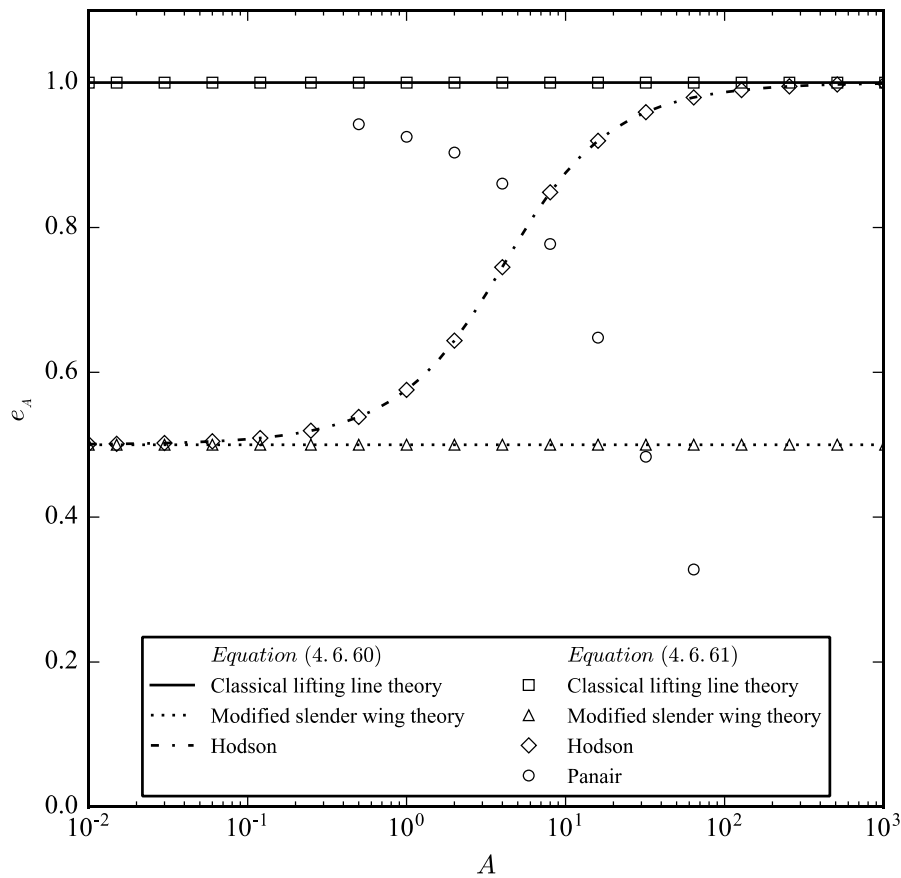


Figure 4.9 Comparison of spanwise lift distributions for tapered wings with  $R_t = 0.75$ .

Finally, we wish to consider how the proposed lifting line formulation affects induced drag calculations. Here we used the same codes, namely Pralines and Panair, to evaluate the lift and drag coefficients of several wings of varying aspect ratios, and then apply Eq. (4.6.61) to compute the aspect ratio efficiency factor for each analysis. These results, along with direct calculations of the aspect ratio efficiency factor using Eq. (4.6.60), are presented in Figure 4.10.

Some difficulty was encountered in obtaining accurate drag results from Panair. In computing lift results, we computed the solution on three different grid sizes and applied Richardson Extrapolation to improve the accuracy of the results. This method could not be applied to the drag results, however, because the results from successively refined grid sizes did not exhibit asymptotic convergence. Instead, each Panair data point presented in Figure 4.10 was computed from a single Panair analysis using a 4%-thick symmetric Joukowski



**Figure 4.10** Sample calculations of the aspect ratio efficiency factor using Pralines and Panair.

airfoil for the cross section and an  $80 \times 80$  grid size. This, however, still did not yield satisfactory results. The Panair data show an inverse trend in  $e_A$  to what is expected, indicating that as aspect ratio increases, both  $\alpha_e$  and  $\alpha_i$  increase. This would seem to violate the boundary condition given by Eq. (4.3.2), bringing into question the validity of the drag calculations produced by Panair.

In contrast, the lifting line results shown in Figure 4.10 agree well with the theory presented in this chapter. The results using classical lifting line theory give an aspect ratio efficiency factor of  $e_A = 1$  regardless of aspect ratio, while the modified slender wing equation gives an aspect ratio efficiency factor of  $e_A = 1/2$ . These represent the theoretical upper and lower limits, respectively, of the aspect ratio efficiency factor. The equation proposed by the present author – see Eqs. (4.6.62)-(4.6.64) – shows a smooth transition between the two limits. While the shape of this transition cannot be confirmed due to the unreliability of the Panair drag results, it can be assumed that the shape is reasonable as it satisfies the boundary condition given by Eq. (4.3.2) and the corresponding lift values have already been shown to be satisfactory. Any alternative would require the influence of an aerodynamic phenomenon that has not been considered here or in the other works reviewed.

## 5 NUMERICAL LIFTING LINE METHOD FOR WINGS OF ARBITRARY ASPECT RATIO

### 5.1 Introduction

In the previous chapter, several equations for the wing lift slope of finite wings have been considered, and a method for modifying classical lifting line theory, Eq. (4.3.14), to match these equations has been presented. This formulation, however, is inapplicable to wings with sweep or dihedral, and is also limited to single isolated lifting surfaces. The numerical lifting line method of Phillips and Snyder [16] is based heavily on classical lifting line theory, but presents a formulation that allows for consideration of sweep, dihedral, and interactions between multiple lifting surfaces. In their original presentation of this method, Phillips and Snyder [16] showed the accuracy to be comparable to numerical panel methods and inviscid computational fluid dynamics solutions, but at a small fraction of the computational cost. It would be advantageous, therefore, to be able to extend the applicability of this numerical formulation to lifting surfaces of low aspect ratio, as was done for classical lifting line theory in the previous section. To do so, we begin with a comprehensive derivation of the method as originally presented by Phillips and Snyder [16]. We will then discuss the necessary modifications to this method to achieve our purpose.

As with classical lifting line theory, a lifting surface in numerical lifting line theory is represented as a series of horseshoe vortices, each horseshoe vortex consisting of a single spanwise vortex segment coincident with the quarter-chord of the wing and two semi-infinite vortex segments extending chordwise downstream. However, in contrast to the overlapping horseshoe vortices shown in Figure 4.1, the lifting surface is composed of non-overlapping, side-by-side horseshoe vortices as shown in Figure 5.1. While a gap is shown between adjacent horseshoe vortices in the figure, this is simply for illustration purposes. In reality, the incoming and outgoing vortex segments of adjacent horseshoe vortices are coincident, and vorticity is shed from the wing at each of these interfaces in an amount equal to the difference in vortex strengths between the two adjacent horseshoe vortices that comprise the interface. While this simple change in arrangement of the horseshoe vortices seems trivial, it affords some significant advantages over the arrangement used in classical lifting line theory. Each horseshoe vortex is now tied to a specific section of the finite wing being modeled, so that the properties of each section are now decoupled from one another. For example, the sweep, dihedral,

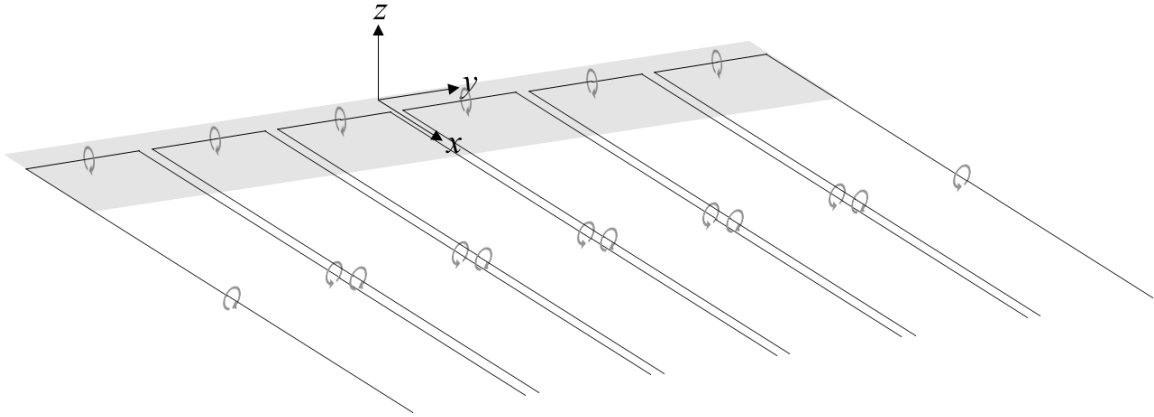


**Figure 5.1 Discrete system of side-by-side horseshoe vortices on a finite wing.**

and section lift slope ( $a_0$ ) can all be specified individually for each section of the wing. In classical lifting line theory, where the largest horseshoe vortex spans from wing tip to wing tip, each of these values is required to be constant over the entire wing.

The fundamental problem we must solve with this new arrangement is the same as that of classical lifting line theory – namely, to determine the vortex strengths  $\Gamma(y)$  such that the boundary condition of Eq. (4.3.1) is satisfied. We shall follow the same general development as was done for classical lifting line theory, but using a more general three-dimensional formulation due to the new arrangement of horseshoe vortices. This complete development can be found in its original form in Phillips and Snyder [16]. We shall then consider how the low aspect ratio modifications presented in the previous chapter can be applied to this numerical method. Finally, we shall compare results from the modified method with those of other approaches.

## 5.2 The Phillips and Snyder Numerical Lifting Line Method

Consider the arbitrary vortex segment  $\overline{OR}$  shown in Figure 5.2. Let  $\mathbf{l}$  be the vector from point  $O$  to point  $R$ , and consider the vortex element  $d\mathbf{l}$  located at point  $Q$ . The velocity induced at point  $P$  by this differential vortex element is given by the Biot-Savart law,

$$d\mathbf{V} = \frac{\Gamma}{4\pi} \frac{d\mathbf{l} \times \mathbf{r}}{r^3} \quad (5.2.1)$$

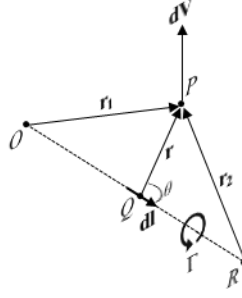


**Figure 5.2** Velocity induced at point  $P$  by an arbitrary vortex segment  $\overline{OR}$ .

Let  $\zeta$  be the ratio of the lengths of the line segments  $\overline{OQ}$  and  $\overline{OR}$ . The vector  $\mathbf{r}$  can be expressed as the difference of the two vectors  $\mathbf{r}_1$  and  $\zeta\mathbf{l}$ , so that the magnitude is given by

$$r = \sqrt{r_1^2 - 2\zeta\mathbf{r}_1 \cdot \mathbf{l} + \zeta^2 l^2} \quad (5.2.2)$$

and the cross product in Eq. (5.2.1) can be rewritten as

$$d\mathbf{l} \times \mathbf{r} = (d\zeta) \times (\mathbf{r}_1 - \zeta\mathbf{l}) = (\mathbf{l} \times \mathbf{r}_1 - \zeta\mathbf{l} \times \mathbf{l}) d\zeta = \mathbf{l} \times \mathbf{r}_1 d\zeta \quad (5.2.3)$$

Using Eqs. (5.2.2) and (5.2.3) in Eq. (5.2.1), we get

$$d\mathbf{V} = \frac{\Gamma}{4\pi} \frac{\mathbf{l} \times \mathbf{r}_1 d\zeta}{(r_1^2 - 2\zeta\mathbf{r}_1 \cdot \mathbf{l} + \zeta^2 l^2)^{3/2}} \quad (5.2.4)$$

The total velocity induced at point  $P$  by the vortex segment  $\overline{OR}$  is then found by integrating Eq. (5.2.4) over the length of the vortex segment,

$$\mathbf{V} = \frac{\Gamma(\mathbf{l} \times \mathbf{r}_1)}{4\pi} \int_0^1 \frac{d\zeta}{(r_1^2 - 2\zeta\mathbf{r}_1 \cdot \mathbf{l} + \zeta^2 l^2)^{3/2}} = \frac{\Gamma(\mathbf{r}_1 \times \mathbf{r}_2)(r_1 + r_2)}{4\pi r_1 r_2 (r_1 r_2 + \mathbf{r}_1 \cdot \mathbf{r}_2)} \quad (5.2.5)$$

A complete proof of the integral in Eq. (5.2.5) is provided in Appendix L. For a semi-infinite vortex with  $r_2 \rightarrow \infty$  in the direction of the freestream, Eq. (5.2.5) becomes

$$\mathbf{V} = \frac{\Gamma(\mathbf{u}_\infty \times \mathbf{r}_1)}{4\pi r_1 (r_1 - \mathbf{u}_\infty \cdot \mathbf{r}_1)} \quad (5.2.6)$$

where  $\mathbf{u}_\infty$  is the unit vector in the direction of the freestream. The velocity induced at an arbitrary point by a complete horseshoe vortex is then

$$\mathbf{V} = \frac{\Gamma}{4\pi} \left[ \frac{(\mathbf{u}_\infty \times \mathbf{r}_2)}{r_2(r_2 - \mathbf{u}_\infty \cdot \mathbf{r}_2)} + \frac{(r_1 + r_2)(\mathbf{r}_1 \times \mathbf{r}_2)}{r_1 r_2 (r_1 r_2 + \mathbf{r}_1 \cdot \mathbf{r}_2)} - \frac{(\mathbf{u}_\infty \times \mathbf{r}_1)}{r_1(r_1 - \mathbf{u}_\infty \cdot \mathbf{r}_1)} \right] \quad (5.2.7)$$

where  $\mathbf{r}_1$  and  $\mathbf{r}_2$  are now the vectors from the two corner points of the horseshoe vortex to the arbitrary point.

Now consider the discrete system of horseshoe vortices used to represent a finite wing as shown in Figure 5.1. A control point placed anywhere along the quarter-chord of the wing (i.e. the lifting line) will experience an induced velocity due to each horseshoe vortex according to Eq. (5.2.7). The induced downwash vector at the control point by a system of  $n$  horseshoe vortices is then given by

$$\mathbf{w}_i = \sum_{j=1}^n \frac{\Gamma_j}{4\pi} \left[ \frac{(\mathbf{u}_\infty \times \mathbf{r}_{j2})}{r_{j2}(r_{j2} - \mathbf{u}_\infty \cdot \mathbf{r}_{j2})} + \frac{(r_{j1} + r_{j2})(\mathbf{r}_{j1} \times \mathbf{r}_{j2})}{r_{j1} r_{j2} (r_{j1} r_{j2} + \mathbf{r}_{j1} \cdot \mathbf{r}_{j2})} - \frac{(\mathbf{u}_\infty \times \mathbf{r}_{j1})}{r_{j1}(r_{j1} - \mathbf{u}_\infty \cdot \mathbf{r}_{j1})} \right] \quad (5.2.8)$$

where  $\mathbf{r}_{j1}$  and  $\mathbf{r}_{j2}$  are the vectors from the two corner points of the  $j$ th horseshoe vortex to the control point.

The velocity vector at the control point can now be expressed as the sum of the freestream velocity and the induced downwash, namely

$$\mathbf{V} = \mathbf{V}_\infty + \mathbf{w}_i \quad (5.2.9)$$

Note that the middle term within the square brackets of Eq. (5.2.8) is indeterminate when the angle between  $\mathbf{r}_{j1}$  and  $\mathbf{r}_{j2}$  is  $\pm 180^\circ$ . However, this condition is only satisfied when the control point lies exactly on the axis of the vortex. Since the velocity induced by a straight vortex segment along its axis is zero, the appropriate value for this term is zero anytime  $\mathbf{r}_{j1}$  and  $\mathbf{r}_{j2}$  are coaxial.

In the development of classical lifting line theory, Prandtl [10,11] used the Kutta-Joukowski theorem given by Eq. (4.3.10) to relate the lift force to the circulation for any spanwise section of the wing. Phillips and Snyder [16] take a similar approach, but use the more general three-dimensional vortex lifting law (see Saffman [101]). This can be written for a differential segment  $d\mathbf{l}$  of the lifting line as

$$d\mathbf{F} = \rho_\infty \Gamma \mathbf{V} \times d\mathbf{l} \quad (5.2.10)$$

Following Prandtl's development of classical lifting line theory, we can equate the magnitude of this spanwise differential force to the lift predicted by 2D airfoil theory, namely

$$|d\mathbf{F}| = \frac{1}{2} \rho_\infty V_\infty^2 a_0 \alpha_e dS \quad (5.2.11)$$

where

$$\alpha_e = \tan^{-1} \left( \frac{\mathbf{V} \cdot \mathbf{u}_n}{\mathbf{V} \cdot \mathbf{u}_a} \right) \quad (5.2.12)$$

is the effective angle of attack,  $\mathbf{u}_n$  is the unit vector normal to the local airfoil chord, and  $\mathbf{u}_a$  is the unit vector aligned axially with the local airfoil chord. Both vectors  $\mathbf{u}_n$  and  $\mathbf{u}_a$  lie within the section plane. Equating the right hand sides of Eqs. (5.2.10) and (5.2.11) gives

$$\rho_\infty \Gamma |\mathbf{V} \times \mathbf{dl}| = \frac{1}{2} \rho_\infty V_\infty^2 a_0 \alpha_e dS \quad (5.2.13)$$

Expressed in this form, Eq. (5.2.13) is a single equation with  $n$  unknowns, namely the vorticities  $\Gamma_{1,2,\dots,n}$  for each horseshoe vortex. The control point, since it has been constrained to lie along the lifting line, also lies along the axis of one of the  $n$  horseshoe vortices. The values of the parameters  $\Gamma$ ,  $\mathbf{V}$ ,  $\mathbf{dl}$ ,  $\alpha_e$ , and  $dS$  in Eq. (5.2.13) are associated with the wing section and corresponding horseshoe vortex along which the control point lies. By placing a control point on each of the  $n$  horseshoe vortices and writing Eq. (5.2.13) for each control point, we generate a system of  $n$  nonlinear equations in  $n$  unknowns that can be solved using an iterative root-finding algorithm such as the Newton-Raphson method.

In Secs. 4.3 and 4.6, we were able to develop closed-form relations for the lift and drag coefficients of wings with elliptic lift distributions. Development of similar equations using the numerical formulation of Phillips and Snyder [16] is not straightforward due to the discrete summation and the vector notation used in the formulation. Instead, a solver that implements this method can compute the resultant force vector at each control point and then compute a vector sum the forces over the wing. Lift and drag components relative to the freestream can then be computed using the vector dot product.

In the original paper by Phillips and Snyder [16], results using this method are shown to be equivalent to those of classical lifting line theory for straight elliptic wings of various aspect ratios. Additionally, results are shown to be in good agreement with experimental and high-order numerical results for straight wings, wings with sweep, and wings with dihedral. However, in all comparisons the aspect ratios are greater than 4. Figure 5.3 compares wing lift slope results computed using the numerical lifting line method of Phillips and Snyder with results from classical lifting line theory and a vortex panel method. Solutions to the numerical lifting line method were computed using MachUp (see Sec. 2.6.1) with 100 nodes per semispan and a section



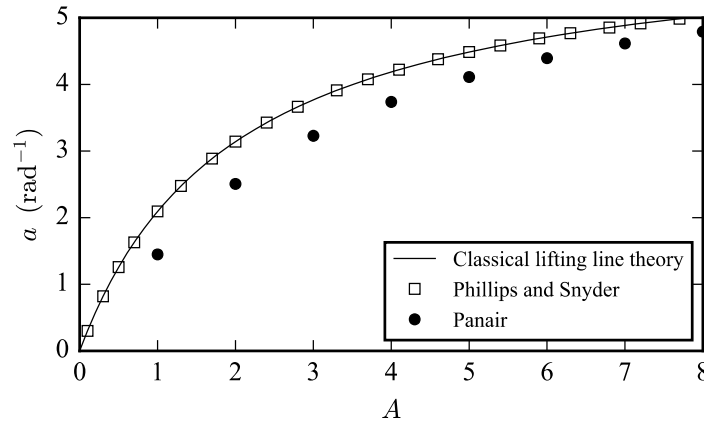


**Figure 5.3 Comparison of wing lift slope calculations for finite elliptic wings.**

lift slope of  $a_0 = 2\pi$ . Solutions to classical lifting line theory were computed using Eq. (4.6.3) with a section lift slope of  $a_0 = 2\pi$ . Vortex panel method results were computed using Panair [98–100]. From these data it is clear that the numerical lifting line method of Phillips and Snyder is subject to the same aspect ratio limitations as classical lifting line theory.

### 5.3 Modifications to the Numerical Lifting Line Method for Wings of Arbitrary Aspect Ratio

As stated in the previous section and illustrated in Figure 5.3, computations performed using the numerical lifting line method of Phillips and Snyder [16] are subject to the same aspect ratio limitations as classical lifting line theory. However, we have already developed a method for modifying classical lifting line theory to accurately account for aspect ratio (see Sec. 4.6). We shall now present a method for applying this same modification to Eq. (5.2.13).

First, we note that the effective angle of attack appears explicitly in Eq. (5.2.13). Solving for  $\alpha_e$  gives

$$\alpha_e = \frac{2\Gamma |\mathbf{V} \times \mathbf{dl}|}{a_0 V_\infty dS} \quad (5.3.1)$$

which is quite similar to Eq. (4.3.13). In Eq. (4.6.47) a correction factor of  $(a_0/R_1)$  has been applied to the effective angle of attack. We therefore, by analogy, apply this same factor here so that Eq. (5.3.1) becomes

$$\alpha_e = \frac{2\Gamma |\mathbf{V} \times \mathbf{dl}|}{a_0 V_\infty dS} \left( \frac{a_0}{R_1} \right) \quad (5.3.2)$$

for arbitrary aspect ratios.

The induced angle of attack does not appear explicitly in Eq. (5.2.13), but the induced downwash given by Eq. (5.2.8) is used in the calculation of  $\mathbf{V}$ , which appears in the left hand side of Eq. (5.2.13) and in the definition for  $\alpha_i$  given by Eq. (5.2.12). Since, by the small angle approximation,

$$\alpha_i = w_i/V_\infty \quad (5.3.3)$$

we conjecture that the induced downwash given by Eq. (5.2.8) must be scaled by the same factor as the induced angle of attack in Eq. (4.6.47), namely  $(\pi A/R_2)$ . This gives

$$\mathbf{w}_i = \left( \frac{\pi A}{R_2} \right) \sum_{j=1}^N \frac{\Gamma_j}{4\pi} \left[ \frac{(\mathbf{u}_\infty \times \mathbf{r}_{j2})}{r_{j2}(r_{j2} - \mathbf{u}_\infty \cdot \mathbf{r}_{j2})} + \frac{(r_{j1} + r_{j2})(\mathbf{r}_{j1} \times \mathbf{r}_{j2})}{r_{j1}r_{j2}(r_{j1}r_{j2} + \mathbf{r}_{j1} \cdot \mathbf{r}_{j2})} - \frac{(\mathbf{u}_\infty \times \mathbf{r}_{j1})}{r_{j1}(r_{j1} - \mathbf{u}_\infty \cdot \mathbf{r}_{j1})} \right] \quad (5.3.4)$$

These two simple changes are all that is required to allow the application of any one of the correction methods described in Sec. 4.6 to the numerical lifting line method of Phillips and Snyder [16]. The nature and complexity of the equations to be solved has not been changed, so that the same algorithms used to solve the unmodified equations can be used to solve the modified ones. For completeness, the equations to be solved for the modified numerical lifting line algorithm are summarized below.

$$\rho_\infty \Gamma |\mathbf{V} \times \mathbf{dl}| \left( \frac{a_0}{R_1} \right) = \frac{1}{2} \rho_\infty V_\infty^2 a_0 \alpha_e dS \quad (5.3.5)$$

$$\alpha_e = \tan^{-1} \left( \frac{\mathbf{V} \cdot \mathbf{u}_n}{\mathbf{V} \cdot \mathbf{u}_a} \right) \quad (5.2.12)$$

$$\mathbf{V} = \mathbf{V}_\infty + \mathbf{w}_i \quad (5.2.9)$$

$$\mathbf{w}_i = \left( \frac{\pi A}{R_2} \right) \sum_{j=1}^N \frac{\Gamma_j}{4\pi} \left[ \frac{(\mathbf{u}_\infty \times \mathbf{r}_{j2})}{r_{j2}(r_{j2} - \mathbf{u}_\infty \cdot \mathbf{r}_{j2})} + \frac{(r_{j1} + r_{j2})(\mathbf{r}_{j1} \times \mathbf{r}_{j2})}{r_{j1}r_{j2}(r_{j1}r_{j2} + \mathbf{r}_{j1} \cdot \mathbf{r}_{j2})} - \frac{(\mathbf{u}_\infty \times \mathbf{r}_{j1})}{r_{j1}(r_{j1} - \mathbf{u}_\infty \cdot \mathbf{r}_{j1})} \right] \quad (5.3.4)$$

As was mentioned in the previous section, closed-form expressions for lift and drag coefficients of wings with elliptic lift distributions are not available based on this numerical formulation, so that they must be computed as a vector summation of the resultant force vectors at each control point. This procedure is the same for the modified formulation described here as for the original formulation of Phillips and Snyder [16] discussed in the previous section, so that the additional rotation of the resultant force vector due to the modifications presented in this section will be automatically accounted for in any application that correctly implements this method.

## 5.4 Results and Discussion

In order to evaluate the effectiveness of the modifications described above, the MachUp source code has been modified to include these changes, and an additional parameter has been added to the input file format to allow selection of the resistance values to be used in an analysis. Figure 5.4 shows a comparison of wing lift slopes computed using this modified version of MachUp with the analytical solutions from Chapter 4 for classical lifting line theory, the modified slender wing equation, and Eqs. (4.6.63)-(4.6.64). Results computed using Panair are also included.

The numerical model for these calculations was composed of 100 spanwise sections for one semispan with a symmetry boundary condition at the wing root. The uniform cross section was modeled as a thin symmetric airfoil with  $a_0 = 2\pi$ . The iterative nonlinear solver was used with a convergence tolerance of  $10^{-10}$ . With these settings, the numerical results agree with the analytical results to at least four digits of precision. Additionally, the differences between the Panair results and the numerical results based on the formulation proposed by the present author are less than 1% for  $A \geq 1$ .

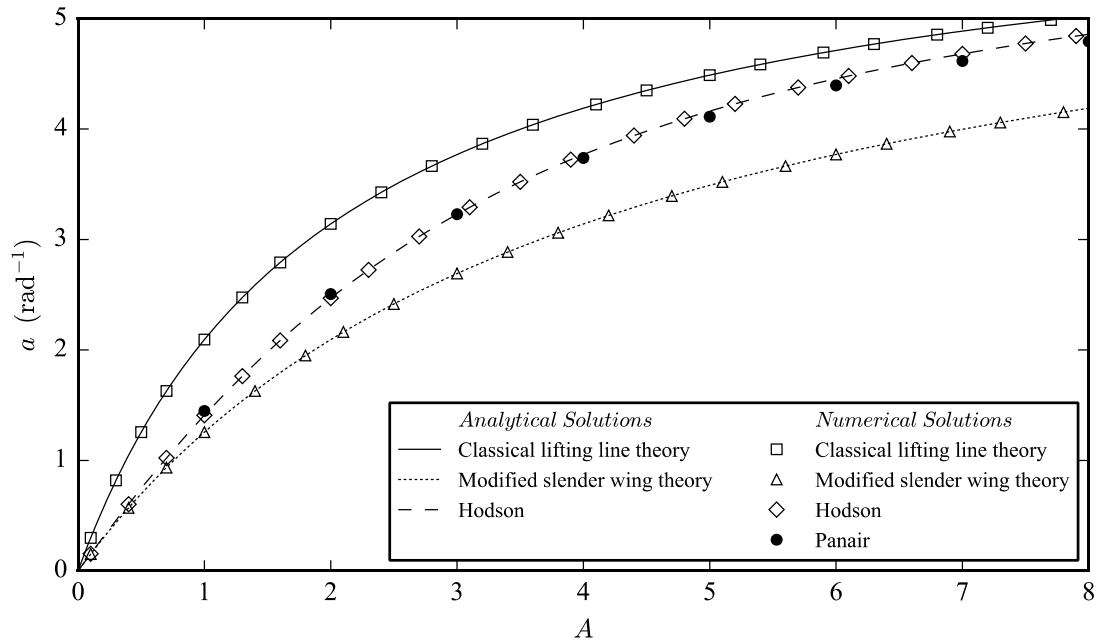


**Figure 5.4** Comparison of analytical and numerical calculations for wing lift slope of elliptic wings.

Figures 5.5-5.7 compare the lift distributions for elliptic, rectangular, and tapered planforms predicted by the modified MachUp code to those predicted by Panair. The results are essentially identical to the analytical results shown in Figures 4.7-4.9. From these data we conclude that the modified equations described in Sec. 5.3 are the numerical equivalent to the analytical lifting line formulation given in Eq. (4.6.47).

This work has considered only isolated wings with no sweep; no geometric or aerodynamic twist; no dihedral; and only elliptic, rectangular, and tapered planforms. The formulation given in Sec. 5.3, however, is not limited to any of these constraints. Previous publications (see Refs. [12–14]) have applied the numerical lifting line algorithm described in Sec.5.2 to a variety of other wing designs with reasonable success. While beyond the scope of the present work, it is expected that the proposed method can produce useful results for arbitrary wing designs.

Figure 5.8 shows aspect ratio efficiency factors computed using MachUp and Panair. The Panair results were discussed in Sec. 4.7. The MachUp results are equivalent to the Pralines results shown in Figure 4.10. This provides added confidence in the derivations leading to Eq. (4.6.59) since that equation is used directly to calculate drag in Pralines but not in MachUp.

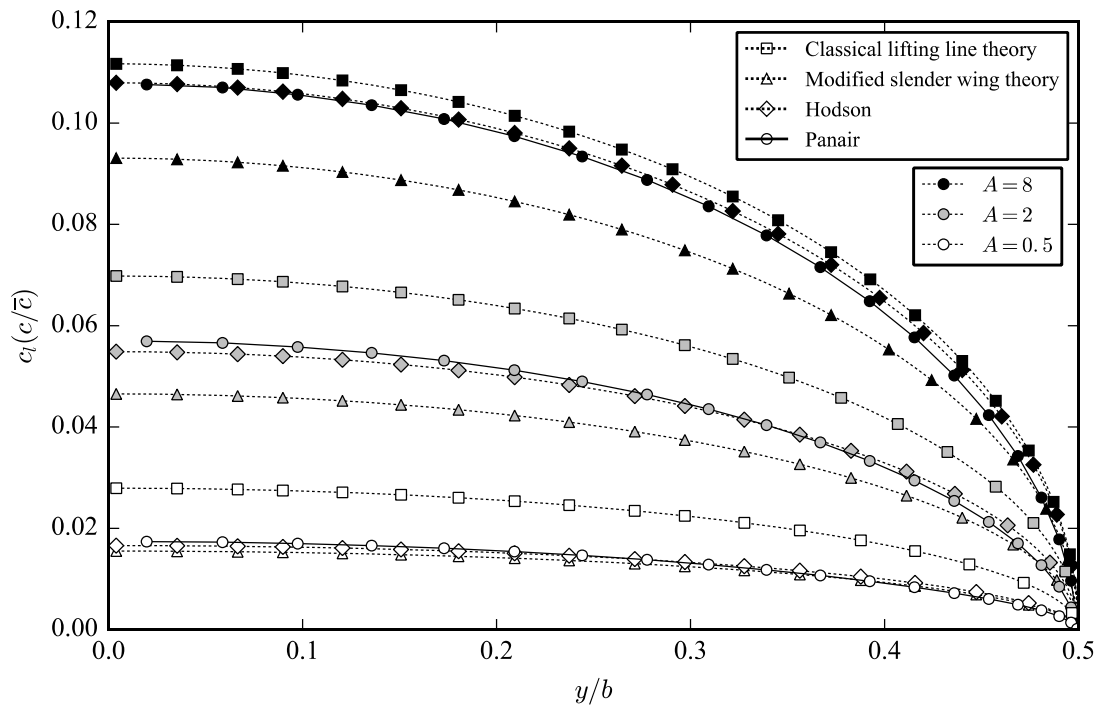


Figure 5.5 Comparison of spanwise lift distributions for elliptic wings.

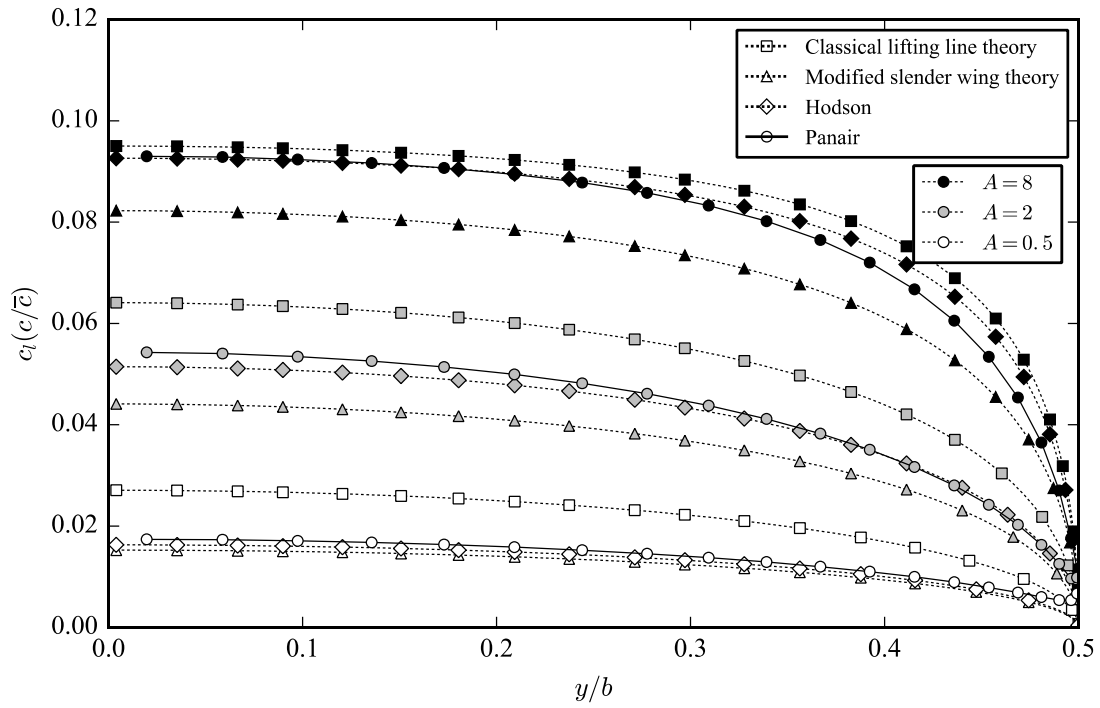


Figure 5.6 Comparison of spanwise lift distributions for rectangular wings.

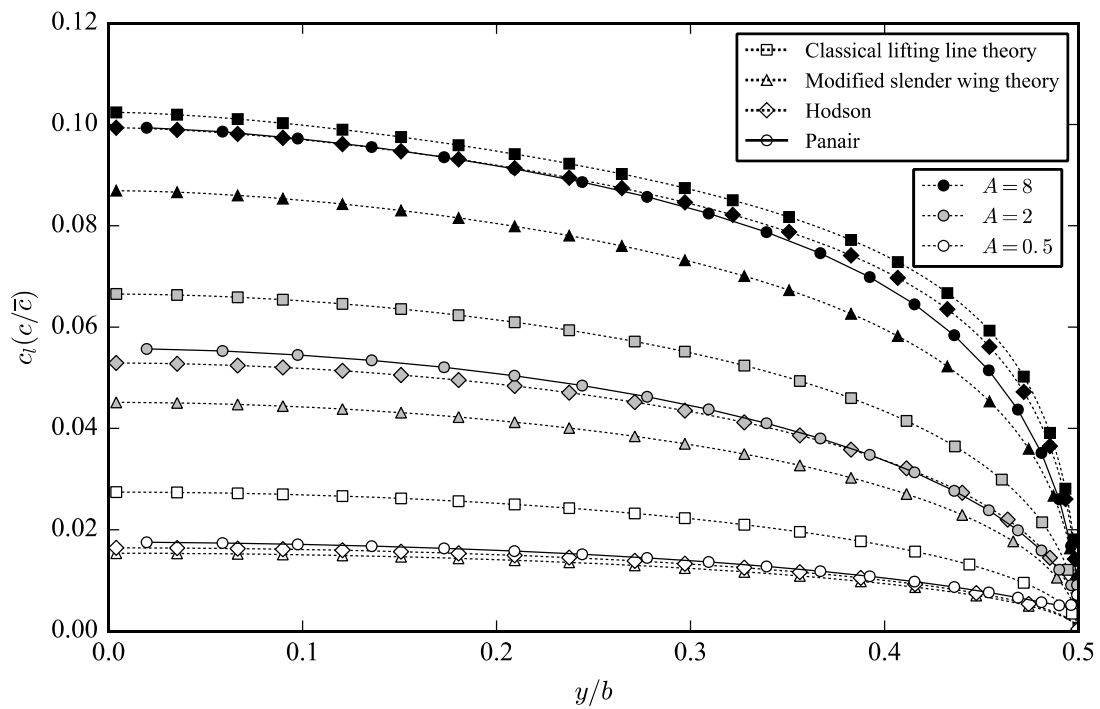
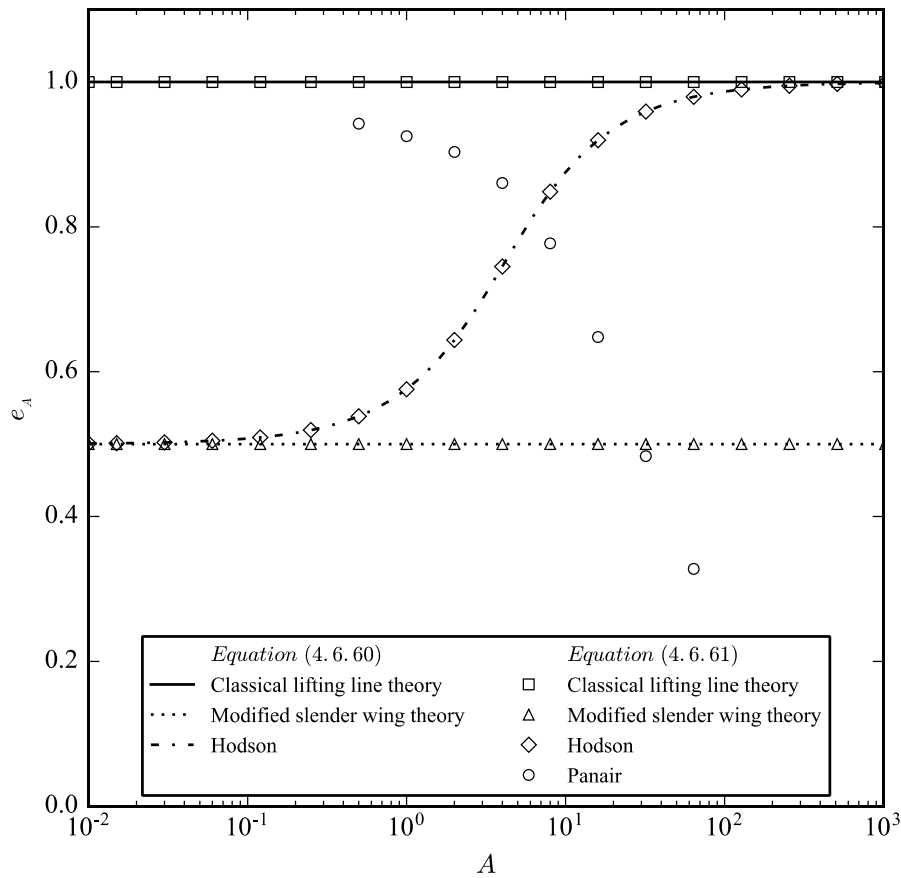


Figure 5.7 Comparison of spanwise lift distributions for tapered wings with  $R_t = 0.75$ .



**Figure 5.8 Sample calculations of the aspect ratio efficiency factor using MachUp and Panair.**

In 2017, Hodson et al. [102] presented wind tunnel data for several subscale test articles of the variable-camber compliant wing (VCCW) developed at the U.S. Air Force Research Laboratory (AFRL). For a description of the VCCW, see Refs. [5,6]. Of particular interest here is the aspect ratio of the VCCW –  $A = 3$  – which falls below the generally accepted range of validity for classical lifting line theory. The data presented by Hodson et al. [102] includes lift, drag, and pitching moment coefficients as functions of angle of attack for five subscale test articles generated from 3D scans of the VCCW in various morphed configurations, as well as three test articles generated from 3D CAD models with uniform NACA 0010, 2410, and 8410 airfoil cross-sections. For a description of each test article, see Ref. [102].

In order to compare numerical results generated with MachUp to the Hodson et al. [102] experimental data, an airfoil database needed to be created containing airfoil coefficients for the different cross sections in

the models. For this analysis, the cross sections were approximated as NACA X410 series airfoils. XFOIL (see Refs. [51,52]) was used to generate viscous airfoil coefficients assuming a Reynolds number based on chord length of  $Re_c = 2.4 \times 10^5$ . The XFOIL results were tabulated for angles of attack between -10 deg and +10 deg. Airfoil coefficient tables for airfoils having 0%, 2%, 4%, 6%, and 8% maximum camber were generated and are listed in Appendix M. Properties for wing sections having maximum camber values between the values listed were linearly interpolated from the two closest airfoils.

Comparisons of lift coefficients for the test articles based on the 3D CAD models are given in Figures 5.9-5.11. Uncertainty bands representing 95% confidence intervals are included on the experimental data. For the CAD-0 and CAD-2 models, the corrected numerical results agree exceptionally well with the experimental data and outperform the numerical results calculated using the classical lifting line formulation. For the CAD-8 model, the corrected numerical results lie slightly below the experimental data but are still within the same range of accuracy as the classical lifting line results. Moreover, they provide a closer approximation to the lift slope for this data than the classical lifting line results provide.

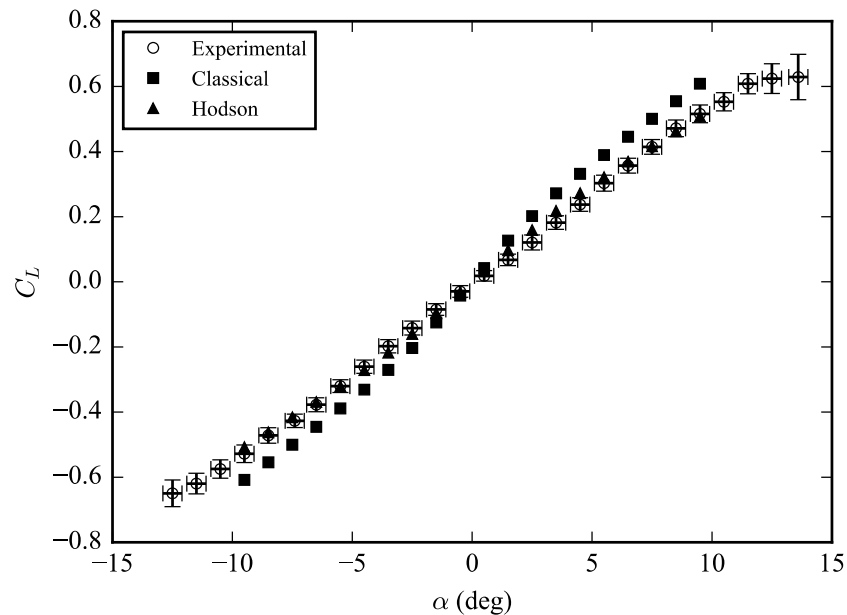


**Figure 5.9 Comparison of numerical and experimental lift coefficients for the CAD-0 test.**

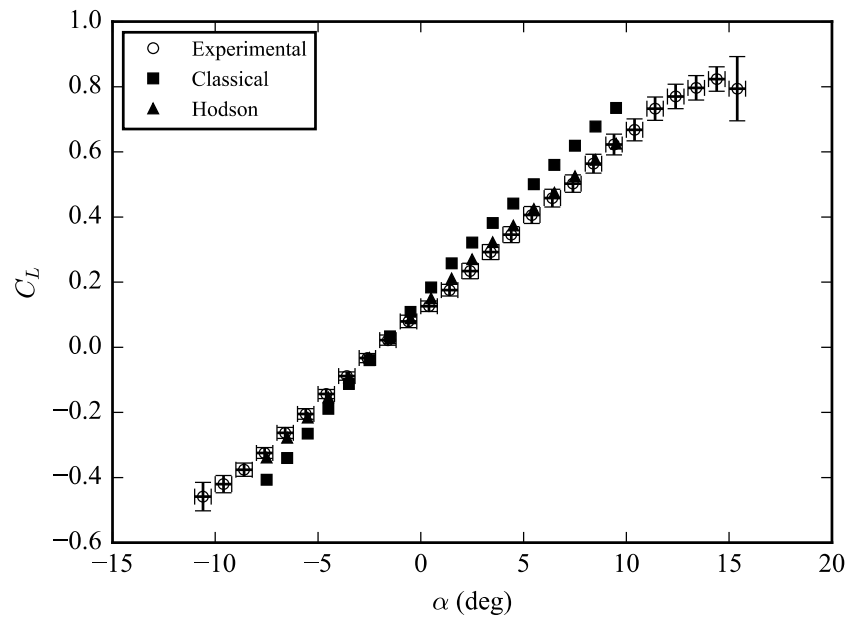


**Figure 5.10** Comparison of numerical and experimental lift coefficients for the CAD-2 test.

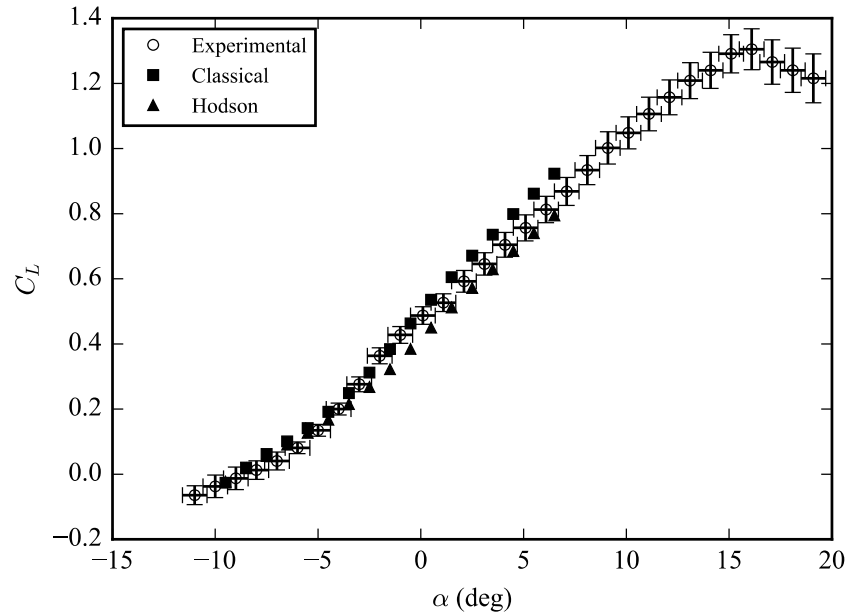


**Figure 5.11** Comparison of numerical and experimental lift coefficients for the CAD-8 test.



Comparisons of lift coefficients for the subscale test articles generated from 3D scans of the VCCW are given in Figures 5.12-5.16. As with the CAD-0 and CAD-2 test articles, the corrected lifting line results for the VCCW-2 and VCCW-CD test articles are in excellent agreement with the experimental data. The corrected lifting line results for the VCCW-8 and VCCW-LW test articles lie slightly below the experimental data but have the correct lift slopes. The corrected numerical results for the VCCW-CU test article are the least satisfactory. They lie further below the experimental results than the classical lifting line results, and though the lift slope is slightly improved it is still too high. The reasons for the discrepancy in the VCCW-CU results are unknown, but there are several possibilities. The actual cross-sectional profiles of the VCCW-CU configuration may differ significantly from the NACA X410 profiles assumed in the numerical analysis. The XFOIL results for the airfoils used in the numerical analyses of the VCCW-CU may be in error, though this would likely also affect the comparisons of other test articles rather than be isolated to a single test article. There may also be an error in the experimental data that was not identified during the uncertainty analysis, though this too would likely also affect the comparisons of other test articles unless the error source was related directly to the setup and installation of the VCCW-CU test article in the wind tunnel. There also remains the possibility that the corrections to lifting line theory implemented here do not accurately account for the effects of thickness, camber, and viscosity, as none of these factors were considered in the theoretical development of the modifications. The VCCW-CU configuration may be such that these discrepancies are significantly amplified. Further investigation of this issue is needed.

Comparisons of drag coefficients for the test articles based on the 3D CAD models are given in Figures 5.17-5.19. In these plots, the numerical results using the corrected formulation and classical lifting line theory are quite similar because the only correction to drag was to the induced drag component, while most of the drag in these analyses comes from parasitic drag. In all three cases and for both numerical models the shape of the drag curve is slightly too concave. The largest source of error here is likely the parasitic drag coefficients determined from the XFOIL results.

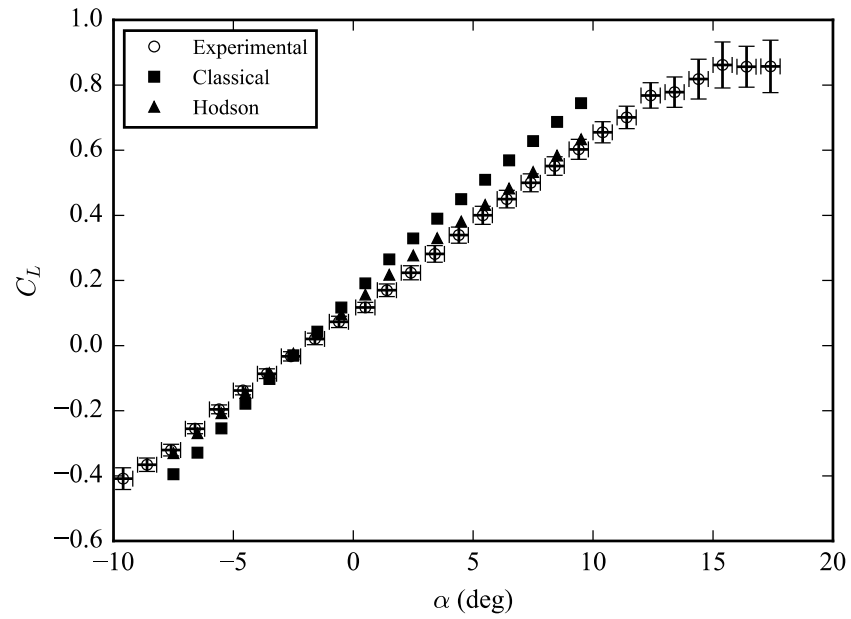


Figure 5.12 Comparison of numerical and experimental lift coefficients for the VCCW-2 test.

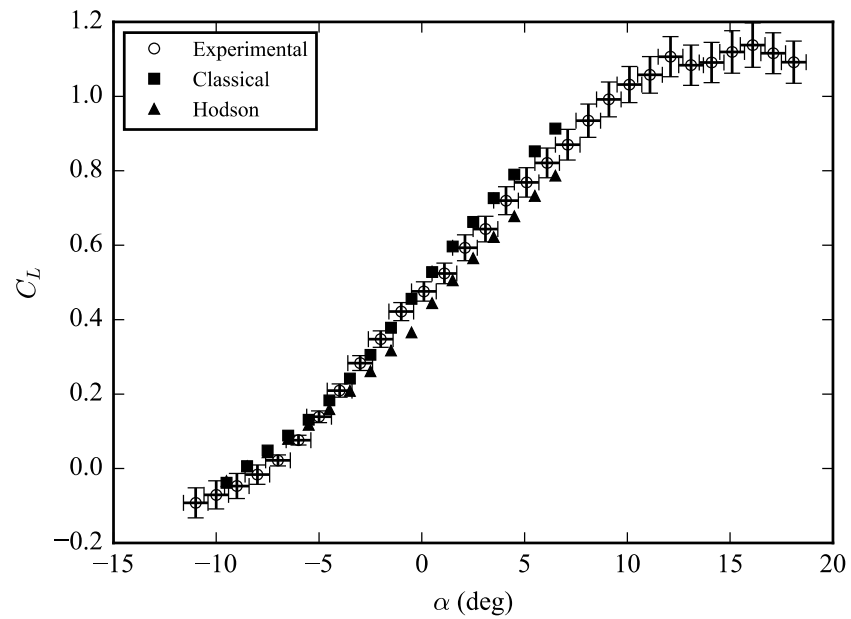


Figure 5.13 Comparison of numerical and experimental lift coefficients for the VCCW-8 test.

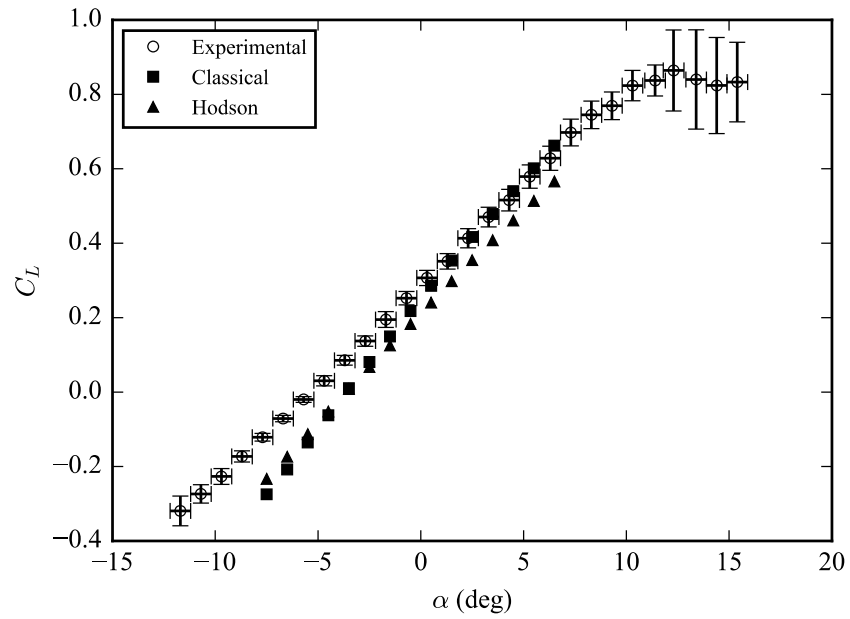


Figure 5.14 Comparison of numerical and experimental lift coefficients for the VCCW-CU test.

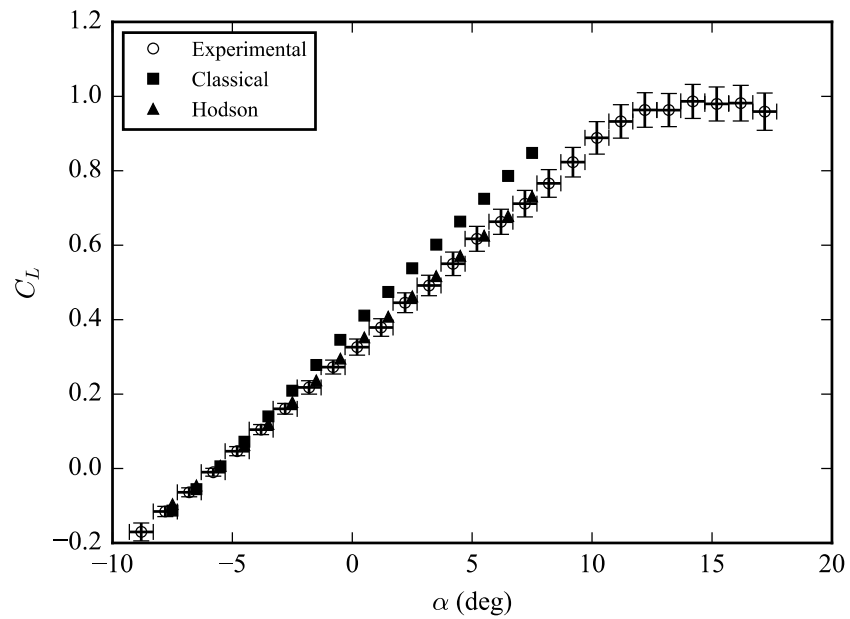


Figure 5.15 Comparison of numerical and experimental lift coefficients for the VCCW-CD test.

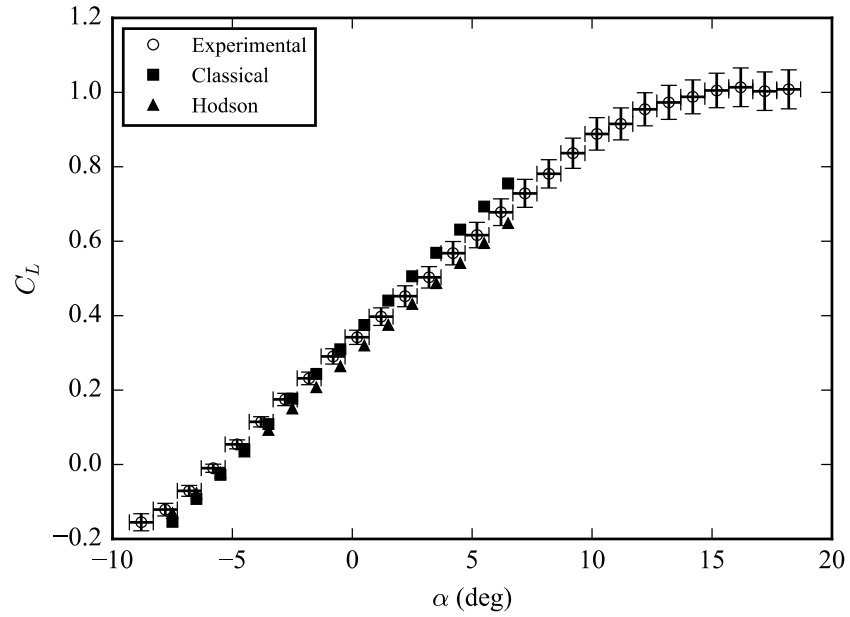


Figure 5.16 Comparison of numerical and experimental lift coefficients for the VCCW-LW test.

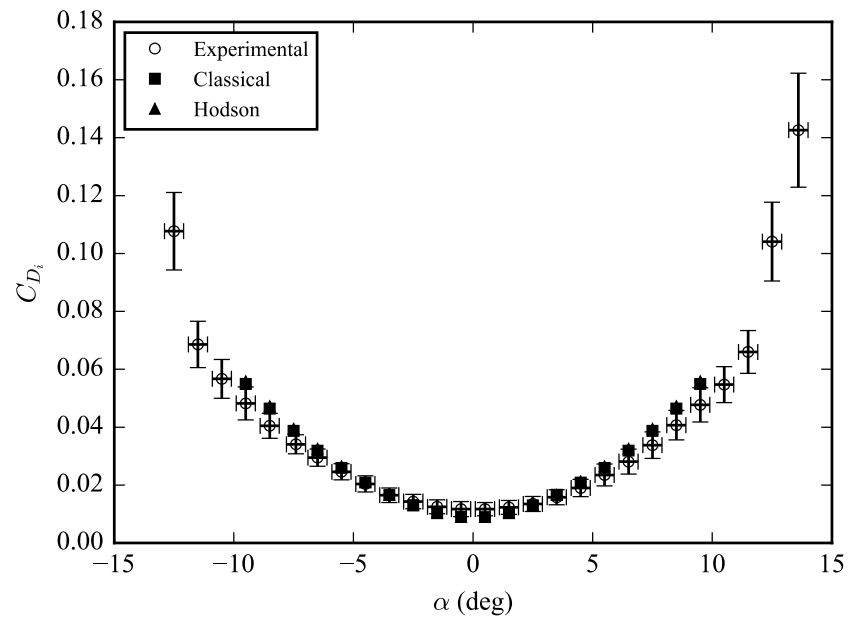


Figure 5.17 Comparison of numerical and experimental drag coefficients for the CAD-0 test.

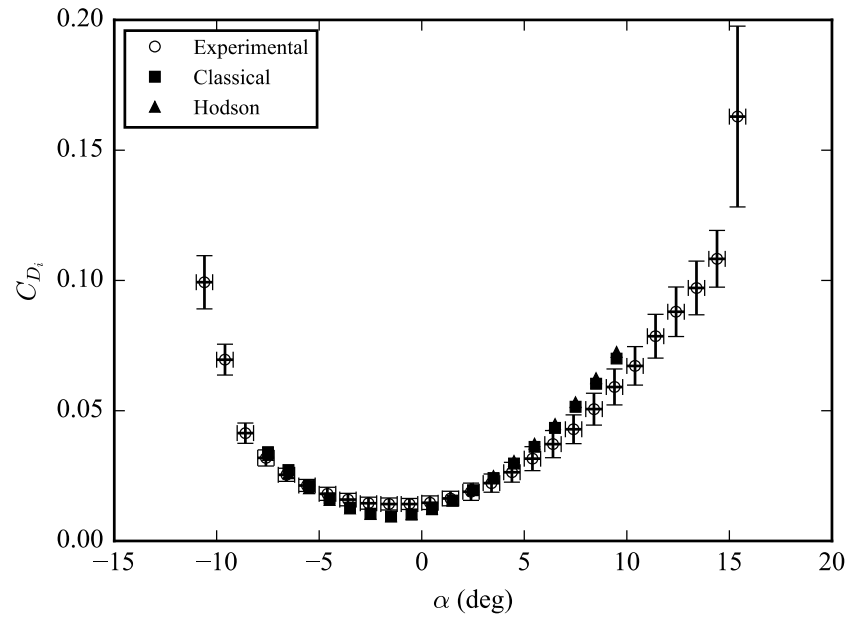


Figure 5.18 Comparison of numerical and experimental drag coefficients for the CAD-2 test.

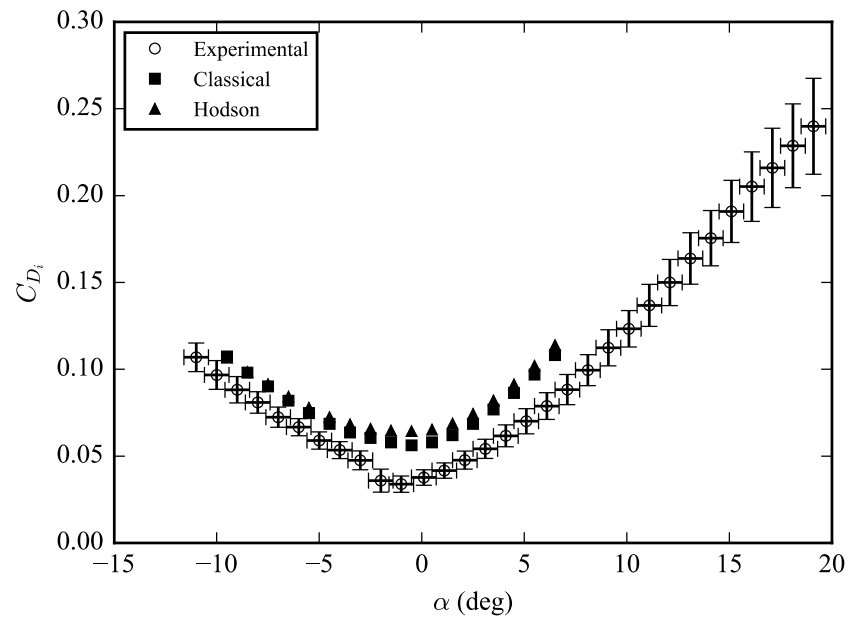
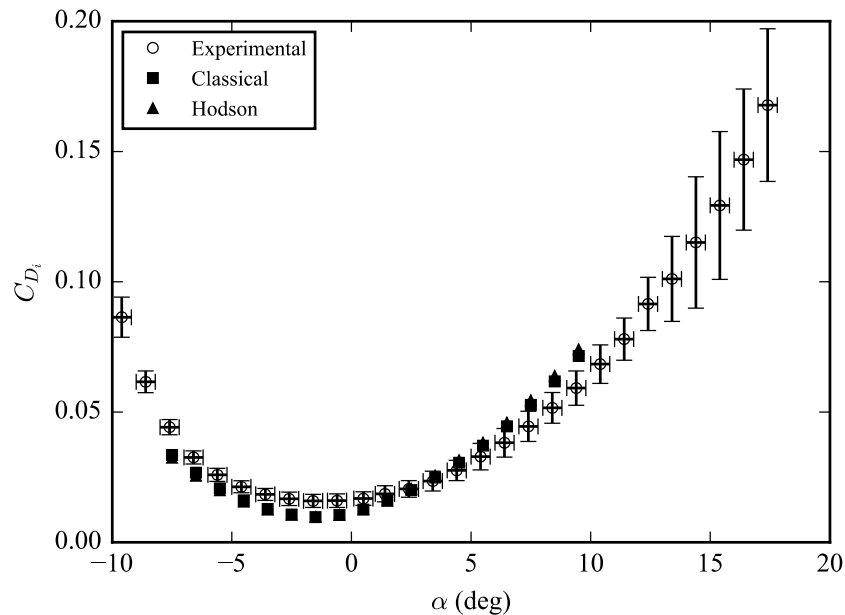
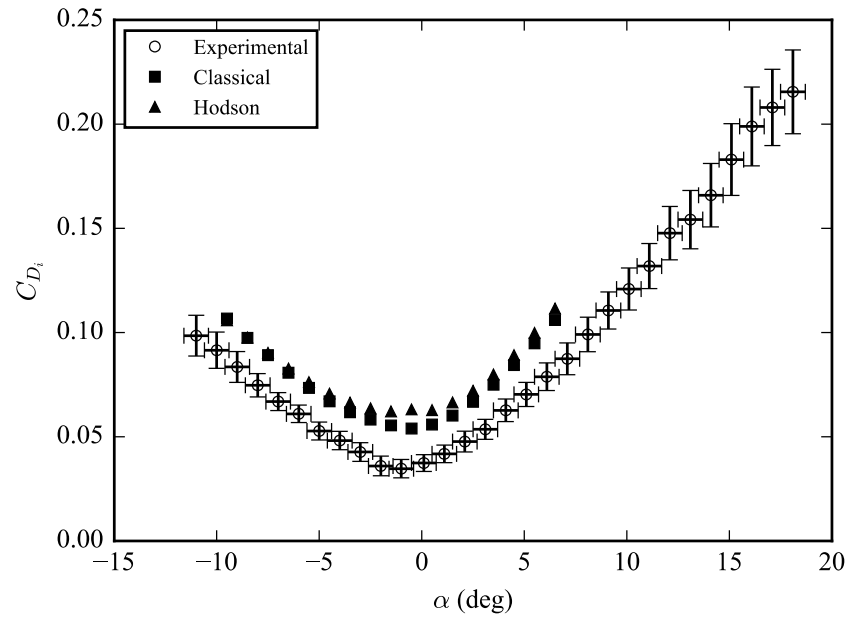


Figure 5.19 Comparison of numerical and experimental drag coefficients for the CAD-8 test.

Comparisons of lift coefficients for the subscale test articles generated from 3D scans of the VCCW are given in Figures 5.20-5.24. Again the differences between the two numerical formulations are mostly quite small, though the corrected model predicts a measurable increase in drag in the case of the VCCW-8 over the classical model. This is because  $\partial C_{D_p} / \partial C_L$  is quite steep in the region at which this wing operates for the NACA 8410 airfoil, so that a relatively small change in lift results in a much larger change in drag. From these plots, only the results for the VCCW-CU model do a reasonable job of matching the experimental data. Results for the other models show too narrow of a drag curve, but this observation is true for both numerical formulations. The most likely source of error here is again the parasitic drag coefficients determined from the XFOIL results. This error is compounded by the fact that the cross-sectional profiles of the scanned models do not match the NACA X410 family of airfoils exactly. Large discrepancies between the cross-sectional profiles and the NACA X410 family of airfoils were noted especially in sections with high camber. Improved estimation of the parasitic drag properties of the airfoils used in these analyses is expected to resolve most of the error seen in these drag calculations.



**Figure 5.20 Comparison of numerical and experimental drag coefficients for the VCCW-2 test.**



**Figure 5.21 Comparison of numerical and experimental drag coefficients for the VCCW-8 test.**

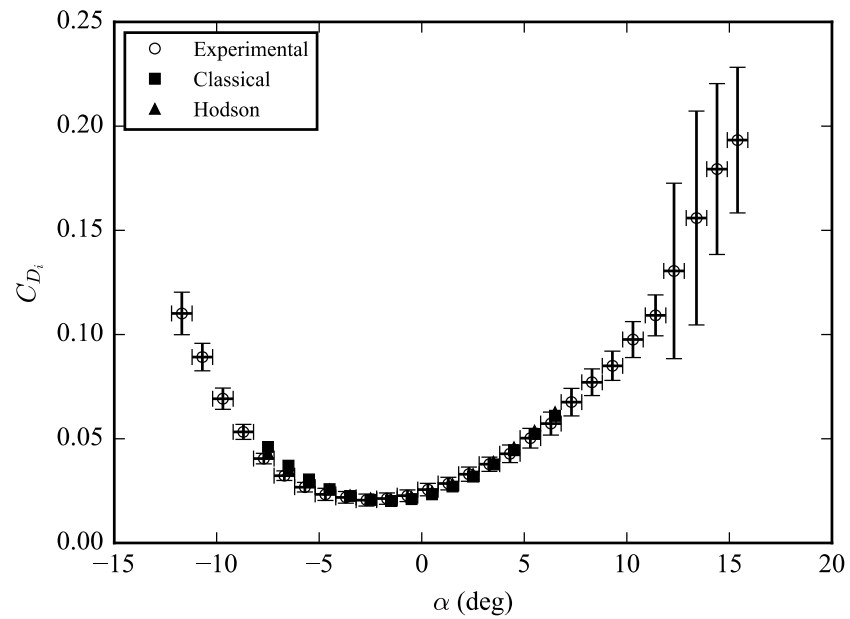


**Figure 5.22 Comparison of numerical and experimental drag coefficients for the VCCW-CU test.**

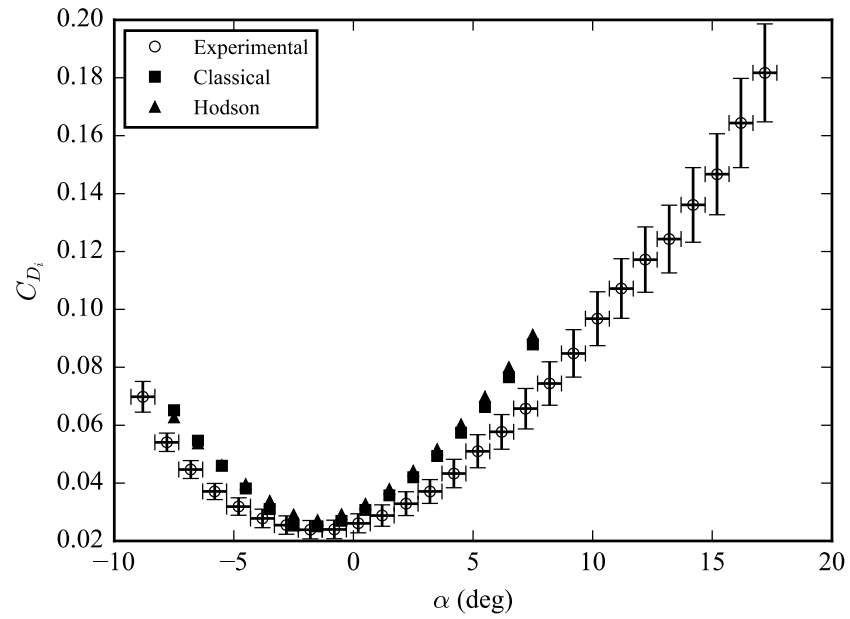


**Figure 5.23** Comparison of numerical and experimental drag coefficients for the VCCW-CD test.

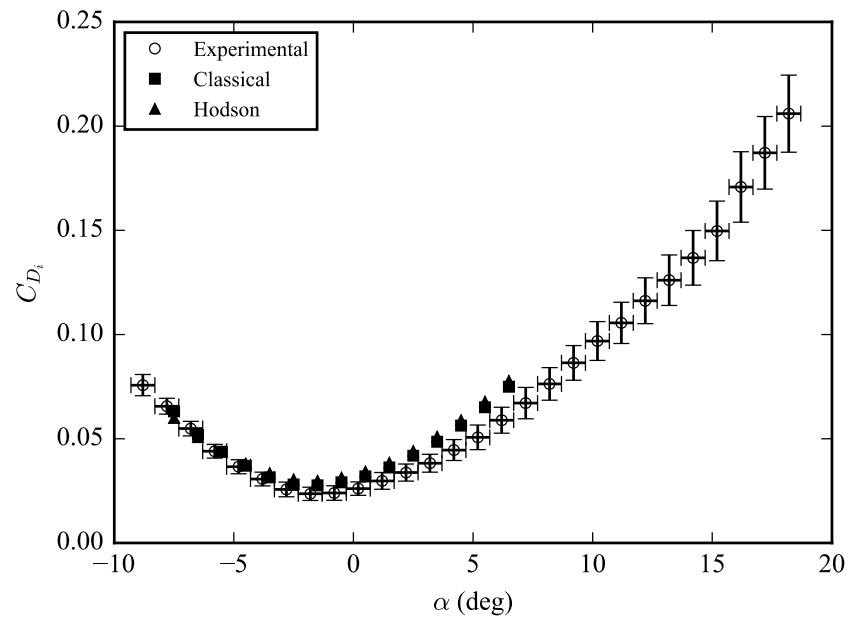


**Figure 5.24** Comparison of numerical and experimental drag coefficients for the VCCW-LW test.



## 6 SUMMARY AND CONCLUSIONS

In this work, several limitations on analysis relative to wing shape optimization have been addressed. First, an efficient method for computing gradients with respect to design parameters in an aerodynamic analysis has been presented and integrated into MachUp, an open-source aerodynamic analysis tool based on a numerical lifting line method. The gradients are computed automatically using DNAD, a forward-mode automatic differentiation package that allows derivatives with respect to multiple input parameters to be computed in a single run. The DNAD module was integrated into the MachUp source code in such a way that inclusion or exclusion of the DNAD module can be controlled entirely at compile-time. In this way, the integration of the DNAD module does not affect the performance of MachUp when derivatives are not needed, and source code modifications are not required to convert between gradient-capable and non-gradient-capable versions of the code. To the author's knowledge, this is the first time this type of integration has been achieved with a practical engineering analysis tool.

Second, a process and suite of tools for performing efficient wing shape optimization has been presented and demonstrated. Optix, an open-source optimization framework that allows objective function evaluations to be run in parallel across available resources, was described in Sec. 3.2 and the source code is listed in Appendix F. Optix is written entirely in Python and is therefore cross-platform, easy to interface with, and easily customizable to a wide range of optimization problems. Its most significant features include the ability to execute independent function evaluations in parallel and to perform quadratic line-searching, both of which have the potential to significantly reduce the time required for complex optimization problems. It can also leverage automatic differentiation capabilities within objective functions to expedite efficient gradient calculations. Currently, constraints must be enforced through use of the penalty function method, and global minimization of non-convex design spaces cannot be guaranteed without the use of an outer wrapper implementing a globally convergent optimization method. These two limitations represent the primary areas of focus for future work in improving and expanding the capabilities of Optix.

Optix and MachUp were used together to solve several inviscid wing shape optimization problems with known solutions, and the solutions were shown to converge toward the correct solution as the number of degrees of freedom was increased. Solutions to several viscous wing shape optimization problems were also solved using this method.

The most significant source of error in the viscous results lies in the aerodynamic properties of the airfoils and the interpolation scheme used for determining aerodynamic properties of intermediate airfoils. Note that this is a problem with the data input to the analysis, however, and not a problem with the analysis tools themselves or the underlying methodology. Improving the accuracy of the airfoil aerodynamic properties and improving the interpolation scheme used for intermediate airfoils should provide the greatest improvement to the accuracy of these results.

Perhaps the most useful product of the optimization work presented in Chapter 3 is the contour plot shown in Figure 3.7. Using high-fidelity analysis tools such as CFD for wing shape optimization is not only computationally prohibitive but also precludes the ability to visualize the design and configuration space of a morphing wing. In this work, we have demonstrated a method for rapidly visualizing the design and configuration space of a finite morphing wing using MachUp. Figure 3.7 illustrates important relationships between lift, induced drag, and parasitic drag and demonstrates how changes in a finite wing design can impact these performance characteristics. The ability demonstrated here to quickly visualize and explore the design and configuration space of a morphing wing is a significant enabler in the push to develop advanced morphing wing technologies.

Although Chapter 3 only considered optimization of planform, geometric twist, and aerodynamic twist on a straight wing, the tools presented can be used to evaluate and optimize geometries of multiple interacting lifting surfaces as well as wings with more complex geometries. Examples of interacting lifting surfaces include the interaction of main wings and stabilizers, wings in formation, wings with winglets, and wings in ground effect. Due to modern composite manufacturing methods, very complex wing shapes can be designed and manufactured. The tools presented in this work can be used to optimize these complex wing designs in both single- and multi-wing systems.

Finally, development of new analytical and numerical formulations of lifting line theory have been presented. These formulations are based heavily on the classical lifting line theory of Prandtl [10,11] and the numerical lifting line method of Phillips and Snyder [16], but also draw on the works of several others (see Refs. [73,79,83,85,88–91,93]) to form a lifting line model accurate over the entire range of aspect ratios, from the slender wing to the infinite wing. The new formulations have been implemented in code and demonstrated to outperform classical lifting line theory in matching the lift results of an inviscid panel code

for elliptic, rectangular, and tapered wings of arbitrary aspect ratio. They were also shown to outperform classical lifting line theory in matching the lift results of a viscous experimental investigation of the VCCW, a low-aspect-ratio rectangular wing with morphable cross-sections.

Drag predictions using the modified analytical and numerical formulations have been shown to agree with the theory presented, but results from Panair were contrary to the theory and no way to reconcile the discrepancies has yet been found. Additionally, drag predictions using the corrected numerical formulation compared to the VCCW experimental data set showed no improvement over classical lifting line theory predictions. Further research on the mechanisms that influence drag for low-aspect-ratio wings is needed to reconcile these data.

## REFERENCES

- [1] Baysal, O., and Eleshaky, M., “Aerodynamic Design Optimization Using Sensitivity Analysis and Computational Fluid Dynamics,” *AIAA Journal*, vol. 30, no. 3, Mar. 1992, pp. 718–725.  
doi:10.2514/3.10977.
- [2] Samareh, J., “Aerodynamic Shape Optimization Based on Free-Form Deformation,” Albany, NY: AIAA, 2004.  
doi:10.2514/6.2004-4630.
- [3] Reuther, J., Jameson, A., Alonso, J., Rimlinger, M., and Saunders, D., “Constrained Multipoint Aerodynamic Shape Optimization Using an Adjoint Formulation and Parallel Computers, Part 2,” *Journal of Aircraft*, vol. 36, no. 1, 1999, pp. 61–74.  
doi:10.2514/2.2414.
- [4] Lyu, Z., Kenway, G., and Martins, J., “Aerodynamic Shape Optimization Investigations of the Common Research Model Wing Benchmark,” *AIAA Journal*, vol. 53, no. 4, Apr. 2015, pp. 968–985.  
doi:10.2514/1.J053318.
- [5] Joo, J., Marks, C., Zientarski, L., and Culler, A., “Variable Camber Compliant Wing – Design,” *23rd AIAA/AHS Adaptive Structures Conference*, Kissimmee, FL: AIAA, 2015.  
doi:10.2514/6.2015-1050.
- [6] Marks, C., Zientarski, L., Culler, A., Hagen, B., Smyers, B., and Joo, J., “Variable Camber Compliant Wing – Wind Tunnel Testing,” *23rd AIAA/AHS Adaptive Structures Conference*, Kissimmee, FL: AIAA, 2015.  
doi:10.2514/6.2015-1051.
- [7] Su, W., Swei, S. S.-M., and Zhu, G., “Optimum Wing Shape of Highly Flexible Morphing Aircraft for Improved Flight Performance,” *Journal of Aircraft*, vol. 53, no. 5, Sep. 2016, pp. 1305–13016.  
doi:10.2514/1.C033490.
- [8] Barbarino, S., Bilgen, O., and Ajaj, R., “A Review of Morphing Aircraft,” *Journal of Intelligent Material Systems and Structures*, vol. 22, Jun. 2011, pp. 823–877. doi:10.1177/1045389X11414084.
- [9] Lanchester, F., *Aerodynamics: Constituting the First Volume of a Complete Work on Aerial Flight*, London: A. Constable, 1907.

- [10] Prandtl, L., “Tragflügel Theorie,” *Nachrichten von der Gesellschaft der Wissenschaften zu Göttingen*, 1918, pp. 451–477.
- [11] Prandtl, L., *Applications of Modern Hydrodynamics to Aeronautics*, NACA, 1921.
- [12] Phillips, W., “Lifting-Line Analysis for Twisted Wings and Washout-Optimized Wings,” *Journal of Aircraft*, vol. 41, no. 1, Jan. 2004, pp. 128–136.  
doi:10.2514/1.262.
- [13] Phillips, W., Alley, N., and Goodrich, W., “Lifting-Line Analysis of Roll Control and Variable Twist,” *Journal of Aircraft*, vol. 41, no. 5, Sep. 2004, pp. 1169–1176.  
doi:10.2514/1.3846.
- [14] Phillips, W. F., and Alley, N. R., “Predicting Maximum Lift Coefficient for Twisted Wings Using Lifting-Line Theory,” *Journal of Aircraft*, vol. 44, no. 3, May 2007, pp. 898–910.  
doi:10.2514/1.25640.
- [15] Katz, J., and Plotkin, A., *Low-Speed Aerodynamics: From Wing Theory to Panel Methods*, McGraw-Hill, 1991.
- [16] Phillips, W., and Snyder, D., “Modern Adaptation of Prandtl’s Classic Lifting-Line Theory,” *Journal of Aircraft*, vol. 37, no. 4, Jul. 2000, pp. 662–670.  
doi:10.2514/2.2649.
- [17] McCormick, B., “The Lifting Line Model,” *Aerodynamics, Aeronautics, and Flight Mechanics*, New York: Wiley, 1994, p. 672.
- [18] Anderson, J., Corda, S., and Van Wie, D., “Numerical Lifting-Line Theory Applied to Drooped Leading-Edge Wings Below and Above Stall,” *Journal of Aircraft*, vol. 17, no. 12, Dec. 1980, pp. 898–904.  
doi:10.2514/3.44690.
- [19] Martins, J., “A Coupled-Adjoint Method for High-Fidelity Aero-Structural Optimization,” Doctoral dissertation, Stanford, 2002.  
<http://aero-comlab.stanford.edu/Papers/martins.thesis.pdf>.
- [20] Simmons, G., *Calculus Gems: Brief Lives and Memorable Mathematics*, Washington, D.C.: The Mathematical Association of America, 2007.

- [21] Courant, R., Friedrichs, K., and Lewy, H., “On the Partial Difference Equations of Mathematical Physics,” *IBM Journal of Research and Development*, vol. 11, Mar. 1967, pp. 215–234.  
doi:10.1147/rd.112.0215.
- [22] Hrennikoff, A., “Solution of Problems of Elasticity by the Framework Method,” *Journal of Applied Mechanics*, vol. 8, no. 4, 1941, pp. A169–A175.
- [23] Courant, R., “Variational Methods for the Solution of Problems of Equilibrium and Vibrations,” *Bulletin of the American Mathematical Society*, vol. 49, pp. 1–23.  
doi:10.1090/s0002-9904-1943-07818-4.
- [24] Thomée, V., “From Finite Differences to Finite Elements: A Short History of Numerical Analysis of Partial Differential Equations,” *Journal of Computational and Applied Mathematics*, vol. 128, no. 1–2, Mar. 2001, pp. 1–54.  
doi:10.1016/S0377-0427(00)00507-0.
- [25] Wengert, R., “A Simple Automatic Derivative Evaluation Program,” *Communications of the ACM*, vol. 7, no. 8, Aug. 1964, pp. 463–464.  
doi:10.1145/355586.364791.
- [26] Griewank, A., and Walther, A., *Evaluating Derivatives: Principles and Techniques of Algorithmic Differentiation*, Philadelphia, PA: Society of Industrial and Applied Mathematics, 2008.  
doi:10.1137/1.9780898717761.
- [27] Rall, L., *Automatic Differentiation: Techniques and Applications*, New York, NY: Springer-Verlag, 1981.
- [28] Corliss, G., Faure, C., Griewank, A., Hascoët, L., and Naumann, U., *Automatic Differentiation of Algorithms: From Simulation to Optimization*, New York, NY: Springer-Verlag New York, Inc., 2002.
- [29] Martins, J., and Hwang, J., “Review and Unification of Methods for Computing Derivatives of Multidisciplinary Computational Models,” *AIAA Journal*, vol. 51, no. 11, Sep. 2013, pp. 2582–2599.  
doi:10.2514/1.J052184.

- [30] Šrajcar, F., Kukulova, Z., and Fitzgibbon, A., “A Benchmark of Selected Algorithmic Differentiation Tools on Some Problems in Computer Vision and Machine Learning,” *Optimization Methods and Software*, vol. 33, no. 4–6, Feb. 2018, pp. 889–906.  
doi:10.1080/10556788.2018.1435651.
- [31] Yu, W., and Blair, M., “DNAD, A Simple Tool for Automatic Differentiation of Fortran Codes Using Dual Numbers,” *Computer Physics Communications*, vol. 184, no. 5, May 2013, pp. 1446–1452.  
doi:10.1016/j.cpc.2012.12.025.
- [32] Spall, R., and Yu, W., “Imbedded Dual-Number Automatic Differentiation for Computational Fluid Dynamics Sensitivity Analysis,” *Journal of Fluids Engineering*, vol. 135, no. 1, Dec. 2012.  
doi:10.1115/1.4023074.
- [33] Pakalapati, S., Sezer, H., and Celik, I., “Implications of using Dual Number Derivatives with a Numerical Solution,” *Proceedings of the ASME 2013 FLuids Engineering Division Summer Meeting*, Jul. 2013.
- [34] LeVeque, R., *Finite Difference Methods for Ordinary and Partial Differential Equations*, Philadelphia, PA: Society of Industrial and Applied Mathematics, 2007.
- [35] Hascoët, L., and Pascual, V., “The Tapenade Automatic Differentiation Tool: Principles, Model, and Specifications,” *ACM Transactions on Mathematical Software*, vol. 39, no. 3, Apr. 2013, pp. 1–20.  
doi:10.1145/2450153.2450158.
- [36] Naumann, U., Utke, J., Heimbach, P., Hill, C., Ozyurt, D., Wunsch, C., Fagan, M., Tallent, N., and Strout, M., “Adjoint Code by Source Transformation with OpenAD/F,” *Proceedings of the European Conference on Computational Fluid Dynamics*, 2006.
- [37] Abdel-Khalik, H., Hovland, P., Lyons, A., Stover, T., and Utke, J., “A Low Rank Approach to Automatic Differentiation,” *Advances in Automatic Differentiation*, vol. 64, 2008, pp. 55–65.  
doi:10.1007/978-3-540-68942-3\_6.
- [38] Qiang, C., Linbo, Z., and Bin, W., “Model Adjointization and its Cost,” *Science in China*, vol. 47, no. 5, Oct. 2004, pp. 587–611.  
doi:10.1360/02yf0440.

- [39] Bischof, C., Carle, A., Khademi, P., and Mauer, A., “ADIFOR 2.0: Automatic Differentiation of Fortran 77 Programs,” *IEEE Computational Science and Engineering*, vol. 3, no. 3, 1996, pp. 18–32.  
doi:10.1109/99.537089.
- [40] Lyness, J., “Numerical Algorithms Based on the Theory of Complex Variable,” *Proceedings of the 1967 22nd ACM National Conference*, 1967, pp. 125–133.  
doi:10.1145/800196.805983.
- [41] Martins, J., Sturdza, P., and Alonso, J., “The Complex-Step Derivative Approximation,” *ACM Transactions on Mathematical Software*, vol. 29, no. 3, Sep. 2003, pp. 245–262.  
doi:10.1145/838250.838251.
- [42] Straka, C., “ADF95: Tool for Automatic Differentiation of a Fortran Code Designed for Large Numbers of Independent Variables,” *Computer Physics Communications*, vol. 168, no. 2, Jun. 2005, pp. 123–139.  
doi:10.1016/j.cpc.2005.01.011.
- [43] Stamatiadis, S., Prosmi, R., and Farantos, S., “AUTO\_DERIV: Tool for Automatic Differentiation of a Fortran Code,” *Computer Physics Communications*, vol. 127, no. 2–3, May 2000, pp. 3443–355.  
doi:10.1016/S0010-4655(99)00513-5.
- [44] Berz, M., Makino, K., Shamseddine, K., Hoffstätter, G., and Weishi, W., “COSY INFINITY and Its Applications in Nonlinear Dynamics,” *Computational Differentiation: Techniques, Applications, and Tools*, M. Berz, C. Bischof, G. Corliss, and A. Griewank, eds., Philadelphia, PA: Society of Industrial and Applied Mathematics, 1996, pp. 363–367.
- [45] Pryce, J., and Reid, J., *AD01, A Fortran 90 Code for Automatic Differentiation*, Oxfordshire, England: Rutherford Appleton Laboratory, 1998.  
<ftp://ftp.numerical.rl.ac.uk/pub/reports/prRAL98057.pdf>. Accessed January 21, 2019.
- [46] Clifford, W., “Preliminary Sketch of Biquaternions,” *Proceedings of the London Mathematical Society*, vol. 4, no. 64, 1973, pp. 381–395.  
doi:10.1112/plms/s1-4.1.381.



- [47] Fike, J., and Alonso, J., “The Development of Hyper-Dual Numbers for Exact Second-Derivative Calculations,” *49th AIAA Aerospace Sciences Meeting Including the New Horizons Forum and Aerospace Exposition*, Jan. 2011.
- [48] Thomas, L., *Elliptic Problems in Linear Differential Equations over a Network*, New York: Columbia University, 1949.
- [49] Hunsaker, D., and Snyder, D., “A Lifting-Line Approach to Estimating Propeller/Wing Interactions,” *24th Applied Aerodynamics Conference*, Jun. 2006.
- [50] Phillips, W., and Hunsaker, D., “Lifting-Line Predictions for Induced Drag and Lift in Ground Effect,” *Journal of Aircraft*, vol. 50, no. 4, Aug. 2013, pp. 1226–1233.  
doi:10.2514/1.C032152.
- [51] Drela, M., “XFOIL: An Analysis and Design System for Low Reynolds Number Airfoils,” *Low Reynolds Number Aerodynamics*, T.J. Mueller, ed., Berlin, Heidelberg: Springer-Verlag, 1989, pp. 1–12.
- [52] Drela, M., and Giles, M., “Viscous-Inviscid Analysis of Transonic and Low Reynolds Number Airfoils,” *AIAA Journal*, vol. 25, no. 10, 1987, pp. 1347–1355.  
doi:10.2514/3.9789.
- [53] Phillips, W., *Mechanics of Flight*, Hoboken, NJ: John Wiley and Sons, Inc., 2010.
- [54] Oliphant, T., *Guide to NumPy*, USA: Trelgol Publishing, 2006.
- [55] Broyden, C., “The Convergence of a Class of Double-Rank Minimization Algorithms,” *Journal of the Institute of Mathematics and Its Applications*, vol. 6, 1970, pp. 76–90.  
doi:10.1093/imamat/6.1.76.
- [56] Fletcher, R., “A New Approach to Variable Metric Algorithms,” *Computer Journal*, vol. 13, no. 3, 1970, pp. 317–322.  
doi:10.12691/ajams-4-5-1.
- [57] Goldfarb, D., “A Family of Variable Metric Updates Derived by Variational Means,” *Mathematics of Computation*, vol. 24, no. 109, 1970, pp. 23–26.  
doi:10.2307/2004873.

- [58] Shanno, D., “Conditioning of Quasi-Newton Methods for Function Minimization,” *Mathematics of Computation*, vol. 24, no. 111, 1970, pp. 647–656.  
doi:10.2307/2004840.
- [59] Nocedal, J., and Wright, S., *Numerical Optimization*, Berlin, New York: Springer-Verlag, 2006.
- [60] Wolfe, P., “Convergence Conditions for Ascent Methods,” *SIAM Review*, vol. 11, no. 2, 1969, pp. 226–235.  
doi:10.1137/1011036.
- [61] Wolfe, P., “Convergence Conditions for Ascent Methods. II: Some Corrections,” *SIAM Review*, vol. 13, no. 2, 1971, pp. 185–188.  
doi:10.1137/1013035.
- [62] Hestenes, M., and Stiefel, E., “Methods of Conjugate Gradients for Solving Linear Systems,” *Journal of Research of the National Bureau of Standards*, vol. 49, no. 6, Dec. 1952, pp. 409–436.  
doi:10.6028/jres.049.044.
- [63] Goldstein, A., “Cauchy’s Method of Minimization,” *Numerische Mathematik*, vol. 4, no. 1, Dec. 1962, pp. 146–150.  
doi:10.1007/BF01386306.
- [64] Armijo, L., “Minimization of Functions Having Lipschitz Continuous First Partial Derivatives,” *Pacific Journal of Mathematics*, vol. 16, no. 1, 1966, pp. 1–3.  
doi:10.2140/pjm.1966.16.1.
- [65] Smith, A., and Coit, D., “Constraint-Handling Techniques – Penalty Functions,” *Handbook of Evolutionary Computation*, Bristol, United Kingdom: Institute of Physics Publishing and Oxford University Press, 1997, p. C5.2:1-6.
- [66] Griva, I., Nash, S., and Sofer, A., *Linear and Nonlinear Optimization*, Society of Industrial and Applied Mathematics, 2009.
- [67] Svanberg, K., “A Class of Globally Convergent Optimization Methods Based on Conservative Convex Separable Approximations,” *SIAM Journal on Optimization*, vol. 12, no. 2, 2002, pp. 555–573.  
doi:10.1137/S1052623499362822.

- [68] Locatelli, M., and Schoen, F., *Global Optimization*, Philadelphia, PA: Society of Industrial and Applied Mathematics, 2013.
- [69] Phillips, W. F., “Lifting-Line Analysis for Twisted Wings and Washout-Optimized Wings,” *Journal of Aircraft*, vol. 41, no. 1, Jan. 2004, pp. 128–136.  
doi:10.2514/1.262.
- [70] Birnbaum, W., “Die tragende Wirbelfläche als Hilfsmittel zur Behandlung des ebenen Problems der Tragflügeltheorie,” *Zeitschrift für angewandte Mathematik und Mechanik*, vol. 3, no. 4, 1923, pp. 290–297.  
doi:10.1002/zamm.19230030408.
- [71] Blenk, H., “Der Eindecker als tragende Wirbelfläche,” *Zeitschrift für angewandte Mathematik und Mechanik*, vol. 5, no. 1, 1925, pp. 36–47.  
doi:10.1002/zamm.19250050104.
- [72] Multhopp, H., *Methods for Calculating the Lift Distribution of Wings (Subsonic Lifting-Surface Theory)*, London: Aeronautical Research Council, 1955.
- [73] Kuchemann, D., *A Simple Method for Calculating the Span and Chordwise Loading on Straight and Swept Wings of any Given Aspect Ratio at Subsonic Speeds.*, Aeronautical Research Council, London, 1952.  
<http://www.dtic.mil/docs/citations/ADA951920>. Accessed November 6, 2018.
- [74] Helmholtz, H., “Theorie der Luftschwingungen in Röhren mit offenen Enden,” *Journal für die Reine und Angewandte Mathematik*, vol. 57, no. 1, 1860, pp. 1–72.
- [75] Anderson, J. D., *Fundamentals of Aerodynamics*, McGraw-Hill, .
- [76] Karamcheti, K., *Principles of Ideal-Fluid Aerodynamics*, New York: Wiley, 1966.
- [77] Munk, M., *The Aerodynamic Forces on Airship Hulls*, NACA, 1924.
- [78] Bollay, W., “A Non-linear Wing Theory and its Application to Rectangular Wings of Small Aspect Ratio,” *Zeitschrift für angewandte Mathematik und Mechanik*, vol. 19, no. 1, Feb. 1939, pp. 21–35.  
doi:10.1002/zamm.19390190103.
- [79] Jones, R., *Properties of Low-Aspect-Ratio Pointed Wings at Speeds Below and Above the Speed of Sound*, Langley Field, VA: NACA Langley Aeronautical Lab., 1946.

- [80] Zimmerman, C., *Characteristics of Clark Y Airfoils of Small Aspect Ratios*, Langley Field, VA: NACA Langley Aeronautical Lab., 1933.
- [81] Zimmerman, C., *Aerodynamic Characteristics of Several Airfoils of Low Aspect Ratio*, Langley Field, VA: NACA Langley Aeronautical Lab., 1935.
- [82] Winter, H., *Flow Phenomena on Plates and Airfoils of Short Span*, Washington, D.C.: NACA, 1936.
- [83] Hauptman, A., and Miloh, T., "On the Exact Solution of the Linearized Lifting-Surface Problem of an Elliptic Wing," *The Quarterly Journal of Mechanics and Applied Mathematics*, vol. 39, no. 1, Feb. 1986, pp. 41–66.  
doi:10.1093/qjmam/39.4.580.
- [84] Prandtl, L., *Recent Work on Airfoil Theory*, Washington, D.C.: NACA, 1940.
- [85] Hauptman, A., and Miloh, T., "Aerodynamic Coefficients of a Thin Elliptic Wing in Unsteady Motion," *AIAA Journal*, vol. 25, no. 6, Jun. 1987, pp. 769–774.
- [86] Smith, J., "Comment on 'Exact and Asymptotic Expressions of the Lift Slope Coefficient of an Elliptic Wing,'" *AIAA Journal*, vol. 28, no. 6, Jun. 1990, p. 1146.  
doi:10.2514/3.48881.
- [87] Laitone, E., "Lift-Curve Slope for Finite-Aspect-Ratio Wings," *Journal of Aircraft*, vol. 26, no. 8, Aug. 1989, pp. 789–790.  
doi:10.2514/3.45841.
- [88] Jones, R., *Correction of the Lifting-Line Theory for the Effect of the Chord*, Washington, D.C.: NACA, 1941.
- [89] Helmbold, H., "Der Unverwundene Ellipsenflügel als Tragende Fläche," *Jahrbuch 1942 der Deutschen Luftfahrtforschung*, 1942, pp. 2–4.
- [90] Van Dyke, M., "Some Inviscid Singular Perturbation Problems," *Perturbation Methods in Fluid Mechanics*, Stanford, CA: The Parabolic Press, 1975, pp. 167–193. Also see Note 13, pp. 239–241.
- [91] Germain, P., "Recent Evolution in Problems and Methods in Aerodynamics," *Journal of the Royal Aeronautical Society*, vol. 71, no. 682, Oct. 1967, pp. 673–691.  
doi:10.1017/S0001924000054324.

- [92] Kida, T., and Miyai, Y., “An Alternative Treatment of Lifting-Line Theory as a Perturbation Problem,” *Journal of Applied Mathematics and Physics*, vol. 29, no. 4, Jul. 1978, pp. 591–607.  
doi:10.1007/BF01601487.
- [93] Van Dyke, M., *Perturbation Methods in Fluid Mechanics*, Stanford, CA: Parabolic Press, 1975.
- [94] Kinner, W., “Über Tragflügel mit kreisförmigem Grundriss,” *Zeitschrift für Angewandte Mathematik und Mechanik*, vol. 16, no. 6, Dec. 1936, pp. 349–352.
- [95] Krienes, K., *The Elliptic Wing Based on the Potential Theory*, Washington, D.C.: NACA, 1941.
- [96] Jordan, P., “On Lifting Wings with Parabolic Tips,” *Zeitschrift für Angewandte Mathematik und Mechanik*, vol. 54, no. 7, 1974, pp. 463–477.
- [97] Medan, R., *Improvements to the Kernel Function Method of Steady, Subsonic Lifting Surface Theory*, Moffett Field, CA: NASA Ames Research Center, 1974.
- [98] Derbyshire, T., and Sidwell, K. W., *PAN AIR Summary Document (version 1.0)*, Moffett Field, CA: NASA Ames Research Center, 1982.  
<https://ntrs.nasa.gov/search.jsp?R=19840020672>. Accessed August 24, 2018.
- [99] Epton, M. A., and Magnus, A. E., *PAN AIR: A computer program for predicting subsonic or supersonic linear potential flows about arbitrary configurations using a higher order panel method. Volume 2: User’s Manual (version 1.0)*, Moffett Field, CA: NASA Ames Research Center, 1981.  
<https://ntrs.nasa.gov/search.jsp?R=19840019629>. Accessed August 24, 2018.
- [100] Epton, M. A., and Magnus, A. E., *PAN AIR: A computer program for predicting subsonic or supersonic linear potential flows about arbitrary configurations using a higher order panel method. Volume 1: Theory document (version 1.1)*, Moffett Field, CA: NASA Ames Research Center, 1981.  
<https://ntrs.nasa.gov/search.jsp?R=19840019629>. Accessed August 24, 2018.
- [101] Saffman, P., *Vortex Dynamics*, Cambridge: Cambridge University Press, 1993.
- [102] Hodson, J., Hunsaker, D., Andrews, B., and Joo, J., “Experimental Results for a Variable Camber Compliant Wing,” Denver, CO: AIAA, 2017, pp. 1–21.  
doi:10.2514/6.2017-4222.

## APPENDICES

## A MODIFIED DNAD SOURCE CODE

```

1  |*****
2  |* Dual Number Automatic Differentiation (DNAD) of Fortran Codes
3  |*-----
4  |* COPYRIGHT (c) Joshua Hodson, All rights reserved, you are free to copy,
5  |* modify, or translate this code to other languages such as c/c++. This is a
6  |* fork of the original Fortran DNAD module developed by Dr. Wenbin Yu. See
7  |* original copyright information below. You can download the original version
8  |* at https://cdmhub.org/resources/374
9  |*
10 |* COPYRIGHT (c) Wenbin Yu, All rights reserved, you are free to copy,
11 |* modify or translate this code to other languages such as c/c++. If
12 |* you find a bug please let me know through wenbinyu.heaven@gmail.com. If
13 |* you added new functions and want to share with others, please let me know
14 |* too. You are welcome to share your successful stories with us through
15 |* http://groups.google.com/group/hifi-comp.
16 |*****
17 |* Acknowledgements
18 |*-----
19 |* The development of DNAD is supported, in part, by the Chief Scientist
20 |* Innovative Research Fund at AFRL/RB WPAFB, and by Department of Army
21 |* SBIR (Topic A08-022) through Advanced Dynamics Inc. The views and
22 |* conclusions contained herein are those of the authors and should not be
23 |* interpreted as necessarily representing the official policies or
24 |* endorsement, either expressed or implied, of the funding agency.
25 |*
26 |* Additional development of DNAD has been supported under a Department of
27 |* Energy (DOE) Nuclear Energy University Program (NEUP) Graduate Fellowship.
28 |* Any opinions, findings, conclusions or recommendations expressed in this
29 |* publication are those of the authors and do not necessarily reflect the
30 |* views of the Department of Energy Office of Nuclear Energy.
31 |*****
32 |* Citation
33 |*-----
34 |* Your citation of the following two papers is appreciated:
35 |* Yu, W. and Blair, M.: "DNAD, a Simple Tool for Automatic Differentiation of
36 |* Fortran Codes Using Dual Numbers," Computer Physics Communications, vol.
37 |* 184, 2013, pp. 1446-1452.
38 |*
39 |* Spall, R. and Yu, W.: "Imbedded Dual-Number Automatic Differentiation for
40 |* CFD Sensitivity Analysis," Journal of Fluids Engineering, vol. 135, 2013,
41 |* 014501.
42 |*****
43 |* Quick Start Guide
44 |*-----
45 |* To integrate DNAD into an existing Fortran program, do the following:
46 |*
47 |*   1. Include the DNAD module in the source files by adding "use dnadmod" to
48 |*      the beginning of all modules, global functions, and global subroutines
49 |*      that include definitions of floating-point variables.
50 |*   2. Redefine all floating-point variables as type(dual). This can be done
51 |*      using precompiler directives so that the integration can be turned on
52 |*      or off at compile-time, eliminating the need for maintaining two
53 |*      separate code bases for the same project.
54 |*   3. All I/O involving floating-point variables will need to be examined.
55 |*      A method will need to be determined for inputting and outputting
56 |*      derivative values. This customization is typically unique for each
57 |*      piece of software and needs to be determined on a case-by-case basis.
58 |*   4. When compiling DNAD, use the compiler option "-Dndv=#", where # is the
59 |*      number of design variables desired. This sizes the derivative array

```

```

60  !*      that is stored with each floating point number.
61  !*      5. When compiling DNAD, use compiler options to specify precision. If no
62  !*      compiler options are specified, DNAD will default to single-precision
63  !*      floating-point arithmetic. Most popular Fortran compilers provide
64  !*      options for specifying precision at compile-time so that it does not
65  !*      have to be hard-coded into the source code. For example, use the
66  !*      "-fdefault-real-8" compiler in gfortran or the "-r8" compiler option
67  !*      with Intel Fortran to compile DNAD as double-precision.
68  !*      6. Modify the compilation process for the target software to include the
69  !*      DNAD module in the resulting executable or library.
70  !*****
71  !* Change Log
72  !*-----
73  !*
74  !* 2016-04-29 Joshua Hodson
75  !* - Updated copyright, acknowledgments, and quick start guide.
76  !* - Removed overloads for single-precision reals.
77  !* - Added tan, dtan, atan, and atan2 intrinsic function overloads.
78  !* - Removed macro for precision and defined all floating-point variables as
79  !*   default real. Compiler options can now be used to set precision.
80  !* - Added checks for undefined derivatives when only constants are used in
81  !*   the calculation (i.e. all partial derivatives are zero). This limits the
82  !*   perpetuation of NaN values in the code.
83  !* - Combined the header and source files into a single file.
84  !*
85  !* 2015-07-29 Joshua Hodson
86  !* - Added maxloc intrinsic function overload.
87  !* - Converted UPPERCase to lowercase for readability.
88  !* - Added macros for defining precision and number of design variables.
89  !* - Renamed module from Dual_Num_Auto_Diff to dnadmod
90  !* - Renamed dual number type from DUAL_NUM to dual
91  !* - Renamed components of dual number type from (xp_ad_, xp_ad_) to (x, dx)
92  !*
93  !* 2014-06-05 Wenbin Yu
94  !* - Forked from original DNAD repository, see https://cdmhub.org/resources/374
95  !*
96  !*****
97
98  ! Number of design variables (default = 1)
99  #ifndef ndv
100 #define ndv 1
101 #endif
102
103 module dnadmod
104
105     implicit none
106
107     private
108
109     real :: negative_one = -1.0
110     type,public:: dual ! make this private will create difficulty to use the
111                        ! original write/read commands, hence x and dx are
112                        ! variables which can be accessed using D%x and D%dx in
113                        ! other units using this module in which D is defined
114                        ! as type(dual).
115         sequence
116         real :: x ! functional value
117         real :: dx(ndv) ! derivative
118     end type dual
119
120

```



```

121 !***** Interfaces for operator overloading
122     public assignment (=)
123     interface assignment (=)
124         module procedure assign_di ! dual=integer, elemental
125         module procedure assign_dr ! dual=real, elemental
126         module procedure assign_id ! integer=dual, elemental
127     end interface
128
129
130     public operator (+)
131     interface operator (+)
132         module procedure add_d ! +dual number, elemental
133         module procedure add_dd ! dual + dual, elemental
134         module procedure add_di ! dual + integer, elemental
135         module procedure add_dr ! dual + real, elemental
136         module procedure add_id ! integer + dual, elemental
137         module procedure add_rd ! real + dual, elemental
138     end interface
139
140     public operator (-)
141     interface operator (-)
142         module procedure minus_d ! negate a dual number,elemental
143         module procedure minus_dd ! dual -dual,elemental
144         module procedure minus_di ! dual-integer,elemental
145         module procedure minus_dr ! dual-real,elemental
146         module procedure minus_id ! integer-dual,elemental
147         module procedure minus_rd ! real-dual,elemental
148     end interface
149
150     public operator (*)
151     interface operator (*)
152         module procedure mult_dd ! dual*dual, elemental
153         module procedure mult_di ! dual*integer,elemental
154         module procedure mult_dr ! dual*real,elemental
155         module procedure mult_id ! integer*dual,elemental
156         module procedure mult_rd ! real*dual,elemental
157     end interface
158
159     public operator (/)
160     interface operator (/)
161         module procedure div_dd ! dual/dual,elemental
162         module procedure div_di ! dual/integer, elemental
163         module procedure div_dr ! dual/real,emental
164         module procedure div_id ! integer/dual, elemental
165         module procedure div_rd ! real/dual, elemental
166     end interface
167
168     public operator (**)
169     interface operator (**)
170         module procedure pow_i ! dual number to an integer power,elemental
171         module procedure pow_r ! dual number to a real power, elemental
172         module procedure pow_d ! dual number to a dual power, elemental
173     end interface
174
175     public operator (==)
176     interface operator (==)
177         module procedure eq_dd ! compare two dual numbers, elemental
178         module procedure eq_di ! compare a dual and an integer, elemental
179         module procedure eq_dr ! compare a dual and a real, elemental
180         module procedure eq_id ! compare integer with a dual number, elemental
181         module procedure eq_rd ! compare a real with a dual number, elemental

```

```

182     end interface
183
184     public operator (<=)
185     interface operator (<=)
186         module procedure le_dd ! compare two dual numbers, elemental
187         module procedure le_di ! compare a dual and an integer, elemental
188         module procedure le_dr ! compare a dual and a real, elemental
189         module procedure le_id ! compare integer with a dual number, elemental
190         module procedure le_rd ! compare a real with a dual number, elemental
191     end interface
192
193     public operator (<)
194     interface operator (<)
195         module procedure lt_dd !compare two dual numbers, elemental
196         module procedure lt_di !compare a dual and an integer, elemental
197         module procedure lt_dr !compare dual with a real, elemental
198         module procedure lt_id ! compare integer with a dual number, elemental
199         module procedure lt_rd ! compare a real with a dual number, elemental
200     end interface
201
202     public operator (>=)
203     interface operator (>=)
204         module procedure ge_dd ! compare two dual numbers, elemental
205         module procedure ge_di ! compare dual with integer, elemental
206         module procedure ge_dr ! compare dual with a real number, elemental
207         module procedure ge_id ! compare integer with a dual number, elemental
208         module procedure ge_rd ! compare a real with a dual number, elemental
209     end interface
210
211     public operator (>)
212     interface operator (>)
213         module procedure gt_dd !compare two dual numbers, elemental
214         module procedure gt_di !compare a dual and an integer, elemental
215         module procedure gt_dr !compare dual with a real, elemental
216         module procedure gt_id ! compare integer with a dual number, elemental
217         module procedure gt_rd ! compare a real with a dual number, elemental
218     end interface
219
220     public operator (/=)
221     interface operator (/=)
222         module procedure ne_dd !compare two dual numbers, elemental
223         module procedure ne_di !compare a dual and an integer, elemental
224         module procedure ne_dr !compare dual with a real, elemental
225         module procedure ne_id ! compare integer with a dual number, elemental
226         module procedure ne_rd ! compare a real with a dual number, elemental
227     end interface
228
229
230 !-----
231 ! Interfaces for intrinsic functions overloading
232 !-----
233     public abs
234     interface abs
235         module procedure abs_d ! absolute value of a dual number, elemental
236     end interface
237
238     public dabs
239     interface dabs
240         module procedure abs_d ! same as abs, used for some old fortran commands
241     end interface
242

```

```

243     public acos
244     interface acos
245         module procedure acos_d ! arccosine of a dual number, elemental
246     end interface
247
248     public asin
249     interface asin
250         module procedure asin_d ! arcsine of a dual number, elemental
251     end interface
252
253     public atan
254     interface atan
255         module procedure atan_d ! arctan of a dual number, elemental
256     end interface
257
258     public atan2
259     interface atan2
260         module procedure atan2_d ! arctan of a dual number, elemental
261     end interface
262
263     public cos
264     interface cos
265         module procedure cos_d ! cosine of a dual number, elemental
266     end interface
267
268     public dcoss
269     interface dcoss
270         module procedure cos_d ! cosine of a dual number, elemental
271     end interface
272
273     public dot_product
274     interface dot_product
275         module procedure dot_product_dd ! dot product two dual number vectors
276     end interface
277
278     public exp
279     interface exp
280         module procedure exp_d ! exponential of a dual number, elemental
281     end interface
282
283     public int
284     interface int
285         module procedure int_d ! integer part of a dual number, elemental
286     end interface
287
288     public log
289     interface log
290         module procedure log_d ! log of a dual number, elemental
291     end interface
292
293     public log10
294     interface log10
295         module procedure log10_d ! log of a dual number, elemental
296     end interface
297
298     public matmul
299     interface matmul
300         module procedure matmul_dd ! multiply two dual matrices
301         module procedure matmul_dv ! multiply a dual matrix with a dual vector
302         module procedure matmul_vd ! multiply a dual vector with a dual matrix
303     end interface

```

```

304
305
306     public max
307     interface max
308         module procedure max_dd ! max of from two to four dual numbers,
309 elemental
310         module procedure max_di ! max of a dual number and an integer, elemental
311         module procedure max_dr ! max of a dual number and a real, elemental
312         module procedure max_rd ! max of a real, and a dual number, elemental
313     end interface
314
315     public dmax1
316     interface dmax1
317         module procedure max_dd ! max of from two to four dual numbers,
318 elemental
319     end interface
320
321     public maxval
322     interface maxval
323         module procedure maxval_d ! maxval of a dual number vector
324     end interface
325
326     public min
327     interface min
328         module procedure min_dd ! min of from two to four dual numbers,
329 elemental
330         module procedure min_dr ! min of a dual and a real, elemental
331     end interface
332
333     public dmin1
334     interface dmin1
335         module procedure min_dd ! min of from two to four dual numbers,
336 elemental
337     end interface
338
339     public minval
340     interface minval
341         module procedure minval_d ! obtain the maxval of a dual number vectgor
342     end interface
343
344     public nint
345     interface nint
346         module procedure nint_d ! nearest integer to the argument, elemental
347     end interface
348
349     public sign
350     interface sign
351         module procedure sign_dd ! sign(a,b) with two dual numbers, elemental
352         module procedure sign_rd ! sign(a,b) with a real and a dual, elemental
353     end interface
354
355     public sin
356     interface sin
357         module procedure sin_d ! obtain sine of a dual number, elemental
358     end interface
359
360     public dsin
361     interface dsin
362         module procedure sin_d ! obtain sine of a dual number, elemental
363     end interface

```

```

361     public tan
362     interface tan
363         module procedure tan_d ! obtain sine of a dual number, elemental
364     end interface
365
366     public dtan
367     interface dtan
368         module procedure tan_d ! obtain sine of a dual number, elemental
369     end interface
370
371     public sqrt
372     interface sqrt
373         module procedure sqrt_d ! obtain the sqrt of a dual number, elemental
374     end interface
375
376     public sum
377     interface sum
378         module procedure sum_d ! sum a dual array
379     end interface
380
381     public maxloc
382     interface maxloc
383         module procedure maxloc_d ! location of max in a dual array
384     end interface
385
386 contains
387
388 !*****Begin: functions/subroutines for overloading operators
389
390 !***** Begin: (=)
391 !-----
392
393     !-----
394     ! dual = integer
395     ! <u, du> = <i, 0>
396     !-----
397     elemental subroutine assign_di(u, i)
398         type(dual), intent(out) :: u
399         integer, intent(in) :: i
400
401         u%x = real(i) ! This is faster than direct assignment
402         u%dx = 0.0
403
404     end subroutine assign_di
405
406
407     !-----
408     ! dual = real(double)
409     ! <u, du> = <r, 0>
410     !-----
411     elemental subroutine assign_dr(u, r)
412         type(dual), intent(out) :: u
413         real, intent(in) :: r
414
415         u%x = r
416         u%dx = 0.0
417
418     end subroutine assign_dr
419
420
421     !-----

```

```

422     ! integer = dual
423     ! i = <u, du>
424     !-----
425     elemental subroutine assign_id(i, v)
426         type(dual), intent(in) :: v
427         integer, intent(out) :: i
428
429         i = int(v%x)
430
431     end subroutine assign_id
432
433 !***** End: (=)
434 !-----
435
436
437 !***** Begin: (+)
438 !-----
439
440     !-----
441     ! Unary positive
442     ! <res, dres> = +<u, du>
443     !-----
444     elemental function add_d(u) result(res)
445         type(dual), intent(in) :: u
446         type(dual) :: res
447
448         res = u ! Faster than assigning component wise
449
450     end function add_d
451
452
453     !-----
454     ! dual + dual
455     ! <res, dres> = <u, du> + <v, dv> = <u + v, du + dv>
456     !-----
457     elemental function add_dd(u, v) result(res)
458         type(dual), intent(in) :: u, v
459         type(dual) :: res
460
461         res%x = u%x + v%x
462         res%dx = u%dx + v%dx
463
464     end function add_dd
465
466
467     !-----
468     ! dual + integer
469     ! <res, dres> = <u, du> + i = <u + i, du>
470     !-----
471     elemental function add_di(u, i) result(res)
472         type(dual), intent(in) :: u
473         integer, intent(in) :: i
474         type(dual) :: res
475
476         res%x = real(i) + u%x
477         res%dx = u%dx
478
479     end function add_di
480
481
482     !-----

```

```

483      ! dual + double
484      ! <res, dres> = <u, du> + <r, 0> = <u + r, du>
485      !-----
486      elemental function add_dr(u, r) result(res)
487          type(dual), intent(in) :: u
488          real, intent(in) :: r
489          type(dual) :: res
490
491          res%x = r + u%x
492          res%dx = u%dx
493
494      end function add_dr
495
496
497      !-----
498      ! integer + dual
499      ! <res, dres> = <i, 0> + <v, dv> = <i + v, dv>
500      !-----
501      elemental function add_id(i, v) result(res)
502          integer, intent(in) :: i
503          type(dual), intent(in) :: v
504          type(dual) :: res
505
506          res%x = real(i) + v%x
507          res%dx = v%dx
508
509      end function add_id
510
511
512      !-----
513      ! double + dual
514      ! <res, dres> = <r, 0> + <v, dv> = <r + v, dv>
515      !-----
516      elemental function add_rd(r, v) result(res)
517          real, intent(in) :: r
518          type(dual), intent(in) :: v
519          type(dual) :: res
520
521          res%x = r + v%x
522          res%dx = v%dx
523
524      end function add_rd
525
526      !***** End: (+)
527      !-----
528
529
530      !***** Begin: (-)
531      !-----
532
533      !-----
534      ! negate a dual
535      ! <res, dres> = -<u, du>
536      !-----
537      elemental function minus_d(u) result(res)
538          type(dual), intent(in) :: u
539          type(dual) :: res
540
541          res%x = -u%x
542          res%dx = -u%dx
543

```

```

544     end function minus_d
545
546
547     !-----
548     ! dual - dual
549     ! <res, dres> = <u, du> - <v, dv> = <u - v, du - dv>
550     !-----
551     elemental function minus_dd(u, v) result(res)
552         type(dual), intent(in) :: u, v
553         type(dual) :: res
554
555         res%x = u%x - v%x
556         res%dx = u%dx - v%dx
557
558     end function minus_dd
559
560     !-----
561     ! dual - integer
562     ! <res, dres> = <u, du> - i = <u - i, du>
563     !-----
564     elemental function minus_di(u, i) result(res)
565         type(dual), intent(in) :: u
566         integer, intent(in) :: i
567         type(dual) :: res
568
569         res%x = u%x - real(i)
570         res%dx = u%dx
571
572     end function minus_di
573
574
575     !-----
576     ! dual - double
577     ! <res, dres> = <u, du> - r = <u - r, du>
578     !-----
579     elemental function minus_dr(u, r) result(res)
580         type(dual), intent(in) :: u
581         real, intent(in) :: r
582         type(dual) :: res
583
584         res%x = u%x - r
585         res%dx = u%dx
586
587     end function minus_dr
588
589
590     !-----
591     ! integer - dual
592     ! <res, dres> = i - <v, dv> = <i - v, -dv>
593     !-----
594     elemental function minus_id(i, v) result(res)
595         integer, intent(in) :: i
596         type(dual), intent(in) :: v
597         type(dual) :: res
598
599         res%x = real(i) - v%x
600         res%dx = -v%dx
601
602     end function minus_id
603
604

```



```

605  !-----
606  ! double - dual
607  ! <res, dres> = r - <v, dv> = <r - v, -dv>
608  !-----
609  elemental function minus_rd(r, v) result(res)
610      real, intent(in) :: r
611      type(dual), intent(in) :: v
612      type(dual) :: res
613
614      res%x = r - v%x
615      res%dx = -v%dx
616
617  end function minus_rd
618
619  !***** END: (-)
620  !-----
621
622
623  !***** BEGIN: (*)
624  !-----
625
626  !-----
627  ! dual * dual
628  ! <res, dres> = <u, du> * <v, dv> = <u * v, u * dv + v * du>
629  !-----
630  elemental function mult_dd(u, v) result(res)
631      type(dual), intent(in) :: u, v
632      type(dual) :: res
633
634      res%x = u%x * v%x
635      res%dx = u%x * v%dx + v%x * u%dx
636
637  end function mult_dd
638
639
640  !-----
641  ! dual * integer
642  ! <res, dres> = <u, du> * i = <u * i, du * i>
643  !-----
644  elemental function mult_di(u, i) result(res)
645      type(dual), intent(in) :: u
646      integer, intent(in) :: i
647      type(dual) :: res
648
649      real :: r
650
651      r = real(i)
652      res%x = r * u%x
653      res%dx = r * u%dx
654
655  end function mult_di
656
657  !-----
658  ! dual * double
659  ! <res, dres> = <u, du> * r = <u * r, du * r>
660  !-----
661  elemental function mult_dr(u, r) result(res)
662      type(dual), intent(in) :: u
663      real, intent(in) :: r
664      type(dual) :: res
665

```

```

666         res%x = u%x * r
667         res%dx = u%dx * r
668
669     end function mult_dr
670
671
672     !-----
673     ! integer * dual
674     ! <res, dres> = i * <v, dv> = <i * v, i * dv>
675     !-----
676     elemental function mult_id(i, v) result(res)
677         integer, intent(in) :: i
678         type(dual), intent(in) :: v
679         type(dual) :: res
680
681         real :: r
682
683         r = real(i)
684         res%x = r * v%x
685         res%dx = r * v%dx
686
687     end function mult_id
688
689
690     !-----
691     ! double * dual
692     ! <res, dres> = r * <v, dv> = <r * v, r * dv>
693     !-----
694     elemental function mult_rd(r, v) result(res)
695         real, intent(in) :: r
696         type(dual), intent(in) :: v
697         type(dual) :: res
698
699         res%x = r * v%x
700         res%dx = r * v%dx
701
702     end function mult_rd
703
704     !***** END: (*)
705     !-----
706
707
708     !***** BEGIN: (/)
709     !-----
710
711     !-----
712     ! dual / dual
713     ! <res, dres> = <u, du> / <v, dv> = <u / v, du / v - u * dv / v^2>
714     !-----
715     elemental function div_dd(u, v) result(res)
716         type(dual), intent(in) :: u, v
717         type(dual) :: res
718
719         real :: inv
720
721         inv = 1.0 / v%x
722         res%x = u%x * inv
723         res%dx = (u%dx - res%x * v%dx) * inv
724
725     end function div_dd
726

```

```

727
728 !-----
729 ! dual / integer
730 ! <res, dres> = <u, du> / i = <u / i, du / i>
731 !-----
732 elemental function div_di(u, i) result(res)
733     type(dual), intent(in) :: u
734     integer, intent(in) :: i
735     type(dual) :: res
736
737     real :: inv
738
739     inv = 1.0 / real(i)
740     res%x = u%x * inv
741     res%dx = u%dx * inv
742
743 end function div_di
744
745
746 !-----
747 ! dual / double
748 ! <res, dres> = <u, du> / r = <u / r, du / r>
749 !-----
750 elemental function div_dr(u, r) result(res)
751     type(dual), intent(in) :: u
752     real, intent(in) :: r
753     type(dual) :: res
754
755     real :: inv
756
757     inv = 1.0 / r
758     res%x = u%x * inv
759     res%dx = u%dx * inv
760
761 end function div_dr
762
763
764 !-----
765 ! integer / dual
766 ! <res, dres> = i / <v, dv> = <i / v, -i / v^2 * du>
767 !-----
768 elemental function div_id(i, v) result(res)
769     integer, intent(in) :: i
770     type(dual), intent(in) :: v
771     type(dual) :: res
772
773     real :: inv
774
775     inv = 1.0 / v%x
776     res%x = real(i) * inv
777     res%dx = -res%x * inv * v%dx
778
779 end function div_id
780
781
782 !-----
783 ! double / dual
784 ! <res, dres> = r / <u, du> = <r / u, -r / u^2 * du>
785 !-----
786 elemental function div_rd(r, v) result(res)
787     real, intent(in) :: r

```

```

788     type(dual), intent(in) :: v
789     type(dual) :: res
790
791     real :: inv
792
793     inv = 1.0 / v%x
794     res%x = r * inv
795     res%dx = -res%x * inv * v%dx
796
797     end function div_rd
798
799 !***** END: (/)
800 !-----
801
802 !***** BEGIN: (**)
803 !-----
804
805 !-----
806 ! power(dual, integer)
807 ! <res, dres> = <u, du> ^ i = <u ^ i, i * u ^ (i - 1) * du>
808 !-----
809 elemental function pow_i(u, i) result(res)
810     type(dual), intent(in) :: u
811     integer, intent(in) :: i
812     type(dual) :: res
813
814     real :: pow_x
815
816     pow_x = u%x ** (i - 1)
817     res%x = u%x * pow_x
818     res%dx = real(i) * pow_x * u%dx
819
820     end function pow_i
821
822 !-----
823 ! power(dual, double)
824 ! <res, dres> = <u, du> ^ r = <u ^ r, r * u ^ (r - 1) * du>
825 !-----
826 elemental function pow_r(u, r) result(res)
827     type(dual), intent(in) :: u
828     real, intent(in) :: r
829     type(dual) :: res
830
831     real :: pow_x
832
833     pow_x = u%x ** (r - 1.0)
834     res%x = u%x * pow_x
835     res%dx = r * pow_x * u%dx
836
837     end function pow_r
838
839 !-----
840 ! POWER dual numbers to a dual power
841 ! <res, dres> = <u, du> ^ <v, dv>
842 !     = <u ^ v, u ^ v * (v / u * du + Log(u) * dv)>
843 !-----
844 elemental function pow_d(u, v) result(res)
845     type(dual), intent(in)::u, v
846     type(dual) :: res
847
848     res%x = u%x ** v%x

```

```

849         res%dx = res%x * (v%x / u%x * u%dx + log(u%x) * v%dx)
850
851     end function pow_d
852
853 !***** END: (**)
854 !-----
855
856
857 !***** BEGIN: (==)
858 !-----
859 !-----
860 ! compare two dual numbers,
861 ! simply compare the functional value.
862 !-----
863 elemental function eq_dd(lhs, rhs) result(res)
864     type(dual), intent(in) :: lhs, rhs
865     logical :: res
866
867     res = (lhs%x == rhs%x)
868
869 end function eq_dd
870
871
872 !-----
873 ! compare a dual with an integer,
874 ! simply compare the functional value.
875 !-----
876 elemental function eq_di(lhs, rhs) result(res)
877     type(dual), intent(in) :: lhs
878     integer, intent(in) :: rhs
879     logical :: res
880
881     res = (lhs%x == real(rhs))
882
883 end function eq_di
884
885
886 !-----
887 ! compare a dual number with a real number,
888 ! simply compare the functional value.
889 !-----
890 elemental function eq_dr(lhs, rhs) result(res)
891     type(dual), intent(in) :: lhs
892     real, intent(in) :: rhs
893     logical::res
894
895     res = (lhs%x == rhs)
896
897 end function eq_dr
898
899
900 !-----
901 ! compare an integer with a dual,
902 ! simply compare the functional value.
903 !-----
904 elemental function eq_id(lhs, rhs) result(res)
905     integer, intent(in) :: lhs
906     type(dual), intent(in) :: rhs
907     logical :: res
908
909     res = (lhs == rhs%x)

```

```

910
911     end function eq_id
912
913
914     !-----
915     ! compare a real with a dual,
916     ! simply compare the functional value.
917     !-----
918     elemental function eq_rd(lhs, rhs) result(res)
919         real, intent(in) :: lhs
920         type(dual), intent(in) :: rhs
921         logical :: res
922
923         res = (lhs == rhs%x)
924
925     end function eq_rd
926
927     !***** END: (==)
928     !-----
929
930
931     !***** BEGIN: (<=)
932     !-----
933     !-----
934     ! compare two dual numbers, simply compare
935     ! the functional value.
936     !-----
937     elemental function le_dd(lhs, rhs) result(res)
938         type(dual), intent(in) :: lhs, rhs
939         logical :: res
940
941         res = (lhs%x <= rhs%x)
942
943     end function le_dd
944
945
946     !-----
947     ! compare a dual with an integer,
948     ! simply compare the functional value.
949     !-----
950     elemental function le_di(lhs, rhs) result(res)
951         type(dual), intent(in) :: lhs
952         integer, intent(in) :: rhs
953         logical :: res
954
955         res = (lhs%x <= rhs)
956
957     end function le_di
958
959
960     !-----
961     ! compare a dual number with a real number,
962     ! simply compare the functional value.
963     !-----
964     elemental function le_dr(lhs, rhs) result(res)
965         type(dual), intent(in) :: lhs
966         real, intent(in) :: rhs
967         logical :: res
968
969         res = (lhs%x <= rhs)
970

```

```

971     end function le_dr
972
973
974     !-----
975     ! compare a dual number with an integer,
976     ! simply compare the functional value.
977     !-----
978     elemental function le_id(i, rhs) result(res)
979         integer, intent(in) :: i
980         type(dual), intent(in) :: rhs
981         logical :: res
982
983         res = (i <= rhs%x)
984
985     end function le_id
986
987
988     !-----
989     ! compare a real with a dual,
990     ! simply compare the functional value.
991     !-----
992     elemental function le_rd(lhs, rhs) result(res)
993         real, intent(in) :: lhs
994         type(dual), intent(in) :: rhs
995         logical :: res
996
997         res = (lhs <= rhs%x)
998
999     end function le_rd
1000
1001 !***** END: (<=)
1002 !-----
1003
1004 !***** BEGIN: (<)
1005 !-----
1006     !-----
1007     ! compare two dual numbers, simply compare
1008     ! the functional value.
1009     !-----
1010     elemental function lt_dd(lhs, rhs) result(res)
1011         type(dual), intent(in) :: lhs, rhs
1012         logical :: res
1013
1014         res = (lhs%x < rhs%x)
1015
1016     end function lt_dd
1017
1018
1019     !-----
1020     ! compare a dual with an integer,
1021     ! simply compare the functional value.
1022     !-----
1023     elemental function lt_di(lhs, rhs) result(res)
1024         type(dual), intent(in) :: lhs
1025         integer, intent(in) :: rhs
1026         logical :: res
1027
1028         res = (lhs%x < rhs)
1029
1030     end function lt_di
1031

```

```

1032  !-----
1033  ! compare a dual number with a real number, simply compare
1034  ! the functional value.
1035  !-----
1036  elemental function lt_dr(lhs, rhs) result(res)
1037      type(dual), intent(in) :: lhs
1038      real, intent(in) :: rhs
1039      logical :: res
1040
1041      res = (lhs%x < rhs)
1042
1043  end function lt_dr
1044
1045
1046  !-----
1047  ! compare a dual number with an integer
1048  !-----
1049  elemental function lt_id(i, rhs) result(res)
1050      integer, intent(in) :: i
1051      type(dual), intent(in) :: rhs
1052      logical :: res
1053
1054      res = (i < rhs%x)
1055
1056  end function lt_id
1057
1058
1059  !-----
1060  ! compare a real with a dual
1061  !-----
1062  elemental function lt_rd(lhs, rhs) result(res)
1063      real, intent(in) :: lhs
1064      type(dual), intent(in) :: rhs
1065      logical :: res
1066
1067      res = (lhs < rhs%x)
1068
1069  end function lt_rd
1070
1071  !***** END: (<)
1072  !-----
1073
1074  !***** BEGIN: (>=)
1075  !-----
1076  !-----
1077  ! compare two dual numbers, simply compare
1078  ! the functional value.
1079  !-----
1080  elemental function ge_dd(lhs, rhs) result(res)
1081      type(dual), intent(in) :: lhs, rhs
1082      logical :: res
1083
1084      res = (lhs%x >= rhs%x)
1085
1086  end function ge_dd
1087
1088
1089  !-----
1090  ! compare a dual with an integer
1091  !-----
1092  elemental function ge_di(lhs, rhs) result(res)

```



```

1093     type(dual), intent(in) :: lhs
1094     integer, intent(in) :: rhs
1095     logical :: res
1096
1097     res = (lhs%x >= rhs)
1098
1099 end function ge_di
1100
1101
1102 !-----
1103 ! compare a dual number with a real number, simply compare
1104 ! the functional value.
1105 !-----
1106 elemental function ge_dr(lhs, rhs) result(res)
1107     type(dual), intent(in) :: lhs
1108     real, intent(in) :: rhs
1109     logical :: res
1110
1111     res = (lhs%x >= rhs)
1112
1113 end function ge_dr
1114
1115
1116 !-----
1117 ! compare a dual number with an integer
1118 !-----
1119 elemental function ge_id(i, rhs) result(res)
1120     integer, intent(in) :: i
1121     type(dual), intent(in) :: rhs
1122     logical :: res
1123
1124     res = (i >= rhs%x)
1125
1126 end function ge_id
1127
1128
1129 !-----
1130 ! compare a real with a dual
1131 !-----
1132 elemental function ge_rd(lhs, rhs) result(res)
1133     real, intent(in) :: lhs
1134     type(dual), intent(in) :: rhs
1135     logical :: res
1136
1137     res = (lhs >= rhs%x)
1138
1139 end function ge_rd
1140
1141 !***** END: (>=)
1142 !-----
1143
1144 !***** BEGIN: (>)
1145 !-----
1146 !-----
1147 ! compare two dual numbers, simply compare
1148 ! the functional value.
1149 !-----
1150 elemental function gt_dd(lhs, rhs) result(res)
1151     type(dual), intent(in) :: lhs, rhs
1152     logical :: res
1153

```

```

1154         res = (lhs%x > rhs%x)
1155
1156     end function gt_dd
1157
1158
1159     !-----
1160     ! compare a dual with an integer
1161     !-----
1162     elemental function gt_di(lhs, rhs) result(res)
1163         type(dual), intent(in) :: lhs
1164         integer, intent(in) :: rhs
1165         logical :: res
1166
1167         res = (lhs%x > rhs)
1168
1169     end function gt_di
1170
1171
1172     !-----
1173     ! compare a dual number with a real number, simply compare
1174     ! the functional value.
1175     !-----
1176     elemental function gt_dr(lhs, rhs) result(res)
1177         type(dual), intent(in) :: lhs
1178         real, intent(in) :: rhs
1179         logical :: res
1180
1181         res = (lhs%x > rhs)
1182
1183     end function gt_dr
1184
1185
1186     !-----
1187     ! compare a dual number with an integer
1188     !-----
1189     elemental function gt_id(i, rhs) result(res)
1190         integer, intent(in) :: i
1191         type(dual), intent(in) :: rhs
1192         logical :: res
1193
1194         res = (i > rhs%x)
1195
1196     end function gt_id
1197
1198
1199     !-----
1200     ! compare a real with a dual
1201     !-----
1202     elemental function gt_rd(lhs, rhs) result(res)
1203         real, intent(in) :: lhs
1204         type(dual), intent(in) :: rhs
1205         logical :: res
1206
1207         res = (lhs > rhs%x)
1208
1209     end function gt_rd
1210
1211     !***** END: (>)
1212     !-----
1213
1214     !***** BEGIN: (/=)

```

```

1215 !-----
1216 !-----
1217 ! compare two dual numbers, simply compare
1218 ! the functional value.
1219 !-----
1220 elemental function ne_dd(lhs, rhs) result(res)
1221     type(dual), intent(in) :: lhs, rhs
1222     logical :: res
1223
1224     res = (lhs%x /= rhs%x)
1225
1226 end function ne_dd
1227
1228
1229 !-----
1230 ! compare a dual with an integer
1231 !-----
1232 elemental function ne_di(lhs, rhs) result(res)
1233     type(dual), intent(in) :: lhs
1234     integer, intent(in) :: rhs
1235     logical :: res
1236
1237     res = (lhs%x /= rhs)
1238
1239 end function ne_di
1240
1241
1242 !-----
1243 ! compare a dual number with a real number, simply compare
1244 ! the functional value.
1245 !-----
1246 elemental function ne_dr(lhs, rhs) result(res)
1247     type(dual), intent(in) :: lhs
1248     real, intent(in) :: rhs
1249     logical :: res
1250
1251     res = (lhs%x /= rhs)
1252
1253 end function ne_dr
1254
1255
1256 !-----
1257 ! compare a dual number with an integer
1258 !-----
1259 elemental function ne_id(i, rhs) result(res)
1260     integer, intent(in) :: i
1261     type(dual), intent(in) :: rhs
1262     logical :: res
1263
1264     res = (i /= rhs%x)
1265
1266 end function ne_id
1267
1268
1269 !-----
1270 ! compare a real with a dual
1271 !-----
1272 elemental function ne_rd(lhs, rhs) result(res)
1273     real, intent(in) :: lhs
1274     type(dual), intent(in) :: rhs
1275     logical :: res

```

```

1276
1277         res = (lhs /= rhs%x)
1278
1279     end function ne_rd
1280
1281 !***** END: (/=)
1282 !-----
1283
1284 !-----
1285 ! Absolute value of dual numbers
1286 ! <res, dres> = abs(<u, du>) = <abs(u), du * sign(u)>
1287 !-----
1288 elemental function abs_d(u) result(res)
1289     type(dual), intent(in) :: u
1290     type(dual) :: res
1291     integer :: i
1292
1293     if(u%x > 0) then
1294         res%x = u%x
1295         res%dx = u%dx
1296     else if (u%x < 0) then
1297         res%x = -u%x
1298         res%dx = -u%dx
1299     else
1300         res%x = 0.0
1301         do i = 1, ndv
1302             if (u%dx(i) .eq. 0.0) then
1303                 res%dx(i) = 0.0
1304             else
1305                 res%dx(i) = set_NaN()
1306             end if
1307         end do
1308     endif
1309
1310 end function abs_d
1311
1312
1313 !-----
1314 ! ACOS of dual numbers
1315 ! <res, dres> = acos(<u, du>) = <acos(u), -du / sqrt(1 - u^2)>
1316 !-----
1317 elemental function acos_d(u) result(res)
1318     type(dual), intent(in) :: u
1319     type(dual) :: res
1320
1321     res%x = acos(u%x)
1322     if (u%x == 1.0 .or. u%x == -1.0) then
1323         res%dx = set_Nan() ! Undefined derivative
1324     else
1325         res%dx = -u%dx / sqrt(1.0 - u%x**2)
1326     end if
1327
1328 end function acos_d
1329
1330
1331 !-----
1332 ! ASIN of dual numbers
1333 ! <res, dres> = asin(<u, du>) = <asin(u), du / sqrt(1 - u^2)>
1334 !-----
1335 elemental function asin_d(u) result(res)
1336     type(dual), intent(in) :: u

```

```

1337         type(dual) :: res
1338
1339         res%x = asin(u%x)
1340         if (u%x == 1.0 .or. u%x == -1.0) then
1341             res%dx = set_NaN() ! Undefined derivative
1342         else
1343             res%dx = u%dx / sqrt(1.0 - u%x**2)
1344         end if
1345
1346     end function asin_d
1347
1348
1349     !-----
1350     ! ATAN of dual numbers
1351     ! <res, dres> = atan(<u, du>) = <atan(u), du / (1 + u^2)>
1352     !-----
1353     elemental function atan_d(u) result(res)
1354         type(dual), intent(in) :: u
1355         type(dual) :: res
1356
1357         res%x = atan(u%x)
1358         res%dx = u%dx / (1.0 + u%x**2)
1359
1360     end function atan_d
1361
1362
1363     !-----
1364     ! ATAN2 of dual numbers
1365     ! <res, dres> = atan2(<u, du>, <v, dv>)
1366     !               = <atan2(u, v), v / (u^2 + v^2) * du - u / (u^2 + v^2) * dv>
1367     !-----
1368     elemental function atan2_d(u, v) result(res)
1369         type(dual), intent(in) :: u, v
1370         type(dual) :: res
1371
1372         real :: usq_plus_vsqu
1373
1374         res%x = atan2(u%x, v%x)
1375
1376         usq_plus_vsqu = u%x**2 + v%x**2
1377         res%dx = v%dx / usq_plus_vsqu * u%dx - u%dx / usq_plus_vsqu * v%dx
1378
1379     end function atan2_d
1380
1381
1382     !-----
1383     ! COS of dual numbers
1384     ! <res, dres> = cos(<u, du>) = <cos(u), -sin(u) * du>
1385     !-----
1386     elemental function cos_d(u) result(res)
1387         type(dual), intent(in) :: u
1388         type(dual) :: res
1389
1390         res%x = cos(u%x)
1391         res%dx = -sin(u%x) * u%dx
1392
1393     end function cos_d
1394
1395
1396     !-----
1397     ! DOT PRODUCT two dual number vectors

```

```

1398 ! <res, dres> = <u, du> . <v, dv> = <u . v, u . dv + v . du>
1399 !-----
1400 function dot_product_dd(u, v) result(res)
1401     type(dual), intent(in) :: u(:), v(:)
1402     type(dual) :: res
1403
1404     integer :: i
1405
1406     res%x = dot_product(u%x, v%x)
1407     do i = 1, ndv
1408         res%dx(i) = dot_product(u%x, v%dx(i)) + dot_product(v%x, u%dx(i))
1409     end do
1410
1411 end function dot_product_dd
1412
1413
1414 !-----
1415 ! EXPONENTIAL OF dual numbers
1416 ! <res, dres> = exp(<u, du>) = <exp(u), exp(u) * du>
1417 !-----
1418 elemental function exp_d(u) result(res)
1419     type(dual), intent(in) :: u
1420     type(dual) :: res
1421
1422     real :: exp_x
1423
1424     exp_x = exp(u%x)
1425     res%x = exp_x
1426     res%dx = u%dx * exp_x
1427
1428 end function exp_d
1429
1430
1431 !-----
1432 ! Convert dual to integer
1433 ! i = int(<u, du>) = int(u)
1434 !-----
1435 elemental function int_d(u) result(res)
1436     type(dual), intent(in) :: u
1437     integer :: res
1438
1439     res = int(u%x)
1440
1441 end function int_d
1442
1443
1444 !-----
1445 ! LOG OF dual numbers, defined for u%x>0 only
1446 ! the error control should be done in the original code
1447 ! in other words, if u%x<=0, it is not possible to obtain LOG.
1448 ! <res, dres> = log(<u, du>) = <log(u), du / u>
1449 !-----
1450 elemental function log_d(u) result(res)
1451     type(dual), intent(in) :: u
1452     type(dual) :: res
1453
1454     real :: inv
1455
1456     inv = 1.0 / u%x
1457     res%x = log(u%x)
1458     res%dx = u%dx * inv

```

```

1459
1460 end function log_d
1461
1462
1463 !-----
1464 ! LOG10 OF dual numbers,defined for u%x>0 only
1465 ! the error control should be done in the original code
1466 ! in other words, if u%x<=0, it is not possible to obtain LOG.
1467 ! <res, dres> = log10(<u, du>) = <log10(u), du / (u * log(10))>
1468 ! LOG<u,up>=<LOG(u),up/u>
1469 !-----
1470 elemental function log10_d(u) result(res)
1471     type(dual), intent(in) :: u
1472     type(dual) :: res
1473
1474     real :: inv
1475
1476     inv = 1.0 / (u%x * log(10.0))
1477     res%x = log10(u%x)
1478     res%dx = u%dx * inv
1479
1480 end function log10_d
1481
1482
1483 !-----
1484 ! MULTIPLY two dual number matrices
1485 ! <res, dres> = <u, du> . <v, dv> = <u . v, du . v + u . dv>
1486 !-----
1487 function matmul_dd(u,v) result(res)
1488     type(dual), intent(in) :: u(:,,:), v(:,:)
1489     type(dual) :: res(size(u,1), size(v,2))
1490
1491     integer :: i
1492
1493     res%x = matmul(u%x, v%x)
1494     do i = 1, ndv
1495         res%dx(i) = matmul(u%dx(i), v%x) + matmul(u%x, v%dx(i))
1496     end do
1497
1498 end function matmul_dd
1499
1500
1501 !-----
1502 ! MULTIPLY a dual number matrix with a dual number
1503 ! vector
1504 !
1505 ! <u,up>.<v,vp>=<u.v,up.v+u.vp>
1506 !-----
1507 function matmul_dv(u, v) result(res)
1508     type(dual), intent(in) :: u(:,,:), v(:)
1509     type(dual) :: res(size(u,1))
1510     integer :: i
1511
1512     res%x = matmul(u%x, v%x)
1513     do i = 1, ndv
1514         res%dx(i) = matmul(u%dx(i), v%x) + matmul(u%x, v%dx(i))
1515     end do
1516
1517 end function matmul_dv
1518
1519

```

```

1520 !-----
1521 ! MULTIPLY a dual vector with a dual matrix
1522 !
1523 ! <u,up>.<v,vp>=<u.v,up.v+u.vp>
1524 !-----
1525 function matmul_vd(u, v) result(res)
1526     type(dual), intent(in) :: u(:,), v(:,)
1527     type(dual) :: res(size(v, 2))
1528     integer::i
1529
1530     res%x = matmul(u%x, v%x)
1531     do i = 1, ndv
1532         res%dx(i) = matmul(u%dx(i), v%x) + matmul(u%x, v%dx(i))
1533     end do
1534
1535 end function matmul_vd
1536
1537 !-----
1538 ! Obtain the max of 2 to 5 dual numbers
1539 !-----
1540 elemental function max_dd(val1, val2, val3, val4, val5) result(res)
1541     type(dual), intent(in) :: val1, val2
1542     type(dual), intent(in), optional :: val3, val4, val5
1543     type(dual) :: res
1544
1545     if (val1%x > val2%x) then
1546         res = val1
1547     else
1548         res = val2
1549     endif
1550     if(present(val3))then
1551         if(res%x < val3%x) res = val3
1552     endif
1553     if(present(val4))then
1554         if(res%x < val4%x) res = val4
1555     endif
1556     if(present(val5))then
1557         if(res%x < val5%x) res = val5
1558     endif
1559
1560 end function max_dd
1561
1562
1563 !-----
1564 ! Obtain the max of a dual number and an integer
1565 !-----
1566 elemental function max_di(u, i) result(res)
1567     type(dual), intent(in) :: u
1568     integer, intent(in) :: i
1569     type(dual) :: res
1570
1571     if (u%x > i) then
1572         res = u
1573     else
1574         res = i
1575     endif
1576
1577 end function max_di
1578
1579 !-----
1580 ! Obtain the max of a dual number and a real number

```



```

1581  !-----
1582  elemental function max_dr(u, r) result(res)
1583      type(dual), intent(in) :: u
1584      real, intent(in) :: r
1585      type(dual) :: res
1586
1587      if (u%x > r) then
1588          res = u
1589      else
1590          res = r
1591      endif
1592
1593  end function max_dr
1594
1595
1596  !-----
1597  ! Obtain the max of a real and a dual
1598  !-----
1599  elemental function max_rd(n, u) result(res)
1600      real, intent(in) :: n
1601      type(dual), intent(in) :: u
1602      type(dual) :: res
1603
1604      if (u%x > n) then
1605          res = u
1606      else
1607          res = n
1608      endif
1609
1610  end function max_rd
1611
1612
1613  !-----
1614  ! Obtain the max value of vector u
1615  !-----
1616  function maxval_d(u) result(res)
1617      type(dual), intent(in) :: u(:)
1618      integer :: iloc(1)
1619      type(dual) :: res
1620
1621      iloc=maxloc(u%x)
1622      res=u(iloc(1))
1623
1624  end function maxval_d
1625
1626
1627  !-----
1628  ! Obtain the min of 2 to 4 dual numbers
1629  !-----
1630  elemental function min_dd(val1, val2, val3, val4) result(res)
1631      type(dual), intent(in) :: val1, val2
1632      type(dual), intent(in), optional :: val3, val4
1633      type(dual) :: res
1634
1635      if (val1%x < val2%x) then
1636          res = val1
1637      else
1638          res = val2
1639      endif
1640      if(present(val3))then
1641          if(res%x > val3%x) res = val3

```

```

1642         endif
1643         if(present(val4))then
1644             if(res%x > val4%x) res = val4
1645         endif
1646     end function min_dd
1647
1648
1649
1650     !-----
1651     ! Obtain the min of a dual and a double
1652     !-----
1653     elemental function min_dr(u, r) result(res)
1654         type(dual), intent(in) :: u
1655         real, intent(in) :: r
1656         type(dual) :: res
1657
1658         if (u%x < r) then
1659             res = u
1660         else
1661             res = r
1662         endif
1663     end function min_dr
1664
1665
1666
1667     !-----
1668     ! Obtain the min value of vector u
1669     !-----
1670     function minval_d(u) result(res)
1671         type(dual), intent(in) :: u(:)
1672         integer :: iloc(1)
1673         type(dual) :: res
1674
1675         iloc=minloc(u%x)
1676         res=u(iloc(1))
1677     end function minval_d
1678
1679
1680
1681     !-----
1682     !Returns the nearest integer to u%x, ELEMENTAL
1683     !-----
1684     elemental function nint_d(u) result(res)
1685         type(dual), intent(in) :: u
1686         integer :: res
1687
1688         res=nint(u%x)
1689     end function nint_d
1690
1691
1692
1693     !-----
1694     ! SIGN(a,b) with two dual numbers as inputs,
1695     ! the result will be |a| if b%x>=0, -|a| if b%x<0,ELEMENTAL
1696     !-----
1697     elemental function sign_dd(val1, val2) result(res)
1698         type(dual), intent(in) :: val1, val2
1699         type(dual) :: res
1700
1701         if (val2%x < 0.0) then
1702             res = -abs(val1)

```

```

1703     else
1704         res = abs(val1)
1705     endif
1706
1707 end function sign_dd
1708
1709
1710 !-----
1711 ! SIGN(a,b) with one real and one dual number as inputs,
1712 ! the result will be |a| if b%x>=0, -|a| if b%x<0,ELEMENTAL
1713 !-----
1714 elemental function sign_rd(val1, val2) result(res)
1715     real, intent(in) :: val1
1716     type(dual), intent(in) :: val2
1717     type(dual) :: res
1718
1719     if (val2%x < 0.0) then
1720         res = -abs(val1)
1721     else
1722         res = abs(val1)
1723     endif
1724
1725 end function sign_rd
1726
1727
1728 !-----
1729 ! SIN of dual numbers
1730 ! <res, dres> = sin(<u, du>) = <sin(u), cos(u) * du>
1731 !-----
1732 elemental function sin_d(u) result(res)
1733     type(dual), intent(in) :: u
1734     type(dual) :: res
1735
1736     res%x = sin(u%x)
1737     res%dx = cos(u%x) * u%dx
1738
1739 end function sin_d
1740
1741
1742 !-----
1743 ! TAN of dual numbers
1744 ! <res, dres> = tan(<u, du>) = <tan(u), du / cos(u)^2>
1745 !-----
1746 elemental function tan_d(u) result(res)
1747     type(dual), intent(in) :: u
1748     type(dual) :: res
1749
1750     res%x = tan(u%x)
1751     res%dx = u%dx / cos(u%x)**2
1752
1753 end function tan_d
1754
1755
1756 !-----
1757 ! SQR of dual numbers
1758 ! <res, dres> = sqrt(<u, du>) = <sqrt(u), du / (2 * sqrt(u))>
1759 !-----
1760 elemental function sqrt_d(u) result(res)
1761     type(dual), intent(in) :: u
1762     type(dual) :: res
1763     integer :: i

```

```

1764
1765     res%x = sqrt(u%x)
1766
1767     if (res%x .ne. 0.0) then
1768         res%dx = 0.5 * u%dx / res%x
1769     else
1770         do i = 1, ndv
1771             if (u%dx(i) .eq. 0.0) then
1772                 res%dx(i) = 0.0
1773             else
1774                 res%dx(i) = set_NaN()
1775             end if
1776         end do
1777     end if
1778
1779 end function sqrt_d
1780
1781
1782 !-----
1783 ! Sum of a dual array
1784 !-----
1785 function sum_d(u) result(res)
1786     type(dual), intent(in) :: u(:)
1787     type(dual) :: res
1788     integer :: i
1789
1790     res%x = sum(u%x)
1791     do i = 1, ndv
1792         res%dx(i) = sum(u%dx(i))
1793     end do
1794
1795 end function sum_d
1796
1797
1798 !-----
1799 ! Find the location of the max value in an
1800 ! array of dual numbers
1801 !-----
1802 function maxloc_d(array) result(ind)
1803     type(dual), intent(in) :: array(:)
1804     integer :: ind(1)
1805
1806     ind = maxloc(array%x)
1807
1808 end function maxloc_d
1809
1810
1811 elemental function set_NaN() result(res)
1812     real :: res
1813
1814     res = sqrt(negative_one)
1815
1816 end function set_NaN
1817
1818 end module dnadmod

```

## B ONE-DIMENSIONAL SCALAR TRANSPORT SOLVER IN FORTRAN

## B.1 User Interface

```

1  program main
2      use adpsolver
3      use adpio
4      implicit none
5
6      type(adpmodel) :: solver ! adpmodel object
7
8      integer :: nargs ! Number of command line arguments
9      character*80 :: arg ! Command line argument
10     character*80 :: opt ! Option from command line argument
11     character*80 :: val ! Value from command line argument
12
13     character*80 :: infile ! Input file name
14     character*80 :: outfile ! Output file name
15
16     integer :: err ! Error flag
17
18     ! Get command line arguments
19     nargs = command_argument_count()
20     if (nargs .gt. 0) then
21         call get_command_argument(1, infile)
22     else
23         write(*, *) "An input file must be specified."
24         call exit(1)
25     end if
26
27     ! Initialize solver
28     write(*, *) "Initializing solver..."
29     call solver%init()
30
31     ! Read the input file
32     write(*, *) "Reading input file '", trim(infile), "'..."
33     err = readInput(solver, infile)
34     if (err .ne. 0) then
35         write(*, *) "Error reading input file, aborting!"
36         call exit(2)
37     end if
38
39     ! Calculate a solution
40     write(*, *) "Solving..."
41     err = solver%solve()
42     if (err .ne. 0) then
43         write(*, *) "Solution error, aborting!"
44         call exit(3)
45     end if
46
47     ! Determine the output file name
48     if (nargs .gt. 1) then
49         call get_command_argument(2, outfile)
50     else
51         outfile = trim(solver%jobname) // ".out"
52     end if
53
54     ! Write the output
55     write(*, *) "Writing output to file '", trim(outfile), "'..."

```

```

56     err = writeOutput(solver, outfile)
57     if (err .ne. 0) then
58         write(*, *) "Error generating output file!"
59         call exit(4)
60     end if
61
62     call solver%dealloc()
63
64 end program main

```

## B.2 Physics Module

```

1  module adpsolver
2      implicit none
3
4      type :: adpmodel
5          character*80 :: jobname ! Job name
6
7          real :: phi0 ! Scalar value at x = 0
8          real :: phi1 ! Scalar value at x = 1
9
10         real :: u ! Velocity
11         real :: gamma ! Diffusivity
12         real :: c ! Proportionality constant for scalar production
13
14         integer :: npts ! Number of grid points on discretized domain
15                     ! (spaced uniformly from x = 0 to x = 1)
16         real :: dx ! Distance between points in x array
17
18         real, allocatable, dimension(:) :: x ! array of grid coordinates
19         real, allocatable, dimension(:) :: phi ! scalar field function
20
21     contains
22         procedure :: init => adpmodel_init
23         procedure :: alloc => adpmodel_alloc
24         procedure :: dealloc => adpmodel_dealloc
25         procedure :: solve => adpmodel_solve
26         procedure :: solveImplicit => adpmodel_solveImplicit
27
28     end type adpmodel
29
30 contains
31     !!! Initialize an adpmodel object
32     !!!
33     !!! Input:
34     !!!     this = adpmodel object to initialize
35     subroutine adpmodel_init(this)
36         class(adpmodel), intent(inout) :: this
37
38         this%jobname = "ADPSolution1"
39
40         this%phi0 = 1.0d0
41         this%phi1 = 0.0d0
42
43         this%u = 1.0d0
44         this%gamma = 0.1d0
45         this%c = -1.0d0
46
47         this%npts = 11
48     end subroutine adpmodel_init

```

```

49
50
51     !!! Allocate dynamic memory
52     !!!
53     !!! Input:
54     !!!     this = adpmodel object
55     !!!
56     !!! Return:
57     !!!     stat = Error status flag (0 = success,
58     !!!                                     1 = Allocation error)
59 integer function adpmodel_alloc(this) result(stat)
60     class(adpmodel), intent(inout) :: this
61
62     integer :: n
63     integer :: err
64
65     ! Initialize error flags
66     err = 0
67     stat = 0
68
69     call this%dealloc()
70
71     n = this%npts
72     allocate(this%x(n), this%phi(n), stat = err)
73     if (err .ne. 0) then
74         write(*, *) "Error: Could not allocate arrays!"
75         stat = 1
76     end if
77 end function adpmodel_alloc
78
79
80     !!! Deallocate dynamic memory
81     !!!
82     !!! Input:
83     !!!     this = adpmodel object
84 subroutine adpmodel_dealloc(this)
85     class(adpmodel), intent(inout) :: this
86
87     if (allocated(this%phi)) deallocate(this%phi)
88     if (allocated(this%x)) deallocate(this%x)
89 end subroutine adpmodel_dealloc
90
91
92     !!! Run the solution
93     !!!
94     !!! Input:
95     !!!     this = adpmodel object
96     !!!
97     !!! Return:
98     !!!     stat = Error status (0 = success,
99     !!!                                     1 = problem not overdamped,
100    !!!                                     2 = error allocating arrays,
101    !!!                                     3 = error executing solver)
102 integer function adpmodel_solve(this) result(stat)
103     class(adpmodel), intent(inout) :: this
104
105     integer :: err ! Temporary error flag
106     integer :: i ! Loop control variable
107
108     ! Initialize the error flags
109     err = 0

```

```

110     stat = 0
111
112     ! Make sure we are in the overdamped regime
113     if (this%u**2 .le. 4.0d0 * this%c * this%gamma) then
114         write(*, *) "Error: The specified properties do not meet ", &
115             "the overdamping requirement for this analysis."
116         stat = 1
117         return
118     end if
119
120     ! Allocate solution arrays
121     err = this%alloc()
122     if (err .ne. 0) then
123         stat = 2
124         return
125     end if
126
127     ! Populate x array for npts
128     this%dx = 1.0d0 / (this%npts - 1)
129     do i = 1, this%npts
130         this%x(i) = (i - 1) * this%dx
131     end do
132
133     ! Solve the problem
134     err = this%solveImplicit()
135
136     ! Check solution status
137     if (err .ne. 0) then
138         stat = 3
139         return
140     end if
141
142 end function adpmodel_solve
143
144
145 !!! Solve the problem implicitly
146 !!!
147 !!! Inputs:
148 !!!     this = AdvectionSolver object
149 !!!
150 !!! Return:
151 !!!     stat = Error status (0 = success)
152 integer function adpmodel_solveImplicit(this) result(stat)
153     class(adpmodel), intent(inout) :: this
154
155     integer :: i, j ! Loop control variables
156     integer :: n ! Shortcut to npts
157     real, dimension(:), allocatable :: ld ! Lower diagonal vector
158     real, dimension(:), allocatable :: md ! Middle diagonal vector
159     real, dimension(:), allocatable :: ud ! Upper diagonal vector
160     real, dimension(:), allocatable :: bc ! BC vector
161
162     real :: aE, aW, aP ! Matrix coefficients
163     real :: w ! temporary variable
164
165     ! Initialize error flag
166     stat = 0
167
168     ! Allocate the solution matrix and BC vector
169     n = this%npts
170     allocate(bc(n), ld(n), md(n), ud(n))

```



```

171         bc = 0.0d0
172         ld = 0.0d0
173         md = 0.0d0
174         ud = 0.0d0
175
176         ! Calculate the matrix coefficients (1st-order upwinding)
177         aW = -this%gamma / this%dx**2; aE = aW
178         if (this%u > 0.0d0) then
179             aW = aW - this%u / this%dx
180         else
181             aE = aE + this%u / this%dx
182         end if
183
184         aP = -aE - aW - this%c
185
186         ! Populate the diagonal and BC vectors
187         bc(1) = this%phi0
188         md(1) = 1.0d0
189         do i = 2, n - 1
190             bc(i) = 0.0d0
191             ld(i) = aW
192             md(i) = aP
193             ud(i) = aE
194         end do
195         bc(n) = this%phi1
196         md(n) = 1.0d0
197
198         do i = 2, n
199             w = ld(i) / md(i - 1)
200             md(i) = md(i) - w * ud(i - 1)
201             bc(i) = bc(i) - w * bc(i - 1)
202         end do
203
204         this%phi(n) = bc(n) / md(n)
205         do i = n - 1, 1, -1
206             this%phi(i) = (bc(i) - ud(i) * this%phi(i + 1)) / md(i)
207         end do
208
209         deallocate(bc, ld, md, ud)
210
211     end function adpmodel_solveImplicit
212
213 end module adpsolver

```

### B.3 I/O Module

```

1  module adpio
2      use adpsolver
3      implicit none
4
5      integer, parameter :: ioUnit = 10 ! IO unit for files
6
7      contains
8          !!! Read and parse the input file
9          !!!
10         !!! Input:
11         !!!     model = adpmodel object
12         !!!     filename = Name of input file to read/parse
13         !!!
14         !!! Return:

```

```

15      !!!      stat = Error status (0 = success,
16      !!!      1 = error opening input file,
17      !!!      2 = error parsing card(s))
18  integer function readInput(model, filename) result(stat)
19      class(adpmodel), intent(inout) :: model
20      character*80, intent(in) :: filename ! Name of input file
21
22      character*80 :: card
23      character*80 :: id
24
25      integer :: err ! I/O error flag
26
27      ! Initialize the error flags
28      err = 0
29      stat = 0
30
31      ! Open the file for reading
32      open(unit = ioUnit, file = filename, status = 'old', &
33      & action = 'read', iostat = err)
34      if (err .ne. 0) then
35          write(*, '(A)') "ERROR: The input file could not be read."
36          write(*, '(A, A)') "    Filename = ", trim(filename)
37          write(*, '(A, I3)') "    I/O Error = ", err
38          close(ioUnit)
39          stat = 1
40          return
41      end if
42
43      ! Begin processing input cards
44      read(ioUnit, '(A)', iostat = err) card
45      do while (.not. is_iostat_end(err))
46          ! Remove all whitespace from card
47          card = removeWhitespace(card)
48
49          if (card(1:1) .eq. '*') then
50              write(*, '(A, 1X, A)') "Found card:", trim(card)
51              err = parseCard(model, card)
52              if (err .ne. 0) then
53                  stat = 2
54              end if
55          else if (len(trim(card)) .gt. 1) then
56              write(*, '(A, 1X, A)') "Found comment:", trim(card)
57          end if
58
59          ! Read the next card
60          read(ioUnit, '(A)', iostat = err) card
61      end do
62
63      if (stat .eq. 2) then
64          write(*, *) "Error: Some input cards were not processed."
65      end if
66
67      close(unit = ioUnit)
68
69  end function readInput
70
71
72      !!! Parse an input card and extract all parameter data
73      !!!
74      !!! Input:
75      !!!      model = adpmodel object

```

```

76      !!!      card = Input card to parse and extract data from
77      !!!
78      !!! Return:
79      !!!      stat = Error status flag (0 = success,
80      !!!                                     1 = I/O error parsing card,
81      !!!                                     2 = error parsing words on card,
82      !!!                                     3 = invalid word parameter name,
83      !!!                                     4 = invalid card ID)
84      integer function parseCard(model, card) result(stat)
85      class(adpmodel), intent(inout) :: model
86      character*80, intent(in) :: card ! Card string
87
88      character*80 :: id ! Card ID (first word on card)
89      integer :: nWords ! Number of words on card (excludes ID)
90      character*80 :: word ! List of words on card (excludes ID)
91
92      integer :: i ! Loop control variable
93      integer :: ind ! End index of last word
94      integer :: err ! Error flag
95
96      character*80 :: paramName ! Parameter name
97      character*80 :: paramValue ! Parameter value
98
99      ! Initialize the error flags
100     err = 0
101     stat = 0
102
103     ! Get the card ID (first word on card)
104     read(card, *, iostat = err) id
105     if (err .ne. 0) then
106         write(*, *) "Unknown error parsing card ID:", trim(card)
107         stat = 1
108         return
109     end if
110
111     ! Get the number of remaining words
112     nwords = count(transfer(card, 'A', len(trim(card)))) == ",")
113
114     ! Get the words
115     ind = index(card, trim(id)) + len(trim(id)) + 1 ! Add 1 for comma
116     do i = 1, nWords
117         ! Read the next word from the card
118         read(card(ind:80), *, iostat = err) word
119         if (err .ne. 0) then
120             write(*, '(A, I2, A, A)') "Unknown error parsing word ", &
121                 & i, ":", trim(card)
122             stat = 2
123             return
124         end if
125
126         ! Get the starting index of the next word (add 1 for comma)
127         ind = index(card, trim(word)) + len(trim(word)) + 1
128
129         ! Parse the word to extract the parameter name and value
130         err = parseArg(word, paramName, paramValue)
131         if (err .ne. 0) then
132             write(*, '(A, I2, A, A)') "Invalid string on word ", &
133                 & i, ":", trim(card)
134             stat = 2
135             cycle
136         end if

```

```

137
138     ! Extract the data based on card type
139     select case(id)
140     case ("*job")
141         err = setJobField(model, paramName, paramValue)
142     case ("*bcs")
143         err = setBCField(model, paramName, paramValue)
144     case ("*props")
145         err = setPropsField(model, paramName, paramValue)
146     case ("*grid")
147         err = setGridField(model, paramName, paramValue)
148     case ("*solver")
149         err = setSolverField(model, paramName, paramValue)
150     case default
151         write(*, '(2X, A, A, A)') "Unrecognized card ID: ", &
152             & trim(id), ". Card skipped!"
153         stat = 4
154         return
155     end select
156
157     ! Check for an error setting fields
158     if (err .ne. 0) then
159         stat = 3
160     end if
161 end do
162
163 end function parseCard
164
165
166 !!! Set a field from the job card
167 !!!
168 !!! Input:
169 !!!     this = adpmodel object
170 !!!     paramName = Name of field to set
171 !!!     paramValue = String representation of parameter value
172 !!!
173 !!! Return:
174 !!!     stat = Error status flag (0 = success,
175 !!!                               1 = Unrecognized parameter name)
176 integer function setJobField(model, paramName, paramValue) result (stat)
177     class(adpmodel), intent(inout) :: model
178     character*80, intent(in) :: paramName ! Parameter name
179     character*80, intent(in) :: paramValue ! Parameter value
180
181     ! Initialize the error flag
182     stat = 0
183
184     select case(paramName)
185     case ("name")
186         model%jobName = paramValue
187     case default
188         write(*, '(6X, A)') &
189             & "Unrecognized parameter name on job card:", &
190             & trim(paramName)
191         stat = 1
192     end select
193
194 end function setJobField
195
196
197 !!! Set a field from the bcs card

```

```

198      !!!
199      !!! Input:
200      !!!      model = adpmodel object
201      !!!      paramName = Name of field to set
202      !!!      paramValue = String representation of parameter value
203      !!!
204      !!! Return:
205      !!!      stat = Error status flag (0 = success,
206      !!!                               1 = Unrecognized parameter name)
207      integer function setBCField(model, paramName, paramValue) result(stat)
208      class(adpmodel), intent(inout) :: model
209      character*80, intent(in) :: paramName ! Parameter name
210      character*80, intent(in) :: paramValue ! Parameter value
211
212      ! Initialize the error flag
213      stat = 0
214
215      select case(paramName)
216      case ("phi0")
217          model%phi0 = stringToReal(paramValue)
218      case ("phi1")
219          model%phi1 = stringToReal(paramValue)
220      case default
221          write(*, '(6X, A, 1X, A)') &
222              & "Unrecognized parameter name on bcs card:", &
223              & trim(paramName)
224          stat = 1
225      end select
226      end function setBCField
227
228
229      !!! Set a field from the props card
230      !!!
231      !!! Input:
232      !!!      model = adpmodel object
233      !!!      paramName = Name of field to set
234      !!!      paramValue = String representation of parameter value
235      !!!
236      !!! Return:
237      !!!      stat = Error status flag (0 = success,
238      !!!                               1 = Unrecognized parameter name)
239      integer function setPropsField(model, paramName, paramValue) result(stat)
240      class(adpmodel), intent(inout) :: model
241      character*80, intent(in) :: paramName ! Parameter name
242      character*80, intent(in) :: paramValue ! Parameter value
243
244      ! Initialize the error flag
245      stat = 0
246
247      select case(paramName)
248      case ("u")
249          model%u = stringToReal(paramValue)
250      case ("gamma")
251          model%gamma = stringToReal(paramValue)
252      case ("c")
253          model%c = stringToReal(paramValue)
254      case default
255          write(*, '(6X, A, 1X, A)') &
256              & "Unrecognized parameter name on props card:", &
257              & trim(paramName)
258          stat = 1

```

```

259         end select
260     end function setPropsField
261
262
263     !!! Set a field from the grid card
264     !!!
265     !!! Input:
266     !!!     model = adpmodel object
267     !!!     paramName = Name of field to set
268     !!!     paramValue = String representation of parameter value
269     !!!
270     !!! Return:
271     !!!     stat = Error status flag (0 = success,
272     !!!         1 = Unrecognized parameter name)
273 integer function setGridField(model, paramName, paramValue) result(stat)
274     class(adpmodel), intent(inout) :: model
275     character*80, intent(in) :: paramName ! Parameter name
276     character*80, intent(in) :: paramValue ! Parameter value
277
278     ! Initialize the error flag
279     stat = 0
280
281     select case(paramName)
282     case ("npts")
283         model%npts = stringToInt(paramValue)
284     case default
285         write(*, '(6X, A, 1X, A)') &
286             & "Unrecognized parameter name on grid card:", &
287             & trim(paramName)
288         stat = 1
289     end select
290 end function setGridField
291
292
293     !!! Set a field from the model card
294     !!!
295     !!! Input:
296     !!!     model = adpsolver object
297     !!!     paramName = Name of field to set
298     !!!     paramValue = String representation of parameter value
299     !!!
300     !!! Return:
301     !!!     stat = Error status flag (0 = success,
302     !!!         1 = Unrecognized parameter name)
303 integer function setSolverField(model, paramName, paramValue) result(stat)
304     class(adpmodel), intent(inout) :: model
305     character*80, intent(in) :: paramName ! Parameter name
306     character*80, intent(in) :: paramValue ! Parameter value
307
308     ! Initialize the error flag
309     stat = 0
310
311     select case(paramName)
312     case ("method")
313         select case(paramValue)
314         case ("analytical")
315             model%method = analytical
316         case ("implicit")
317             model%method = implicit
318         case default
319             write(*, '(6X, A, 1X, A)') &

```

```

320         & "Unrecognized solution method:", paramValue
321     end select
322     case ("derivatives")
323         select case (paramValue)
324             case ("yes")
325                 model%computeDerivatives = .true.
326             case ("no")
327                 model%computeDerivatives = .false.
328             case default
329                 write(*, '(A)') "Derivatives option must be ", &
330                     & "yes/no. Defaulting to no."
331         end select
332     case default
333         write(*, '(6X, A, 1X, A)') &
334             & "Unrecognized parameter name on solver card:", &
335             & trim(paramName)
336         stat = 1
337     end select
338
339 end function setSolverField
340
341
342 REAL function stringToReal(str) result (val)
343     character*80, intent(in) :: str ! String to convert
344
345     integer :: err ! I/O error status
346
347     read(str, *, iostat = err) val
348     if (err .ne. 0) then
349         write(*, '(6X, A, A)') "Error converting string to real: ", str
350     end if
351 end function stringToReal
352
353
354 integer function stringToInt(str) result (val)
355     character*80, intent(in) :: str ! String to convert
356
357     integer :: err ! I/O error status
358
359     read(str, *, iostat = err) val
360     if (err .ne. 0) then
361         write(*, '(6X, A, A)') "Error converting string to int: ", str
362     end if
363 end function stringToInt
364
365
366 !!! Write the results to an output file
367 !!!
368 !!! Inputs:
369 !!!     model = adpmodel object
370 !!!     filename_opt = Optional output filename (defaults to jobName.out)
371 !!!
372 !!! Return:
373 !!!     stat = Error status (0 = success,
374 !!!                         1 = Error opening output file)
375 integer function writeOutput(model, filename_opt) result(stat)
376     class(adpmodel), intent(inout) :: model ! adpmodel object
377     character*80, intent(in), optional :: filename_opt ! Optional filename
378
379     character*80 :: filename ! Output file name
380     integer :: err ! Error status flag

```

```

381
382     stat = 0
383
384     ! Get the filename to write to
385     if (present(filename_opt)) then
386         filename = filename_opt
387     else
388         filename = trim(model%jobname) // ".out"
389     end if
390
391     ! Open the output file for writing
392     open(unit = ioUnit, file = filename, action = 'write', iostat = err)
393     if (err .ne. 0) then
394         write(*, *) "Error: Unable to open output file for writing."
395         stat = 1
396         return
397     end if
398
399     ! Write the header and results
400     call writeData(model)
401
402     ! Close the output file
403     close(unit = ioUnit)
404
405 end function writeOutput
406
407
408 subroutine writeData(model)
409     class(adpmodel), intent(inout) :: model ! adpmodel object
410
411     integer :: i, j ! Loop control variable
412     character*80 :: fmtString
413
414     if (model%method .eq. analytical .and. model%computeDerivatives) then
415         ! Header
416         write(ioUnit, '(A)') "x,phi,dPhi/dX,dPhi/dU,dPhi/dGamma,dPhi/dC"
417
418         ! Results
419         write(fmtString, *) '(5(ES23.15, ", ", ES23.15))'
420         do i=1, model%npts
421             write(ioUnit, fmtString) model%x(i), model%phi(i), &
422                 & model%dPhi_dU(i), model%dPhi_dGamma(i), model%dPhi_dC(i)
423         end do
424     else
425         ! Header
426         write(ioUnit, '(A)') "x,phi"
427
428         ! Results
429         write(fmtString, *) '(ES23.15, ", ", ES23.15)'
430         do i=1, model%npts
431             write(ioUnit, fmtString) model%x(i), model%phi(i)
432         end do
433     end if
434 end subroutine writeData
435
436
437
438 character*80 function removeWhitespace(str) result(mstr)
439     character*80, intent(in) :: str
440
441     integer :: i ! Loop control variable

```



```

442     integer :: l ! Length of modified string
443
444     character, parameter :: tab = achar(9) ! Tab character
445
446     ! Initialize length of modified string to 0
447     l = 0
448     mstr = char(0)
449
450     ! Loop over each character in unmodified string
451     do i = 1, len(str)
452         ! Only consider non-space, non-tab characters
453         if (str(i:i) .ne. ' ' .and. str(i:i) .ne. tab) then
454             l = l + 1 ! Increment the count
455             mstr(1:l) = str(i:i) ! Add the non-whitespace character
456         end if
457     end do
458 end function removeWhitespace
459
460
461 !!! Parse an argument to determine the name and value
462 !!!
463 !!! Input:
464 !!!     arg = Argument string to parse
465 !!!
466 !!! Output:
467 !!!     argName = name extracted from argument string
468 !!!     argValue = value extracted from argument string
469 !!!
470 !!! Return:
471 !!!     stat = Error status (0 = success,
472 !!!                               1 = argument value missing,
473 !!!                               2 = argument name and value missing)
474 integer function parseArg(arg, argName, argValue) result(stat)
475     character*80, intent(in) :: arg ! Argument string to parse
476     character*80, intent(out) :: argName ! Name of argument
477     character*80, intent(out) :: argValue ! Value of argument
478
479     character*80 :: trimmedArg
480     integer :: ind ! Index of equal sign in argument
481
482     argName = ""
483     argValue = ""
484
485     trimmedArg = trim(adjustl(arg))
486     ind = index(trimmedArg, "=")
487     if (len(trimmedArg) .eq. 0) then
488         stat = 2
489         return
490     else if (ind .eq. 0) then
491         argName = trimmedArg
492         stat = 1
493     else
494         argName = trimmedArg(1 : ind - 1)
495         argValue = trimmedArg(ind + 1 :)
496         stat = 0
497     end if
498 end function parseArg
499
500 end module adpio

```

## C SUMMARY OF CODE CHANGES TO APPENDIX B FOR DNAD INTEGRATION

**C.1 Changes to adpsolver Module**

Original: lines 1-2

```

1  module adpsolver
2      implicit none

```

Modified: lines 1-6

```

1  module adpsolver
2      #ifdef dnad
3          use dnadmod
4      #define real type(dual)
5      #endif
6      implicit none

```

**C.2 Changes to adpio Module**

Original: lines 1-2

```

1  module adpio
2      implicit none

```

Modified: lines 1-6

```

1  module adpio
2      #ifdef dnad
3          use dnadmod
4      #define real type(dual)
5      #endif
6      use adpsolver

```

Original: lines 5-7

```

5      integer, parameter :: ioUnit = 10 ! IO unit for files
6
7  contains

```

Modified: lines 9-16

```

9      integer, parameter :: ioUnit = 10 ! IO unit for files
10 #ifdef dnad
11     integer, parameter :: maxdvs = 3 ! Maximum number of derivatives supported
12     integer :: dvcount = 0 ! Count of partial derivatives requested
13     character*80, dimension(maxdvs) :: dvnames = "" ! List of derivative names
14 #endif
15
16 Contains

```

Original: lines 149-150

```

149         err = setSolverField(model, paramName, paramValue)
150     case default

```

Modified: lines 158-163

```

158             err = setSolverField(model, paramName, paramValue)
159 #ifdef dnad
160         case ("dnad")
161             err = setDNADField(model, paramName, paramValue)
162 #endif
163         case default

```

Original: lines 339-342

```

339     end function setSolverField
340
341
342     real function stringToReal(str) result (val)

```

Modified: lines 352-414

```

352     end function setSolverField
353
354
355 #ifdef dnad
356     !!! Set a field from the dnad card
357     !!!
358     !!! Input:
359     !!!     model = adpmodel object
360     !!!     paramName = Name of field to set
361     !!!     paramValue = String representation of parameter value
362     !!!
363     !!! Return:
364     !!!     stat = Error status flag (0 = success,
365     !!!                                     1 = Unrecognized parameter name,
366     !!!                                     2 = Number of allowed dvs exceeded)
367     integer function setDNADField(model, paramName, paramValue) result(stat)
368     class(adpmodel), intent(inout) :: model
369     character(len=*) , intent(in) :: paramName ! Parameter name
370     character(len=*) , intent(in) :: paramValue ! Parameter value
371
372     ! Initialize the error flag
373     stat = 0
374
375     select case(paramName)
376     case ("dv")
377         ! Check number of design variables
378         if (dvcount .ge. ndv) then
379             write(*, '(6X, A, I0, A, /, 6X, A, A)') &
380                 & "The maximum number of design variables (", &
381                 & ndv, ") has been reached.", paramValue, &
382                 & " will not be included as a design variable."
383         else
384             select case(paramValue)
385             case ("u")
386                 dvcount = dvcount + 1
387                 model%u%dx(dvcount) = 1.0
388                 dvnames(dvcount) = "dPhi/dU"
389             case ("gamma")
390                 dvcount = dvcount + 1
391                 model%gamma%dx(dvcount) = 1.0
392                 dvnames(dvcount) = "dPhi/dGamma"

```

```

393         case ("c")
394             dvcount = dvcount + 1
395             model%dx(dvcount) = 1.0
396             dvnames(dvcount) = "dPhi/dC"
397         case default
398             write(*, '(6X, A, 1X, A)') &
399                 & "Unrecognized design variable:", &
400                 & paramValue
401         end select
402     end if
403     case default
404         write(*, '(6X, A, 1X, A)') &
405             & "Unrecognized parameter name on dnad card:", &
406             & trim(paramName)
407         stat = 1
408     end select
409
410     end function setDNADfield
411 #endif
412
413
414     REAL function stringToReal(str) result (val)

```

Original: lines 405-408

```

405     end function writeOutput
406
407
408     subroutine writeData(model)

```

Modified: lines 477-481

```

477     end function writeOutput
478
479
480 #ifndef dnad
481     subroutine writeData(model)

```

Original: lines 435-438

```

435     end subroutine writeData
436
437
438     character*80 function removeWhitespace(str) result(mstr)

```

Modified: lines 508-546

```

508     end subroutine writeData
509 #else
510     subroutine writeData(model)
511         class(adpmodel), intent(inout) :: model ! adpmodel object
512
513         integer :: i, j ! Loop control variable
514         character*80 :: fmtString
515
516         if (model%method .eq. analytical .and. model%computeDerivatives) then
517             ! Header
518             write(fmtString, *) '(', 4 + dvcount, '(A, ",")', A)'

```

```

519         write(ioUnit, fmtString) "x", "phi", "dPhi/dU", "dPhi/dGamma", &
520         & "dPhi/dC", (trim(dvnames(j))//"_AD", j=1, dvcount)
521
522         ! Results
523         write(fmtString, *) '(', 4 + dvcount, '(ES23.15, ", "), ES23.15)'
524         do i=1, model%npts
525             write(ioUnit, fmtString) model%x(i)%x, model%phi(i)%x, &
526             & model%dPhi_dU(i)%x, model%dPhi_dGamma(i)%x, &
527             & model%dPhi_dC(i)%x, (model%phi(i)%dx(j), j=1, dvcount)
528         end do
529     else
530         ! Header
531         write(fmtString, *) '(', 1 + dvcount, '(A, ", "), A)'
532         write(ioUnit, fmtString) "x", "phi", &
533         & (trim(dvnames(j))//"_AD", j=1, dvcount)
534
535         ! Results
536         write(fmtString, *) '(', 1 + dvcount, '(ES23.15, ", "), ES23.15)'
537         do i=1, model%npts
538             write(ioUnit, fmtString) model%x(i)%x, model%phi(i)%x, &
539             & (model%phi(i)%dx(j), j=1, dvcount)
540         end do
541     end if
542 end subroutine writeData
543 #endif
544
545
546 character*80 function removeWhitespace(str) result(mstr)

```

## D SUMMARY OF CODE CHANGES TO MACHUP FOR DNAD INTEGRATION

### D.1 Changes to loads\_m Module

Original: lines 1-2

```
1  module loads_m
2      use plane_m
```

Modified: lines 1-6

```
1  module loads_m
2      #ifdef dnad
3          use dnadmod
4      #define real type(dual)
5      #endif
6      use plane_m
```

Original: lines 58-61

```
58  real :: ans(7),P(3),percent,span,chord
59  120 Format(A15, 100ES25.13)
60
61  !Get filename if specified
```

Modified: lines 62-68

```
62  real :: ans(7),P(3),percent,span,chord
63  real :: zero
64  120 Format(A15, 100ES25.13)
65
66  zero = 0.0
67
68  !Get filename if specified
```

### D.2 Changes to plane\_m Module

Original: lines 1-2

```
1  module plane_m
2      use myjson_m
```

Modified: lines 1-6

```
1  module plane_m
2      #ifdef dnad
3          use dnadmod
4      #define real type(dual)
5      #endif
6      use myjson_m
```

Original: lines 150-174

```

150     call t%json%get('plane.name', cval); call json_check(); t%name = trim(cval)
151     t%CG(1) = json_file_required_real(t%json,'plane.CGx')
152     t%CG(2) = json_file_required_real(t%json,'plane.CGy')
153     t%CG(3) = json_file_required_real(t%json,'plane.CGz')
154
155     t%Sr = json_file_required_real(t%json,'reference.area')
156     t%long_r = json_file_required_real(t%json,'reference.longitudinal_length')
157     t%lat_r = json_file_required_real(t%json,'reference.lateral_length')
158
159     t%alpha = json_file_required_real(t%json,'condition.alpha'); t%alpha =
t%alpha*pi/180.0
160     t%beta = json_file_optional_real(t%json,'condition.beta',0.0); t%beta =
t%beta*pi/180.0
161
162     t%omega(1) = json_file_optional_real(t%json,'condition.omega.roll',0.0)
163     t%omega(2) = json_file_optional_real(t%json,'condition.omega.pitch',0.0)
164     t%omega(3) = json_file_optional_real(t%json,'condition.omega.yaw',0.0)
165
166     t%hag = json_file_optional_real(t%json,'condition.ground',0.0)
167     if(t%hag.gt.0.0) t%groundplane = 1
168
169     call t%json%get('solver.type', cval); call json_check(); solver = trim(cval)
170     jacobian_converged = json_file_optional_real(t%json,'solver.convergence',
1.0e-6)
171     jacobian_omega = json_file_optional_real(t%json,'solver.relaxation',0.9)
172     nonlinear_maxiter = json_file_optional_integer(t%json,'solver.maxiter',100)
173
174     call t%json%get('airfoil_DB', cval); call json_check(); DB_Airfoil =
trim(cval)

```

Modified: lines 154-178

```

154     call t%json%get('plane.name', cval); call json_check(); t%name = trim(cval)
155     call myjson_get(t%json,'plane.CGx', t%CG(1))
156     call myjson_get(t%json,'plane.CGy', t%CG(2))
157     call myjson_get(t%json,'plane.CGz', t%CG(3))
158
159     call myjson_get(t%json,'reference.area', t%Sr)
160     call myjson_get(t%json,'reference.longitudinal_length', t%long_r)
161     call myjson_get(t%json,'reference.lateral_length', t%lat_r)
162
163     call myjson_get(t%json,'condition.alpha',t%alpha); t%alpha=t%alpha*pi/180.0
164     call myjson_get(t%json,'condition.beta',t%beta,0.0); t%beta=t%beta*pi/180.0
165
166     call myjson_get(t%json,'condition.omega.roll', t%omega(1), 0.0)
167     call myjson_get(t%json,'condition.omega.pitch', t%omega(2), 0.0)
168     call myjson_get(t%json,'condition.omega.yaw', t%omega(3), 0.0)
169
170     call myjson_get(t%json,'condition.ground', t%hag, 0.0)
171     if(t%hag.gt.0.0) t%groundplane = 1
172
173     call t%json%get('solver.type', cval); call json_check(); solver = trim(cval)
174     call myjson_get(t%json,'solver.convergence', jacobian_converged, 1.0e-6)
175     call myjson_get(t%json,'solver.relaxation', jacobian_omega, 0.9)
176     call myjson_get(t%json,'solver.maxiter', nonlinear_maxiter, 100)
177
178     call t%json%get('airfoil_DB', cval); call json_check(); DB_Airfoil =
trim(cval)

```

Original: lines 193-196

```

193         call json_check();
194         call t%json%get('controls.'//trim(j_cont%name)//'.deflection',
t%controls(icontrol)%deflection);
195         call json_check()
196         t%controls(icontrol)%deflection = pi/180.0*t%controls(icontrol)%
deflect

```

Modified: lines 197-199

```

197         call json_check();
198         call myjson_get(t%json, 'controls.'//trim(j_cont%name)//
'.deflection', t%controls(icontrol)%deflection)
199         t%controls(icontrol)%deflection = pi/180.0*t%controls(icontrol)%
deflect

```

Original: lines 232-251

```

232         call t%json%get('wings.'//trim(j_wing%name)//'.ID', t%wings(iwing)%ID);
call json_check()
233         call t%json%get('wings.'//trim(j_wing%name)//'.side', cval);
call json_check();
234         t%wings(iwing)%orig_side = trim(cval)
235         call t%json%get('wings.'//trim(j_wing%name)//'.connect.ID',
t%wings(iwing)%connectid); call json_check()
236         call t%json%get('wings.'//trim(j_wing%name)//'.connect.location', cval);
call json_check();
237         t%wings(iwing)%connectend = trim(cval)
238         call t%json%get('wings.'//trim(j_wing%name)//'.connect.dx',
t%wings(iwing)%doffset(1)); call json_check()
239         call t%json%get('wings.'//trim(j_wing%name)//'.connect.dy',
t%wings(iwing)%doffset(2)); call json_check()
240         call t%json%get('wings.'//trim(j_wing%name)//'.connect.dz',
t%wings(iwing)%doffset(3)); call json_check()
241         call t%json%get('wings.'//trim(j_wing%name)//'.connect.yoffset',
t%wings(iwing)%dy); call json_check()
242         call t%json%get('wings.'//trim(j_wing%name)//'.span',
t%wings(iwing)%span); call json_check()
243         call t%json%get('wings.'//trim(j_wing%name)//'.sweep', sweep);
call json_check()
244         call t%json%get('wings.'//trim(j_wing%name)//'.dihedral', dihedral);
call json_check()
245         call t%json%get('wings.'//trim(j_wing%name)//'.mounting_angle', mount);
call json_check()
246         call t%json%get('wings.'//trim(j_wing%name)//'.washout', washout); call
json_check()
247         call t%json%get('wings.'//trim(j_wing%name)//'.root_chord',
t%wings(iwing)%chord_1); call json_check()
248         call t%json%get('wings.'//trim(j_wing%name)//'.tip_chord',
t%wings(iwing)%chord_2); call json_check()
249
250         call t%json%get('wings.'//trim(j_wing%name)//'.sweep_definition',
t%wings(iwing)%sweep_definition);
251         if(json_failed()) t%wings(iwing)%sweep_definition=1

```



Modified: lines 235-254

```

235         call t%json%get('wings.'//trim(j_wing%name)//'.ID', t%wings(iwing)%ID);
call json_check()
236         call t%json%get('wings.'//trim(j_wing%name)//'.side', cval); call
json_check();
237         t%wings(iwing)%orig_side = trim(cval)
238         call t%json%get('wings.'//trim(j_wing%name)//'.connect.ID',
t%wings(iwing)%connectid); call json_check()
239         call t%json%get('wings.'//trim(j_wing%name)//'.connect.location', cval);
call json_check();
240         t%wings(iwing)%connectend = trim(cval)
241         call myjson_get(t%json, 'wings.'//trim(j_wing%name)//'.connect.dx',
t%wings(iwing)%doffset(1))
242         call myjson_get(t%json, 'wings.'//trim(j_wing%name)//'.connect.dy',
t%wings(iwing)%doffset(2))
243         call myjson_get(t%json, 'wings.'//trim(j_wing%name)//'.connect.dz',
t%wings(iwing)%doffset(3))
244         call myjson_get(t%json, 'wings.'//trim(j_wing%name)//'.connect.yoffset',
t%wings(iwing)%dy)
245         call myjson_get(t%json, 'wings.'//trim(j_wing%name)//'.span',
t%wings(iwing)%span)
246         call myjson_get(t%json, 'wings.'//trim(j_wing%name)//'.sweep', sweep)
247         call myjson_get(t%json, 'wings.'//trim(j_wing%name)//'.dihedral',
dihedral)
248         call myjson_get(t%json, 'wings.'//trim(j_wing%name)//'.mounting_angle',
mount)
249         call myjson_get(t%json, 'wings.'//trim(j_wing%name)//'.washout', washout)
250         call myjson_get(t%json, 'wings.'//trim(j_wing%name)//'.root_chord',
t%wings(iwing)%chord_1)
251         call myjson_get(t%json, 'wings.'//trim(j_wing%name)//'.tip_chord',
t%wings(iwing)%chord_2)
252
253         call t%json%get('wings.'//trim(j_wing%name)//'.sweep_definition',
t%wings(iwing)%sweep_definition);
254         if(json_failed()) t%wings(iwing)%sweep_definition=1

```

Original: lines 286-303

```

286         !control surface defs
287         call t%json%get('wings.'//trim(j_wing%name)//'.control.span_root',
t%wings(iwing)%control_span_root);
288         if(json_failed()) then
289             call json_clear_exceptions()
290             t%wings(iwing)%has_control_surface = 0
291         else
292             t%wings(iwing)%has_control_surface = 1
293             call t%json%get('wings.'//trim(j_wing%name)//'.control.span_root',
t%wings(iwing)%control_span_root);
294             call json_check()
295             call t%json%get('wings.'//trim(j_wing%name)//'.control.span_tip',
t%wings(iwing)%control_span_tip );
296             call json_check()

```

```

297         call t%json%get('wings.'//trim(j_wing%name)//'.control.chord_root',
t%wings(iwing)%control_chord_root);
298         call json_check()
299         call t%json%get('wings.'//trim(j_wing%name)//'.control.chord_tip',
t%wings(iwing)%control_chord_tip );
300         call json_check()
301         call t%json%get('wings.'//trim(j_wing%name)//'.control.is_sealed',
t%wings(iwing)%control_is_sealed);
302         call json_check()
303     end if

```

Modified: lines 289-302

```

289     !control surface defs
290     call myjson_get(t%json, 'wings.'//trim(j_wing%name)//
'.control.span_root', t%wings(iwing)%control_span_root, -1.0)
291
292     if(t%wings(iwing)%control_span_root < 0.0) then
293         call json_clear_exceptions()
294         t%wings(iwing)%has_control_surface = 0
295     else
296         t%wings(iwing)%has_control_surface = 1
297         call myjson_get(t%json, 'wings.'//trim(j_wing%name)//
'.control.span_tip', t%wings(iwing)%control_span_tip)
298         call myjson_get(t%json, 'wings.'//trim(j_wing%name)//
'.control.chord_root', t%wings(iwing)%control_chord_root)
299         call myjson_get(t%json, 'wings.'//trim(j_wing%name)//
'.control.chord_tip', t%wings(iwing)%control_chord_tip)
300         call t%json%get('wings.'//trim(j_wing%name)//'.control.is_sealed',
t%wings(iwing)%control_is_sealed);
301         call json_check()
302     end if

```

Original: lines 377-384

```

377     case ('linear')
378         airfoils(i)%aL0 = json_file_required_real(f_json,trim(prefix)//
'properties.alpha_L0');
379         airfoils(i)%CLa = json_file_required_real(f_json,trim(prefix)//
'properties.CL_alpha');
380         airfoils(i)%CmL0 = json_file_required_real(f_json,trim(prefix)//
'properties.Cm_L0');
381         airfoils(i)%Cma = json_file_required_real(f_json,trim(prefix)//
'properties.Cm_alpha');
382         airfoils(i)%CD0 = json_file_required_real(f_json,trim(prefix)//
'properties.CD_min');
383         airfoils(i)%CLmax = json_file_optional_real(f_json,trim(prefix)//
'properties.CL_max',-1.0);
384         airfoils(i)%has_data_file = 0

```

Modified: lines 376-383

```

376     case ('linear')
377         call myjson_get(f_json, trim(prefix)//'properties.alpha_L0',
airfoils(i)%aL0);
378         call myjson_get(f_json, trim(prefix)//'properties.CL_alpha',
airfoils(i)%CLa);
379         call myjson_get(f_json, trim(prefix)//'properties.Cm_L0',
airfoils(i)%CmL0);

```

```

380         call myjson_get(f_json, trim(prefix)//'properties.Cm_alpha',
airfoils(i)%Cma);
381         call myjson_get(f_json, trim(prefix)//'properties.CD_min',
airfoils(i)%CD0);
382         call myjson_get(f_json, trim(prefix)//'properties.CL_max',
airfoils(i)%CLmax, -1.0);
383         airfoils(i)%has_data_file = 0

```

Original: lines 604-607

```

604         if(trim(j_mix%name).eq.trim(t%controls(icontrol)%name)) then
605             call t%json%get('wings.'//trim(t%wings(iwing)%name)
//'.control.mix.'//trim(j_mix%name), ratio);
606             call json_check()
607             if(t%controls(icontrol)%is_symmetric.eq.1) then

```

Modified: lines 603-605

```

603         if(trim(j_mix%name).eq.trim(t%controls(icontrol)%name)) then
604             call myjson_get(t%json, 'wings.'// trim(t%wings(iwing)%
name) //'.'control.mix.'//trim(j_mix%name), ratio)
605             if(t%controls(icontrol)%is_symmetric.eq.1) then

```

Original: lines 720-722

```

720     integer :: i
721     real :: time1,time2
722     call cpu_time(time1)

```

Modified: lines 718-720

```

718     integer :: i
719     REAL :: time1,time2
720     call cpu_time(time1)

```

Original: lines 1133-1136

```

1133     real :: A(3,3),Atemp(3,3),X(3),B(3),span,span1,span2,span3,F0(3),F1(3),P(3),
percent
1134     120 Format(A15, 100ES25.13)
1135
1136     filename = trim(adjustl(t%master_filename))//'_loads.txt'

```

Modified: lines 1131-1137

```

1131     real :: A(3,3),Atemp(3,3),X(3),B(3),span,span1,span2,span3,F0(3),F1(3),P(3),
percent
1132     real :: zero
1133     120 Format(A15, 100ES25.13)
1134
1135     zero = 0.0
1136
1137     filename = trim(adjustl(t%master_filename))//'_loads.txt'

```

Original: lines 1153-1155

```
1153  call ds_create_from_data(dist,30,2,rawdata)
1154  call ds_cubic_setup(dist,1,2,0.0,2,0.0)
1155  call ds_print_data(dist)
```

Modified: lines 1154-1156

```
1153  call ds_create_from_data(dist,30,2,rawdata)
1154  call ds_cubic_setup(dist, 1, 2, zero, 2, zero)
1155  call ds_print_data(dist)
```

### D.3 Changes to special\_functions\_m Module

Original: lines 1-2

```
1  module special_functions_m
2      use plane_m
```

Modified: lines 1-6

```
1  module special_functions_m
2      #ifdef dnad
3          use dnadmod
4      #define real type(dual)
5      #endif
6          use plane_m
```

Original: lines 459-460

```
459  start_alpha = json_optional_real(json_command, 'start_alpha', 0.0)
460  start_alpha = (start_alpha+1.0)*pi/180.0
```

Modified: lines 463-464

```
463  call myjson_get(json_command, 'start_alpha', start_alpha, 0.0)
464  start_alpha = (start_alpha+1.0)*pi/180.0
```

Original: lines 469-471

```
469  do ialpha = -10, 300, 1
470      t%alpha = real(ialpha)/10.0*pi/180.0 + start_alpha
471      call plane_run_current(t)
```

Modified: lines 473-475

```
473  do ialpha = -10, 300, 1
474      t%alpha = REAL(ialpha)/10.0*pi/180.0 + start_alpha
475      call plane_run_current(t)
```

Original: lines 581-598

```

581     write(*,*) 'Using control surface: ',trim(controlname)
582
583     call json_get(json_command,'CL',CL_target,json_found)
584
585     if(json_failed()) then
586         call json_clear_exceptions()
587         trimType = 2
588
589         CW_target = json_required_real(json_command,'CW');
590         climb=json_optional_real(json_command,'climb',0.0); climb=climb*pi/180.0
591         thrust_x = json_optional_real(json_command,'thrust.x',0.0);
592         thrust_z = json_optional_real(json_command,'thrust.z',0.0);
593         thrust_a = json_optional_real(json_command,'thrust.angle',0.0);
594
595     else !trim using CL, Cm
596         trimType = 1
597         Cm_target = json_optional_real(json_command,'Cm',0.0);
598     end if

```

Modified: lines 585-602

```

585     write(*,*) 'Using control surface: ',trim(controlname)
586
587     call myjson_get(json_command, 'CL', CL_target, -1.0)
588
589     if(CL_target < 0.0) then
590         call json_clear_exceptions()
591         trimType = 2
592
593         call myjson_get(json_command, 'CW', CW_target)
594         call myjson_get(json_command,'climb',climb,0.0); climb=climb*pi/180.0
595         call myjson_get(json_command, 'thrust.x', thrust_x, 0.0);
596         call myjson_get(json_command, 'thrust.z', thrust_z, 0.0);
597         call myjson_get(json_command, 'thrust.angle', thrust_a, 0.0);
598
599     else !trim using CL, Cm
600         trimType = 1
601         call myjson_get(json_command, 'Cm', Cm_target, 0.0);
602     end if

```

Original: lines 606-611

```

606     de = t%controls(icontrol)%deflection !radians
607
608     delta = json_optional_real(json_command,'delta',0.5);
609     maxres = json_optional_real(json_command,'convergence',1.0e-10);
610     relaxation = json_optional_real(json_command,'relaxation',1.0);
611     maxiter = json_optional_integer(json_command,'maxiter',50);

```

Modified: lines 610-615

```

610     de = t%controls(icontrol)%deflection !radians
611
612     call myjson_get(json_command, 'delta', delta, 0.5);
613     call myjson_get(json_command, 'convergence', maxres, 1.0e-10);
614     call myjson_get(json_command, 'relaxation', relaxation, 1.0);
615     call myjson_get(json_command, 'maxiter', maxiter, 50);

```

Original: lines 755-769

```

755     write(*,*) '----- Finding alpha to target CL -----'
756
757     CL_target = json_required_real(json_command,'CL');
758
759     !store alpha and de in case no solution is found
760     alpha_temp = t%alpha !radians
761
762     alpha = 0.0 !t%alpha !radians
763
764     delta = json_optional_real(json_command,'delta',0.5);
765     maxres = json_optional_real(json_command,'convergence',1.0e-10);
766     relaxation = json_optional_real(json_command,'relaxation',1.0);
767     maxiter = json_optional_integer(json_command,'maxiter',50);
768
769     write(*,*)

```

Modified: lines 759-773

```

759     write(*,*) '----- Finding alpha to target CL -----'
760
761     call myjson_get(json_command, 'CL', CL_target);
762
763     !store alpha and de in case no solution is found
764     alpha_temp = t%alpha !radians
765
766     alpha = 0.0 !t%alpha !radians
767
768     call myjson_get(json_command, 'delta', delta, 0.5);
769     call myjson_get(json_command, 'convergence', maxres, 1.0e-10);
770     call myjson_get(json_command, 'relaxation', relaxation, 1.0);
771     call myjson_get(json_command, 'maxiter', maxiter, 50);
772
773     write(*,*)

```

Original: lines 843-855

```

843     type(plane_t) :: t
844     character(len=:),allocatable :: cval
845     character(100) :: target_var, change_var
846     real :: result,x0,x1,xnew,f0,f1, target_val, tolerance
847     integer :: ios
848
849     !Read json target info
850     call t%json%get('run.target.variable', cval); call json_check();
    target_var = trim(cval)
851     call t%json%get('run.target.value', target_val); call json_check()
852     call t%json%get('run.target.tolerance', tolerance); call json_check()
853     call t%json%get('run.target.change', cval); call json_check();
    change_var = trim(cval)
854
855     write(*,*) '    target variable = ',trim(target_var)

```

Modified: lines 847-857

```

847     type(plane_t) :: t
848     character(len=:), allocatable :: target_var, change_var
849     real :: result,x0,x1,xnew,f0,f1, target_val, tolerance

```

```

850
851     !Read json target info
852     call myjson_get(t%json, 'run.target.variable', target_var)
853     call myjson_get(t%json, 'run.target.value', target_val)
854     call myjson_get(t%json, 'run.target.tolerance', tolerance)
855     call myjson_get(t%json, 'run.target.change', change_var)
856
857     write(*,*) '      target variable = ',trim(target_var)

```

Original: lines 922-927

```

922         call json_get(json_command,trim(c_var%name)//'.file', cval,json_found);
call json_check(); var_file = trim(cval)
923         save_file = json_optional_integer(json_command,trim(c_var%name)//
'.save', 0)
924
925         call f_json%load_file(filename = var_file);          call json_check()
926         call f_json%get(trim(var_name), var_value);          call json_check()
927         call json_value_add(p_root, trim(c_var%name), var_value)

```

Modified: lines 924-929

```

924         call json_get(json_command,trim(c_var%name)//'.file', cval,json_found);
call json_check(); var_file = trim(cval)
925         call myjson_get(json_command,trim(c_var%name)//'.save', save_file, 0);
926
927         call f_json%load_file(filename = var_file);          call json_check()
928         call myjson_get(f_json, trim(var_name), var_value)
929         call json_value_add(p_root, trim(c_var%name), var_value)

```

Original: lines 961-964

```

961     call f_json%load_file(filename = fn);          call json_check()
962     call f_json%get(trim(fitness_var), fitness_val); call json_check()
963
964     open(unit = 10, File = 'fitness.txt', action = 'write', iostat = ios)

```

Modified: lines 963-966

```

963     call f_json%load_file(filename = fn);          call json_check()
964     call myjson_get(f_json, trim(fitness_var), fitness_val)
965
966     open(unit = 10, File = 'fitness.txt', action = 'write', iostat = ios)

```

Original: lines 984-989

```

984     call f_json%load_file(filename = fn);          call json_check()
985     call f_json%get('total.MyAirplane.CD', CD);    call json_check()
986     call f_json%get('total.Wing_1_left.Cl', Cl);    call json_check()
987     call f_json%get('total.Wing_1_left.Cn', Cn);    call json_check()
988
989     if(opt_type.eq.1) then

```

Modified: lines 986-991

```

986     call f_json%load_file(filename = fn);           call json_check()
987     call myjson_get(f_json, 'total.MyAirplane.CD', CD)
988     call myjson_get(f_json, 'total.MyAirplane.Cl', Cl)
989     call myjson_get(f_json, 'total.MyAirplane.Cn', Cn)
990
991     if(opt_type.eq.1) then

```

Original: lines 1028-1031

```

1028     call f_json%load_file(filename = fn);           call json_check()
1029     call f_json%get(trim(read_var), result);         call json_check()
1030
1031 end subroutine sf_run_single

```

Modified: lines 1030-1033

```

1028     call f_json%load_file(filename = fn);           call json_check()
1029     call myjson_get(f_json, trim(read_var), result)
1030
1031 end subroutine sf_run_single

```

#### D.4 Changes to view\_m Module

Original: lines 1-2

```

1  module view_m
2      use plane_m

```

Modified: lines 1-6

```

1  module view_m
2      #ifdef dnad
3          use dnadmod
4      #define real type(dual)
5      #endif
6          use plane_m

```

Original: line 124

```

124         delta = gpsize/real(gnum)

```

Modified: line 128

```

128         delta = gpsize/REAL(gnum)

```



Original: lines 132-133

```

132      P1(1) = P0(1) - gsize*cos(t%alpha); P1(2) = P0(2) + real(i)*delta;
      P1(3) = P0(3) - gsize*sin(t%alpha)
133      P2(1) = P0(1) + gsize*cos(t%alpha); P2(2) = P0(2) + real(i)*delta;
      P2(3) = P0(3) + gsize*sin(t%alpha)

```

Modified: lines 136-137

```

136      P1(1) = P0(1) - gsize*cos(t%alpha); P1(2) = P0(2) + REAL(i)*delta;
      P1(3) = P0(3) - gsize*sin(t%alpha)
137      P2(1) = P0(1) + gsize*cos(t%alpha); P2(2) = P0(2) + REAL(i)*delta;
      P2(3) = P0(3) + gsize*sin(t%alpha)

```

Original: lines 140-141

```

140      P1(1) = P0(1) - real(i)*delta*cos(t%alpha); P1(2) = P0(2) + gsize;
      P1(3) = P0(3) - real(i)*delta*sin(t%alpha)
141      P2(1) = P0(1) - real(i)*delta*cos(t%alpha); P2(2) = P0(2) - gsize;
      P2(3) = P0(3) - real(i)*delta*sin(t%alpha)

```

Modified: lines 144-145

```

144      P1(1) = P0(1) - REAL(i)*delta*cos(t%alpha); P1(2) = P0(2) + gsize;
      P1(3) = P0(3) - REAL(i)*delta*sin(t%alpha)
145      P2(1) = P0(1) - REAL(i)*delta*cos(t%alpha); P2(2) = P0(2) - gsize;
      P2(3) = P0(3) - REAL(i)*delta*sin(t%alpha)

```

## D.5 Changes to wing\_m Module

Original: lines 1-2

```

1  module wing_m
2      use section_m

```

Modified: lines 1-6

```

1  module wing_m
2      #ifdef dnad
3          use dnadmod
4      #define real type(dual)
5      #endif
6          use section_m

```

Original: lines 71-73

```

71      integer :: isec
72      real :: start(3),qvec(3),nvec(3),avec(3),fvec(3),dtheta,percent_1,percent_2,
      percent_c,chord_1,chord_2,RA,span
73      real :: my_sweep,my_dihedral,my_twist,temp

```

Modified: lines 75-78

```

75      integer :: isec
76      REAL :: dtheta

```

```

77      real :: start(3), qvec(3), nvec(3), avec(3), fvec(3), percent_1, percent_2,
      percent_c, chord_1, chord_2, RA, span
78      real :: my_sweep, my_dihedral, my_twist, temp

```

Original: lines 104-112

```

104     call wing_allocate(t)
105     dtheta = pi/real(t%nSec)
106     t%area = 0.0
107     span = 0.0
108     do isec=1,t%nSec
109         percent_1 = 0.5*(1.0-cos(dtheta*real(isec-1)))
110         percent_2 = 0.5*(1.0-cos(dtheta*real(isec)))
111         percent_c = 0.5*(1.0-cos(dtheta*(real(isec)-0.5)))
112         if(t%side.eq.'left') then !must handle differently for left wing

```

Modified: lines 109-117

```

109     call wing_allocate(t)
110     dtheta = pi/REAL(t%nSec)
111     t%area = 0.0
112     span = 0.0
113     do isec=1,t%nSec
114         percent_1 = 0.5*(1.0-cos(dtheta*REAL(isec-1)))
115         percent_2 = 0.5*(1.0-cos(dtheta*REAL(isec)))
116         percent_c = 0.5*(1.0-cos(dtheta*(REAL(isec)-0.5)))
117         if(t%side.eq.'left') then !must handle differently for left wing

```

Original: lines 274-276

```

274     integer :: isec
275     real :: A,B,C,D,P1(3),P2(3),P3(3),tempv(3),tempr,temp_percent
276     P1(1) = CG(1) - hag*sin(alpha) !offset from CG

```

Modified: lines 279-282

```

279     integer :: isec
280     real :: A,B,C,D,P1(3),P2(3),P3(3),tempv(3),tempr,temp_percent,zero
281     zero = 0.0
282     P1(1) = CG(1) - hag*sin(alpha) !offset from CG

```

Original: lines 295-302

```

295         t%sec(isec)%chord_2 = tempr
296
297         call math_reflect_point(A,B,C,0.0,t%sec(isec)%un,tempv)
298         t%sec(isec)%un = tempv
299         call math_reflect_point(A,B,C,0.0,t%sec(isec)%ua,tempv)
300         t%sec(isec)%ua = tempv
301         call math_reflect_point(A,B,C,0.0,t%sec(isec)%uf,tempv)
302         t%sec(isec)%uf = tempv

```

Modified: lines 301-308

```

301      t%sec(isec)%chord_2 = tempr
302
303      call math_reflect_point(A,B,C,zero,t%sec(isec)%un,tempv)
304      t%sec(isec)%un = tempv
305      call math_reflect_point(A,B,C,zero,t%sec(isec)%ua,tempv)
306      t%sec(isec)%ua = tempv
307      call math_reflect_point(A,B,C,zero,t%sec(isec)%uf,tempv)
308      t%sec(isec)%uf = tempv

```

## D.6 Changes to airfoil\_m Module

Original: lines 1-2

```

1  module airfoil_m
2      use dataset_m

```

Modified: lines 1-6

```

1  module airfoil_m
2      #ifdef dnad
3          use dnadmod
4      #define real type(dual)
5      #endif
6          use dataset_m

```

## D.7 Changes to atmosphere\_m Module

Original: lines 1-2

```

1  module atmosphere_m
2      use dataset_m

```

Modified: lines 1-6

```

1  module atmosphere_m
2      #ifdef dnad
3          use dnadmod
4      #define real type(dual)
5      #endif
6          use dataset_m

```

Original: line 12

```

12      real :: temp(36,7)

```

Modified: lines 17-20

```

17      real :: temp(36,7)
18      real :: zero
19
20      zero = 0.0

```

Original: lines 52-55

```

52      call ds_create_from_data(t%properties,36,7,temp(:, :))
53      call ds_cubic_setup(t%properties,1,2,0.0,2,0.0)
54
55  end subroutine atm_create

```

Modified: lines 60-63

```

60      call ds_create_from_data(t%properties,36,7,temp(:, :))
61      call ds_cubic_setup(t%properties,1,2,zero,2,zero)
62
63  end subroutine atm_create

```

## D.8 Changes to dataset\_m Module

Original: lines 1-2

```

1  module dataset_m
2      use math_m

```

Modified: lines 1-6

```

1  module dataset_m
2      #ifdef dnad
3          use dnadmod
4      #define real type(dual)
5      #endif
6          use math_m

```

## D.9 Changes to math\_m Module

Original: lines 1-4

```

1  module math_m
2      implicit none
3      real, parameter :: pi = 3.1415926535897932
4      contains

```

Modified: lines 1-9

```

1  module math_m
2      #ifdef dnad
3          use dnadmod
4      #define real type(dual)
5      #endif
6
7      implicit none
8      REAL, parameter :: pi = 3.1415926535897932
9      contains

```

Original: lines 225-229

```

225      INTEGER::n,D,info
226      REAL,DIMENSION(n)::B,X
227      REAL,DIMENSION(n,n)::A

```

```

228
229     INTEGER,allocatable,DIMENSION(:) :: INDX

```

Modified: lines 230-234

```

230     INTEGER::n,D,info
231     real,DIMENSION(n)::B,X
232     real,DIMENSION(n,n)::A
233
234     INTEGER,allocatable,DIMENSION(:) :: INDX

```

Original: lines 274-277

```

274     REAL, PARAMETER :: TINY=1.5D-16
275     REAL AMAX,DUM, SUM, A(N,N)
276     REAL,ALLOCATABLE,DIMENSION(:) :: VV
277     INTEGER N, CODE, D, INDX(N)

```

Modified: lines 279-282

```

279     REAL, PARAMETER :: TINY=1.5D-16
280     real AMAX,DUM, SUM, A(N,N)
281     real,ALLOCATABLE,DIMENSION(:) :: VV
282     INTEGER N, CODE, D, INDX(N)

```

Original: lines 356-357

```

356     integer :: N
357     REAL SUM, A(N,N),B(N)
358     INTEGER INDX(N)

```

Modified: lines 361-363

```

361     integer :: N
362     real SUM, A(N,N),B(N)
363     INTEGER INDX(N)

```

## D.10 Changes to section\_m Module

Original: lines 1-2

```

1  module section_m
2      use airfoil_m

```

Modified: lines 1-6

```

1  module section_m
2      #ifdef dnad
3          use dnadmod
4      #define real type(dual)
5      #endif
6      use airfoil_m

```

## D.11 Changes to myjson\_m Module

Original: lines 1-134

```

1  module myjson_m
2      use json_m
3      implicit none
4
5      logical :: json_found
6
7  contains
8
9  !-----
10 -
11 real function json_required_real(json,name)
12     implicit none
13     type(json_value),intent(in),pointer :: json
14     character(len=*) :: name
15     real :: value
16
17     call json_get(json, name, value, json_found)
18     if(json_failed()) then
19         write(*,*) 'Error: Unable to read required value: ',name
20         STOP
21     end if
22
23     json_required_real = value
24 end function json_required_real
25 !-----
26 -
27 real function json_optional_real(json,name,default_value)
28     implicit none
29     type(json_value),intent(in),pointer :: json
30     character(len=*) :: name
31     real :: value, default_value
32
33     call json_get(json, name, value, json_found)
34     if((.not.json_found) .or. json_failed()) then
35         write(*,*) trim(name), ' set to ',default_value
36         value = default_value
37         call json_clear_exceptions()
38     end if
39
40     json_optional_real = value
41 end function json_optional_real
42 !-----
43 -
44 integer function json_optional_integer(json,name,default_value)
45     implicit none
46     type(json_value),intent(in),pointer :: json
47     character(len=*) :: name
48     integer :: value, default_value
49
50     call json_get(json, name, value, json_found)
51     if((.not.json_found) .or. json_failed()) then
52         write(*,*) trim(name), ' set to ',default_value
53         value = default_value
54         call json_clear_exceptions()
55     end if

```

```

55
56     json_optional_integer = value
57 end function json_optional_integer
58
59 !-----
-
60 real function json_file_required_real(json,name)
61     implicit none
62     type(json_file) :: json
63     character(len=*) :: name
64     real :: value
65
66     call json%get(name, value)
67     if(json_failed()) then
68         write(*,*) 'Error: Unable to read required value: ',name
69         STOP
70     end if
71
72     json_file_required_real = value
73 end function json_file_required_real
74
75 !-----
-
76 real function json_file_optional_real(json,name,default_value)
77     implicit none
78     type(json_file) :: json
79     character(len=*) :: name
80     real :: value, default_value
81
82     call json%get(name, value)
83     if(json_failed()) then
84         write(*,*) name, ' set to ',default_value
85         value = default_value
86         call json_clear_exceptions()
87     end if
88
89     json_file_optional_real = value
90 end function json_file_optional_real
91
92 !-----
-
93 integer function json_file_optional_integer(json,name,default_value)
94     implicit none
95     type(json_file) :: json
96     character(len=*) :: name
97     integer :: value, default_value
98
99     call json%get(name, value)
100    if(json_failed()) then
101        write(*,*) trim(name), ' set to ',default_value
102        value = default_value
103        call json_clear_exceptions()
104    end if
105
106    json_file_optional_integer = value
107 end function json_file_optional_integer
108
109 !-----
-
110 subroutine json_check()
111     if(json_failed()) then

```

```

112         call print_json_error_message()
113         STOP
114     end if
115 end subroutine json_check
116 !-----
-
117 subroutine print_json_error_message()
118     implicit none
119     character(len=:),allocatable :: error_msg
120     logical :: status_ok
121
122     !get error message:
123     call json_check_for_errors(status_ok, error_msg)
124
125     !print it if there is one:
126     if (.not. status_ok) then
127         write(*,'(A)') error_msg
128         deallocate(error_msg)
129         call json_clear_exceptions()
130     end if
131
132 end subroutine print_json_error_message
133
134 end module myjson_m

```

Modified: lines 1-305

```

1  module myjson_m
2  #ifdef dnad
3      use dnadmod
4  #ifndef ndv
5      #define ndv 1
6  #endif
7  #endif
8      use json_m
9      implicit none
10
11      logical :: json_found
12  #ifdef dnad
13      integer, save :: n_design_vars = 0
14  #endif
15
16      interface myjson_get
17          module procedure :: myjson_value_get_real, myjson_file_get_real
18  #ifdef dnad
19          module procedure :: myjson_value_get_dual, myjson_file_get_dual
20  #endif
21          module procedure :: myjson_value_get_integer, myjson_file_get_integer
22          module procedure :: myjson_file_get_string
23      end interface myjson_get
24
25  #ifdef dnad
26      interface json_value_add
27          module procedure :: myjson_value_add_dual, myjson_value_add_dual_vec
28      end interface
29  #endif
30
31  contains
32
33  !-----
34  subroutine myjson_value_get_real(json, name, value, default_value)

```



```

35     implicit none
36     type(json_value),intent(in),pointer :: json
37     character(len=*), intent(in) :: name
38     real, intent(out) :: value
39     real, intent(in), optional :: default_value
40
41     call json_get(json, name, value, json_found)
42     if(json_failed() .or. (.not. json_found)) then
43         if (present(default_value)) then
44             write(*,*) trim(name),' set to ',default_value
45             value = default_value
46             call json_clear_exceptions()
47         else
48             write(*,*) 'Error: Unable to read required value: ',name
49             STOP
50         end if
51     end if
52 end subroutine myjson_value_get_real
53
54 #ifdef dnad
55 !-----
56 subroutine myjson_value_get_dual(json, name, value, default_value)
57     implicit none
58     type(json_value),intent(in),pointer :: json
59     character(len=*), intent(in) :: name
60     type(dual), intent(out) :: value
61     real, intent(in), optional :: default_value
62
63     real, dimension(:), allocatable :: vec
64
65     call json_get(json, name, value%x, json_found)
66     if(json_failed() .or. (.not. json_found)) then
67         call json_clear_exceptions()
68         call json_get(json, name, vec, json_found)
69         if(json_found .and. (.not. json_failed())) then
70             value = vec(1) ! This will initialize derivatives to zero
71             if(vec(2) /= 0) then
72                 if(n_design_vars < ndv) then
73                     n_design_vars = n_design_vars + 1
74                     value%dx(n_design_vars) = vec(2)
75                 else
76                     write(*,*) 'Error: The number of design variables ', &
77                         & 'exceeds the compiled limit: ', ndv
78                     write(*,*) '      Reduce the number of design ', &
79                         & 'variables, or increase the limit by'
80                     write(*,*) '      specifying -Dndv=<num> when compiling.'
81                     STOP
82                 end if
83             end if
84         else
85             if (present(default_value)) then
86                 value = default_value
87                 write(*,*) trim(name),' set to ', value
88                 call json_clear_exceptions()
89             else
90                 write(*,*) 'Error: Unable to read required value: ',name
91                 STOP
92             end if
93         end if
94     end if
95 end if

```

```

96  end subroutine myjson_value_get_dual
97
98  #endif
99  !-----
100 subroutine myjson_value_get_integer(json, name, value, default_value)
101   implicit none
102   type(json_value),intent(in),pointer :: json
103   character(len=*), intent(in) :: name
104   integer, intent(out) :: value
105   integer, intent(in), optional :: default_value
106
107   call json_get(json, name, value, json_found)
108   if(.not.json_found .or. json_failed()) then
109     if (present(default_value)) then
110       write(*,*) trim(name), ' set to ', default_value
111       value = default_value
112       call json_clear_exceptions()
113     else
114       write(*,*) 'Error: Unable to read required value: ', name
115       STOP
116     end if
117   end if
118
119 end subroutine myjson_value_get_integer
120
121 !-----
122 subroutine myjson_file_get_real(json, name, value, default_value)
123   implicit none
124   type(json_file) :: json
125   character(len=*), intent(in) :: name
126   real, intent(out) :: value
127   real, intent(in), optional :: default_value
128
129   call json%get(name, value)
130   if(json_failed()) then
131     if (present(default_value)) then
132       write(*,*) trim(name), ' set to ', default_value
133       value = default_value
134       call json_clear_exceptions()
135     else
136       write(*,*) 'Error: Unable to read required value: ', trim(name)
137       STOP
138     end if
139   end if
140
141 end subroutine myjson_file_get_real
142
143 #ifdef dnad
144 !-----
145 subroutine myjson_file_get_dual(json, name, value, default_value)
146   implicit none
147   type(json_file) :: json
148   character(len=*), intent(in) :: name
149   type(dual), intent(out) :: value
150   real, intent(in), optional :: default_value
151
152   real :: temp
153   real, dimension(:), allocatable :: vec
154
155   call json%get(name, temp)
156   if(.not. json_failed()) then

```

```

157         value = temp ! Derivatives not specified, initialize to zero
158     else
159         call json_clear_exceptions()
160         call json%get(name, vec)
161         if(.not. json_failed()) then
162             value = vec(1) ! This will initialize derivatives to zero
163             if(vec(2) /= 0) then
164                 if(n_design_vars < ndv) then
165                     n_design_vars = n_design_vars + 1
166                     value%dx(n_design_vars) = vec(2)
167                 else
168                     write(*,*) 'Error: The number of design variables ', &
169                         & 'exceeds the compiled limit: ', ndv
170                     write(*,*) '      Reduce the number of design ', &
171                         & 'variables, or increase the limit by'
172                     write(*,*) '      specifying -Dndv=<num> when compiling.'
173                     STOP
174                 end if
175             end if
176         else
177             if (present(default_value)) then
178                 value = default_value
179                 write(*,*) trim(name), ' set to ', value
180                 call json_clear_exceptions()
181             else
182                 write(*,*) 'Error: Unable to read required value: ', trim(name)
183                 STOP
184             end if
185         end if
186     end if
187
188 end subroutine myjson_file_get_dual
189
190 #endif
191 !-----
192 subroutine myjson_file_get_integer(json, name, value, default_value)
193     implicit none
194     type(json_file) :: json
195     character(len=*) , intent(in) :: name
196     integer, intent(out) :: value
197     integer, intent(in), optional :: default_value
198
199     call json%get(name, value)
200     if(json_failed()) then
201         if (present(default_value)) then
202             write(*,*) trim(name), ' set to ', default_value
203             value = default_value
204             call json_clear_exceptions()
205         else
206             write(*,*) 'Error: Unable to read required value: ', name
207             STOP
208         end if
209     end if
210 end subroutine myjson_file_get_integer
211
212 !-----
213 subroutine myjson_file_get_string(json, name, value)
214     implicit none
215     type(json_file) :: json
216     character(len=*) , intent(in) :: name
217     character(:), allocatable, intent(out) :: value

```

```

218
219     call json%get(name, value)
220     if(json_failed()) then
221         write(*,*) 'Error: Unable to read required value: ',name
222         STOP
223     end if
224
225     value = trim(value)
226 end subroutine myjson_file_get_string
227
228 !-----
229 subroutine json_check()
230     if(json_failed()) then
231         call print_json_error_message()
232         STOP
233     end if
234 end subroutine json_check
235 !-----
236 subroutine print_json_error_message()
237     implicit none
238     character(len=:),allocatable :: error_msg
239     logical :: status_ok
240
241     !get error message:
242     call json_check_for_errors(status_ok, error_msg)
243
244     !print it if there is one:
245     if (.not. status_ok) then
246         write(*,'(A)') error_msg
247         deallocate(error_msg)
248         call json_clear_exceptions()
249     end if
250
251 end subroutine print_json_error_message
252
253 #ifdef dnad
254 subroutine myjson_value_add_dual(me, name, val)
255
256     implicit none
257
258     type(json_value), pointer :: me
259     character(len=*),intent(in) :: name
260     type(dual),intent(in) :: val
261
262     real,allocatable,dimension(:) :: vec
263     integer :: vec_length
264
265     ! Dual numbers are written to json as a vector: [u, du/dx, du/dy, ...]
266     vec_length = size(val%dx) + 1
267     allocate(vec(vec_length))
268     vec(1) = val%x
269     vec(2:) = val%dx
270
271     call json_value_add(me, name, vec)
272
273 end subroutine myjson_value_add_dual
274
275 subroutine myjson_value_add_dual_vec(me, name, val)
276
277     implicit none
278

```

```

279     type(json_value), pointer          :: me
280     character(len=*),intent(in)       :: name
281     type(dual),dimension(:),intent(in) :: val
282
283     type(json_value),pointer :: var
284     integer :: i
285
286     !create the variable as an array:
287     call json_value_create(var)
288     call to_array(var,name)
289
290     !populate the array:
291     do i=1,size(val)
292         call json_value_add(var, '', val(i))
293     end do
294
295     !add it:
296     call json_value_add(me, var)
297
298     !cleanup:
299     nullify(var)
300
301 end subroutine myjson_value_add_dual_vec
302 !*****
303
304 #endif
305 end module myjson_m

```

## E EXAMPLE MACHUP INPUT FILES

## E.1 Example JSON-Formatted Input File

```

{
  "run": {
    "targetcl": {
      "CL": 0.5, "delta": 0.1, "relaxation": 1.0, "maxiter": 100,
      "convergence": 1.0E-12, "run": 1
    },
    "forces": {"run": 1},
    "distributions": {"run": 1},
    "stl": {"run": 1}
  },
  "solver": { "type": "nonlinear", "convergence": 1.0E-12, "relaxation": 0.9 },
  "plane": { "name": "MyAirplane", "CGx": 0, "CGy": 0, "CGz": 0 },
  "reference": { "area": 8.0, "longitudinal_length": 1.0, "lateral_length": 8.0 },
  "condition": { "alpha": 5.0, "beta": 0.0 },
  "airfoil_DB": "./AirfoilDB",
  "wings": {
    "wing_main": {
      "name": "wing_main", "ID": 1, "is_main": 1, "side": "both",
      "connect": {
        "ID": 0, "location": "tip", "dx": 0, "dy": 0, "dz": 0, "yoffset": 0
      },
      "span": 4, "mounting_angle": 0,
      "sweep": 0.0, "dihedral": 0.0, "washout": 0,
      "root_chord": 1.27323954473516, "tip_chord": -1,
      "airfoils": { "NACA_2412": "" },
      "grid": 100,
      "control": {}
    }
  }
}

```

## E.2 Example Parameter File for a NACA 2412 Airfoil in Inviscid Incompressible Flow

```

{
  "NACA_2412": {
    "properties": {
      "type": "linear",
      "alpha_L0": -0.0380,
      "CL_alpha": 6.8583,
      "Cm_L0": 0.0,
      "Cm_alpha": 0.0,
      "CD0": 0.0,
      "CD0_L": 0.0,
      "CD0_L2": 0.0,
      "CL_max": 1.4,
      "Comments": "All angles in radians and slopes in 1/radians"
    }
  }
}

```

### E.3 Example Profile File for a NACA 2412 Airfoil

```

50
1.0000000000000000E+00 -7.1367152187917782E-09
9.9585604667663574E-01 -3.1594577012583613E-04
9.8349648714065552E-01 -1.2519687879830599E-03
9.6313685178756714E-01 -2.7746756095439196E-03
9.3513005971908569E-01 -4.8345020040869713E-03
8.9995884895324707E-01 -7.3724603280425072E-03
8.5822510719299316E-01 -1.0325845330953598E-02
8.1063729524612427E-01 -1.3630562461912632E-02
7.5799691677093506E-01 -1.7218593508005142E-02
7.0118451118469238E-01 -2.1010775119066238E-02
6.4114278554916382E-01 -2.4906730279326439E-02
5.7886141538619995E-01 -2.8774760663509369E-02
5.1535928249359131E-01 -3.2445460557937622E-02
4.5166760683059692E-01 -3.5712052136659622E-02
3.8890376687049866E-01 -3.8347791880369186E-02
3.2840368151664734E-01 -4.0438853204250336E-02
2.7069056034088135E-01 -4.1869580745697021E-02
2.1664057672023773E-01 -4.2349778115749359E-02
1.6707630455493927E-01 -4.1626252233982086E-02
1.2276169657707214E-01 -3.9503570646047592E-02
8.4396116435527802E-02 -3.5854429006576538E-02
5.2605386823415756E-02 -3.0618341639637947E-02
2.7930552139878273E-02 -2.3790119215846062E-02
1.0814117267727852E-02 -1.5401563607156277E-02
1.5862619038671255E-03 -5.5013755336403847E-03
4.6834559179842472E-04 5.7065724395215511E-03
7.6267276890575886E-03 1.7224393784999847E-02
2.3013709113001823E-02 2.8722338378429413E-02
4.6425748616456985E-02 3.9908505976200104E-02
7.7515803277492523E-02 5.0407152622938156E-02
1.1579234898090363E-01 5.9802222996950150E-02
1.6062285006046295E-01 6.7684493958950043E-02
2.1124278008937836E-01 7.3695354163646698E-02
2.6677113771438599E-01 7.7561683952808380E-02
3.2623127102851868E-01 7.9118162393569946E-02
3.8857534527778625E-01 7.8316092491149902E-02
4.5230948925018311E-01 7.5411744415760040E-02
5.1669228076934814E-01 7.0949688553810120E-02
5.8073848485946655E-01 6.5182760357856750E-02
6.4338487386703491E-01 5.8385424315929413E-02
7.0359897613525391E-01 5.0850689411163330E-02
7.6039564609527588E-01 4.2882818728685379E-02
8.1285268068313599E-01 3.4793458878993988E-02
8.6012434959411621E-01 2.6899019256234169E-02
9.0145480632781982E-01 1.9516089931130409E-02
9.3618875741958618E-01 1.2953279539942741E-02
9.6377998590469360E-01 7.4985213577747345E-03
9.8379832506179810E-01 3.4026026260107756E-03
9.9593400955200195E-01 8.6140306666493416E-04
1.0000000000000000E+00 7.1367152187917782E-09

```

## F OPTIX SOURCE CODE

```

1  import json
2  from myjson import myjson
3  from collections import OrderedDict, Iterable
4  import numpy as np
5  import os
6  import shutil
7  import time
8
9  import multiprocessing
10
11 np.set_printoptions(precision = 14)
12
13 zero = 1.0e-20
14
15
16 class objective_model(object):
17     """Defines the evaluation model of an objective function
18
19     This class defines a model consisting of an objective function that can be
20     evaluated individually and with gradients. The class allows this function
21     to be executed at multiple design points, either synchronously or
22     asynchronously (using the Python multiprocessing module).
23
24     Two methods for evaluating the function are used. The first method is
25     required and evaluates only the function itself, while the second method
26     is optional and evaluates the function and its gradient with respect to the
27     design variables. If the second function is not provided, a second-order
28     central differencing scheme is used to approximate gradients when needed.
29     """
30     def __init__(self,
31                 objective_fcn,
32                 objective_fcn_with_gradient = None,
33                 max_processes = 1,
34                 dx = 0.01
35                 ):
36         """Constructor
37
38         Constructor for the objective_model class
39
40         Inputs
41         -----
42         objective_fcn:
43             The function to evaluate through this model. The function should
44             accept two arguments. The first argument is a list of design
45             variable values specifying a fixed design point. The second
46             argument is the case number assigned to the evaluation. The
47             function should return a single result that is the value of the
48             objective function at the specified design point.
49         objective_fcn_with_gradient:
50             The function to evaluate through this model when gradients are
51             requested. The function should accept the same two arguments as
52             objective_fcn. The function should return two results: the value
53             of the objective function at the specified design point and the
54             gradient of the objective function at the specified design point.
55             Note that the first return value should be equal to the
56             objective_fcn return value for a given design point.
57
58             If objective_fcn_with_gradient is not specified (default), a
59             second-order central difference approximation will be used with

```



```

60         objective_fcn when gradients are needed.
61
62     max_processes:
63         The maximum number of simultaneous processes to use. If set to 1
64         (default), all function evaluations will be executed sequentially.
65         Otherwise, the Python multiprocessing module will be used to
66         execute multiple function evaluations simultaneously.
67
68     dx:
69         The perturbation size to use if the second-order central difference
70         approximation is used to estimate the gradient of the function. If
71         objective_fcn_with_gradient is specified, dx is not used.
72     """
73     # Set the objective function
74     self.obj_fcn = objective_fcn
75
76     # Set the gradient function
77     if objective_fcn_with_gradient is not None:
78         # Use the user-specified function to calculate gradients
79         self.obj_fcn_with_gradient = objective_fcn_with_gradient
80     else:
81         # Use central differencing scheme to approximate the gradient
82         self.obj_fcn_with_gradient = self.central_difference
83         self.dx = dx
84
85     # Set the maximum number of simultaneous processes
86     self.max_processes = max_processes
87
88     # Initialize the number of function/gradient evaluations
89     self.n_fcn_evals = 0
90     self.n_grad_evals = 0
91
92
93     def evaluate(self, design_points):
94         """Evaluate the function at multiple design points
95
96         This routine evaluates the objective function at multiple design
97         points, each specified by a list of design variables.
98
99         Inputs
100         -----
101         design_points = A list of design points. A design point is defined by
102                        a list of design variables that are passed into the
103                        objective function for a single evaluation. Therefore,
104                        design_points is a list of lists.
105
106         Outputs
107         -----
108         objective = A list of results from the objective function,
109                    corresponding to the value of the objective function at
110                    each design point specified.
111
112         """
113         objective = []
114         if self.max_processes > 1:
115             # Execute function at multiple design points in parallel
116             with multiprocessing.Pool(processes = self.max_processes) as pool:
117                 args = [(design_points[i], i + 1)
118                         for i in range(len(design_points))]
119                 objective = pool.map(self.obj_fcn, args)
120         else:

```

```

121         # Execute function at each design point sequentially
122         for i in range(len(design_points)):
123             objective.append(self.obj_fcn((design_points[i], i + 1)))
124
125     # Increment the number of function evaluations
126     self.n_fcn_evals += len(design_points)
127
128     return objective
129
130
131     def evaluate_gradient(self, design_point):
132         """Evaluate the function and its gradient at a specified design point
133
134         This routine evaluates the objective function and its gradient at a
135         single design point.
136
137         Inputs
138         -----
139         design_point = The design point at which to evaluate the function and
140                       its gradient. The design point is defined as a list of
141                       values, one value for each design variable required by
142                       the objective function.
143
144         Outputs
145         -----
146         objective = The value of the objective function at the specified design
147                   point.
148
149         gradient = The gradient of the objective function at the specified
150                   design point.
151         """
152         objective, gradient = self.obj_fcn_with_gradient((design_point, 0))
153         self.n_fcn_evals += 1
154         self.n_grad_evals += 1
155
156         return objective, gradient
157
158
159     def central_difference(self, args):
160         """Approximate the gradient of a function using central differencing
161
162         This routine approximates the gradient of a specified function with
163         respect to all design variables at a specified design point. The
164         gradient is approximated using second-order central differencing.
165
166         Inputs
167         -----
168         design_point = A list of design variables defining the design point at
169                       which the objective function and its gradient will be
170                       evaluated
171
172         case_id = The case ID to use for the objective function evaluation. The
173                  case IDs for gradient evaluations will be incremented
174                  sequentially starting from (case_id + 1).
175         """
176         design_point = args[0]
177         case_id = args[1]
178         # Initialize a list of objective function arguments by perturbing each
179         # variable by +/-dx
180         n_design_vars = len(design_point)
181         arglist = [(design_point[:, i], i) for i in range(case_id,

```

```

182         case_id + 2 * n_design_vars + 1)]
183     for i in range(1, n_design_vars + 1):
184         argslist[i][0][i - 1] += self.dx
185         argslist[i + n_design_vars][0][i - 1] -= self.dx
186
187     if self.max_processes > 1:
188         # Execute function at multiple design points in parallel
189         with multiprocessing.Pool(processes = self.max_processes) as pool:
190             results = pool.map(self.obj_fcn, argslist)
191     else:
192         # Execute function at each design point sequentially
193         results = []
194         for a in argslist:
195             results.append(self.obj_fcn(a))
196
197     # Get the objective function value at the specified design point
198     objective = results[0]
199
200     # Calculate the gradient of the objective function from results
201     # at the perturbed design points
202     gradient = []
203     for i in range(1, n_design_vars + 1):
204         gradient.append((results[i] - results[i + n_design_vars]) /
205                         (2.0 * self.dx))
206
207     return objective, gradient
208
209
210 class settings(object):
211     """Defines the various settings used by the optimization algorithm
212     """
213     def __init__(self):
214         self.opt_file = 'optimization.txt'
215         self.grad_file = 'gradient.txt'
216         self.verbose = False
217
218         self.nvars = 0
219         self.varnames = []
220         self.varsinit = []
221         self.opton = []
222
223         self.default_alpha = 0.0
224         self.stop_delta = 1.0E-12
225         self.nsearch = 8
226         self.line_search_type = 'quadratic'
227         self.alpha_tol = 0.1
228         self.max_refinements = 100
229         self.rsq_tol = 0.99
230         self.max_alpha_factor = 100
231
232         self.wolfe_armijo = 1.0e-4
233         self.wolfe_curv = 0.9
234
235         self.nconstraints = 0
236         self.constrainttype = []
237         self.constraintnames = []
238         self.constraintvalues = []
239         self.penalty = []
240         self.penalty_factor = []
241
242

```

```

243     def load(settings_file):
244         self = settings()
245         input = myjson(settings_file)
246
247         # Read settings from JSON file
248         json_settings = input.get('settings', OrderedDict)
249         self.default_alpha = json_settings.get('default_alpha', float)
250         self.stop_delta = json_settings.get('stop_delta', float)
251         self.nsearch = json_settings.get('n_search', int)
252         self.line_search_type = json_settings.get('line_search_type', str,
253           'quadratic')
254         self.verbose = json_settings.get('verbose', bool, False) # optional
255
256         self.alpha_tol = json_settings.get('alpha_tol', float, self.alpha_tol)
257         self.max_refinements = json_settings.get('max_refinements', int,
258           self.max_refinements)
259         self.rsq_tol = json_settings.get('rsq_tol', float, self.rsq_tol)
260         self.max_alpha_factor = json_settings.get('max_alpha_factor', int,
261           self.max_alpha_factor)
262
263         self.wolfe_armijo = json_settings.get('wolfe_armijo', float,
264           self.wolfe_armijo)
265         self.wolfe_curv = json_settings.get('wolfe_curvature', float,
266           self.wolfe_curv)
267
268         # Read variables
269         json_variables = input.get('variables', OrderedDict, OrderedDict())
270         self.nvars = 0
271         self.varnames = []
272         self.varsinit = []
273         self.opton = []
274         for var_name in json_variables.data:
275             self.add_variable(var_name,
276                 json_variables.get(var_name + '.init', float),
277                 json_variables.get(var_name + '.opt', str) == 'on')
278
279         # Read constraints
280         json_constraints = input.get('constraints', OrderedDict, OrderedDict())
281         self.nconstraints = len(json_constraints.data)
282         self.nconstraints = 0
283         self.constrainttype = []
284         self.constraintnames = []
285         self.constraintvalues = []
286         self.penalty = []
287         self.penalty_factor = []
288         valid_constraint_types = ['=', '<', '>']
289         for const_name in json_constraints.data:
290             json_constraint_data = json_constraints.get(const_name,
291                 OrderedDict)
292             const_type = json_constraint_data.get('type', str)
293             if const_type not in valid_constraint_types:
294                 print('Unknown constraint type: {0}. Constraint {1} skipped.'
295                     .format(const_type, const_name))
296                 print('Valid constraint types are {0}.'
297                     .format(valid_constraint_types))
298                 continue
299
300             self.constrainttype.append(const_type)
301             self.constraintnames.append(const_name)
302             self.constraintvalues.append(
303                 json_constraint_data.get('value', float))

```

```

304         self.penalty.append(
305             json_constraint_data.get('penalty', float))
306         self.penalty_factor.append(
307             json_constraint_data.get('factor', float))
308
309     return self
310
311
312     def write(self, settings_file):
313         data = OrderedDict()
314         data['settings'] = OrderedDict()
315         data['settings']['default_alpha'] = self.default_alpha
316         data['settings']['stop_delta'] = self.stop_delta
317         data['settings']['n_search'] = self.nsearch
318         data['settings']['line_search_type'] = self.line_search_type
319         data['settings']['verbose'] = self.verbose
320
321         data['settings']['alpha_tol'] = self.alpha_tol
322         data['settings']['max_refinements'] = self.max_refinements
323         data['settings']['rsq_tol'] = self.rsq_tol
324         data['settings']['max_alpha_factor'] = self.max_alpha_factor
325
326         data['settings']['wolfe_armijo'] = self.wolfe_armijo
327         data['settings']['wolfe_curvature'] = self.wolfe_curv
328
329         data['variables'] = OrderedDict()
330         for i in range(self.nvars):
331             data['variables'][self.varnames[i]] = OrderedDict()
332             data['variables'][self.varnames[i]]['init'] = self.varsinit[i]
333             data['variables'][self.varnames[i]]['opt'] = self.opton[i]
334
335         with open(settings_file, 'w') as settings:
336             json.dump(data, settings, indent = 4)
337
338
339     def add_variable(self, varname, varinit, opton = True):
340         if varname in self.varnames:
341             i = self.varnames.index(varname)
342             self.varsinit[i] = varinit
343             self.opton[i] = opton
344         else:
345             self.varnames.append(varname)
346             self.varsinit.append(varinit)
347             self.opton.append(opton)
348             self.nvars += 1
349
350
351     def optimize(obj_model, settings):
352         """
353         """
354         header = ('{0:>4}, {1:>5}, {2:>5}, {3:>20}, {4:>20}, {5:>20}'
355             .format('iter', 'outer', 'inner', 'fitness', 'alpha', 'mag(dx)'))
356         for name in settings.varnames: header += ', {0:>20}'.format(name)
357         with open(settings.opt_file, 'w') as opt_file:
358             opt_file.write(header + '\n')
359
360         with open(settings.grad_file, 'w') as grad_file:
361             grad_file.write(header + '\n')
362
363         print('----- Variables -----')
364         for i in range(settings.nvars):

```

```

365         print('{0} = {1}'.format(settings.varnames[i], settings.varsinit[i]))
366     print('')
367
368     print('----- Constraints -----')
369     for i in range(settings.nconstraints):
370         print('{0}, {1}, {2}'.format(settings.constraintnames[i],
371                                     settings.constrainttype[i], settings.constraintvalues[i]))
372     print('')
373
374     print('----- Settings -----')
375     print('         default alpha: {0}'.format(settings.default_alpha))
376     print('         stopping delta: {0}'.format(settings.stop_delta))
377     print('')
378
379     iter = 0
380     o_iter = 0
381     mag_dx = 1.0
382     design_point = settings.varsinit[:]
383     while mag_dx > settings.stop_delta:
384         design_point_init = np.copy(design_point)
385         i_iter = 0
386
387         print('Constraint Penalties')
388         for i in range(settings.nconstraints):
389             print('{0} {1}'.format(settings.constraintnames[i],
390                                   settings.penalty[i]))
391
392         print('Beginning new update matrix')
393         print(header)
394
395         alpha = 0.0
396         while mag_dx > settings.stop_delta:
397             obj_value, gradient = obj_model.evaluate_gradient(design_point)
398             append_file(iter, o_iter, i_iter, obj_value, alpha, mag_dx,
399                       design_point, gradient, settings)
400
401             # Initialize N to the identity matrix
402             if (i_iter == 0):
403                 N = np.eye(settings.nvars) # n x n
404
405             else:
406                 dx = np.matrix(design_point - design_point_prev) # 1 x n
407                 gamma = np.matrix(gradient - gradient_prev) # 1 x n
408                 NG = N * np.transpose(gamma) # n x 1
409                 denom = dx * np.transpose(gamma) # 1 x 1
410                 N += ((1.0 + np.dot(gamma, NG) / denom)[0,0] *
411                      (np.transpose(dx) * dx) / denom
412                     - ((np.transpose(dx) * (gamma * N)) + (NG * dx)) / denom
413                     )
414
415             # Calculate the second Wolfe condition for the previous
416             # iteration. The curvature condition ensures that the slope is
417             # sufficiently large to contribute to a reduction in the
418             # objective function. If this condition is not met, the inner
419             # loop is stopped and the direction matrix is reset to the
420             # direction of steepest descent.
421             if np.dot(s, gradient) < settings.wolfe_curv *
422                np.dot(s, gradient_prev):
423                 print("Wolfe condition (ii): curvature condition " +
424                       "not satisfied!")
425                 break

```

```

426
427     s = -np.dot(N, gradient)
428     design_point_prev = np.copy(design_point)
429     gradient_prev = np.copy(gradient)
430
431     alpha, design_point = line_search(design_point[:,], obj_value,
432                                     gradient, s, obj_model, settings)
433
434     dx = design_point - design_point_prev
435     mag_dx = np.linalg.norm(dx)
436     i_iter += 1
437     iter += 1
438
439     dx = design_point - design_point_init
440     mag_dx = np.linalg.norm(dx)
441     append_file(iter, o_iter, i_iter, obj_value, alpha, mag_dx,
442               design_point, gradient, settings)
443
444     o_iter += 1
445     for i in range(settings.nconstraints):
446         settings.penalty[i] = (settings.penalty[i] *
447                               settings.penalty_factor[i])
448
449     # Run the final case
450     obj_value = obj_model.obj_fcn((design_point, -1))
451     append_file(iter, o_iter, i_iter, obj_value, 0.0, mag_dx, design_point,
452               gradient, settings)
453     return (obj_value, design_point)
454
455
456 def line_search(design_point, obj_value, gradient, s, obj_model, settings):
457     if settings.line_search_type == 'quadratic':
458         return line_search_quad(design_point, obj_value, gradient, s,
459                                obj_model, settings)
460     else:
461         return line_search_lin(design_point, obj_value, s, obj_model, settings)
462
463
464 def line_search_lin(design_point, obj_value, s, obj_model, settings):
465     if settings.verbose:
466         print('line search -----')
467
468     s_norm = np.linalg.norm(s)
469     alpha = max(settings.default_alpha, 1.1 * settings.stop_delta / s_norm)
470     alpha_mult = settings.nsearch / 2.0
471
472     found_min = False
473     while not found_min:
474         xval, yval = run_mult_cases(settings.nsearch, alpha, s, design_point,
475                                   obj_value, obj_model)
476         if settings.verbose:
477             for i in range(settings.nsearch + 1):
478                 print('{0:5d}, {1:15.7E}, {2:15.7E}'
479                       .format(i, xval[i], yval[i]))
480
481         mincoord = yval.index(min(yval))
482         if yval[1] > yval[0]:
483             if (alpha * s_norm) < settings.stop_delta:
484                 print('Line search within stopping tolerance: alpha = {0}'
485                       .format(alpha))
486                 return alpha, design_point

```

```

487         elif mincoord == 0:
488             if settings.verbose: print('Too big of a step. Reducing alpha')
489             alpha /= alpha_mult
490         else:
491             if mincoord < settings.nsearch: found_min = True
492             else: alpha *= alpha_mult
493     else:
494         if settings.verbose: print('mincoord = {0}'.format(mincoord))
495         if mincoord == 0: return alpha, design_point
496         elif mincoord < settings.nsearch: found_min = True
497         else: alpha *= alpha_mult
498
499     a1 = xval[mincoord - 1]
500     a2 = xval[mincoord]
501     a3 = xval[mincoord + 1]
502     f1 = yval[mincoord - 1]
503     f2 = yval[mincoord]
504     f3 = yval[mincoord + 1]
505
506     da = a2 - a1
507     alpha = a1 + da * (4.0 * f2 - f3 - 3.0 * f1) / (2.0 * (2.0 * f2 - f3 - f1))
508     if alpha > a3 or alpha < a1:
509         if f2 > f1: alpha = a1
510         else: alpha = a2
511
512     for i in range(len(design_point)):
513         design_point[i] += alpha * s[i]
514
515     if settings.verbose: print('Final alpha = {0}'.format(alpha))
516     return alpha, design_point
517
518
519 def line_search_quad(design_point, obj_value, gradient, s, obj_model, settings):
520     """Perform a quadratic line search to minimize the objective function
521
522     This subroutine evaluates the objective function multiple times in the
523     direction of s and fits a parabola to the results using a least-squares
524     algorithm to identify the minimum value for the objective function in
525     the current direction.
526
527     Inputs
528     -----
529     design_point = A list of design variables defining the design point at
530                   which to begin the line search
531
532     obj_value = The value of the objective function at the specified design
533                point.
534     gradient = The gradient of the objective function at the specified design
535               point.
536
537     s = The direction matrix defining the direction in which to conduct the
538         line search.
539
540     obj_model = The objective model object
541
542     settings = The optimization settings object
543     Outputs
544     -----
545     alpha_min = The alpha corresponding to the minimum value of the objective
546                function in the current direction
547

```



```

548 design_point = The design point corresponding to the minimum value of the
549                 objective function in the current direction
550 """
551 if settings.verbose:
552     print('Performing quadratic line search...')
553
554 # Determine the initial step size to use in the direction of s
555 stop_delta = settings.stop_delta / np.linalg.norm(s)
556 alpha = max(settings.default_alpha, 1.1 * stop_delta)
557
558 found_min = False
559 line_search_min = (0.0, obj_value)
560 alpha_history = []
561
562 # Determine the maximum number of adjustments in alpha to attempt.
563 nadjust = int(np.ceil(-np.log10(stop_delta) /
564                   np.log10(np.ceil(settings.nsearch / 2))))
565
566 for i in range(nadjust):
567     # Compute the objective function multiple times in the direction of s
568     alphas, obj_vals = run_mult_cases(settings.nsearch, alpha, s,
569                                       design_point, obj_value, obj_model)
570     alpha_history.append(alpha)
571
572     # Save the minimum data point for later comparisons
573     ind = obj_vals.index(min(obj_vals))
574     if obj_vals[ind] < line_search_min[1]:
575         line_search_min = (alphas[ind], obj_vals[ind])
576     alpha_min_est = line_search_min[0]
577
578     if settings.verbose:
579         for j in range(settings.nsearch + 1):
580             print('{:5d}, {:23.15E}, {:23.15E}'.format(
581                 j, alphas[j], obj_vals[j]))
582
583     # Check for invalid results
584     if np.isnan(obj_vals).any():
585         print('Found NaN')
586         break
587
588     # Check for plateau
589     if min(obj_vals) == max(obj_vals):
590         print('Objective function has plateaued')
591         break
592
593     # Check stopping criteria
594     if alpha <= stop_delta and ind < settings.nsearch - 1:
595         print('stopping criteria met')
596         break
597
598     # Fit a quadratic through the data and find the resulting minimum
599     q = quadratic(np.asarray(alphas), np.asarray(obj_vals))
600     (alpha_min_est, obj_value_est) = q.vertex()
601
602     if (alpha_min_est is None or alpha_min_est < 0 or not q.convex() or
603         q.rsq < settings.rsq_tol):
604         # Can't find a better minimum by curve fitting all data points.
605         # Try a quadratic through minimum and two closest neighbors.
606         left = min(max(ind - 1, 0), len(alphas) - 3)
607         right = left + 3
608         q = quadratic(np.asarray(alphas[left:right]),

```

```

609         np.asarray(obj_vals[left:right]))
610         (alpha_min_est, obj_value_est) = q.vertex()
611
612         if (alpha_min_est is None or alpha_min_est < 0 or not q.convex()):
613             if ind == settings.nsearch:
614                 # If minimum is at the end, try increasing alpha
615                 alpha_min_est = alpha * 4
616             elif ind == 0:
617                 # If minimum is at beginning, try reducing alpha
618                 alpha_min_est = alpha / 2
619             else:
620                 # Can't find a better minimum by curve fitting,
621                 # so just use the current minimum.
622                 break
623
624         # Set alpha for next iteration
625         alpha = max(alpha / settings.max_alpha_factor,
626                     min(alpha * settings.max_alpha_factor,
627                         alpha_min_est / np.ceil(settings.nsearch / 2.0)))
628         print('alpha for next iteration = ', alpha)
629
630         # Check to see if we've already tried close to this alpha
631         alpha_close = min(alpha_history, key=lambda a: abs(a - alpha) / alpha)
632         delta = abs(alpha_close - alpha) / alpha
633         if delta <= settings.alpha_tol:
634             break
635
636         # Update design point based on alpha that minimized objective function
637         alpha_min = line_search_min[0]
638         design_point[:] += alpha_min * s[:]
639
640         # Calculate the first Wolfe condition. This is a measure of how much the
641         # step length (alpha) decreases the objective function, but has no effect
642         # on the behavior of the quadratic line search.
643         armijo = obj_value + settings.wolfe_armijo * alpha_min * np.dot(s, gradient)
644         if line_search_min[1] > armijo:
645             print("Wolfe condition (i): Armijo rule not satisfied.")
646
647         if settings.verbose: print('Line search minimized at alpha = {0}'
648                                   .format(alpha_min))
649         return alpha_min, design_point
650
651
652 def run_mult_cases(nevals, alpha, s, dp0, obj_fcn0, obj_model):
653     # Calculate linearly distributed alphas for the line search
654     alphas = [(i * alpha) for i in range(nevals + 1)]
655
656     # Set up the design points in the direction of the line search
657     design_points = []
658     for i in range(nevals):
659         design_points.append([(dp0[j] + alphas[i + 1] * s[j])
660                               for j in range(len(dp0))])
661
662     # Evaluate the function at each design point
663     obj_fcn_values = [obj_fcn0] + obj_model.evaluate(design_points)
664
665     return alphas, obj_fcn_values
666
667
668 def append_file(iter, o_iter, i_iter, obj_fcn_value, alpha, mag_dx,
669                design_point, gradient, settings):

```

```

670 msg = ('{0:4d}, {1:5d}, {2:5d}, {3: 20.13E}, {4: 20.13E}, {5: 20.13E}'
671         .format(iter, o_iter, i_iter, obj_fcn_value, alpha, mag_dx))
672 values_msg = msg
673 for value in design_point:
674     values_msg = ('{0}, {1: 20.13E}'.format(values_msg, value))
675 print(values_msg)
676 with open(settings.opt_file, 'a') as opt_file:
677     print(values_msg, file = opt_file)
678
679 grad_msg = msg
680 for grad in gradient:
681     grad_msg = ('{0}, {1: 20.13E}'.format(grad_msg, grad))
682 with open(settings.grad_file, 'a') as grad_file:
683     print(grad_msg, file = grad_file)
684
685
686 class quadratic(object):
687     """Class for fitting, evaluating, and interrogating quadratic functions
688     This class is used for fitting a quadratic function to a data set
689     evaluating the function at specific points, and determining the
690     characteristics of the function.
691     """
692     def __init__(self, x, y):
693         """
694         Construct a quadratic object from tabulated data.
695         Quadratic is of the form  $f(x) = ax^2 + bx + c$ 
696         Inputs
697         -----
698         x = List of independent values
699         y = List of dependent values
700         """
701         super().__init__()
702
703         # Calculate the quadratic coefficients
704         x_sq = [xx**2 for xx in x]
705         A = np.vstack([x_sq, x, np.ones(len(x))]).T
706         self.a, self.b, self.c = np.linalg.lstsq(A, y)[0]
707
708         # Calculate the coefficient of determination
709         f = [self.f(xx) for xx in x]
710         ssres = ((f - y)**2).sum()
711         sstot = ((y - y.mean())**2).sum()
712
713         if abs(sstot) < zero:
714             # Data points actually formed a horizontal line
715             self.rsq = 0.0
716         else:
717             self.rsq = 1 - ssres / sstot
718
719
720     def convex(self):
721         """
722         Test to see if the quadratic is convex (opens up).
723         """
724         # Convex has positive curvature (2nd derivative)
725         #  $f''(x) = 2a$ , so  $a > 0$  corresponds to convex
726         return (self.a > 0)
727
728
729     def vertex(self):
730         """

```

```

731     Find the coordinates of the vertex
732     """
733     if self.a != 0.0:
734         # Find x where f'(x) = 2ax + b = 0
735         x = -0.5 * self.b / self.a
736         return (x, self.f(x))
737     else:
738         # Quadratic is actually a line, no minimum!
739         return (None, None)
740
741
742     def f(self, x):
743         """
744         Evaluate the quadratic function at x
745         """
746         if x is not None: return self.a * x**2 + self.b * x + self.c
747         else: return None
748
749
750     class myjson:
751         def __init__(self, filename=None, parent=None, data=None, path=None):
752             self.file = ''
753             self.data = OrderedDict()
754             self.path = ''
755
756             if filename is not None: self.load(filename)
757             elif parent is not None:
758                 self.file = parent.file
759                 self.data = data
760                 self.path = parent.path + path
761
762
763         def load(self, filename):
764             if not os.path.isfile(filename):
765                 print('Error: Cannot find file "{0}". Make sure'.format(filename))
766                 print('the path is correct and the file is accessible.')
767                 raise IOError(filename)
768
769             self.file = filename
770             with open(self.file) as file:
771                 self.data = json.load(file, object_pairs_hook = OrderedDict)
772
773
774         def get(self, value_path, value_type, default_value = None):
775             abs_path = self.path + '.' + value_path
776
777             json_data = self.data
778             for path in value_path.split('.'):
779                 try:
780                     json_data = json_data[path]
781                 except KeyError as exc:
782                     if default_value is None:
783                         print('Error: required JSON path not found. Op aborted.')
784                         print('Missing path is "{0}"'.format(abs_path))
785                         raise
786                     else:
787                         json_data = default_value
788
789             if not isinstance(value_type, Iterable): value_type = [value_type]
790             if type(json_data) not in value_type:
791                 print('Error: JSON value is of an incorrect type.')

```

```
792         print('          Expected {0} but found {1}'
793               .format(value_type, type(json_data)))
794         print('          Invalid path is "{0}"'.format(abs_path))
795         raise KeyError(value_path)
796
797     if type(json_data) is OrderedDict:
798         return myjson(parent = self, data = json_data, path = value_path)
799     else:
800         return json_data
801
802
803 def load(filename):
804     return myjson(filename)
```

## G INPUT FILES AND PYTHON SCRIPTS FOR WING SHAPE OPTIMIZATION

The sections below list the Python scripts and main input file required to run the optimization analyses presented in Secs. 3.3 and 3.4. The objective functions (`evaluate` and `evaluate_with_gradient`) and the `get_list_of_vars` helper function are contained in a single Python script file called `obj_fcn.py`. Required MachUp executables, the main input file (`input.json`), and all other supporting input files referenced in the main input file must be contained in a folder called `OrigFiles` that must reside within the current working directory. An airfoil database must also exist within the current working directory that contains all the necessary airfoils referenced by the input files. Note that the files in this database will be different between inviscid and viscous analyses.

### G.1 Main Optimization Execution Script

```

1  import optix
2  import argparse
3  import obj_fcn
4  from timeit import default_timer as timer
5
6  parser = argparse.ArgumentParser()
7  parser.add_argument('-nchord',
8                      help = '-nchord N (Number of chord control points)',
9                      type = int, required = False, default = 0)
10 parser.add_argument('-ntwist',
11                     help = '-ntwist N (Number of twist control points)',
12                     type = int, required = False, default = 0)
13 parser.add_argument('-ncamber',
14                     help = '-ncamber N (Number of camber control points)',
15                     type = int, required = False, default = 0)
16 args = parser.parse_args()
17 nchord = args.nchord
18 ntwist = args.ntwist
19 ncamber = args.ncamber
20
21 # Create a settings object
22 settings = optix.settings()
23 settings.default_alpha = 1.0
24 settings.stop_delta = 1e-10
25 settings.nsearch = 4
26 settings.line_search_type = 'quadratic'
27 settings.verbose = True
28 settings.alpha_tol = 0.1
29 settings.max_refinements = 100
30 settings.rsq_tol = 0.99
31 settings.max_alpha_factor = 100
32 settings.wolfe_armijo = 0.0001
33 settings.wolfe_curvature = 0.9
34
35 # Set up the control point parameters
36 for i in range(nchord):
37     settings.add_variable('chord{}'.format(i), 1.0, True)
38

```

```

39 for i in range(1, ntwist):
40     settings.add_variable('twist{}'.format(i), 0.0, True)
41
42 for i in range(ncamber):
43     settings.add_variable('camber{}'.format(i), 1.0, True)
44
45 settings.write('settings.json')
46
47 # Number of design variables
48 ndv = nchord + ntwist + ncamber + 1 # Add 1 for angle of attack
49 if nchord > 0: ndv += 2 # Add 1 for area and 1 for longitudinal length
50 if ntwist > 0: ndv -= 1 # Subtract 1 for root twist
51
52 # Create the objective model
53 model = optix.objective_model(obj_fcn.evaluate,
54                               obj_fcn.evaluate_with_gradient, max_processes = 4)
55
56 # Begin the optimization
57 start = timer()
58 optix.optimize(model, settings)
59
60 end = timer()
61 print("Optimization time: {0} seconds.".format(end - start))
62 print("Number of function evaluations: {0}".format(model.n_fcn_evals))
63 print("Number of gradient evaluations: {0}".format(model.n_grad_evals))

```

## G.2 Objective Function (obj\_fcn.evaluate)

```

1  import os
2  import shutil
3  import json
4  import numpy as np
5  from collections import OrderedDict
6
7  def evaluate(args):
8
9      # Get the list of variables
10     with open('settings.json', 'r') as settings_file:
11         settings_data = json.load(settings_file,
12                                   object_pairs_hook = OrderedDict)
13
14     chord = get_list_of_vars(settings_data, 'chord', 0.01, 3.0, args[0])
15     twist = get_list_of_vars(settings_data, 'twist', -90.0, 90.0, args[0])
16     camber = get_list_of_vars(settings_data, 'camber', 0.0, 5.0, args[0])
17
18     case_id = args[1]
19
20     # Get the current working directory
21     work_dir = os.getcwd()
22
23     # Get the current working directory and case directory names
24     orig_dir = work_dir + '/' + 'OrigFiles'
25     case_dir = work_dir + '/' + str(case_id)
26
27     # Remove existing folder with same case ID
28     if os.path.exists(case_dir): shutil.rmtree(case_dir)
29
30     # Copy original files into case directory
31     shutil.copytree(orig_dir, case_dir)
32

```

```

33     # Make the temporary directory current
34     os.chdir(case_dir)
35
36     # Generate chord input file
37     if len(chord) > 0:
38         # Get the desired area, wingspan, and average chord
39         with open('input.json', 'r') as input_file:
40             input_data = json.load(input_file, object_pairs_hook = OrderedDict)
41             area = input_data['reference']['area']
42             b = input_data['reference']['lateral_length']
43             cavg = area / b
44
45         # Calculate the chord length at the wing tip
46         c_tip = 2.0 * len(chord) * cavg - chord[0] - 2.0 * sum(chord[1:])
47         chord += [c_tip]
48
49         # Write the chord files
50         y_chord = np.linspace(0.0, 1.0, len(chord))
51         design_vars = {}
52         for i in range(len(chord)):
53             row = 'r' + str(i + 1)
54             design_vars[row] = {}
55             design_vars[row]['c1'] = y_chord[i]
56             design_vars[row]['c2'] = chord[i]
57         with open('chord_left.json', 'w') as data_file:
58             json.dump(design_vars, data_file, sort_keys = False, indent = 4)
59         with open('chord_right.json', 'w') as data_file:
60             json.dump(design_vars, data_file, sort_keys = False, indent = 4)
61
62     # Generate twist input file
63     if len(twist) > 0:
64         twist = [0.0] + twist
65         y_twist = np.linspace(0.0, 1.0, len(twist))
66         design_vars = {}
67         for i in range(len(twist)):
68             row = 'r' + str(i + 1)
69             design_vars[row] = {}
70             design_vars[row]['c1'] = y_twist[i]
71             design_vars[row]['c2'] = twist[i]
72         with open('twist_left.json', 'w') as data_file:
73             json.dump(design_vars, data_file, sort_keys = False, indent = 4)
74         with open('twist_right.json', 'w') as data_file:
75             json.dump(design_vars, data_file, sort_keys = False, indent = 4)
76
77     # Generate camber input file
78     if len(camber) > 0:
79         y_camber = np.linspace(0.0, 1.0, len(camber))
80         design_vars = {}
81         for i in range(len(camber)):
82             row = 'r' + str(i + 1)
83             design_vars[row] = {}
84             design_vars[row]['c1'] = y_camber[i]
85             design_vars[row]['c2'] = camber[i]
86         with open('af_ratio_left.json', 'w') as data_file:
87             json.dump(design_vars, data_file, sort_keys = False, indent = 4)
88         with open('af_ratio_right.json', 'w') as data_file:
89             json.dump(design_vars, data_file, sort_keys = False, indent = 4)
90
91     # Execute MachUp with DNAD integration
92     os.system('./MachUp_DNAD1.out input.json > out.txt')
93

```



```

94     # Extract cost function from MachUp results
95     with open('input_forces.json') as forces_file:
96         forces_data = json.load(forces_file)
97
98     # Get the drag and DNAD derivatives
99     cd = forces_data['total']['MyAirplane']['CD'][0]
100
101     # Move to the original work directory
102     os.chdir(work_dir)
103
104     return cd

```

### G.3 Objective Function with Gradient Calculations (obj\_fcn.evaluate\_with\_gradient)

```

1  import os
2  import shutil
3  import json
4  import numpy as np
5  from collections import OrderedDict
6
7  def evaluate_gradient(args):
8      # Get the list of variables
9      with open('settings.json', 'r') as settings_file:
10         settings_data = json.load(settings_file, object_pairs_hook =
OrderedDict)
11
12         chord = get_list_of_vars(settings_data, 'chord', 0.1, 10.0, args[0])
13         twist = get_list_of_vars(settings_data, 'twist', -90.0, 90.0, args[0])
14         camber = get_list_of_vars(settings_data, 'camber', 0.0, 4.0, args[0])
15         ndv = len(chord) + len(twist) + len(camber) + 1 # Add 1 for alpha
16         if len(chord) > 0: ndv += 1 # Add 1 for chord at wingtip
17
18         case_id = args[1]
19
20         # Get the current working directory
21         work_dir = os.getcwd()
22
23         # Get the current working directory and case directory names
24         orig_dir = work_dir + '/' + 'OrigFiles'
25         case_dir = work_dir + '/' + str(case_id)
26
27         # Remove existing folder with same case ID
28         if os.path.exists(case_dir): shutil.rmtree(case_dir)
29
30         # Copy original files into case directory
31         shutil.copytree(orig_dir, case_dir)
32
33         # Make the temporary directory current
34         os.chdir(case_dir)
35
36
37
38         # Generate chord input file
39         if len(chord) > 0:
40             # Get the desired area, wingspan, and average chord
41             with open('input.json', 'r') as input_file:
42                 input_data = json.load(input_file, object_pairs_hook = OrderedDict)
43                 area = input_data['reference']['area']
44                 b = input_data['reference']['lateral_length']
45                 cavg = area / b

```

```

46
47     # Calculate the chord length at the wing tip
48     c_tip = 2.0 * len(chord) * cavg - chord[0] - 2.0 * sum(chord[1:])
49     chord += [c_tip]
50
51     # Write the chord files
52     y_chord = np.linspace(0.0, 1.0, len(chord))
53     design_vars = {}
54     for i in range(len(chord)):
55         row = 'r' + str(i + 1)
56         design_vars[row] = {}
57         design_vars[row]['c1'] = y_chord[i]
58         design_vars[row]['c2'] = [chord[i], 1.0]
59     with open('chord_left.json', 'w') as data_file:
60         json.dump(design_vars, data_file, sort_keys = False, indent = 4)
61     design_vars = {}
62     for i in range(len(chord)):
63         row = 'r' + str(i + 1)
64         design_vars[row] = {}
65         design_vars[row]['c1'] = y_chord[i]
66         design_vars[row]['c2'] = chord[i]
67     with open('chord_right.json', 'w') as data_file:
68         json.dump(design_vars, data_file, sort_keys = False, indent = 4)
69
70     # Generate twist input file
71     if len(twist) > 0:
72         twist = [0.0] + twist
73         y_twist = np.linspace(0.0, 1.0, len(twist))
74         design_vars = {}
75         for i in range(len(twist)):
76             row = 'r' + str(i + 1)
77             design_vars[row] = {}
78             design_vars[row]['c1'] = y_twist[i]
79             design_vars[row]['c2'] = [twist[i], 1.0] if i > 0 else twist[i]
80         with open('twist_left.json', 'w') as data_file:
81             json.dump(design_vars, data_file, sort_keys = False, indent = 4)
82
83         for i in range(len(twist)):
84             row = 'r' + str(i + 1)
85             design_vars[row] = {}
86             design_vars[row]['c1'] = y_twist[i]
87             design_vars[row]['c2'] = twist[i]
88         with open('twist_right.json', 'w') as data_file:
89             json.dump(design_vars, data_file, sort_keys = False, indent = 4)
90
91     # Generate camber input file
92     if len(camber) > 0:
93         y_camber = np.linspace(0.0, 1.0, len(camber))
94         design_vars = {}
95         for i in range(len(camber)):
96             row = 'r' + str(i + 1)
97             design_vars[row] = {}
98             design_vars[row]['c1'] = y_camber[i]
99             design_vars[row]['c2'] = [camber[i], 1.0]
100         with open('af_ratio_left.json', 'w') as data_file:
101             json.dump(design_vars, data_file, sort_keys = False, indent = 4)
102
103         for i in range(len(camber)):
104             row = 'r' + str(i + 1)
105             design_vars[row] = {}
106             design_vars[row]['c1'] = y_camber[i]

```

```

107         design_vars[row]['c2'] = camber[i]
108         with open('af_ratio_right.json', 'w') as data_file:
109             json.dump(design_vars, data_file, sort_keys = False, indent = 4)
110
111     # Execute MachUp with DNAD integration
112     os.system('./MachUp_DNAD{}.out input.json > out.txt'.format(ndv))
113
114     # Extract cost function from MachUp results
115     with open('input_forces.json') as forces_file:
116         forces_data = json.load(forces_file)
117
118     # Get the induced drag and DNAD derivatives
119     cd = forces_data['total']['MyAirplane']['CD'][0]
120
121     # Calculate the gradient
122     grad_left = forces_data['total']['MyAirplane']['CD'][2:]
123     grad = [2 * gl for gl in grad_left]
124     if len(chord) > 0:
125         # Get d(CD)/d(c_tip)
126         dCD_dctip = grad[len(chord) - 1]
127
128         # Remove derivative for wingtip chord from gradient
129         grad = grad[:len(chord) - 1] + grad[len(chord):]
130
131         # Apply the partial derivative factor for the wingtip chord
132         grad[0] += -dCD_dctip
133         for i in range(1, len(chord) - 1):
134             grad[i] += -2.0 * dCD_dctip
135
136     # Move to the original work directory
137     os.chdir(work_dir)
138
139     return cd, grad

```

#### G.4 Helper Function for Extracting Variable Names (get\_list\_of\_vars)

```

1 def get_list_of_vars(settings_data, prefix, minval, maxval, allvalues = None):
2     # Get a mask identifying indices for variables with matching prefix
3     mask = [var.find(prefix) == 0 for var in settings_data['variables']]
4
5     # If allvalues is not specified, get initial values from settings file
6     if allvalues is None:
7         allvalues = [settings_data['variables'][var]['init']
8                     for var in settings_data['variables']]
9
10    # Unpack variables with matching prefix into a list
11    values = [min(max(allvalues[i], minval), maxval)
12             for i in range(len(allvalues)) if mask[i]]
13
14    # Return the resulting list
15    return values

```

#### G.5 Main MachUp Input File

```

{
    "run": {
        "targetcl": {
            "CL": 0.5,

```

```

        "delta": 0.1,
        "relaxation": 1.0,
        "maxiter": 100,
        "convergence": 1.000001E-12,
        "run": 1
    },
    "forces": {"run": 1},
    "distributions": {"run": 0},
    "stl": {"run": 0}
},
"solver": {
    "type": "nonlinear",
    "convergence": 1.000001E-12,
    "relaxation": 0.9
},
"plane": {
    "name": "MyAirplane",
    "CGx": 0,
    "CGy": 0,
    "CGz": 0
},
"reference": {
    "area": 8.0,
    "longitudinal_length": 1.0,
    "lateral_length": 8.0
},
"condition": {
    "alpha": 3.0,
    "beta": 0.0
},
"airfoil_DB": "../AirfoilDatabase",
"wings": {
    "Wing_left": {
        "name": "Wing_1",
        "ID": 1,
        "is_main": 1,
        "side": "left",
        "connect": {
            "ID": 0,
            "location": "tip",
            "dx": 0,
            "dy": 0,
            "dz": 0,
            "yoffset": 0
        },
        "span": 4,
        "sweep": 0.0,
        "dihedral": 0.0,
        "mounting_angle": 0,
        "washout": 0,
        "washout_file": "twist_left.json",
        "root_chord": 1,
        "tip_chord": 1,
        "chord_file": "chord_left.json",
        "airfoils": {
            "NACA_n2412": "",
            "NACA_0012": "",
            "NACA_2412": "",
            "NACA_4412": "",
            "NACA_6412": "",
            "NACA_8412": ""
        }
    }
}

```

```

    },
    "af_ratio_file": "af_ratio_left.json",
    "grid": 100,
    "control": {}
  },
  "Wing_right": {
    "name": "Wing_right",
    "ID": 1,
    "is_main": 1,
    "side": "right",
    "connect": {
      "ID": 0,
      "location": "tip",
      "dx": 0,
      "dy": 0,
      "dz": 0,
      "yoffset": 0
    },
    "span": 4,
    "sweep": 0.0,
    "dihedral": 0.0,
    "mounting_angle": 0,
    "washout": 0,
    "washout_file": "twist_right.json",
    "root_chord": 1,
    "tip_chord": 1,
    "chord_file": "chord_right.json",
    "airfoils": {
      "NACA_n2412": "",
      "NACA_0012": "",
      "NACA_2412": "",
      "NACA_4412": "",
      "NACA_6412": "",
      "NACA_8412": ""
    },
    "af_ratio_file": "af_ratio_right.json",
    "grid": 100,
    "control": {}
  }
}

```

## H AERODYNAMIC CALCULATIONS USING PANAIR

Panair is an open-source Fortran code that implements a high-order panel method for performing potential flow analysis of arbitrary geometries. It was originally developed by Boeing Military Airplane Development under contract to NASA in the latter part of the twentieth century, and has seen wide use in industry and academia since that time. Source code,<sup>\*</sup> documentation,<sup>†,‡,§</sup> and a list of research publications<sup>\*\*</sup> related to Panair can be found online. Because of its established reliability in performing aerodynamic calculations, Panair has been used in the present research to perform baseline calculations against which the accuracy of various formulations of lifting line theory can be measured.

In order to rapidly process finite wing models of different configurations with Panair, several functions were added to the MachUp source code for converting wing geometry data into properly-formatted Panair input files. These functions are listed in Appendix I. For each wing configuration analyzed, a MachUp input file was generated with the planform shape, airfoil geometry, and number of spanwise sections defined. MachUp was then executed to generate a Panair input file for this geometry. The Panair input file was then processed by Panair to calculate pressure distributions over the wing surface. Upon successful execution, Panair produces an output file that defines the predicted pressure coefficient at each node specified in the input file. A suite of Python scripts were used to integrate the pressures calculated by Panair to determine the spanwise section lift distribution and the total lift generated by the wing.

A wing representation in the Panair input file is divided into two panel networks – one representing the upper surface of the wing and another representing the lower surface. For rectangular and tapered wings, where the tip chord is nonzero, a third panel network is needed to define an endcap to close the volume of the wing. This endcap network is automatically added to the Panair input file by MachUp. Since all wings considered in the present work are symmetric about the root plane, a symmetry boundary condition is defined at the root so that only one semispan of the wing is modeled. A representative Panair input file is included in Appendix J. This model represents an elliptic wing with an aspect ratio of  $A = 4$ , an average chord length of

---

<sup>\*</sup> <http://www.pdas.com/panairdownload.html>

<sup>†</sup> <https://ntrs.nasa.gov/archive/nasa/casi.ntrs.nasa.gov/19840020672.pdf>

<sup>‡</sup> <https://ntrs.nasa.gov/archive/nasa/casi.ntrs.nasa.gov/19920013405.pdf>

<sup>§</sup> <https://ntrs.nasa.gov/archive/nasa/casi.ntrs.nasa.gov/19920013622.pdf>

<sup>\*\*</sup> <http://www.pdas.com/panairrefs.html>

$c_{\text{avg}} = 1\text{m}$ , and a symmetric Joukowski airfoil with maximum thickness  $\bar{t}_{\text{max}} = 4\%$ . The wing is operating at a geometric angle of attack of  $\alpha = 1\text{deg}$  in incompressible flow with freestream density  $\rho_{\infty} = 1\text{kg/m}^3$  and velocity  $V_{\infty} = 1\text{m/s}$ . There are 11 chordwise nodes and 21 spanwise nodes each for the upper and lower wing surface networks, defining a combined  $20 \times 20$  mesh of panels for a total of 400 panels in the model. The spanwise lift distribution computed using this input file is shown in Figure H.1.

The physical scale of the model was found to have a noticeable effect on the pressure results, especially near the wing tip and for fine panel meshes. The source of this variation in the results based on physical scale is unknown since the pressure coefficients written to the Panair output file are nondimensional. It is theorized that data written to and read from intermediate solution files on disk during the solution process may be of limited precision so that, when read in, rounding error is introduced into the solution. If true, this rounding error could then be reduced by increasing the physical scale of the model so that more digits of precision are written to disk. This theory has not been tested, however, and a different source of error may be present in the code. In order to alleviate this problem, multiple Panair solutions were evaluated with increasing scales until a reasonably converged solution was achieved. An example of this using a mesh size of  $80 \times 80$  panels for the elliptic wing described previously is shown in Figure H.2. For the wing configurations considered in this work, the results become independent of scale for  $\bar{c} \geq 5\text{m}$ .

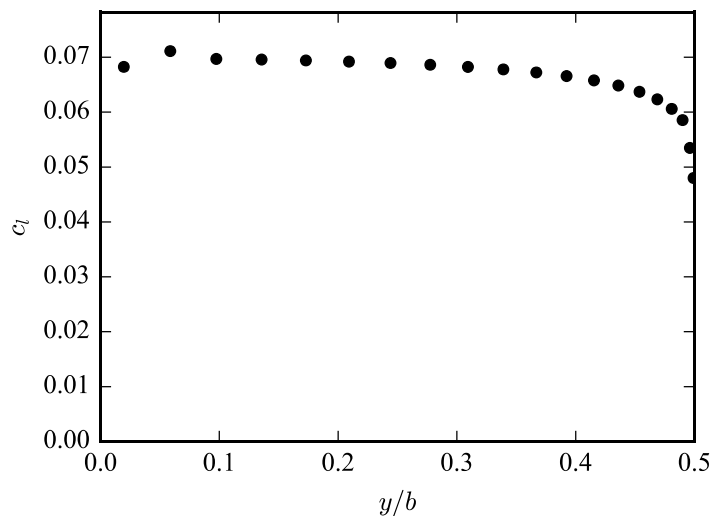


**Figure H.1** Lift distribution with a  $20 \times 20$  mesh for an elliptic wing with  $A = 4$  and  $\bar{t}_{\text{max}} = 4\%$ .

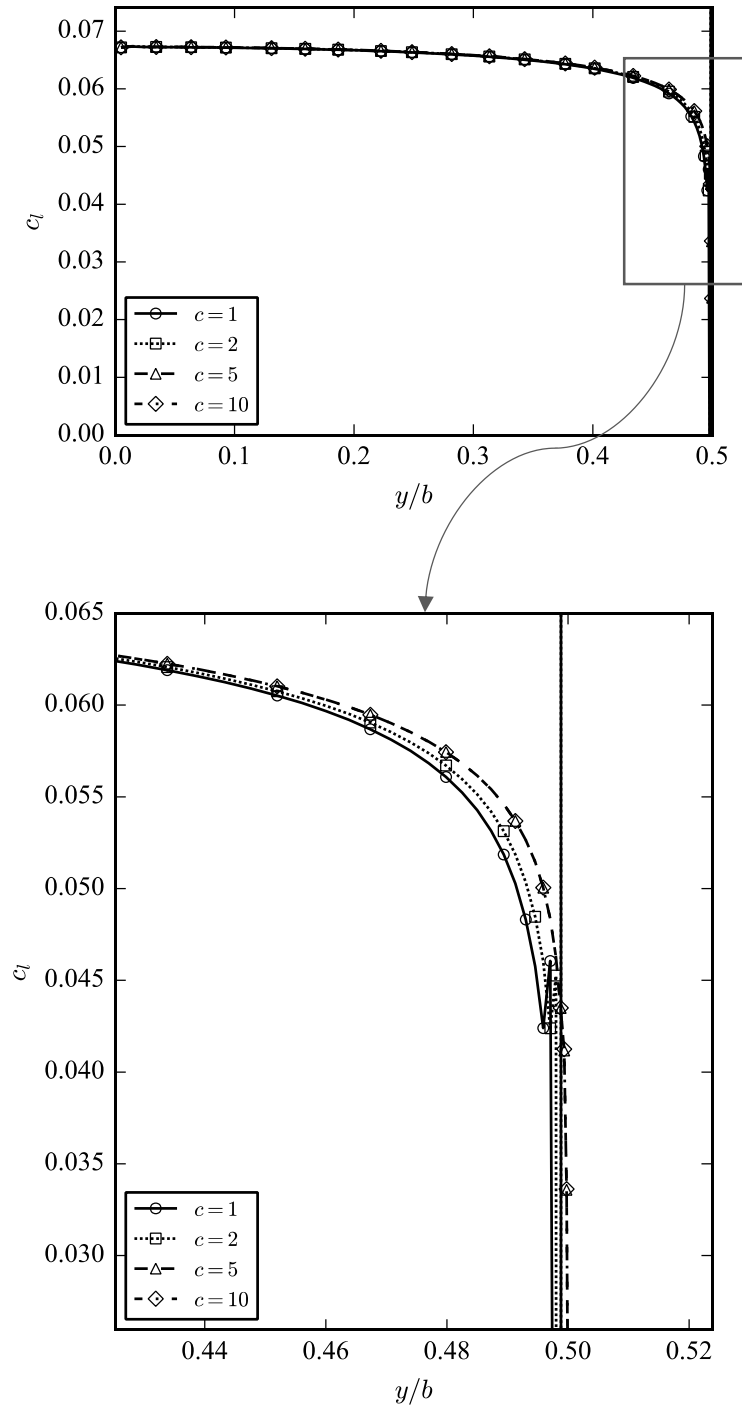


**Figure H.2** Lift distributions as a function of average chord length with an  $80 \times 80$  mesh for an elliptic wing with  $A = 4$  and  $\bar{t}_{\max} = 4\%$ .



The number of panels that can be included in a Panair model is extremely limited, driven by the state of computer hardware available at the time Panair was developed. In order to obtain the most accurate results possible, three models of successively increasing mesh sizes (  $20 \times 20$  ,  $40 \times 40$  , and  $80 \times 80$  ) were used for each wing configuration, and the results were extrapolated using Richardson Extrapolation to estimate a fully-grid-resolved solution. A result set showing the extrapolated data for the same wing configuration as has already been described is given in Figure H.3. The extrapolated results are in good agreement with results from the  $80 \times 80$  mesh.

The lifting line calculations presented in Chapters 4 and 5 represent wings having uniform, thin, symmetric sections with  $a_0 = 2\pi$  . Since the wing geometry provided to Panair must have a non-zero thickness, the thin sections were approximated by solving three result sets of successively decreasing airfoil thicknesses (  $\bar{t}_{\max} = 16\%$  ,  $8\%$  , and  $4\%$  ) and extrapolating the results to a solution for  $\bar{t}_{\max} = 0\%$  using a linear least squares regression algorithm. A result set showing the thickness-extrapolation results for the elliptic wing described above is given in Figure H.4. Since the result sets for each airfoil thickness were themselves extrapolated from three Panair analyses of different grid sizes, a total of nine Panair analyses were needed to produce Figure H.4 and each of the Panair datasets used in the comparisons in Chapters 4 and 5.

Most of the low-aspect-ratio models discussed in Chapter 4 were developed for elliptic wings with straight quarter-chords, while others (namely Hauptman and Miloh [83] and Küchemann [73]) were developed for elliptic wings with straight mid-chords. In the interest of facilitating comparisons between these models, Panair was used to quantify the differences in wing lift coefficients and spanwise lift distributions between these two wing configurations. Figure H.5 shows wing lift coefficients computed using Panair for aspect ratios ranging from 1 to 8. Figure H.6 shows the spanwise lift distributions (scaled by the local chord ratio  $c/\bar{c}$  ) computed using Panair for aspect ratios of 0.5, 2, and 8. From these results we conclude that the differences in lift are negligible between the two configurations, so that comparisons between the different low-aspect-ratio models discussed in Chapter 4 can be made without adjustment to the data.

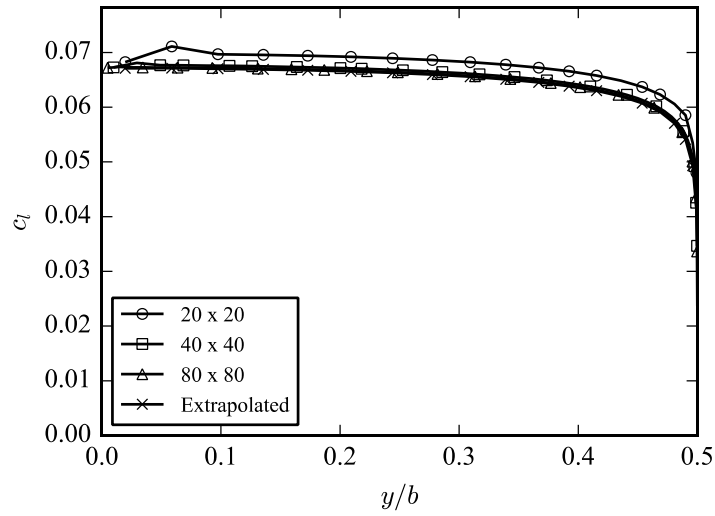


Figure H.3 Mesh refinement and extrapolated results computed for an elliptic wing with  $A = 4$  and

$\bar{t}_{\max} = 4\%$ .

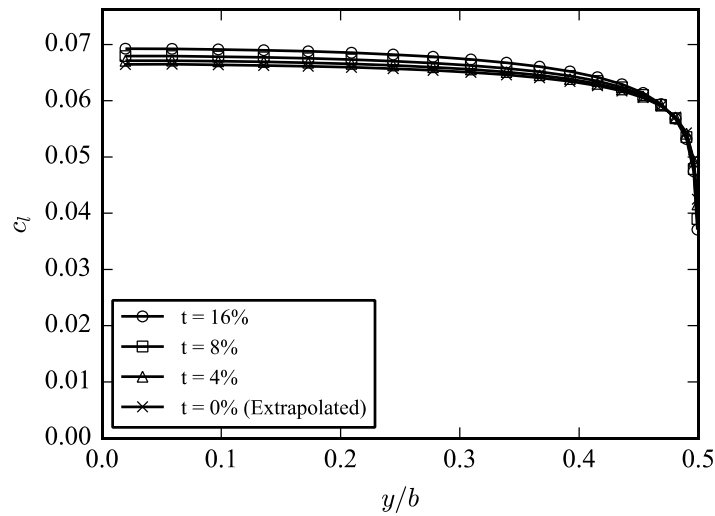
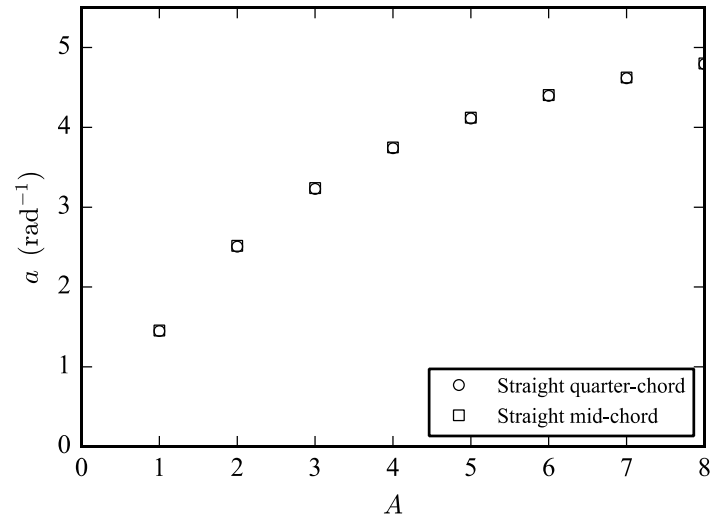
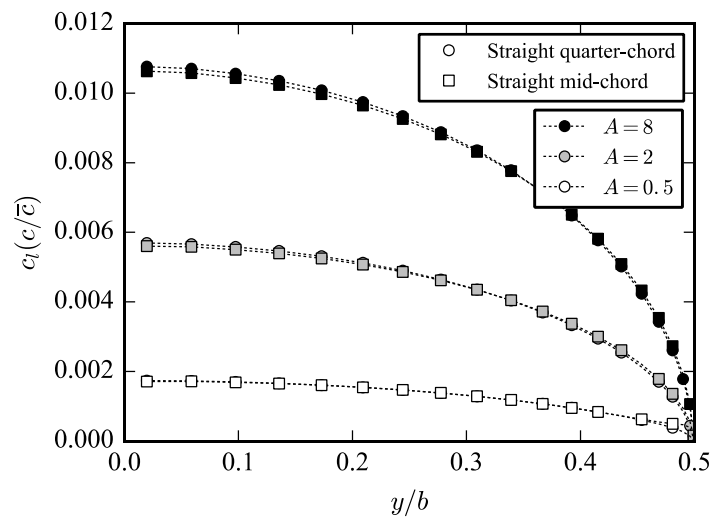


Figure H.4 Lift coefficient results computed for elliptic wings of different airfoil thicknesses with

$A = 4$  and extrapolated results for  $\bar{t}_{\max} = 0\%$ .



**Figure H.5** Comparison of wing lift coefficients for wings with straight quarter-chord and straight mid-chord.



**Figure H.6** Comparison of spanwise lift coefficients for wings with straight quarter-chord and straight mid-chord.

## I MACHUP FUNCTIONS FOR WRITING PANAIR INPUT FILES

```

1  subroutine view_panair(t, json_command)
2      type(plane_t), intent(in) :: t
3      type(json_value), intent(in), pointer :: json_command
4
5      real, allocatable, dimension(:, :) :: af_points
6      character(100) :: filename, upper_network, lower_network, endcap_network
7      integer :: i, iwing, af_datasize, symmetric
8      integer :: ierror = 0
9
10     integer :: endcap_npts
11     real :: endcap_scale
12
13     call myjson_get(json_command, 'endcap_npts', endcap_npts, 0)
14     call myjson_get(json_command, 'endcap_scale', endcap_scale, 1.0)
15
16     do i=1,size(airfoils)
17         call af_create_geom_from_file(airfoils(i),DB_Airfoil)
18     end do
19
20     ! Open the file
21     write(filename, '(A)') trim(adjustl(t%master_filename))//'_view.panair'
22     open(unit = 10, File = trim(adjustl(filename)), action = 'write', iostat =
ierror)
23
24     ! Determine symmetry
25     symmetric = 1
26     do iwing = 1, t%nrealwings
27         if(t%wings(iwing)%orig_side .eq. 'right' .or. t%wings(iwing)%orig_side
.eq. 'left') then
28             symmetric = 0
29         end if
30     end do
31
32     ! Write Header information
33     call view_write_panair_header(t, symmetric)
34
35     do iwing=1,t%nrealwings !real wings
36         ! If symmetric, only write out the right wings
37         if(symmetric .eq. 1 .and. t%wings(iwing)%side .ne. 'right') then
38             cycle
39         end if
40
41         ! Make sure all airfoils have the same number of points
42         af_datasize = t%wings(iwing)%airfoils(1)%p%geom%datasize
43         do i=1, t%wings(iwing)%nairfoils
44             if(t%wings(iwing)%airfoils(i)%p%geom%datasize .ne. af_datasize) then
45                 write(*,*) 'All airfoils for wing ',t%wings(iwing)%name,' must
have same number of nodes.'
46                 stop
47             end if
48         end do
49
50         ! Allocate space for the points on an airfoil
51         if (mod(af_datasize, 2) .eq. 0) af_datasize = af_datasize + 1 ! Must be
odd number of points for Panair!
52         allocate(af_points(af_datasize,3))
53
54         ! Write the network header information
55         call view_write_panair_network_header(t%wings(iwing))

```

```

56
57     ! Write the upper network
58     write(upper_network, '(A, I0)') 'upper_', t%wings(iwing)%ID
59     call view_write_panair_network(t%wings(iwing), af_points,
trim(adjustl(upper_network)), af_datasize, af_datasize / 2 + 1)
60
61     ! Write the lower network
62     write(lower_network, '(A, I0)') 'lower_', t%wings(iwing)%ID
63     call view_write_panair_network(t%wings(iwing), af_points,
trim(adjustl(lower_network)), af_datasize / 2 + 1, 1)
64
65     ! Write the endcap network
66     if(t%wings(iwing)%chord_2 >= 0.0) then
67         write(endcap_network, '(A, I0)') 'endcap_', t%wings(iwing)%ID
68         call view_write_panair_endcap(t%wings(iwing), af_points,
trim(adjustl(endcap_network)), endcap_npts, endcap_scale)
69     end if
70
71     ! Attach a wake to the trailing edge of the upper network
72     call view_write_panair_wake(trim(adjustl(upper_network)))
73     deallocate(af_points)
74 end do
75
76 write(10, "(A)") "$END"
77 close(10)
78
79 end subroutine view_panair
80
81
82 subroutine view_write_panair_header(plane, symmetric)
83     type(plane_t), intent(in) :: plane
84     integer, intent(in) :: symmetric
85
86     write(10, '(A)') '$TITLE'
87     write(10, '(A)') plane%name
88     write(10, '(A)') 'Generated by MachUp'
89     write(10, '(A)') '$DATACHECK'
90     write(10, '(A)') '=ndtchk'
91     write(10, '(A)') '0.0'
92     write(10, '(A)') '$SYMMETRIC'
93     write(10, '(A, T11, A)') '=xzpln', 'xypln'
94     write(10, '(I0, A, T11, A)') symmetric, '.0', '0.0'
95     write(10, '(A)') '$MACH NUMBER'
96     write(10, '(A)') '=amach'
97     write(10, '(F10.6)') 0.0
98     write(10, '(A)') '$CASES'
99     write(10, '(A)') '=nacase'
100    write(10, '(A)') '1.0'
101    write(10, '(A)') '$ANGLES OF ATTACK'
102    write(10, '(A)') '=alpc'
103    write(10, '(F10.6)') 0.0
104    write(10, '(A)') '=alpha(0)'
105    write(10, '(F10.6)') plane%alpha * 180.0 / pi
106    write(10, '(A)') '$YAW ANGLE'
107    write(10, '(A)') '=betc'
108    write(10, '(F10.6)') 0.0
109    write(10, '(A)') '=beta(0)'
110    write(10, '(F10.6)') plane%beta * 180.0 / pi
111    write(10, '(A)') '$REFERENCE DATA'
112    write(10, '(A, T11, A, T21, A)') '=xref', 'yref', 'zref'
113    write(10, '(3F10.6)') 0.0, 0.0, 0.0

```

```

114     write(10, '(A, T11, A, T21, A, T31, A)') '=sref', 'bref', 'cref', 'dref'
115     write(10, '(4F10.6)') plane%Sr, plane%lat_r, plane%long_r, plane%lat_r
116     write(10, '(A)') '$PRINTOUT CONTROL'
117     write(10, '(A, T11, A, T21, A, T31, A, T41, A, T51, A)') '=isings',
'igeomp', 'isingp', 'icontp', 'ibconp', 'iedgep'
118     write(10, '(A, T11, A, T21, A, T31, A, T41, A, T51, A)') '0.0', '0.0',
'0.0', '0.0', '0.0', '0.0'
119     write(10, '(A, T11, A, T21, A, T31, A, T41, A)') '=ipraic', 'nxdgn',
'ioutpr', 'ifmcp', 'icostp'
120     write(10, '(A, T11, A, T21, A, T31, A, T41, A)') '0.0', '0.0', '1.0', '0.0',
'0.0'
121 end subroutine view_write_panair_header
122
123
124 subroutine view_write_panair_network_header(wi)
125     type(wing_t), intent(in) :: wi
126
127     integer :: nnetworks
128
129     if(wi%chord_2 >= 0.0) then
130         nnetworks = 3
131     else
132         nnetworks = 2
133     end if
134
135     ! Write header info
136     write(10, "(A, I0)") "$POINTS for wing ", wi%ID
137     write(10, "(A)") "=kn" ! Number of networks in $POINTS block
138     write(10, "(I0, T2, A)") nnetworks, ".0"
139     write(10, "(A)") "=kt" ! Boundary condition (1 = solid surface)
140     write(10, "(A)") "1.0"
141
142 end subroutine view_write_panair_network_header
143
144
145 subroutine view_write_panair_network(wi, af_points, network, istart, iend)
146     type(wing_t), intent(in) :: wi
147     real, allocatable, dimension(:, :), intent(inout) :: af_points
148     character(len=*), intent(in) :: network
149     integer, intent(in) :: istart, iend
150
151     integer :: isec, isec_start, isec_end, isec_inc
152     type(section_t), pointer :: si
153
154     write(10, "(A, T11, A)") "=nm", "nn"
155     write(10, "(I0, T11, I0, T71, A)") istart - iend + 1, wi%nSec + 1, network
156
157     if(wi%side .eq. "left") then
158         isec_start = wi%nSec
159         isec_end = 1
160         isec_inc = -1
161     else
158         isec_start = 1
159         isec_end = wi%nSec
160         isec_inc = 1
161     end if
162
163     do isec = isec_start, isec_end, isec_inc
164         si => wi%sec(isec)
165         call view_create_local_airfoil_panair(wi, si, 1, af_points)
166         call view_write_panair_points(istart, iend, af_points)
167     end do

```

```

171     end do
172
173     call view_create_local_airfoil_panair(wi, si, 2, af_points)
174     call view_write_panair_points(istart, iend, af_points)
175
176 end subroutine view_write_panair_network
177
178
179 subroutine view_create_local_airfoil_panair(wi, si, sec_side, af_points)
180     type(wing_t), intent(in) :: wi
181     type(section_t), pointer, intent(in) :: si
182     integer, intent(in) :: sec_side
183     real, allocatable, dimension(:,:), intent(inout) :: af_points
184
185     real :: percent, chord, RA
186     integer :: i, mid
187     integer :: af_datasize
188
189     real :: a, b, c
190     real, dimension(3) :: midpoint
191
192     af_datasize = size(af_points, 1)
193     if (mod(af_datasize, 2) .eq. 0) then
194         write(*,*) "Allocated size of af_points must always be odd for Panair
interface!"
195         write(*,*) "If the number of points on an airfoil is even, allocate
af_points to"
196         write(*,*) "one more than this."
197         stop
198     end if
199
200     if(sec_side .eq. 1) then
201         percent = si%percent_1
202     else if(sec_side .eq. 2) then
203         percent = si%percent_2
204     else
205         percent = si%percent_c
206     end if
207
208     if(wi%chord_2 >= 0.0) then
209         chord = wi%chord_1 + percent*(wi%chord_2 - wi%chord_1)
210     else
211         RA = 8.0 * wi%span / pi / wi%chord_1
212         chord = 8.0 * wi%span / pi / RA * sqrt(1.0 - percent**2)
213     end if
214
215     if(sec_side .eq. 1) then
216         call view_create_local_airfoil(si%af1_a, si%af1_b, wi%side,
si%af_weight_1, chord, &
217             & si%twist1, si%dihedral1, si%P1, af_points)
218     else if(sec_side .eq. 2) then
219         call view_create_local_airfoil(si%af2_a, si%af2_b, wi%side,
si%af_weight_2, chord, &
220             & si%twist2, si%dihedral2, si%P2, af_points)
221     else
222         call view_create_local_airfoil(si%afc_a, si%afc_b, wi%side,
si%af_weight_c, chord, &
223             & si%twist, si%dihedral, si%PC, af_points)
224     end if
225

```

```

226      ! If the number of points on an airfoil is even, add an additional point at
the leading edge
227      if (mod(si%af1_a%geom%datasize, 2) .eq. 0) then
228          ! Find the index of the second leading-edge point
229          mid = si%af1_a%geom%datasize / 2 + 1
230
231          ! Calculate the new midpoint between the first and second leading-edge
points
232          midpoint(:) = 0.5 * (af_points(mid - 1, :) + af_points(mid, :))
233
234          ! Fit a parabola through three points at the leading edge
235          call quadratic_fit(af_points(mid - 1 : mid + 1, 3:1:-2), a, b, c)
236          if (.not. isnan(a) .and. .not. isnan(b) .and. .not. isnan(c)) then
237              midpoint(1) = a * midpoint(3)**2 + b * midpoint(3) + c
238          end if
239
240          ! Shift the last half of the point array to the end
241          af_points(si%af1_a%geom%datasize + 1 : mid + 1 : -1, :) =
af_points(si%af1_a%geom%datasize : mid : -1, :)
242
243          ! Place the new midpoint between the two leading-edge points
244          af_points(mid, :) = midpoint(:)
245
246      end if
247
248      do i = 1, af_ddatasize
249          af_points(i, 1) = -af_points(i, 1)
250          af_points(i, 3) = -af_points(i, 3)
251      end do
252
253  end subroutine view_create_local_airfoil_panair
254
255
256  subroutine view_write_panair_points(istart, iend, af_points)
257      integer, intent(in) :: istart, iend
258      real, dimension(:, :), intent(in) :: af_points
259
260      integer :: ipt
261
262      do ipt = istart, iend + 1, -2
263          write(10, "(6F10.6)") af_points(ipt, :), af_points(ipt - 1, :)
264      end do
265      if (ipt == iend) then
266          write(10, "(3F10.6)") af_points(ipt, :)
267      end if
268  end subroutine view_write_panair_points
269
270
271  subroutine view_write_panair_endcap(wi, af_points, network, npts, rscale)
272      type(wing_t), intent(in) :: wi
273      real, allocatable, dimension(:, :), intent(inout) :: af_points
274      character(len=*), intent(in) :: network
275      integer, intent(in) :: npts
276      real, intent(in) :: rscale
277
278      real, allocatable, dimension(:, :), intent(in) :: af_points_scaled, c
279      real :: r
280      real :: theta, theta_start, theta_end, dtheta
281      integer :: i, j, af_mid, af_end
282
283      ! Calculate the midpoint index

```



```

284     af_end = size(af_points, 1)
285     af_mid = (af_end + 1) / 2
286
287     ! Write the network header info
288     write(10, "(A, T11, A)") "=nm", "nn"
289     write(10, "(I0, T11, I0, T71, A)") af_mid, npts + 2, network
290
291     ! Get the airfoil points
292     call view_create_local_airfoil_panair(wi, wi%sec(wi%nSec), 2, af_points)
293     allocate(af_points_scaled(af_mid, 3))
294     allocate(c(af_mid, 3))
295
296     ! Set up theta
297     if(wi%side .eq. 'left') then
298         theta_start = 0.0
299         theta_end = pi
300     else
301         theta_start = pi
302         theta_end = 0.0
303     end if
304     dtheta = (theta_end - theta_start) / REAL(npts + 1)
305
306     ! calculate the centerline of the airfoil (not quite camber line...)
307     c(:, :) = 0.5 * (af_points(1:af_mid, :) + af_points(af_end:af_mid:-1, :))
308
309     theta = theta_start
310     do i = 1, npts + 2
311         ! Scale the airfoil points
312         do j = 1, af_mid
313             r = 0.5 * (af_points(af_end - j + 1, 3) - af_points(j, 3))
314             af_points_scaled(j, 1) = c(j, 1)
315             af_points_scaled(j, 2) = c(j, 2) + rscale * r * sin(theta)
316             af_points_scaled(j, 3) = c(j, 3) + r * cos(theta)
317         end do
318
319         call view_write_panair_points(af_mid, 1, af_points_scaled)
320
321         theta = theta + dtheta
322     end do
323
324 end subroutine view_write_panair_endcap
325
326
327 subroutine view_write_panair_wake(network)
328     character(*), intent(in) :: network
329     write(10, "(A)") "$TRAILING matchw=0"
330     write(10, "(A)") "=kn"
331     write(10, "(A)") "1.0"
332     write(10, "(A, T11, A)") "=kt", "matchw"
333     write(10, "(A, T11, A)") "18.0", "0.0"
334     write(10, "(A, T11, A, T21, A, T31, A)") "=inat", "insd", "xwake", "twake"
335     write(10, "(A, T11, A, T21, A, T31, A, T71, A)") network, "1.0", "10.0",
336     "0.0", "wake"
337 end subroutine view_write_panair_wake

```

## J EXAMPLE PANAIR INPUT FILE

```

$title
myairplane
Generated by MachUp
$DATACHECK
=ndtchk
0.0
$SYMMETRIC
=xzpln    xyp1n
1.0      0.0
$MACH NUMBER
=amach
0.000000
$CASES
=nacase
1.0
$ANGLES OF ATTACK
=alpc
0.000000
=alpha(0)
1.000000
$YAW ANGLE
=betc
0.000000
=beta(0)
0.000000
$REFERENCE DATA
=xref      yref      zref
0.000000  0.000000  0.000000
=sref      bref      cref      dref
4.000000  1.000000  4.000000  1.000000
$PRINTOUT CONTROL
=isings    igeomp    isingp    icontp    ibconp    iedgep
0.0        0.0        0.0        0.0        0.0        0.0
=ipraic    nexdgn    ioutpr    ifmcpr    icostp
0.0        0.0        1.0        0.0        0.0
$POINTS for wing 1
=kn
2.0
=kt
1.0
=nm        nn
11         21
0.954930  0.000000  0.000000  0.918311  0.000000  0.000377
0.813166  0.000000  0.002748  0.652742  0.000000  0.007923
0.456480  0.000000  0.014992  0.246982  0.000000  0.021670
0.047048  0.000000  0.025288  -0.122724  0.000000  0.023915
-0.245660  0.000000  0.017131  -0.310112  0.000000  0.006222
-0.319908  0.000000  -0.000000
0.951986  0.156918  0.000000  0.915480  0.156918  0.000376
0.810659  0.156918  0.002739  0.650729  0.156918  0.007899
0.455073  0.156918  0.014946  0.246220  0.156918  0.021603
0.046903  0.156918  0.025210  -0.122346  0.156918  0.023841
-0.244902  0.156918  0.017078  -0.309156  0.156918  0.006203
-0.318922  0.156918  -0.000000
0.943173  0.312869  0.000000  0.907005  0.312869  0.000372
0.803155  0.312869  0.002714  0.644705  0.312869  0.007826
0.450860  0.312869  0.014807  0.243941  0.312869  0.021403
0.046469  0.312869  0.024977  -0.121213  0.312869  0.023620
-0.242635  0.312869  0.016920  -0.306294  0.312869  0.006146
-0.315969  0.312869  -0.000000
0.928545  0.466891  0.000000  0.892938  0.466891  0.000367

```

upper\_1

0.790698	0.466891	0.002672	0.634706	0.466891	0.007704
0.443867	0.466891	0.014578	0.240158	0.466891	0.021071
0.045748	0.466891	0.024589	-0.119333	0.466891	0.023254
-0.238872	0.466891	0.016658	-0.301544	0.466891	0.006051
-0.311069	0.466891	-0.000000			
0.908192	0.618034	0.000000	0.873366	0.618034	0.000359
0.773367	0.618034	0.002613	0.620794	0.618034	0.007535
0.434138	0.618034	0.014258	0.234894	0.618034	0.020609
0.044745	0.618034	0.024050	-0.116718	0.618034	0.022744
-0.233636	0.618034	0.016293	-0.294934	0.618034	0.005918
-0.304250	0.618034	-0.000000			
0.882240	0.765367	0.000000	0.848409	0.765367	0.000348
0.751268	0.765367	0.002539	0.603055	0.765367	0.007320
0.421732	0.765367	0.013851	0.228181	0.765367	0.020020
0.043467	0.765367	0.023363	-0.113383	0.765367	0.022094
-0.226960	0.765367	0.015827	-0.286506	0.765367	0.005749
-0.295556	0.765367	-0.000000			
0.850849	0.907981	0.000000	0.818221	0.907981	0.000336
0.724536	0.907981	0.002448	0.581597	0.907981	0.007060
0.406727	0.907981	0.013358	0.220062	0.907981	0.019308
0.041920	0.907981	0.022532	-0.109348	0.907981	0.021308
-0.218884	0.907981	0.015264	-0.276312	0.907981	0.005544
-0.285040	0.907981	-0.000000			
0.814211	1.044997	0.000000	0.782989	1.044997	0.000322
0.693338	1.044997	0.002343	0.556554	1.044997	0.006756
0.389213	1.044997	0.012783	0.210587	1.044997	0.018476
0.040115	1.044997	0.021562	-0.104640	1.044997	0.020391
-0.209459	1.044997	0.014607	-0.264414	1.044997	0.005306
-0.272766	1.044997	-0.000000			
0.772554	1.175571	0.000000	0.742929	1.175571	0.000305
0.657865	1.175571	0.002223	0.528079	1.175571	0.006410
0.369300	1.175571	0.012129	0.199812	1.175571	0.017531
0.038063	1.175571	0.020459	-0.099286	1.175571	0.019348
-0.198743	1.175571	0.013859	-0.250886	1.175571	0.005034
-0.258811	1.175571	-0.000000			
0.726134	1.298896	0.000000	0.698289	1.298896	0.000287
0.618336	1.298896	0.002090	0.496349	1.298896	0.006025
0.347110	1.298896	0.011400	0.187806	1.298896	0.016478
0.035776	1.298896	0.019229	-0.093320	1.298896	0.018185
-0.186801	1.298896	0.013027	-0.235811	1.298896	0.004732
-0.243260	1.298896	-0.000000			
0.675237	1.414214	0.000000	0.649344	1.414214	0.000267
0.574995	1.414214	0.001943	0.461558	1.414214	0.005603
0.322780	1.414214	0.010601	0.174642	1.414214	0.015323
0.033268	1.414214	0.017881	-0.086779	1.414214	0.016910
-0.173708	1.414214	0.012114	-0.219282	1.414214	0.004400
-0.226209	1.414214	-0.000000			
0.620177	1.520812	0.000000	0.596395	1.520812	0.000245
0.528109	1.520812	0.001785	0.423922	1.520812	0.005146
0.296460	1.520812	0.009736	0.160402	1.520812	0.014073
0.030555	1.520812	0.016423	-0.079703	1.520812	0.015531
-0.159543	1.520812	0.011126	-0.201402	1.520812	0.004041
-0.207764	1.520812	-0.000000			
0.561294	1.618034	0.000000	0.539770	1.618034	0.000222
0.477967	1.618034	0.001615	0.383672	1.618034	0.004657
0.268312	1.618034	0.008812	0.145172	1.618034	0.012737
0.027654	1.618034	0.014864	-0.072136	1.618034	0.014057
-0.144395	1.618034	0.010069	-0.182279	1.618034	0.003657
-0.188037	1.618034	-0.000000			
0.498949	1.705280	0.000000	0.479816	1.705280	0.000197
0.424878	1.705280	0.001436	0.341057	1.705280	0.004140

0.238510	1.705280	0.007833	0.129048	1.705280	0.011322
0.024583	1.705280	0.013213	-0.064123	1.705280	0.012495
-0.128357	1.705280	0.008951	-0.162033	1.705280	0.003251
-0.167151	1.705280	-0.000000			
0.433529	1.782013	0.000000	0.416904	1.782013	0.000171
0.369170	1.782013	0.001248	0.296339	1.782013	0.003597
0.207238	1.782013	0.006806	0.112127	1.782013	0.009838
0.021359	1.782013	0.011481	-0.055716	1.782013	0.010857
-0.111527	1.782013	0.007777	-0.140788	1.782013	0.002825
-0.145235	1.782013	-0.000000			
0.365436	1.847759	0.000000	0.351422	1.847759	0.000144
0.311185	1.847759	0.001052	0.249793	1.847759	0.003032
0.174687	1.847759	0.005737	0.094516	1.847759	0.008293
0.018005	1.847759	0.009677	-0.046965	1.847759	0.009152
-0.094010	1.847759	0.006556	-0.118675	1.847759	0.002381
-0.122423	1.847759	-0.000000			
0.295089	1.902113	0.000000	0.283774	1.902113	0.000117
0.251282	1.902113	0.000849	0.201708	1.902113	0.002448
0.141060	1.902113	0.004633	0.076322	1.902113	0.006696
0.014539	1.902113	0.007814	-0.037924	1.902113	0.007390
-0.075913	1.902113	0.005294	-0.095830	1.902113	0.001923
-0.098857	1.902113	-0.000000			
0.222924	1.944740	0.000000	0.214375	1.944740	0.000088
0.189830	1.944740	0.000641	0.152380	1.944740	0.001850
0.106563	1.944740	0.003500	0.057657	1.944740	0.005059
0.010983	1.944740	0.005903	-0.028649	1.944740	0.005583
-0.057348	1.944740	0.003999	-0.072394	1.944740	0.001453
-0.074681	1.944740	-0.000000			
0.149384	1.975377	0.000000	0.143655	1.975377	0.000059
0.127207	1.975377	0.000430	0.102111	1.975377	0.001239
0.071409	1.975377	0.002345	0.038636	1.975377	0.003390
0.007360	1.975377	0.003956	-0.019198	1.975377	0.003741
-0.038430	1.975377	0.002680	-0.048512	1.975377	0.000973
-0.050045	1.975377	-0.000000			
0.074923	1.993835	0.000000	0.072050	1.993835	0.000030
0.063800	1.993835	0.000216	0.051214	1.993835	0.000622
0.035815	1.993835	0.001176	0.019378	1.993835	0.001700
0.003691	1.993835	0.001984	-0.009629	1.993835	0.001876
-0.019274	1.993835	0.001344	-0.024331	1.993835	0.000488
-0.025100	1.993835	-0.000000			
-0.000000	2.000000	-0.000000	-0.000000	2.000000	-0.000000
-0.000000	2.000000	-0.000000	-0.000000	2.000000	-0.000000
-0.000000	2.000000	-0.000000	-0.000000	2.000000	-0.000000
-0.000000	2.000000	-0.000000	-0.000000	2.000000	-0.000000
-0.000000	2.000000	-0.000000	-0.000000	2.000000	-0.000000
-0.000000	2.000000	-0.000000	-0.000000	2.000000	-0.000000
-0.000000	2.000000	-0.000000	-0.000000	2.000000	-0.000000

=nm

nn

11

21

lower\_1

-0.319908	0.000000	-0.000000	-0.310112	0.000000	-0.006223
-0.245660	0.000000	-0.017131	-0.122724	0.000000	-0.023915
0.047048	0.000000	-0.025288	0.246982	0.000000	-0.021670
0.456480	0.000000	-0.014992	0.652742	0.000000	-0.007923
0.813166	0.000000	-0.002748	0.918311	0.000000	-0.000377
0.954930	0.000000	-0.000000			
-0.318922	0.156918	-0.000000	-0.309156	0.156918	-0.006203
-0.244902	0.156918	-0.017078	-0.122346	0.156918	-0.023841
0.046903	0.156918	-0.025210	0.246220	0.156918	-0.021603
0.455073	0.156918	-0.014946	0.650730	0.156918	-0.007899
0.810659	0.156918	-0.002739	0.915480	0.156918	-0.000376
0.951986	0.156918	-0.000000			
-0.315969	0.312869	-0.000000	-0.306294	0.312869	-0.006146

-0.242635	0.312869	-0.016920	-0.121213	0.312869	-0.023620
0.046469	0.312869	-0.024977	0.243941	0.312869	-0.021403
0.450860	0.312869	-0.014807	0.644705	0.312869	-0.007826
0.803155	0.312869	-0.002714	0.907005	0.312869	-0.000372
0.943173	0.312869	-0.000000			
-0.311069	0.466891	-0.000000	-0.301544	0.466891	-0.006051
-0.238872	0.466891	-0.016658	-0.119333	0.466891	-0.023254
0.045748	0.466891	-0.024589	0.240158	0.466891	-0.021071
0.443867	0.466891	-0.014578	0.634706	0.466891	-0.007704
0.790698	0.466891	-0.002672	0.892938	0.466891	-0.000367
0.928545	0.466891	-0.000000			
-0.304250	0.618034	-0.000000	-0.294934	0.618034	-0.005918
-0.233636	0.618034	-0.016293	-0.116718	0.618034	-0.022744
0.044745	0.618034	-0.024050	0.234894	0.618034	-0.020609
0.434138	0.618034	-0.014258	0.620794	0.618034	-0.007535
0.773367	0.618034	-0.002613	0.873366	0.618034	-0.000359
0.908192	0.618034	-0.000000			
-0.295556	0.765367	-0.000000	-0.286506	0.765367	-0.005749
-0.226960	0.765367	-0.015827	-0.113382	0.765367	-0.022094
0.043467	0.765367	-0.023363	0.228181	0.765367	-0.020020
0.421732	0.765367	-0.013851	0.603055	0.765367	-0.007320
0.751268	0.765367	-0.002539	0.848409	0.765367	-0.000348
0.882240	0.765367	-0.000000			
-0.285040	0.907981	-0.000000	-0.276312	0.907981	-0.005544
-0.218884	0.907981	-0.015264	-0.109348	0.907981	-0.021308
0.041920	0.907981	-0.022532	0.220062	0.907981	-0.019308
0.406727	0.907981	-0.013358	0.581597	0.907981	-0.007060
0.724536	0.907981	-0.002448	0.818221	0.907981	-0.000336
0.850849	0.907981	-0.000000			
-0.272766	1.044997	-0.000000	-0.264414	1.044997	-0.005306
-0.209459	1.044997	-0.014607	-0.104640	1.044997	-0.020391
0.040115	1.044997	-0.021562	0.210587	1.044997	-0.018476
0.389213	1.044997	-0.012783	0.556554	1.044997	-0.006756
0.693338	1.044997	-0.002343	0.782989	1.044997	-0.000322
0.814211	1.044997	-0.000000			
-0.258811	1.175571	-0.000000	-0.250886	1.175571	-0.005034
-0.198743	1.175571	-0.013859	-0.099286	1.175571	-0.019348
0.038063	1.175571	-0.020459	0.199812	1.175571	-0.017531
0.369300	1.175571	-0.012129	0.528079	1.175571	-0.006410
0.657865	1.175571	-0.002223	0.742929	1.175571	-0.000305
0.772554	1.175571	-0.000000			
-0.243260	1.298896	-0.000000	-0.235811	1.298896	-0.004732
-0.186801	1.298896	-0.013027	-0.093320	1.298896	-0.018185
0.035776	1.298896	-0.019229	0.187806	1.298896	-0.016478
0.347110	1.298896	-0.011400	0.496349	1.298896	-0.006025
0.618336	1.298896	-0.002090	0.698289	1.298896	-0.000287
0.726134	1.298896	-0.000000			
-0.226209	1.414214	-0.000000	-0.219282	1.414214	-0.004400
-0.173708	1.414214	-0.012114	-0.086779	1.414214	-0.016910
0.033268	1.414214	-0.017881	0.174643	1.414214	-0.015323
0.322780	1.414214	-0.010601	0.461558	1.414214	-0.005603
0.574995	1.414214	-0.001943	0.649344	1.414214	-0.000267
0.675237	1.414214	-0.000000			
-0.207764	1.520812	-0.000000	-0.201402	1.520812	-0.004041
-0.159543	1.520812	-0.011126	-0.079703	1.520812	-0.015531
0.030555	1.520812	-0.016423	0.160402	1.520812	-0.014073
0.296460	1.520812	-0.009736	0.423922	1.520812	-0.005146
0.528109	1.520812	-0.001785	0.596395	1.520812	-0.000245
0.620177	1.520812	-0.000000			
-0.188037	1.618034	-0.000000	-0.182279	1.618034	-0.003657
-0.144395	1.618034	-0.010069	-0.072136	1.618034	-0.014057

```

0.027654 1.618034 -0.014864 0.145172 1.618034 -0.012737
0.268312 1.618034 -0.008812 0.383672 1.618034 -0.004657
0.477967 1.618034 -0.001615 0.539770 1.618034 -0.000222
0.561294 1.618034 -0.000000
-0.167151 1.705280 -0.000000 -0.162033 1.705280 -0.003251
-0.128357 1.705280 -0.008951 -0.064123 1.705280 -0.012495
0.024583 1.705280 -0.013213 0.129048 1.705280 -0.011322
0.238510 1.705280 -0.007833 0.341057 1.705280 -0.004140
0.424878 1.705280 -0.001436 0.479816 1.705280 -0.000197
0.498949 1.705280 -0.000000
-0.145235 1.782013 -0.000000 -0.140788 1.782013 -0.002825
-0.111527 1.782013 -0.007777 -0.055716 1.782013 -0.010857
0.021359 1.782013 -0.011481 0.112127 1.782013 -0.009838
0.207238 1.782013 -0.006806 0.296339 1.782013 -0.003597
0.369170 1.782013 -0.001248 0.416904 1.782013 -0.000171
0.433529 1.782013 -0.000000
-0.122423 1.847759 -0.000000 -0.118675 1.847759 -0.002381
-0.094010 1.847759 -0.006556 -0.046965 1.847759 -0.009152
0.018005 1.847759 -0.009677 0.094516 1.847759 -0.008293
0.174687 1.847759 -0.005737 0.249793 1.847759 -0.003032
0.311185 1.847759 -0.001052 0.351422 1.847759 -0.000144
0.365436 1.847759 -0.000000
-0.098857 1.902113 -0.000000 -0.095830 1.902113 -0.001923
-0.075913 1.902113 -0.005294 -0.037924 1.902113 -0.007390
0.014539 1.902113 -0.007814 0.076322 1.902113 -0.006696
0.141060 1.902113 -0.004633 0.201708 1.902113 -0.002448
0.251282 1.902113 -0.000849 0.283774 1.902113 -0.000117
0.295089 1.902113 -0.000000
-0.074681 1.944740 -0.000000 -0.072394 1.944740 -0.001453
-0.057348 1.944740 -0.003999 -0.028649 1.944740 -0.005583
0.010983 1.944740 -0.005903 0.057657 1.944740 -0.005059
0.106563 1.944740 -0.003500 0.152380 1.944740 -0.001850
0.189830 1.944740 -0.000641 0.214375 1.944740 -0.000088
0.222924 1.944740 -0.000000
-0.050045 1.975377 -0.000000 -0.048512 1.975377 -0.000973
-0.038430 1.975377 -0.002680 -0.019198 1.975377 -0.003741
0.007360 1.975377 -0.003956 0.038636 1.975377 -0.003390
0.071409 1.975377 -0.002345 0.102111 1.975377 -0.001239
0.127207 1.975377 -0.000430 0.143655 1.975377 -0.000059
0.149384 1.975377 -0.000000
-0.025100 1.993835 -0.000000 -0.024331 1.993835 -0.000488
-0.019274 1.993835 -0.001344 -0.009629 1.993835 -0.001876
0.003691 1.993835 -0.001984 0.019378 1.993835 -0.001700
0.035815 1.993835 -0.001176 0.051214 1.993835 -0.000622
0.063800 1.993835 -0.000216 0.072050 1.993835 -0.000030
0.074923 1.993835 -0.000000
-0.000000 2.000000 -0.000000 -0.000000 2.000000 -0.000000
-0.000000 2.000000 -0.000000 -0.000000 2.000000 -0.000000
-0.000000 2.000000 -0.000000 -0.000000 2.000000 -0.000000
-0.000000 2.000000 -0.000000 -0.000000 2.000000 -0.000000
-0.000000 2.000000 -0.000000 -0.000000 2.000000 -0.000000
-0.000000 2.000000 -0.000000
$TRAILING matchw=0
=kn
1.0
=kt      matchw
18.0     0.0
=inat    insd      xwake      twake
upper_1  1.0       10.0       0.0
$END
wake_1

```

## K PRALINES SOURCE CODE

**K.1 Pralines Main Program (main.f90)**

```

1  program PrandtlsLiftingLine
2      use LiftingLineInterface
3
4      implicit none
5
6      !Begin execution
7      call BeginLiftingLineInterface()
8
9  end program

```

**K.2 Interface Module (liftinglineinterface.f90)**

```

1  module LiftingLineInterface
2      use class_Planform
3      use LiftingLineSetters
4      use LiftingLineSolver
5      use LiftingLineOutput
6      use LiftingLineSolver_Test
7
8      implicit none
9
10 contains
11     subroutine BeginLiftingLineInterface()
12         type(Planform) :: pf
13         character*2 :: inp = 'A'
14
15         call InitPlanform(pf)
16
17         do while(inp /= 'Q')
18             inp = PlanformParameters(pf)
19             if (inp == 'A') then
20                 call ComputeCMatrixAndCoefficients(pf)
21                 call OutputPlanform(pf)
22                 do while(inp /= 'Q' .and. inp /= 'B')
23                     inp = OperatingConditions(pf)
24                     if (inp /= 'Q') then
25                         call UpdateOperatingConditions(pf, inp)
26                     end if
27                 end do
28             else if (inp /= 'Q') then
29                 call UpdatePlanformParameters(pf, inp)
30             end if
31         end do
32     end subroutine BeginLiftingLineInterface
33
34     character*2 function PlanformParameters(pf) result(inp)
35         type(Planform), intent(inout) :: pf
36
37         character*80 :: msg
38
39         ! Clear the screen and output the header
40         call system('cls')
41         call OutputHeader()
42

```

```

43      ! Display options to user
44      write(6, '(28x, a)') "Planform Design Menu"
45      write(6, *)
46      write(6, '(a)') "Select from the following menu options:"
47      write(6, *)
48
49      ! Wing parameters
50      write(6, '(2x, a)') "Wing Parameters:"
51
52      msg = "WT - Edit wing type"
53      call DisplayMessageWithTextDefault(msg, GetWingType(pf), 4)
54
55      msg = "N - Edit number of nodes per semispan"
56      call DisplayMessageWithIntegerDefault(msg, (pf%NNodes + 1) / 2, 4)
57
58      msg = "RA - Edit aspect ratio"
59      call DisplayMessageWithRealDefault(msg, pf%AspectRatio, 4)
60
61      if (pf%WingType == Tapered) then
62          msg = "RT - Edit taper ratio"
63          call DisplayMessageWithRealDefault(msg, pf%TaperRatio, 4)
64      end if
65
66      msg = "S - Edit section lift slope"
67      call DisplayMessageWithRealDefault(msg, pf%SectionLiftSlope, 4)
68
69      if (pf%WingType == Combination) then
70          msg = "TZ - Edit z/b at the transition from tapered to elliptic"
71          call DisplayMessageWithRealDefault(msg, pf%TransitionPoint, 4)
72
73          msg = "TC - Edit c/croot at the transition from tapered to elliptic"
74          call DisplayMessageWithRealDefault(msg, pf%TransitionChord, 4)
75      end if
76
77      if (pf%WingType /= Elliptic) then
78          msg = "WD - Toggle washout distribution type"
79          call DisplayMessageWithTextDefault(msg,
GetWashoutDistributionType(pf), 4)
80      end if
81
82      msg = "LC - Edit low-aspect-ratio correction method"
83      call DisplayMessageWithTextDefault(msg, GetLowAspectRatioMethod(pf), 4)
84
85      ! Aileron parameters
86      write(6, *)
87      write(6, '(2x, a)') "Aileron Parameters:"
88
89      msg = "ZR - Edit z/b of aileron root"
90      call DisplayMessageWithRealDefault(msg, pf%AileronRoot, 4)
91
92      msg = "ZT - Edit z/b of aileron tip"
93      call DisplayMessageWithRealDefault(msg, pf%AileronTip, 4)
94
95      msg = "PH - Make hinge line parallel with quarter-chord line?"
96      call DisplayMessageWithLogicalDefault(msg, pf%ParallelHingeLine, 4)
97
98      msg = "CR - Edit cf/c of aileron root"
99      call DisplayMessageWithRealDefault(msg, pf%FlapFractionRoot, 4)
100
101      msg = "CT - Edit cf/c of aileron tip"
102      call DisplayMessageWithRealDefault(msg, pf%FlapFractionTip, 4)

```



```

103
104     msg = "HE - Edit aileron hinge efficiency"
105     call DisplayMessageWithRealDefault(msg, pf%HingeEfficiency, 4)
106
107     ! Output and Plotting options
108     write(6, *)
109     write(6, '(2x, a)') "Output and Plotting Options:"
110     msg = "C - Output C matrix and Fourier Coefficients?"
111     call DisplayMessageWithLogicalDefault(msg, pf%OutputMatrices, 4)
112
113     msg = "F - Edit output file name"
114     call DisplayMessageWithTextDefault(msg, pf%FileName, 4)
115
116     write(6, '(4x, a)') "PP - Plot planform in ES-Plot"
117
118     ! Main Execution commands
119     write(6, *)
120     write(6, '(2x, a)') "A - Advance to Operating Conditions Menu"
121     write(6, '(2x, a)') "T - Test solver against Problem 1.34b solution"
122     write(6, '(2x, a)') "Q - Quit"
123
124     write(6, *)
125     write(6, '(a)') "Your selection: "
126
127     inp = GetCharacterInput(" ")
128     write(6, *)
129 end function PlanformParamters
130
131 character*2 function OperatingConditions(pf) result(inp)
132     type(Planform), intent(inout) :: pf
133
134     integer :: i
135     character*80 :: msg
136
137     ! Clear the screen and output the header
138     call system('cls')
139     call OutputHeader()
140
141     ! Output the Planform summary
142     call OutputPlanformSummary(6, pf)
143     call OutputOperatingConditions(6, pf)
144     call OutputFlightCoefficients(6, pf)
145     write(6, '(80a)') ("*", i=1,80)
146
147     ! Display options to user
148     write(6, '(28x, a)') "Operating Conditions Menu"
149     write(6, *)
150     write(6, '(a)') "Select from the following menu options:"
151
152     ! Operating Conditions
153     write(6, *)
154     write(6, '(2x, a)') "Operating Conditions:"
155
156     msg = "AA - Edit root aerodynamic angle of attack"
157     call DisplayMessageWithAngleDefault(msg, pf%AngleOfAttack, 4)
158
159     msg = "CL - Edit coefficient of lift"
160     call DisplayMessageWithRealDefault(msg, pf%LiftCoefficient, 4)
161
162     msg = "OW - Use optimum total washout"
163     call DisplayMessageWithLogicalDefault(msg, pf%UseOptimumWashout, 4)

```

```

164
165     msg = "W - Edit total amount of washout"
166     call DisplayMessageWithAngleDefault(msg, pf%Washout, 4)
167
168     msg = "AD - Edit aileron deflection"
169     call DisplayMessageWithAngleDefault(msg, pf%AileronDeflection, 4)
170
171     msg = "SR - Use steady dimensionless rolling rate"
172     call DisplayMessageWithLogicalDefault(msg, pf%UseSteadyRollingRate, 4)
173
174     msg = "R - Edit dimensionless rolling rate"
175     call DisplayMessageWithRealDefault(msg, pf%RollingRate, 4)
176
177     ! Plotting options
178     write(6, *)
179     write(6, '(2x, a)') "Plotting Options:"
180     write(6, '(4x, a)') "PP - Plot Planform in ES-Plot"
181     write(6, '(4x, a)') "PW - Plot Dimensionless Washout Distribution in ES-
Plot"
182     write(6, '(4x, a)') "PL - Plot Section Lift Distribution in ES-Plot"
183     write(6, '(4x, a)') "WL - Write Section Lift Distribution to
'liftdistribution.dat'"
184     write(6, '(4x, a)') "PN - Plot Normalized Section Lift Coefficient in
ES-Plot"
185     write(6, '(4x, a)') "WN - Write Normalized Section Lift Coefficient in
ES-Plot"
186
187     ! Main Execution commands
188     write(6, *)
189     msg = "S - Save Flight coefficients to output file"
190     call DisplayMessageWithTextDefault(msg, pf%FileName, 2)
191
192     write(6, '(2x, a)') "B - Back to Planform Design Menu"
193     write(6, '(2x, a)') "Q - Quit"
194
195     write(6, *)
196     write(6, '(a)') "Your selection: "
197
198     inp = GetCharacterInput(" ")
199     write(6, *)
200 end function OperatingConditions
201
202 subroutine UpdatePlanformParameters(pf, input)
203     type(Planform), intent(inout) :: pf
204     character*2, intent(in) :: input
205
206     ! Process input command
207     ! Wing parameters
208     if (input == 'WT') then
209         call EditWingType(pf)
210     else if (input == 'N') then
211         call EditNNodes(pf)
212     else if (input == 'RA') then
213         call EditAspectRatio(pf)
214     else if (input == 'RT' .and. pf%WingType == Tapered) then
215         call EditTaperRatio(pf)
216     else if (input == 'S') then
217         call EditLiftSlope(pf)
218     else if (input == 'TZ' .and. pf%WingType == Combination) then
219         call EditTransitionPoint(pf)
220     else if (input == 'TC' .and. pf%WingType == Combination) then

```

```

221         call EditTransitionChord(pf)
222     else if (input == 'WD' .and. pf%WingType /= Elliptic) then
223         call EditWashoutDistribution(pf)
224     else if (input == 'LC') then
225         call EditLowAspectRatioCorrectionMethod(pf)
226
227     ! Aileron parameters
228     else if (input == 'ZR') then
229         call EditAileronRoot(pf)
230     else if (input == 'ZT') then
231         call EditAileronTip(pf)
232     else if (input == 'PH') then
233         call ToggleParallelHinge(pf)
234     else if (input == 'CR') then
235         call EditFlapFractionRoot(pf)
236     else if (input == 'CT') then
237         call EditFlapFractionTip(pf)
238     else if (input == 'HE') then
239         call EditHingeEfficiency(pf)
240
241     ! Output options
242     else if (input == 'C') then
243         pf%OutputMatrices = .not. pf%OutputMatrices
244     else if (input == 'F') then
245         call EditFileName(pf)
246     else if (input == 'PP') then
247         call PlotPlanform(pf)
248
249     ! Testing options
250     else if (input == 'T') then
251         call TestLiftingLineSolver()
252     end if
253 end subroutine UpdatePlanformParameters
254
255 subroutine UpdateOperatingConditions(pf, input)
256     type(Planform), intent(inout) :: pf
257     character*2, intent(in) :: input
258
259     ! Operating Conditions
260     if (input == 'AA') then
261         call EditAngleOfAttack(pf)
262     else if (input == 'CL') then
263         call EditLiftCoefficient(pf)
264     else if (input == 'OW') then
265         call ToggleUseOptimumWashout(pf)
266     else if (input == 'W') then
267         call EditWashout(pf)
268     else if (input == 'AD') then
269         call EditAileronDeflection(pf)
270     else if (input == 'SR') then
271         call ToggleUseSteadyRollingRate(pf)
272     else if (input == 'R') then
273         call EditRollingRate(pf)
274
275     ! Output and Plotting options
276     else if (input == 'PP') then
277         call PlotPlanform(pf)
278     else if (input == 'PW') then
279         call PlotWashout(pf)
280     else if (input == 'PL') then
281         call PlotSectionLiftDistribution(pf)

```

```

282     else if (input == 'WL') then
283         call WriteSectionLiftDistribution(pf)
284     else if (input == 'PN') then
285         call PlotNormalizedLiftCoefficient(pf)
286     else if (input == 'WN') then
287         call WriteNormalizedLiftCoefficient(pf)
288     else if (input == 'S') then
289         call OutputFlightConditions(pf)
290     end if
291
292     call ComputeFlightConditions(pf)
293 end subroutine UpdateOperatingConditions
294
295 subroutine EditWingType(pf)
296     type(Planform), intent(inout) :: pf
297
298     logical :: cont
299     character*2 :: inp
300
301     write(6, *)
302     write(6, '(a)') "Select from the following wing type options:"
303     write(6, '(2x, a)') "T - Tapered"
304     write(6, '(2x, a)') "E - Elliptic"
305     write(6, '(2x, a)') "C - Combination (Tapered with elliptic tip)"
306     write(6, *)
307     write(6, '(a)') "Your selection: "
308
309     cont = .true.
310     do while(cont)
311         inp = GetCharacterInput(" ")
312         write(6, *)
313
314         if (inp == "T") then
315             call SetWingType(pf, Tapered)
316             cont = .false.
317         else if (inp == "E") then
318             call SetWingType(pf, Elliptic)
319             cont = .false.
320         else if (inp == "C") then
321             call SetWingType(pf, Combination)
322             cont = .false.
323         else
324             write(6, '(a)') "Invalid input, please make a selection from the
above menu."
325         end if
326     end do
327 end subroutine EditWingType
328
329 subroutine EditTransitionPoint(pf)
330     type(Planform), intent(inout) :: pf
331
332     character*80 :: msg
333     real*8 :: tp_old
334     logical :: isValid
335
336     tp_old = pf%TransitionPoint
337
338     msg = "Enter z/b at the transition point from tapered to elliptic"
339     call DisplayMessageWithRealDefault(msg, pf%TransitionPoint, 0)
340     call SetTransitionPoint(pf, GetRealInput(0.0d0, 0.5d0,
pf%TransitionPoint))

```

```

341
342     isValid = AreCombinationWingCoefficientsValid(pf)
343     do while(.not. isValid)
344         call SetTransitionPoint(pf, tp_old)
345         write(6, *)
346         write(6, '(a)') "The input provided results in invalid ellipse
coefficients."
347         write(6, '(a)') "Try a new value or press <ENTER> to accept
default."
348
349         call SetTransitionPoint(pf, GetRealInput(0.0d0, 0.5d0,
pf%TransitionPoint))
350         isValid = AreCombinationWingCoefficientsValid(pf)
351     end do
352 end subroutine EditTransitionPoint
353
354 subroutine EditTransitionChord(pf)
355     type(Planform), intent(inout) :: pf
356
357     character*80 :: msg
358     real*8 :: tc_old
359     logical :: isValid
360
361     tc_old = pf%TransitionChord
362
363     msg = "Enter c/croot at the transition point from tapered to elliptic"
364     call DisplayMessageWithRealDefault(msg, pf%TransitionChord, 0)
365     call SetTransitionChord(pf, GetRealInput(0.0d0, 10.0d0,
pf%TransitionChord))
366
367     isValid = AreCombinationWingCoefficientsValid(pf)
368     do while(.not. isValid)
369         call SetTransitionChord(pf, tc_old)
370         write(6, *)
371         write(6, '(a)') "The input provided results in invalid ellipse
coefficients."
372         write(6, '(a)') "Try a new value or press <ENTER> to accept
default."
373
374         call SetTransitionChord(pf, GetRealInput(0.0d0, 2.0d0,
pf%TransitionChord))
375         isValid = AreCombinationWingCoefficientsValid(pf)
376     end do
377 end subroutine EditTransitionChord
378
379 subroutine EditWashoutDistribution(pf)
380     type(Planform), intent(inout) :: pf
381
382     if (pf%WashoutDistribution == Linear) then
383         call SetWashoutDistribution(pf, Optimum)
384     else
385         call SetWashoutDistribution(pf, Linear)
386     end if
387 end subroutine EditWashoutDistribution
388
389 subroutine EditLowAspectRatioCorrectionMethod(pf)
390     type(Planform), intent(inout) :: pf
391
392     logical :: cont
393     character*2 :: inp
394

```

```

395     write(6, *)
396     write(6, '(a)') "Select from the following low-aspect-ratio correction
methods:"
397     write(6, '(2x, a)') "C - Classical Lifting Line Theory (no correction)"
398     write(6, '(2x, a)') "H - Hodson"
399     write(6, '(2x, a)') "M - Modified Slender Wing"
400     write(6, '(2x, a)') "K - Kuchemann"
401     write(6, *)
402     write(6, '(a)') "Your selection: "
403
404     cont = .true.
405     do while(cont)
406         inp = GetCharacterInput(" ")
407         write(6, *)
408
409         if (inp == "C") then
410             call SetLowAspectRatioMethod(pf, Classical)
411             cont = .false.
412         else if (inp == "H") then
413             call SetLowAspectRatioMethod(pf, Hodson)
414             cont = .false.
415         else if (inp == "M") then
416             call SetLowAspectRatioMethod(pf, ModifiedSlender)
417             cont = .false.
418         else if (inp == "K") then
419             call SetLowAspectRatioMethod(pf, Kuchemann)
420             cont = .false.
421         else
422             write(6, '(a)') "Invalid input, please make a selection from the
above menu."
423         end if
424     end do
425     end subroutine
426
427     subroutine EditNNodes(pf)
428         type(Planform), intent(inout) :: pf
429
430         character*80 :: msg
431         integer :: npss
432         character*80 :: int_str
433
434         npss = (pf%NNodes + 1) / 2
435
436         msg = "Enter number of nodes per semispan or press <ENTER> to accept
default"
437         call DisplayMessageWithIntegerDefault(msg, npss, 0)
438         call SetNNodes(pf, GetIntInput(4, 1000, npss))
439     end subroutine EditNNodes
440
441     subroutine EditAspectRatio(pf)
442         type(Planform), intent(inout) :: pf
443
444         character*80 :: msg
445
446         write(6, *)
447         msg = "Enter new aspect ratio or press <ENTER> to accept default"
448         call DisplayMessageWithRealDefault(msg, pf%AspectRatio, 0)
449         call SetAspectRatio(pf, GetRealInput(1.0d-12, 100.0d0, pf%AspectRatio))
450     end subroutine EditAspectRatio
451
452     subroutine EditTaperRatio(pf)

```

```

453     type(Planform), intent(inout) :: pf
454
455     character*80 :: msg
456
457     write(6, *)
458     msg = "Enter new taper ratio or press <ENTER> to accept default"
459     call DisplayMessageWithRealDefault(msg, pf%TaperRatio, 0)
460     call SetTaperRatio(pf, GetRealInput(0.0d0, 100.0d0, pf%TaperRatio))
461 end subroutine EditTaperRatio
462
463 subroutine EditLiftSlope(pf)
464     type(Planform), intent(inout) :: pf
465
466     character*80 :: msg
467
468     write(6, *)
469     msg = "Enter new section lift slope or press <ENTER> to accept default"
470     call DisplayMessageWithRealDefault(msg, pf%SectionLiftSlope, 0)
471     call SetSectionLiftSlope(pf, GetRealInput(-100.0d0 * pi, 100.0d0 * pi, &
472     & pf%SectionLiftSlope))
473 end subroutine EditLiftSlope
474
475 subroutine EditAileronRoot(pf)
476     type(Planform), intent(inout) :: pf
477
478     character*80 :: msg
479
480     write(6, *)
481     msg = "Enter new z/b for aileron root or press <ENTER> to accept
default"
482     call DisplayMessageWithRealDefault(msg, pf%AileronRoot, 0)
483     call SetAileronRoot(pf, GetRealInput(0.0d0, pf%AileronTip,
pf%AileronRoot))
484 end subroutine EditAileronRoot
485
486 subroutine EditAileronTip(pf)
487     type(Planform), intent(inout) :: pf
488
489     character*80 :: msg
490
491     write(6, *)
492     msg = "Enter new z/b for aileron tip or press <ENTER> to accept default"
493     call DisplayMessageWithRealDefault(msg, pf%AileronTip, 0)
494     call SetAileronTip(pf, GetRealInput(pf%AileronRoot, 0.5d0,
pf%AileronTip))
495 end subroutine EditAileronTip
496
497 subroutine EditFlapFractionRoot(pf)
498     type(Planform), intent(inout) :: pf
499
500     character*80 :: msg
501
502     write(6, *)
503     if (pf%ParallelHingeLine) then
504         write(6, '(a)') "NOTE: Hinge is no longer constrained to be parallel
with quarter-chord line."
505     end if
506
507     msg = "Enter new cf/c at aileron root or press <ENTER> to accept
default"
508     call DisplayMessageWithRealDefault(msg, pf%DesiredFlapFractionRoot, 0)

```

```

509         call SetFlapFractionRoot(pf, GetRealInput(0.0d0, 1.0d0,
pf%DesiredFlapFractionRoot))
510     end subroutine EditFlapFractionRoot
511
512     subroutine EditFlapFractionTip(pf)
513         type(Planform), intent(inout) :: pf
514
515         character*80 :: msg
516
517         write(6, *)
518         msg = "Enter new cf/c at aileron tip or press <ENTER> to accept default"
519         call DisplayMessageWithRealDefault(msg, pf%FlapFractionTip, 0)
520         call SetFlapFractionTip(pf, GetRealInput(0.0d0, 1.0d0,
pf%FlapFractionTip))
521     end subroutine EditFlapFractionTip
522
523     subroutine ToggleParallelHinge(pf)
524         type(Planform), intent(inout) :: pf
525
526         if (pf%ParallelHingeLine) then
527             call SetFlapFractionRoot(pf, pf%DesiredFlapFractionRoot)
528         else
529             call SetParallelHingeLine(pf)
530         end if
531     end subroutine ToggleParallelHinge
532
533     subroutine EditHingeEfficiency(pf)
534         type(Planform), intent(inout) :: pf
535
536         character*80 :: msg
537
538         write(6, *)
539         msg = "Enter aileron hinge efficiency or press <ENTER> to accept
default"
540         call DisplayMessageWithRealDefault(msg, pf%HingeEfficiency, 0)
541         call SetHingeEfficiency(pf, GetRealInput(0.0d0, 1.0d0,
pf%HingeEfficiency))
542     end subroutine EditHingeEfficiency
543
544     subroutine EditDeflectionEfficiency(pf)
545         type(Planform), intent(inout) :: pf
546
547         character*80 :: msg
548
549         write(6, *)
550         msg = "Enter deflection efficiency or press <ENTER> to accept default"
551         call DisplayMessageWithRealDefault(msg, pf%DeflectionEfficiency, 0)
552         call SetDeflectionEfficiency(pf, GetRealInput(0.0d0, 1.0d0, &
& pf%DeflectionEfficiency))
553     end subroutine EditDeflectionEfficiency
554
555     subroutine EditFileName(pf)
556         type(Planform), intent(inout) :: pf
557
558         character*80 :: msg
559
560         write(6, *)
561         msg = "Enter output file name or press <ENTER> to accept default"
562         call DisplayMessageWithTextDefault(msg, pf%FileName, 0)
563         call SetFileName(pf, GetStringInput(pf%FileName))
564     end subroutine EditFileName

```



```

566
567     subroutine EditAngleOfAttack(pf)
568         type(Planform), intent(inout) :: pf
569
570         character*80 :: msg
571
572         write(6, *)
573         write(6, '(a, a)') "NOTE: This operation will calculate a new lift ", &
574             & "coefficient and optimum washout."
575
576         msg = "Enter angle of attack or press <ENTER> to accept default"
577         call DisplayMessageWithAngleDefault(msg, pf%DesiredAngleOfAttack, 0)
578         call SetAngleOfAttack(pf, GetRealInput(-12.0d0, 12.0d0, &
579             & pf%DesiredAngleOfAttack * 180.0d0 / pi))
580     end subroutine EditAngleOfAttack
581
582     subroutine EditLiftCoefficient(pf)
583         type(Planform), intent(inout) :: pf
584
585         character*80 :: msg
586         real*8 :: mn, mx, dflt
587
588         mn = CL1(pf%CLa, -12.0d0 * pi / 180.0d0, pf%EW, pf%Washout)
589         mx = CL1(pf%CLa, 12.0d0 * pi / 180.0d0, pf%EW, pf%Washout)
590         if (pf%DesiredLiftCoefficient < mn) then
591             dflt = mn
592         else if (pf%DesiredLiftCoefficient > mx) then
593             dflt = mx
594         else
595             dflt = pf%DesiredLiftCoefficient
596         end if
597
598         write(6, *)
599         write(6, '(a, a)') "NOTE: This operation will calculate a new alpha ", &
600             & "and optimum washout"
601         msg = "Enter lift coefficient or press <ENTER> to accept default"
602         call DisplayMessageWithRealDefault(msg, dflt, 0)
603         call SetLiftCoefficient(pf, GetRealInput(mn, mx, dflt))
604     end subroutine EditLiftCoefficient
605
606     subroutine EditWashout(pf)
607         type(Planform), intent(inout) :: pf
608
609         character*80 :: msg
610
611         write(6, *)
612         if (pf%UseOptimumWashout) then
613             write(6, '(a)') "NOTE: Use of optimum total washout has been
disabled."
614         end if
615         msg = "Enter total washout or press <ENTER> to accept default"
616         call DisplayMessageWithAngleDefault(msg, pf%DesiredWashout, 0)
617         call SetWashout(pf, GetRealInput(-12.0d0, 12.0d0, pf%DesiredWashout *
180.0d0 / pi))
618     end subroutine EditWashout
619
620     subroutine ToggleUseOptimumWashout(pf)
621         type(Planform), intent(inout) :: pf
622
623         if (pf%UseOptimumWashout) then
624             call SetWashout(pf, pf%DesiredWashout * 180.0d0 / pi)

```

```

625         else
626             call SetOptimumWashout(pf)
627         end if
628     end subroutine ToggleUseOptimumWashout
629
630     subroutine EditAileronDeflection(pf)
631         type(Planform), intent(inout) :: pf
632
633         character*80 :: msg
634
635         write(6, *)
636         msg = "Enter aileron deflection or press <ENTER> to accept default"
637         call DisplayMessageWithAngleDefault(msg, pf%AileronDeflection, 0)
638         call SetAileronDeflection(pf, GetRealInput(-12.0d0, 12.0d0, &
639             & pf%AileronDeflection * 180.0d0 / pi))
640     end subroutine EditAileronDeflection
641
642     subroutine ToggleUseSteadyRollingRate(pf)
643         type(Planform), intent(inout) :: pf
644
645         pf%UseSteadyRollingRate = .not. pf%UseSteadyRollingRate
646         if (pf%UseSteadyRollingRate) then
647             call SetSteadyRollingRate(pf)
648         else
649             call SetRollingRate(pf, pf%DesiredRollingRate)
650         end if
651     end subroutine ToggleUseSteadyRollingRate
652
653     subroutine EditRollingRate(pf)
654         type(Planform), intent(inout) :: pf
655
656         character*80 :: msg
657
658         write(6, *)
659
660         if (pf%UseSteadyRollingRate) then
661             write(6, '(a)') "NOTE: Use of steady rolling rate has been
disabled."
662         end if
663
664         msg = "Enter dimensionless rolling rate or press <ENTER> to accept
default"
665         call DisplayMessageWithRealDefault(msg, pf%DesiredRollingRate, 0)
666         call SetRollingRate(pf, GetRealInput(-100.0d0, 100.0d0,
pf%DesiredRollingRate))
667     end subroutine EditRollingRate
668
669     subroutine DisplayMessageWithRealDefault(msg, dflt, tab)
670         character*80, intent(in) :: msg ! Message to be displayed
671         real*8, intent(in) :: dflt ! Default value to show in parenthesis
672         integer, intent(in) :: tab ! Size of indentation to use
673
674         call DisplayMessageWithTextDefault(msg, FormatReal(dflt, 5), tab)
675     end subroutine DisplayMessageWithRealDefault
676
677     subroutine DisplayMessageWithAngleDefault(msg, dflt, tab)
678         character*80, intent(in) :: msg ! Message to be displayed
679         real*8, intent(in) :: dflt ! Default value to show in parenthesis
680         integer, intent(in) :: tab ! Size of indentation to use
681
682         character*80 :: dflt_deg

```

```

683
684         write(dflt_deg, '(a, a)') trim(FormatReal(dflt * 180.0d0 / pi, 5)), "
degrees"
685         call DisplayMessageWithTextDefault(msg, dflt_deg, tab)
686     end subroutine DisplayMessageWithAngleDefault
687
688     subroutine DisplayMessageWithIntegerDefault(msg, dflt, tab)
689         character*80, intent(in) :: msg ! Message to be displayed
690         integer, intent(in) :: dflt ! Default value to show in parenthesis
691         integer, intent(in) :: tab ! Size of indentation to use
692
693         call DisplayMessageWithTextDefault(msg, FormatInteger(dflt), tab)
694     end subroutine DisplayMessageWithIntegerDefault
695
696     subroutine DisplayMessageWithTextDefault(msg, dflt, tab)
697         character*80, intent(in) :: msg ! Message to be displayed
698         character*80, intent(in) :: dflt ! Default value to show in parenthesis
699         integer, intent(in) :: tab ! Size of indentation to use
700
701         character*80 :: msg_fmt
702
703         if (tab == 0) then
704             msg_fmt = "(a, a, a, a)"
705         else
706             write(msg_fmt, '(a, i1, a)') "(", tab, "x, a, a, a, a)"
707         end if
708
709         write(6, msg_fmt) trim(msg), " ( ", trim(dflt), " )"
710     end subroutine DisplayMessageWithTextDefault
711
712     subroutine DisplayMessageWithLogicalDefault(msg, dflt, tab)
713         character*80, intent(in) :: msg ! Message to be displayed
714         logical, intent(in) :: dflt ! Default value to show in parenthesis
715         integer, intent(in) :: tab ! Size of indentation to use
716
717         character*80 :: tf
718
719         if (dflt) then
720             tf = "True"
721         else
722             tf = "False"
723         end if
724         call DisplayMessageWithTextDefault(msg, tf, tab)
725
726     end subroutine DisplayMessageWithLogicalDefault
727
728 end module LiftingLineInterface

```

### K.3 Planform Class Module (class\_Planform.f90)

```

1  module class_Planform
2      use Utilities
3      implicit none
4
5      public :: Planform
6
7      ! Supported wing types
8      enum, bind(C)
9          enumerator :: Tapered = 1, Elliptic = 2, Combination = 3
10     end enum

```

```

11
12     ! Supported washout distribution types
13     enum, bind(C)
14         enumerator :: Linear = 1, Optimum = 2
15     end enum
16
17     ! Supported low-aspect-ratio methods
18     enum, bind(C)
19         enumerator :: Classical=1, Hodson=2, ModifiedSlender=3, Kuchemann=4
20     end enum
21
22     type Planform
23         ! Wing Parameters
24         integer :: WingType = Tapered ! Wing type
25         integer :: WashoutDistribution = Linear ! Washout distribution type
26         integer :: NNodes = 99 ! Total number of nodes
27         real*8 :: AspectRatio = 5.56d0 ! Aspect ratio
28         real*8 :: TaperRatio = 1.0d0 ! Taper ratio (tapered wing only)
29         real*8 :: TransitionPoint = 0.25d0 ! Transition point (Combination wing
only)
30         real*8 :: TransitionChord = 1.0d0 ! c/croot at transtion point
(Combination wing only)
31         real*8 :: SectionLiftSlope = 2.0d0 * pi ! Section lift slope
32         real*8 :: AileronRoot = 0.253d0 ! Location of aileron root (z/b)
33         real*8 :: AileronTip = 0.438d0 ! Location of aileron tip (z/b)
34         logical :: ParallelHingeLine = .true. ! Is the hinge line parallel to
the
35                                     ! quarter-chord line? When true,
36                                     ! FlapFractionTip will be
calculated
37         real*8 :: DesiredFlapFractionRoot = 0.28d0 ! Desired flap fraction at
aileron root (cf/c)
38         real*8 :: FlapFractionRoot = 0.28d0 ! Flap fraction at aileron root
(cf/c)
39         real*8 :: FlapFractionTip = 0.25d0 ! Flap fraction at aileron tip (cf/c)
40         real*8 :: HingeEfficiency = 0.85d0 ! Aileron hinge efficiency
41         real*8 :: DeflectionEfficiency = 1.0d0 ! Aileron deflection efficiency
42         integer :: LowAspectRatioMethod = Classical ! Low-Aspect-Ratio
correction method
43
44         ! Coefficients for Tapered wing with elliptic tip
45         real*8 :: C1 = 0.0d0 ! Represents transition point
46         real*8 :: C2 = 0.0d0 ! Represents slope of tapered section
47         real*8 :: C3 = 0.0d0 ! Represents secondary axis of ellipse
48         real*8 :: C4 = 0.0d0 ! Represents ellipse center offset
49         real*8 :: C5 = 0.0d0 ! Represents croot/b
50
51         ! Output Options
52         logical :: OutputMatrices = .true. ! Write C Matrix and Fourier
coefficients to output file?
53         character*80 :: FileName = "planform.out" ! Name of output file
54
55         ! Operating Conditions
56         real*8 :: DesiredAngleOfAttack = pi / 36.0d0 ! Desired root aerodynamic
angle of Attack
57                                     ! (alpha - alpha_L0), in
radians
58                                     ! When specified, a new
LiftCoefficient is calculated
59         real*8 :: AngleOfAttack = pi / 36.0d0 ! Root Aerodynamic Angle of Attack
! (alpha - alpha_L0), in radians
60

```

```

61         real*8 :: DesiredLiftCoefficient = 0.4d0 ! Desired lift coefficient
62                                     ! When specified, a new
AngleOfAttack is calculated
63         real*8 :: LiftCoefficient = 0.4d0 ! Lift coefficient (user input,
ignored if SpecifyAlpha == .true.)
64         real*8 :: DesiredWashout = 0.0d0 ! Desired total washout, in radians
65         real*8 :: OptimumWashout1 = 0.0d0 ! Optimum total washout, in radians
(Eq. 1.8.37)
66         real*8 :: OptimumWashout2 = 0.0d0 ! Optimum total washout, in radians
(Eq. 1.8.42)
67         real*8 :: Washout = 0.0d0 ! Total washout to use
68         logical :: UseOptimumWashout = .true. ! Use the optimum total washout?
69         real*8 :: AileronDeflection = 0.0d0 ! Aileron deflection, in radians
70         real*8 :: DesiredRollingRate = 0.0d0 ! Desired dimensionless rolling
rate (constant over wingspan)
71         real*8 :: RollingRate = 0.0d0 ! Dimensionless rolling rate (constant
over wingspan)
72         logical :: SpecifyAlpha = .true. ! Was alpha specified?
73                                     ! .true. = Use desired alpha to
calculate CL
74                                     ! .false. = Use desired CL to calculate
alpha
75         logical :: UseSteadyRollingRate = .true. ! Use the steady dimensionless
rolling rate?
76
77         ! Planform Calculations
78         real*8, allocatable, dimension(:, :) :: BigC, BigC_Inv
79         real*8, allocatable, dimension(:) :: a, b, c, d, BigA
80         real*8, allocatable, dimension(:) :: Omega
81         logical :: IsAllocated = .false.
82
83         ! Lift Coefficient Calculations
84         real*8 :: KL ! Lift slope factor
85         real*8 :: EW ! Washout effectiveness (epsilon omega)
86         real*8 :: CLa ! Wing lift slope (derivative of CL with respect to alpha)
87         real*8 :: CL1 ! Lift Coefficient (Eq. 1.8.24)
88         real*8 :: CL2 ! Lift Coefficient (Eq. 1.8.5)
89
90         ! Drag Coefficient Calculations
91         real*8 :: KD ! Induced drag factor
92         real*8 :: KDL ! Lift-washout contribution to induced drag
93         real*8 :: KDW ! Washout contribution to induced drag
94         real*8 :: ES ! Span efficiency factor
95         real*8 :: CDi1 ! Induced drag coefficient (Eq. 1.8.25)
96         real*8 :: CDi2 ! Induced drag coefficient (Eq. 1.8.6)
97         real*8 :: CDi3 ! Induced drag coefficient (Eq. 32, Wing Flapping paper)
98
99         ! Roll/yaw calculations
100        real*8 :: CRM_da ! Change in rolling moment coefficient with respect
to alpha
101        real*8 :: CRM_pbar ! Change in rolling moment coefficient with respect
to rolling rate
102        real*8 :: CRM ! Rolling moment coefficient
103        real*8 :: CYM ! Yawing moment coefficient
104
105    end type Planform
106
107    contains
108        character*80 function GetWingType(pf) result(name)
109            type(Planform), intent(in) :: pf
110
111

```

```

111         if (pf%WingType .eq. Tapered) then
112             name = "Tapered"
113         else if (pf%WingType .eq. Elliptic) then
114             name = "Elliptic"
115         else if (pf%WingType .eq. Combination) then
116             name = "Tapered with elliptic tip"
117         else
118             name = "Unknown"
119         end if
120     end function GetWingType
121
122     character*80 function GetWashoutDistributionType(pf) result(name)
123         type(Planform), intent(in) :: pf
124
125         if (pf%WashoutDistribution .eq. Linear) then
126             name = "Linear"
127         else if (pf%WashoutDistribution .eq. Optimum) then
128             name = "Optimum"
129         else
130             name = "Unknown"
131         end if
132     end function GetWashoutDistributionType
133
134     character*80 function GetLowAspectRatioMethod(pf) result(name)
135         type(Planform), intent(in) :: pf
136
137         if (pf%LowAspectRatioMethod .eq. Classical) then
138             name = "Classical"
139         else if (pf%LowAspectRatioMethod .eq. Hodson) then
140             name = "Hodson"
141         else if (pf%LowAspectRatioMethod .eq. ModifiedSlender) then
142             name = "Modified Slender Wing"
143         else if (pf%LowAspectRatioMethod .eq. Kuchemann) then
144             name = "Kuchemann"
145         else
146             name = "Unknown"
147         end if
148     end function GetLowAspectRatioMethod
149
150     real*8 function theta_i(i, nnodes) result(theta)
151         integer, intent(in) :: i
152         integer, intent(in) :: nnodes
153
154         if (i < 1 .or. i > nnodes) then
155             write(6, '(a, i3)') "ERROR: Function theta_i called with i = ",
156 i
157             if (i < 1) then
158                 theta = 0.0d0
159             else
160                 theta = pi
161             end if
162         else
163             theta = real(i-1, 8) / real(nnodes - 1, 8) * pi
164         end if
165     end function theta_i
166
167     real*8 function theta_zb(zb) result(theta)
168         real*8, intent(in) :: zb ! z/b
169
170         if (zb < -0.5d0 .or. zb > 0.5d0) then

```

```

170         write(6, '(a, f7.4)') "ERROR: Function theta_d called with z/b =
", zb
171         if (zb < -0.5d0) then
172             theta = 0.0d0
173         else
174             theta = pi
175         end if
176     else
177         theta = acos(-2.0d0 * zb)
178     end if
179 end function theta_zb
180
181 real*8 function c_over_b_i(pf, i) result(cb)
182     type(Planform), intent(in) :: pf
183     integer, intent(in) :: i
184
185     real*8 :: theta
186
187     theta = theta_i(i, pf%NNodes)
188     cb = c_over_b(pf, theta)
189 end function c_over_b_i
190
191 real*8 function c_over_b_zb(pf, zb) result(cb)
192     type(Planform), intent(in) :: pf
193     real*8, intent(in) :: zb ! z/b
194
195     real*8 :: theta
196
197     theta = theta_zb(zb)
198     cb = c_over_b(pf, theta)
199 end function c_over_b_zb
200
201 real*8 function c_over_b(pf, theta) result(cb)
202     type(Planform), intent(in) :: pf
203     real*8, intent(in) :: theta
204
205     real*8 :: zb, u
206
207     if (pf%WingType == Tapered) then
208         ! Calculate c/b for tapered wing
209         cb = (2.0d0 * (1.0d0 - (1.0d0 - pf%TaperRatio) * &
210             & dabs(cos(theta)))) / (pf%AspectRatio * (1.0d0 +
211 pf%TaperRatio))
212     else if (pf%WingType == Elliptic) then
213         ! Calculate c/b for elliptic wing
214         cb = (4.0d0 * sin(theta)) / &
215             & (pi * pf%AspectRatio)
216     else if (pf%WingType == Combination) then
217         ! Calculate c/b for combination wing
218         zb = abs(z_over_b(theta))
219         if (zb <= pf%TransitionPoint) then
220             cb = pf%C5 * (1.0d0 - pf%C2 * zb)
221         else
222             u = (zb - pf%C4) / (0.5d0 - pf%C4)
223             cb = pf%C5 * pf%C3 * sqrt(1.0d0 - u**2)
224         end if
225     else
226         ! Unknown wing type!
227         stop "**** Unknown Wing Type ****"
228     end if
229 end function c_over_b

```

```

229
230  real*8 function z_over_b_i(i, nnodes) result(zb)
231      integer, intent(in) :: i
232      integer, intent(in) :: nnodes
233
234      zb = z_over_b(theta_i(i, nnodes))
235  end function z_over_b_i
236
237  real*8 function z_over_b(theta) result(zb)
238      real*8, intent(in) :: theta
239
240      zb = -0.5d0 * cos(theta)
241  end function z_over_b
242
243  real*8 function cf_over_c_i(pf, i) result(cfc)
244      type(Planform), intent(in) :: pf
245      integer, intent(in) :: i
246
247      real*8 :: zbi
248
249      zbi = z_over_b_i(i, pf%NNodes)
250      if (Compare(dabs(zbi), pf%AileronRoot, zero) == -1 .or. &
251          & Compare(dabs(zbi), pf%AileronTip, zero) == 1) then
252          cfc = 0.0d0
253      else
254          cfc = 0.75d0 - y_i(pf, i) / c_over_b_i(pf, i)
255      end if
256  end function cf_over_c_i
257
258  real*8 function y_i(pf, i) result(y)
259      type(Planform), intent(in) :: pf
260      integer, intent(in) :: i
261
262      real*8 :: zb_i, cb_i
263      real*8 :: zb_root, cfc_root, theta_root, cb_root, y_root
264      real*8 :: zb_tip, cfc_tip, theta_tip, cb_tip, y_tip
265      real*8 :: slope, offst
266
267      zb_root = pf%AileronRoot
268      cfc_root = pf%FlapFractionRoot
269      theta_root = theta_zb(zb_root)
270      cb_root = c_over_b(pf, theta_root)
271      y_root = (0.75d0 - cfc_root) * cb_root
272
273      zb_tip = pf%AileronTip
274      cfc_tip = pf%FlapFractionTip
275      theta_tip = theta_zb(zb_tip)
276      cb_tip = c_over_b(pf, theta_tip)
277      y_tip = (0.75d0 - cfc_tip) * cb_tip
278
279      slope = (y_tip - y_root) / (zb_tip - zb_root)
280      offst = y_root - slope * zb_root
281
282      zb_i = z_over_b_i(i, pf%NNodes)
283      y = slope * dabs(zb_i) + offst
284  end function y_i
285
286  real*8 function FlapEffectiveness(pf, i) result(eps_f)
287      type(Planform), intent(in) :: pf
288      integer, intent(in) :: i
289

```



```

290         real*8 :: theta_f, eps_fi
291
292         theta_f = acos(2.0d0 * cf_over_c_i(pf, i) - 1.0d0)
293         eps_fi = 1.0d0 - (theta_f - sin(theta_f)) / pi
294         eps_f = eps_fi * pf%HingeEfficiency * pf%DeflectionEfficiency
295     end function FlapEffectiveness
296
297     subroutine DeallocateArrays(pf)
298         type(Planform), intent(inout) :: pf
299
300         if (pf%IsAllocated) then
301             deallocate(pf%BigC)
302             deallocate(pf%BigC_Inv)
303             deallocate(pf%a)
304             deallocate(pf%b)
305             deallocate(pf%c)
306             deallocate(pf%d)
307             deallocate(pf%BigA)
308             deallocate(pf%Omega)
309
310             pf%IsAllocated = .false.
311         end if
312     end subroutine DeallocateArrays
313
314     subroutine AllocateArrays(pf)
315         type(Planform), intent(inout) :: pf
316
317         if (pf%IsAllocated) call DeallocateArrays(pf)
318
319         allocate(pf%BigC(pf%NNodes, pf%NNodes))
320         allocate(pf%BigC_Inv(pf%NNodes, pf%NNodes))
321         allocate(pf%a(pf%NNodes))
322         allocate(pf%b(pf%NNodes))
323         allocate(pf%c(pf%NNodes))
324         allocate(pf%d(pf%NNodes))
325         allocate(pf%BigA(pf%NNodes))
326         allocate(pf%Omega(pf%NNodes))
327         pf%IsAllocated = .true.
328     end subroutine AllocateArrays
329
330 end module class_Planform

```

#### K.4 Module of Setter Functions (liftinglinesetters.f90)

```

1  module LiftingLineSetters
2      use class_Planform
3      implicit none
4
5      contains
6          subroutine InitPlanform(pf)
7              type(Planform), intent(inout) :: pf
8
9              call SetParallelHingeLine(pf)
10         end subroutine InitPlanform
11
12         ! Planform Parameters
13         subroutine SetWingType(pf, wingType)
14             type(Planform), intent(inout) :: pf
15             integer, intent(in) :: wingType
16

```

```

17         if (pf%WingType /= wingType) then
18             pf%WingType = wingType
19             call DeallocateArrays(pf)
20
21             if (pf%WingType == Combination) then
22                 call SetCombinationWingCoefficients(pf)
23             else if (pf%ParallelHingeLine) then
24                 call SetParallelHingeLine(pf)
25             end if
26             if (pf%WingType == Elliptic) then
27                 pf%WashoutDistribution = Linear
28             end if
29         end if
30     end subroutine SetWingType
31
32     subroutine SetWashoutDistribution(pf, washoutDist)
33         type(Planform), intent(inout) :: pf
34         integer, intent(in) :: washoutDist
35
36         if (pf%WingType /= Elliptic .and. pf%WashoutDistribution /= washoutDist)
37             then
38                 pf%WashoutDistribution = washoutDist
39                 call DeallocateArrays(pf)
40             end if
41         end subroutine SetWashoutDistribution
42
43     subroutine SetLowAspectRatioMethod(pf, lowAspectRatioMethod)
44         type(Planform), intent(inout) :: pf
45         integer, intent(in) :: lowAspectRatioMethod
46
47         if (pf%LowAspectRatioMethod /= lowAspectRatioMethod) then
48             pf%LowAspectRatioMethod = lowAspectRatioMethod
49             call DeallocateArrays(pf)
50         end if
51     end subroutine SetLowAspectRatioMethod
52
53     subroutine SetTransitionPoint(pf, tp)
54         type(Planform), intent(inout) :: pf
55         real*8, intent(in) :: tp
56
57         if (Compare(pf%TransitionPoint, tp, zero) /= 0) then
58             pf%TransitionPoint = tp
59             call DeallocateArrays(pf)
60             call SetCombinationWingCoefficients(pf)
61         end if
62     end subroutine SetTransitionPoint
63
64     subroutine SetTransitionChord(pf, tc)
65         type(Planform), intent(inout) :: pf
66         real*8, intent(in) :: tc
67
68         if (Compare(pf%TransitionChord, tc, zero) /= 0) then
69             pf%TransitionChord = tc
70             call DeallocateArrays(pf)
71             call SetCombinationWingCoefficients(pf)
72         end if
73     end subroutine SetTransitionChord
74
75     subroutine SetCombinationWingCoefficients(pf)
76         type(Planform), intent(inout) :: pf

```

```

77      real*8 :: u, asin_u
78
79      pf%C1 = pf%TransitionPoint
80      pf%C2 = (1.0d0 - pf%TransitionChord) / pf%C1
81      pf%C4 = (pf%C1 - 0.25d0 * pf%C2) / (pf%C1 * pf%C2 - pf%C2 + 1.0d0)
82      u = (pf%C1 - pf%C4) / (0.5d0 - pf%C4)
83      asin_u = asin(u)
84      pf%C3 = (1.0d0 - pf%C1 * pf%C2) / sqrt(1.0d0 - u**2)
85      pf%C5 = 1.0d0 / (pf%AspectRatio * (2.0d0 * pf%C1 - pf%C1**2 * pf%C2 + &
86          & 0.5d0 * pf%C3 * (0.5d0 - pf%C4) * (pi - 2.0d0 * asin_u - &
87          & sin(2.0d0 * asin_u))))
88
89      if (pf%ParallelHingeLine) then
90          call SetParallelHingeLine(pf)
91      end if
92  end subroutine SetCombinationWingCoefficients
93
94  logical function AreCombinationWingCoefficientsValid(pf) result(isValid)
95      type(Planform), intent(in) :: pf
96
97      real*8 :: u, d1, d2
98
99      u = (pf%C1 - pf%C4) / (0.5d0 - pf%C4)
100     d1 = -pf%C2
101     d2 = -(pf%C3 * u) / (sqrt(1.0d0 - u**2) * (0.5d0 - pf%C4))
102
103     if (Compare(pf%C1, 0.0d0, zero) /= 1 .and. &
104         & Compare(pf%C1, 0.5d0, zero) /= -1) then
105         isValid = .false.
106     else if (Compare(pf%C1 * pf%C2 - pf%C2 + 1.0d0, 0.0d0, zero) == 0) then
107         isValid = .false.
108     else if (Compare(pf%C4, 0.5d0, zero) == 0) then
109         isValid = .false.
110     else if (Compare(dabs(u), 1.0d0, zero) /= -1) then
111         isValid = .false.
112     else if (Compare(d1, d2, zero) /= 0) then
113         isValid = .false.
114     else
115         isValid = .true.
116     end if
117 end function AreCombinationWingCoefficientsValid
118
119 subroutine SetNNodes(pf, npss)
120     type(Planform), intent(inout) :: pf
121     integer, intent(in) :: npss
122
123     integer :: nnodes
124
125     nnodes = npss * 2 - 1
126     if (pf%NNodes /= nnodes) then
127         pf%NNodes = nnodes
128         call DeallocateArrays(pf)
129     end if
130 end subroutine SetNNodes
131
132 subroutine SetAspectRatio(pf, ra)
133     type(Planform), intent(inout) :: pf
134     real*8, intent(in) :: ra
135
136     if (Compare(pf%AspectRatio, ra, zero) /= 0) then
137         pf%AspectRatio = ra

```

```

138         call DeallocateArrays(pf)
139     end if
140 end subroutine SetAspectRatio
141
142 subroutine SetTaperRatio(pf, rt)
143     type(Planform), intent(inout) :: pf
144     real*8, intent(in) :: rt
145
146     if (Compare(pf%TaperRatio, rt, zero) /= 0) then
147         pf%TaperRatio = rt
148         call DeallocateArrays(pf)
149
150         if (pf%ParallelHingeline) then
151             call SetParallelHingeline(pf)
152         end if
153     end if
154 end subroutine SetTaperRatio
155
156 subroutine SetSectionLiftSlope(pf, cla_sec)
157     type(Planform), intent(inout) :: pf
158     real*8, intent(in) :: cla_sec
159
160     if (Compare(pf%SectionLiftSlope, cla_sec, zero) /= 0) then
161         pf%SectionLiftSlope = cla_sec
162         call DeallocateArrays(pf)
163     end if
164 end subroutine SetSectionLiftSlope
165
166 subroutine SetAileronRoot(pf, ar)
167     type(Planform), intent(inout) :: pf
168     real*8, intent(in) :: ar
169
170     if (Compare(pf%AileronRoot, ar, zero) /= 0) then
171         pf%AileronRoot = ar
172         call DeallocateArrays(pf)
173     end if
174 end subroutine SetAileronRoot
175
176 subroutine SetAileronTip(pf, at)
177     type(Planform), intent(inout) :: pf
178     real*8, intent(in) :: at
179
180     if (Compare(pf%AileronTip, at, zero) /= 0) then
181         pf%AileronTip = at
182         call DeallocateArrays(pf)
183     end if
184 end subroutine SetAileronTip
185
186 subroutine SetParallelHingeline(pf)
187     type(Planform), intent(inout) :: pf
188
189     real*8 :: cfc_root_par
190
191     pf%ParallelHingeline = .true.
192     cfc_root_par = ParallelRootFlapFraction(pf)
193     if (Compare(pf%FlapFractionRoot, cfc_root_par, zero) /= 0) then
194         pf%FlapFractionRoot = cfc_root_par
195         call DeallocateArrays(pf)
196     end if
197 end subroutine SetParallelHingeline
198

```

```

199  subroutine SetFlapFractionRoot(pf, cfc_root)
200      type(Planform), intent(inout) :: pf
201      real*8, intent(in) :: cfc_root
202
203      pf%ParallelHingeLine = .false.
204      pf%DesiredFlapFractionRoot = cfc_root
205      if (Compare(pf%FlapFractionRoot, cfc_root, zero) /= 0) then
206          pf%FlapFractionRoot = cfc_root
207          call DeallocateArrays(pf)
208      end if
209  end subroutine SetFlapFractionRoot
210
211  subroutine SetFlapFractionTip(pf, cfc_tip)
212      type(Planform), intent(inout) :: pf
213      real*8, intent(in) :: cfc_tip
214
215      if (Compare(pf%FlapFractionTip, cfc_tip, zero) /= 0) then
216          pf%FlapFractionTip = cfc_tip
217          call DeallocateArrays(pf)
218
219          if (pf%ParallelHingeLine) then
220              call SetParallelHingeLine(pf)
221          end if
222      end if
223  end subroutine SetFlapFractionTip
224
225  subroutine SetHingeEfficiency(pf, eff_hinge)
226      type(Planform), intent(inout) :: pf
227      real*8, intent(in) :: eff_hinge
228
229      if (Compare(pf%HingeEfficiency, eff_hinge, zero) /= 0) then
230          pf%HingeEfficiency = eff_hinge
231          call DeallocateArrays(pf)
232      end if
233  end subroutine SetHingeEfficiency
234
235  subroutine SetDeflectionEfficiency(pf, eff_def)
236      type(Planform), intent(inout) :: pf
237      real*8, intent(in) :: eff_def
238
239      if (Compare(pf%DeflectionEfficiency, eff_def, zero) /= 0) then
240          pf%DeflectionEfficiency = eff_def
241          call DeallocateArrays(pf)
242      end if
243  end subroutine SetDeflectionEfficiency
244
245  subroutine ToggleOutputMatrices(pf)
246      type(Planform), intent(inout) :: pf
247
248      pf%OutputMatrices = .not. pf%OutputMatrices
249  end subroutine ToggleOutputMatrices
250
251  subroutine SetFileName(pf, filename)
252      type(Planform), intent(inout) :: pf
253      character*80, intent(in) :: filename
254
255      pf%FileName = trim(filename)
256  end subroutine SetFileName
257
258
259  ! Operating Conditions

```

```

260     subroutine SetAngleOfAttack(pf, alpha)
261         type(Planform), intent(inout) :: pf
262         real*8, intent(in) :: alpha
263
264         pf%SpecifyAlpha = .true.
265         pf%DesiredAngleOfAttack = alpha * pi / 180.0d0
266         pf%AngleOfAttack = pf%DesiredAngleOfAttack
267         if (pf%UseOptimumWashout) then
268             call SetOptimumWashout(pf)
269         end if
270         pf%LiftCoefficient = CL1(pf%CLa, pf%AngleOfAttack, pf%EW, pf%Washout)
271     end subroutine SetAngleOfAttack
272
273     subroutine SetLiftCoefficient(pf, cl)
274         type(Planform), intent(inout) :: pf
275         real*8, intent(in) :: cl
276
277         pf%SpecifyAlpha = .false.
278         pf%DesiredLiftCoefficient = cl
279         pf%LiftCoefficient = pf%DesiredLiftCoefficient
280         if (pf%UseOptimumWashout) then
281             call SetOptimumWashout(pf)
282         end if
283         pf%AngleOfAttack = RootAlpha(pf%CLa, pf%LiftCoefficient, pf%EW,
284 pf%Washout)
285     end subroutine SetLiftCoefficient
286
287     subroutine SetAileronDeflection(pf, da)
288         type(Planform), intent(inout) :: pf
289         real*8, intent(in) :: da
290
291         pf%AileronDeflection = da * pi / 180.0d0
292     end subroutine SetAileronDeflection
293
294     subroutine SetWashout(pf, washout)
295         type(Planform), intent(inout) :: pf
296         real*8, intent(in) :: washout
297
298         pf%DesiredWashout = washout * pi / 180.0d0
299         pf%Washout = pf%DesiredWashout
300         pf%UseOptimumWashout = .false.
301         if (pf%SpecifyAlpha) then
302             pf%LiftCoefficient = CL1(pf%CLa, pf%AngleOfAttack, pf%EW,
303 pf%Washout)
304         else
305             pf%AngleOfAttack = RootAlpha(pf%CLa, pf%LiftCoefficient, pf%EW,
306 pf%Washout)
307         end if
308     end subroutine SetWashout
309
310     subroutine SetOptimumWashout(pf)
311         type(Planform), intent(inout) :: pf
312
313         logical :: cont
314         integer :: i
315         real*8 :: oldCL, newCL, resCL
316         real*8 :: oldOmega, newOmega, resOmega
317
318         if (pf%SpecifyAlpha) then
319             oldCL = pf%LiftCoefficient
320             oldOmega = pf%Washout

```

```

318         cont = .true.
319         i = 0
320         do while (i < 100 .or. (cont .and. i < 1000))
321             i = i + 1
322             newOmega = OptimumWashout1(pf%KDL, oldCL, pf%KDW, pf%CLa)
323             newCL = CL1(pf%CLa, pf%AngleOfAttack, pf%EW, newOmega)
324
325             resCL = Residual(oldCL, newCL)
326             resOmega = Residual(oldOmega, newOmega)
327
328             cont = (Compare(resCL, 0.0d0, zero) /= 0 .or. Compare(resOmega,
0.0d0, zero) /= 0)
329             oldOmega = newOmega
330             oldCL = newCL
331         end do
332
333         if (i >= 1000) then
334             stop "**** Max number of convergence iterations reached! ****"
335         else
336             pf%LiftCoefficient = newCL
337             pf%OptimumWashout1 = newOmega
338         end if
339     end if
340
341     pf%OptimumWashout1 = OptimumWashout1(pf%KDL, pf%LiftCoefficient, &
& pf%KDW, pf%CLa)
342
343     if (pf%WashoutDistribution == Optimum) then
344         pf%OptimumWashout2 = OptimumWashout2(pf, pf%LiftCoefficient, &
pf%AspectRatio, pf%SectionLiftSlope)
345     end if
346
347     pf%Washout = pf%OptimumWashout1
348     pf%UseOptimumWashout = .true.
349
350     if (.not. pf%SpecifyAlpha) then
351         pf%AngleOfAttack = RootAlpha(pf%CLa, pf%LiftCoefficient, pf%EW,
pf%Washout)
352     end if
353 end subroutine SetOptimumWashout
354
355 subroutine SetRollingRate(pf, rollingrate)
356     type(Planform), intent(inout) :: pf
357     real*8, intent(in) :: rollingrate
358
359     pf%DesiredRollingRate = rollingrate
360     pf%RollingRate = rollingrate
361     pf%UseSteadyRollingRate = .false.
362 end subroutine
363
364 subroutine SetSteadyRollingRate(pf)
365     type(Planform), intent(inout) :: pf
366
367     real*8 :: steady_pbar
368
369     pf%RollingRate = SteadyRollingRate(pf)
370     pf%UseSteadyRollingRate = .true.
371 end subroutine SetSteadyRollingRate
372
373 real*8 function ParallelRootFlapFraction(pf) result(cfc_root_par)
374     type(Planform), intent(in) :: pf
375
376     real*8 :: cb_root, cfc_root

```

```

377     real*8 :: cb_tip, cfc_tip
378
379     cb_tip = c_over_b_zb(pf, pf%AileronTip)
380     cfc_tip = pf%FlapFractionTip
381     cb_root = c_over_b_zb(pf, pf%AileronRoot)
382     cfc_root_par = 0.75d0 - cb_tip / cb_root * (0.75d0 - cfc_tip)
383 end function ParallelRootFlapFraction
384
385 real*8 function RootAlpha(cla, cl, ew, omega) result(alpha)
386     real*8, intent(in) :: cla
387     real*8, intent(in) :: cl
388     real*8, intent(in) :: ew
389     real*8, intent(in) :: omega
390
391     alpha = cl / cla + ew * omega
392 end function RootAlpha
393
394 real*8 function SteadyRollingRate(pf) result(pbar_steady)
395     type(Planform), intent(in) :: pf
396
397     ! Calculate steady dimensionless rolling rate (Eq. 1.8.59)
398     pbar_steady = -pf%CRM_da / pf%CRM_pbar * pf%AileronDeflection
399 end function SteadyRollingRate
400
401 real*8 function OptimumWashout1(kdl, cl, kdw, cla) result(ow1)
402     real*8, intent(in) :: kdl
403     real*8, intent(in) :: cl
404     real*8, intent(in) :: kdw
405     real*8, intent(in) :: cla
406
407     ow1 = (kdl * cl) / (2.0d0 * kdw * cla)
408 end function OptimumWashout1
409
410 real*8 function OptimumWashout2(pf, cl, ra, ls) result(ow2)
411     type(Planform), intent(in) :: pf
412     real*8, intent(in) :: cl
413     real*8, intent(in) :: ra
414     real*8, intent(in) :: ls
415
416     ow2 = (4.0d0 * cl) / (pi * ra * ls * c_over_b(pf, pi / 2.0d0))
417 end function OptimumWashout2
418
419 real*8 function CL1(cla, alpha, ew, w) result(cl)
420     real*8, intent(in) :: cla
421     real*8, intent(in) :: alpha
422     real*8, intent(in) :: ew
423     real*8, intent(in) :: w
424
425     cl = cla * (alpha - ew * w) ! Eq. 1.8.24
426 end function CL1
427
428 real*8 function CL2(ra, bigA1) result(cl)
429     real*8, intent(in) :: ra
430     real*8, intent(in) :: bigA1
431
432     cl = pi * ra * bigA1 ! Eq. 1.8.5
433 end function CL2
434
435 real*8 function CDi1(pf) result(cdi)
436     type(Planform), intent(in) :: pf
437

```



```

438     real*8 :: n, a0, A, r1, r2
439
440     a0 = pf%SectionLiftSlope
441     A = pf%AspectRatio
442
443     ! Set the low aspect ratio method parameters
444     if (pf%LowAspectRatioMethod == Hodson) then
445         r1 = a0
446         r2 = A * (pi - atan((2.0 * a0) / (pi * A)))
447     else if (pf%LowAspectRatioMethod == ModifiedSlender) then
448         r1 = a0
449         r2 = 0.5 * pi * A
450     else if (pf%LowAspectRatioMethod == Kuchemann) then
451         n = 1.0 - 0.5 * (1.0 + (a0 / (pi * A))**2)**(-0.25)
452         r1 = 2 * n * a0 / (1.0 - pi * n / tan(pi * n))
453         r2 = pi * A / (2.0 * n)
454     else ! Assume Classical
455         r1 = a0
456         r2 = pi * A
457     end if
458
459     cdi = (pf%CL1**2 * (1.0d0 + pf%KD) - pf%KDL * pf%CL1 * pf%CLa * &
460           & pf%Washout + pf%KDW * (pf%CLa * pf%Washout)**2) / (pi * A) &
461           & * (r1 / r2) * (pi * A) / a0 ! Low-RA correction
462 end function CDi1
463
464 real*8 function CDi2(pf) result(cdi)
465     type(Planform), intent(in) :: pf
466
467     integer :: i
468
469     cdi = 0.0d0
470     do i = 1, pf%NNodes
471         cdi = cdi + real(i, 8) * pf%BigA(i)**2
472     end do
473     cdi = cdi * pi * pf%AspectRatio
474 end function CDi2
475
476 real*8 function CDi3(pf) result(cdi)
477     type(Planform), intent(in) :: pf
478
479     integer :: i
480     real*8 :: ri
481
482     cdi = 0.0d0
483     do i = 1, pf%NNodes
484         ri = real(i, 8)
485         cdi = cdi + ri * pf%BigA(i)**2
486     end do
487     cdi = (cdi - 0.5d0 * pf%RollingRate * pf%BigA(2)) * pi * pf%AspectRatio
488 end function CDi3
489
490 end module LiftingLineSetters

```

## K.5 Solver Module (liftinglinesolver.f90)

```

1  module LiftingLineSolver
2      use class_Planform
3      use LiftingLineSetters
4      use LiftingLineOutput

```

```

5      use matrix
6      implicit none
7
8  contains
9      subroutine ComputeCMatrixAndCoefficients(pf)
10         type(Planform), intent(inout) :: pf
11
12         write(6, '(a)') "Calculating C matrix and Fourier coefficients, please
wait..."
13         write(6, '(a, a, a)') "Estimated calculation time: ", &
14             & trim(FormatReal(pf%NNodes**2 * 1.0d-5, 3)), " seconds"
15         write(6, *)
16
17         if (.not. pf%IsAllocated) then
18             if (pf%WingType == Combination) then
19                 call SetCombinationWingCoefficients(pf)
20             end if
21
22             call AllocateArrays(pf)
23
24             call ComputeC(pf, pf%BigC)
25             call ComputeCInverse(pf, pf%BigC_Inv)
26             call ComputeFourierCoefficients_a(pf, pf%a)
27             call ComputeFourierCoefficients_b(pf, pf%b, pf%Omega)
28             call ComputeFourierCoefficients_c(pf, pf%c)
29             call ComputeFourierCoefficients_d(pf, pf%d)
30
31             call ComputeLiftCoefficientParameters(pf)
32             call ComputeDragCoefficientParameters(pf)
33             call ComputeRollCoefficientParameters(pf)
34             call ComputeFlightConditions(pf)
35         end if
36     end subroutine ComputeCMatrixAndCoefficients
37
38     subroutine ComputeFourierCoefficients_a(pf, a)
39         type(Planform), intent(in) :: pf
40         real*8, intent(out) :: a(pf%NNodes)
41
42         real*8 :: ones(pf%NNodes)
43         integer :: i
44         integer :: nnodes
45
46         nnodes = pf%NNodes
47         ones = (/ (1.0d0, i=1, nnodes) /)
48         if (pf%WingType == Tapered .and. Compare(pf%TaperRatio, 0.0d0, zero) ==
0) then
49             ones(1) = 0.0d0
50             ones(nnodes) = 0.0d0
51         end if
52
53         a = matmul(pf%BigC_Inv, ones)
54     end subroutine ComputeFourierCoefficients_a
55
56     subroutine ComputeFourierCoefficients_b(pf, b, omega)
57         type(Planform), intent(in) :: pf
58         real*8, intent(out) :: b(pf%NNodes)
59         real*8, intent(out) :: omega(pf%NNodes)
60
61         real*8 :: croot_over_b, theta
62         integer :: i
63         integer :: nnodes

```

```

64
65     nnodes = pf%NNodes
66     if (pf%WashoutDistribution == Linear) then
67         omega = (/ (dabs(cos(theta_i(i, nnodes))), i=1, nnodes) /)
68         if (pf%WingType == Tapered .and. Compare(pf%TaperRatio, 0.0d0, zero)
== 0) then
69             omega(1) = 0.0d0
70             omega(nnodes) = 0.0d0
71         end if
72     else if (pf%WashoutDistribution == Optimum) then
73         croot_over_b = c_over_b(pf, pi / 2.0d0)
74         do i = 1, nnodes
75             theta = theta_i(i, nnodes)
76             omega(i) = 1.0d0 - sin(theta) / (c_over_b(pf, theta) /
croot_over_b)
77         end do
78
79         if (pf%WingType == Combination) then
80             omega(1) = 1.0d0 - sqrt(1.0d0 - 2.0d0 * pf%C4) / pf%C3
81             omega(nnodes) = omega(1)
82         else if (pf%WingType == Tapered .and. Compare(pf%TaperRatio, 0.0d0,
zero) == 0) then
83             omega(1) = 2.0d0
84             omega(nnodes) = 2.0d0
85         end if
86     else
87         write(6, '(a)') "Unknown washout distribution type!"
88         stop
89     end if
90
91     b = matmul(pf%BigC_Inv, omega)
92 end subroutine ComputeFourierCoefficients_b
93
94 subroutine ComputeFourierCoefficients_c(pf, c)
95     type(Planform), intent(in) :: pf
96     real*8, intent(out) :: c(pf%NNodes)
97
98     real*8 :: chi(pf%NNodes)
99     real*8 :: zbi
100    integer :: i
101    integer :: nnodes
102
103    nnodes = pf%NNodes
104    do i = 1, nnodes
105        zbi = z_over_b_i(i, nnodes)
106        chi(i) = -sign(FlapEffectiveness(pf, i), zbi)
107    end do
108
109    if (pf%WingType == Tapered .and. Compare(pf%TaperRatio, 0.0d0, zero) ==
0) then
110        chi(1) = 0.0d0
111        chi(nnodes) = 0.0d0
112    end if
113
114    c = matmul(pf%BigC_Inv, chi)
115 end subroutine ComputeFourierCoefficients_c
116
117 subroutine ComputeFourierCoefficients_d(pf, d)
118     type(Planform), intent(in) :: pf
119     real*8, intent(out) :: d(pf%NNodes)
120

```

```

121     real*8 :: cos_theta(pf%NNodes)
122     integer :: i
123     integer :: nnodes
124
125     nnodes = pf%NNodes
126     cos_theta = (/ (cos(theta_i(i, nnodes))), i=1, nnodes) /)
127     if (pf%WingType == Tapered .and. Compare(pf%TaperRatio, 0.0d0, zero) ==
0) then
128         cos_theta(1) = 0.0d0
129         cos_theta(nnodes) = 0.0d0
130     end if
131
132     d = matmul(pf%BigC_Inv, cos_theta)
133 end subroutine ComputeFourierCoefficients_d
134
135 subroutine ComputeBigACoefficients(pf, bigA)
136     type(Planform), intent(in) :: pf
137     real*8, intent(out) :: bigA(pf%NNodes)
138
139     integer :: i
140
141     do i = 1, pf%NNodes
142         bigA(i) = pf%a(i) * pf%AngleOfAttack - pf%b(i) * pf%Washout + &
143             & pf%c(i) * pf%AileronDeflection + pf%d(i) * pf%RollingRate
144     end do
145 end subroutine ComputeBigACoefficients
146
147 subroutine ComputeLiftCoefficientParameters(pf)
148     type(Planform), intent(inout) :: pf
149
150     pf%KL = Kappa_L(pf%AspectRatio, pf%SectionLiftSlope, pf%a(1))
151     pf%EW = Epsilon_Omega(pf%a(1), pf%b(1))
152     pf%CLa = C_L_alpha(pf%AspectRatio, pf%a(1))
153 end subroutine ComputeLiftCoefficientParameters
154
155 subroutine ComputeDragCoefficientParameters(pf)
156     type(Planform), intent(inout) :: pf
157
158     pf%KD = Kappa_D(pf%NNodes, pf%a)
159     pf%ES = SpanEfficiencyFactor(pf%KD)
160     pf%KDL = Kappa_DL(pf%NNodes, pf%a, pf%b)
161     pf%KDW = Kappa_DOmega(pf%NNodes, pf%a, pf%b)
162 end subroutine ComputeDragCoefficientParameters
163
164 subroutine ComputeRollCoefficientParameters(pf)
165     type(Planform), intent(inout) :: pf
166
167     pf%CRM_da = CRM_dAlpha(pf%AspectRatio, pf%c(2))
168     pf%CRM_pbar = CRM_PBar(pf%AspectRatio, pf%d(2))
169 end subroutine ComputeRollCoefficientParameters
170
171 real*8 function Kappa_L(ra, cla_section, a1) result(kl)
172     real*8, intent(in) :: ra
173     real*8, intent(in) :: cla_section
174     real*8, intent(in) :: a1
175
176     kl = 1.0d0 / ((1.0d0 + pi * ra / cla_section) * a1) - 1.0d0
177 end function Kappa_L
178
179 real*8 function Epsilon_Omega(a1, b1) result(ew)
180     real*8, intent(in) :: a1

```

```

181         real*8, intent(in) :: b1
182
183         ew = b1 / a1
184     end function Epsilon_Omega
185
186     real*8 function C_L_alpha(ra, a1) result(cla)
187         real*8, intent(in) :: ra
188         real*8, intent(in) :: a1
189
190         cla = pi * ra * a1
191     end function C_L_alpha
192
193     real*8 function Kappa_D(nnodes, a) result(kd)
194         integer, intent(in) :: nnodes
195         real*8, intent(in) :: a(nnodes)
196
197         integer :: i
198
199         kd = 0.0d0
200         do i = 2, nnodes
201             kd = kd + real(i, 8) * (a(i) / a(1))**2
202         end do
203     end function Kappa_D
204
205     real*8 function SpanEfficiencyFactor(kd) result(es)
206         real*8, intent(in) :: kd
207         es = 1.0d0 / (1.0d0 + kd)
208     end function SpanEfficiencyFactor
209
210     real*8 function Kappa_DL(nnodes, a, b) result(kd1)
211         integer, intent(in) :: nnodes
212         real*8, intent(in) :: a(nnodes)
213         real*8, intent(in) :: b(nnodes)
214
215         integer :: i
216
217         kd1 = 0.0d0
218         do i = 2, nnodes
219             kd1 = kd1 + real(i, 8) * a(i) / a(1) * &
220                 & (b(i) / b(1) - a(i) / a(1))
221         end do
222         kd1 = kd1 * 2.0d0 * b(1) / a(1)
223     end function Kappa_DL
224
225     real*8 function Kappa_DOmega(nnodes, a, b) result(kdw)
226         integer, intent(in) :: nnodes
227         real*8, intent(in) :: a(nnodes)
228         real*8, intent(in) :: b(nnodes)
229
230         integer :: i
231
232         kdw = 0.0d0
233         do i = 2, nnodes
234             kdw = kdw + real(i, 8) * (b(i) / b(1) - a(i) / a(1))**2
235         end do
236         kdw = kdw * (b(1) / a(1))**2
237     end function Kappa_DOmega
238
239     real*8 function CRM_dAlpha(ra, c2) result(crmda)
240         real*8, intent(in) :: ra
241         real*8, intent(in) :: c2

```

```

242
243     crmda = -pi * ra / 4.0d0 * c2
244 end function CRM_dAlpha
245
246 real*8 function CRM_PBar(ra, d2) result(crmmpbar)
247     real*8, intent(in) :: ra
248     real*8, intent(in) :: d2
249
250     crmpbar = -pi * ra / 4.0d0 * d2
251 end function CRM_PBar
252
253 subroutine ComputeFlightConditions(pf)
254     type(Planform), intent(inout) :: pf
255
256     ! Make sure planform characteristics have been computed
257     if (.not. pf%IsAllocated) then
258         call ComputeCMatrixAndCoefficients(pf)
259     end if
260
261     ! Compute root aerodynamic angle of attack, if necessary
262     if (.not. pf%SpecifyAlpha) then
263         pf%AngleOfAttack = RootAlpha(pf%CLa, pf%LiftCoefficient, pf%EW,
pf%Washout)
264     else
265         pf%LiftCoefficient = CL1(pf%CLa, pf%AngleOfAttack, pf%EW,
pf%Washout)
266     end if
267
268     ! Compute optimum total washout, if necessary
269     if (pf%UseOptimumWashout) then
270         call SetOptimumWashout(pf)
271     else
272         call SetWashout(pf, pf%DesiredWashout * 180.0d0 / pi)
273     end if
274
275     ! Compute steady rolling rate, if necessary
276     if (pf%UseSteadyRollingRate) then
277         call SetSteadyRollingRate(pf)
278     end if
279
280     ! Compute BigA Fourier Coefficients
281     call ComputeBigACoefficients(pf, pf%BigA)
282
283     ! Compute lift coefficients
284     call ComputeLiftCoefficients(pf)
285
286     ! Compute drag coefficient
287     call ComputeDragCoefficients(pf)
288
289     ! Compute roll coefficient
290     pf%CRM = CRoll(pf%CRM_da, pf%CRM_pbar, pf%AileronDeflection,
pf%RollingRate)
291
292     ! Compute yaw coefficient
293     pf%CYM = CYaw(pf, pf%CL1, pf%BigA)
294 end subroutine ComputeFlightConditions
295
296 subroutine ComputeLiftCoefficients(pf)
297     type(Planform), intent(inout) :: pf
298
299     pf%CL1 = CL1(pf%CLa, pf%AngleOfAttack, pf%EW, pf%Washout)

```

```

300     pf%CL2 = CL2(pf%AspectRatio, pf%BigA(1))
301 end subroutine ComputeLiftCoefficients
302
303 subroutine ComputeDragCoefficients(pf)
304     type(Planform), intent(inout) :: pf
305
306     pf%CDi1 = CDi1(pf)
307     pf%CDi2 = CDi2(pf)
308     pf%CDi3 = CDi3(pf)
309 end subroutine ComputeDragCoefficients
310
311 real*8 function CRoll(crmda, crmpbar, da, pbar) result(crm)
312     real*8, intent(in) :: crmda
313     real*8, intent(in) :: crmpbar
314     real*8, intent(in) :: da
315     real*8, intent(in) :: pbar
316
317     crm = crmda * da + crmpbar * pbar
318 end function CRoll
319
320 real*8 function CYaw(pf, cl, bigA) result(cym)
321     type(Planform), intent(in) :: pf
322     real*8, intent(in) :: cl
323     real*8, intent(in) :: bigA(pf%NNodes)
324
325     integer :: i
326     integer :: nnodes
327     nnodes = pf%NNodes
328
329     cym = cl / 8.0d0 * (6.0d0 * bigA(2) - pf%RollingRate) + &
330         & pi * pf%AspectRatio / 8.0d0 * (10.0d0 * bigA(2) - &
331         & pf%RollingRate) * bigA(3)
332     do i = 4, nnodes
333         cym = cym + 0.25d0 * pi * pf%AspectRatio * &
334             & (2.0d0 * real(i, 8) - 1.0d0) * bigA(i-1) * bigA(i)
335     end do
336 end function CYaw
337
338 subroutine ComputeC(pf, c)
339     type(Planform), intent(in) :: pf
340     real*8, intent(inout) :: c(pf%NNodes, pf%NNodes)
341
342     integer :: i
343     integer :: nnodes
344
345     nnodes = pf%NNodes
346
347     ! Compute values for i=1, i=N
348     call C1j_Nj(c, pf)
349
350     ! Compute values for i=2 to i=N-1
351     do i = 2, nnodes-1
352         call Cij(c, i, pf)
353     end do
354 end subroutine ComputeC
355
356 subroutine ComputeCInverse(pf, c_inv)
357     type(Planform), intent(in) :: pf
358     real*8, intent(inout) :: c_inv(pf%NNodes, pf%NNodes)
359
360     call matinv_gauss(pf%NNodes, pf%BigC, c_inv)

```

```

361     end subroutine ComputeCInverse
362
363     subroutine C1j_Nj(c, pf)
364         real*8, dimension(:,:), intent(inout) :: c
365         type(Planform), intent(in) :: pf
366
367         integer :: j
368         integer :: jsq
369         integer :: nnode
370         real*8 :: cb0
371
372         nnode = pf%NNodes
373         do j = 1, nnode
374             jsq = j**2
375             c(1, j) = real(jsq, 8)
376             c(nnode, j) = real((-1)**(j + 1) * jsq, 8)
377         end do
378
379         cb0 = c_over_b(pf, pi)
380         if (dabs(cb0) < 1.0d-10) then
381             call C1j_Nj_zero_chord(c, pf)
382         end if
383
384     end subroutine C1j_Nj
385
386     subroutine Cij(c, i, pf)
387         real*8, dimension(:,:), intent(inout) :: c
388         integer, intent(in) :: i
389         type(Planform), intent(in) :: pf
390
391         integer :: j
392         integer :: nnode
393         real*8 :: theta
394         real*8 :: cb
395         real*8 :: sin_theta
396         real*8 :: a0, A, r1, r2, r1y
397         real*8 :: n
398
399         nnode = pf%NNodes
400         theta = theta_i(i, nnode)
401         cb = c_over_b_i(pf, i)
402         sin_theta = sin(theta)
403
404         a0 = pf%SectionLiftSlope
405         A = pf%AspectRatio
406
407         ! Set the low aspect ratio method parameters
408         if (pf%LowAspectRatioMethod == Hodson) then
409             r1 = a0 * (A / cb * sin_theta)**exp(-8.0 * A)
410             r2 = A * (pi - atan((2.0 * a0) / (pi * A)))
411         else if (pf%LowAspectRatioMethod == ModifiedSlender) then
412             r1 = a0
413             r2 = 0.5 * pi * A
414         else if (pf%LowAspectRatioMethod == Kuchemann) then
415             n = 1.0 - 0.5 * (1.0 + (a0 / (pi * A))**2)**(-0.25)
416             r1 = 2 * n * a0 / (1.0 - pi * n / tan(pi * n))
417             r2 = pi * A / (2.0 * n)
418         else ! Assume Classical
419             r1 = a0
420             r2 = pi * A
421         end if

```



```

422
423     do j = 1, nnode
424         c(i, j) = (4.0d0 / (pf%SectionLiftSlope * cb) * (a0 / r1) + &
425             & real(j, 8) / sin_theta * ((pi * A) / r2)) * sin(real(j, 8) *
theta)
426     end do
427 end subroutine Cij
428
429 subroutine C1j_Nj_zero_chord(c, pf)
430     real*8, dimension(:, :, intent(inout)) :: c
431     type(Planform), intent(in) :: pf
432
433     integer :: j, n
434
435     n = pf%NNodes
436
437     if (pf%WingType == Tapered) then
438         do j = 1, n
439             c(1, j) = 2.0d0 * pf%AspectRatio * (1.0d0 + real(j, 8))
440             c(n, j) = real((-1)**(j + 1), 8) * c(1, j)
441         end do
442     else if (pf%WingType == Elliptic) then
443         do j = 1, n
444             c(1, j) = c(1, j) + real(j, 8) * pi * &
445                 & pf%AspectRatio / pf%SectionLiftSlope
446             c(n, j) = c(n, j) + real((-1)**(j + 1) * j, 8) * pi * &
447                 & pf%AspectRatio / pf%SectionLiftSlope
448         end do
449     else if (pf%WingType == Combination) then
450         ! TODO: Add code for combination wing type
451         do j = 1, n
452             c(1, j) = c(1, j) + 4.0d0 * real(j, 8) * &
453                 & sqrt(1.0d0 - 2.0d0 * pf%C4) / &
454                 & (pf%C3 * pf%C5 * pf%SectionLiftSlope)
455             c(n, j) = c(n, j) + 4.0d0 * real((-1)**(j + 1) * j, 8) * &
456                 & sqrt(1.0d0 - 2.0d0 * pf%C4) / &
457                 & (pf%C3 * pf%C5 * pf%SectionLiftSlope)
458         end do
459     else
460         stop "**** Unknown Wing Type ****"
461     end if
462
463 end subroutine C1j_Nj_zero_chord
464
465 end module LiftingLineSolver

```

## K.6 Output Module (liftinglineoutput.f90)

```

1  module LiftingLineOutput
2      use Utilities
3      use class_Planform
4      use LiftingLineSetters
5      use matrix
6      implicit none
7
8  contains
9      subroutine OutputHeader()
10         integer :: i
11
12         write(6, ('(80a)')) ("*", i=1, 80)

```

```

13     write(6, '(34x, a)') "Pralines v1.0"
14     write(6, *)
15     write(6, '(28x, a)') "Author: Josh Hodson"
16     write(6, '(28x, a)') "Release Date: 20 Nov 2013"
17     write(6, *)
18     write(6, '(80a)') ("*", i=1, 80)
19 end subroutine OutputHeader
20
21 subroutine OutputPlanform(pf)
22     type(Planform), intent(in) :: pf
23
24     ! Open a clean file for output
25     open(unit=10, file=pf%FileName, action='WRITE')
26
27     ! Output the planform summary to output file
28     call OutputPlanformSummary(10, pf)
29
30     ! Output C matrix and fourier coefficients to output file
31     if (pf%OutputMatrices) then
32         call OutputC(10, pf%NNodes, pf%BigC)
33         call OutputCInverse(10, pf%NNodes, pf%BigC_Inv)
34         call OutputFourierCoefficients(10, pf)
35     end if
36
37     ! Close the output file
38     close(unit=10)
39 end subroutine OutputPlanform
40
41 subroutine OutputLiftCoefficientParameters(u, pf)
42     integer, intent(in) :: u ! Output unit
43     type(Planform), intent(in) :: pf
44
45     write(u, '(a)') "Lift Coefficient Parameters:"
46     write(u, '(2x, a, f20.15)') "KL    = ", pf%KL
47     write(u, '(2x, a, f20.15)') "CL,a  = ", pf%CLa
48     write(u, '(2x, a, f20.15)') "EW    = ", pf%EW
49     write(u, *)
50 end subroutine OutputLiftCoefficientParameters
51
52 subroutine OutputDragCoefficientParameters(u, pf)
53     integer, intent(in) :: u ! Output unit
54     type(Planform), intent(in) :: pf
55
56     write(u, '(a)') "Drag Coefficient Parameters:"
57     write(u, '(2x, a, f20.15)') "KD    = ", pf%KD
58     write(u, '(2x, a, f20.15)') "KDL   = ", pf%KDL
59     write(u, '(2x, a, f20.15)') "KDW   = ", pf%KDW
60     write(u, '(2x, a, f20.15)') "es    = ", pf%ES
61     write(u, *)
62 end subroutine OutputDragCoefficientParameters
63
64 subroutine OutputRollCoefficientParameters(u, pf)
65     integer, intent(in) :: u ! Output unit
66     type(Planform), intent(in) :: pf
67
68     write(u, '(a)') "Rolling Moment Coefficient Parameters:"
69     write(u, '(2x, a, f20.15)') "Cl,da = ", pf%CrM_da
70     write(u, '(2x, a, f20.15)') "Cl,pb = ", pf%CrM_pbar
71     write(u, *)
72 end subroutine OutputRollCoefficientParameters
73

```

```

74     subroutine OutputFlightConditions(pf)
75         type(Planform), intent(in) :: pf
76
77         ! Open the file and append flight conditions to end
78         open(unit=10, file=pf%FileName, access="append")
79
80         ! Output flight conditions to output file
81         call OutputOperatingConditions(10, pf)
82         call OutputFlightCoefficients(10, pf)
83
84         ! Close the output file
85         close(unit=10)
86     end subroutine OutputFlightConditions
87
88     subroutine OutputOperatingConditions(u, pf)
89         integer, intent(in) :: u ! Output unit
90         type(Planform), intent(in) :: pf
91
92         write(u, '(a15, 19x, 1x, a1, f20.15, 1x, a)') "Optimum washout", &
93             & "=", pf%OptimumWashout1 * 180.0d0 / pi, "degrees (Eq. 1.8.37)"
94         if (pf%WashoutDistribution == Optimum) then
95             write(u, '(a15, 19x, 1x, a1, f20.15, 1x, a)') "Optimum washout", &
96                 & "=", pf%OptimumWashout2 * 180.0d0 / pi, "degrees (Eq. 1.8.42)"
97         end if
98         write(u, '(a28, 6x, 1x, a1, f20.15, 1x, a)') "Washout used in
calculations", &
99             & "=", pf%Washout * 180.0d0 / pi, "degrees"
100        write(u, '(a18, 16x, 1x, a1, f20.15, 1x, a)') &
101            & "Aileron deflection", "=", &
102            & pf%AileronDeflection * 180.0d0 / pi, "degrees"
103        write(u, '(a33, 1x, 1x, a1, f20.15)') &
104            & "Steady dimensionless rolling rate", "=", SteadyRollingRate(pf)
105        write(u, '(a31, 3x, 1x, a1, f20.15)') &
106            & "Dimensionless rolling rate used", "=", pf%RollingRate
107        write(u, '(a32, 2x, 1x, a1, f20.15, 1x, a)') &
108            & "Root aerodynamic angle of attack", "=", &
109            & pf%AngleOfAttack * 180.0d0 / pi, "degrees"
110        write(u, *)
111    end subroutine OutputOperatingConditions
112
113    subroutine OutputFlightCoefficients(u, pf)
114        integer, intent(in) :: u ! Output unit
115        type(Planform), intent(in) :: pf
116
117        write(u, '(a)') "Flight Coefficients:"
118        write(u, '(2x, a, f20.15, a)') "CL    = ", pf%CL1, " (Eq. 1.8.24)"
119        write(u, '(2x, a, f20.15, a)') "CL    = ", pf%CL2, " (Eq. 1.8.5)"
120        write(u, '(2x, a, f20.15, a)') "CDi    = ", pf%CDi1, " (Eq. 1.8.25)"
121        write(u, '(2x, a, f20.15, a)') "CDi    = ", pf%CDi2, " (Eq. 1.8.6)"
122        write(u, '(2x, a, f20.15, a)') "CDi    = ", pf%CDi3, " (Exact)"
123        write(u, '(2x, a, f20.15)') "Croll = ", pf%CRM
124        write(u, '(2x, a, f20.15)') "Cyaw  = ", pf%CYM
125        write(u, *)
126    end subroutine OutputFlightCoefficients
127
128    subroutine OutputPlanformSummary(u, pf)
129        integer, intent(in) :: u
130        type(Planform), intent(in) :: pf
131
132        character*80 :: fmt_str
133        integer :: len_nnodes

```

```

134
135     len_nnodes = int(log10(real(pf%NNodes))) + 1
136     write(fmt_str, '(a,i1,a,i1,a)') "(2x, a15, 11x, 1x, a1, 3x, i", &
137         & len_nnodes, ", 1x, a, i", len_nnodes, ",a)"
138
139     write(u, '(a)') "Planform Summary:"
140
141     ! Wing type
142     write(u, '(2x, a9, 17x, 1x, a1, 3x, a)') "Wing type", "=", &
143         & trim(GetWingType(pf))
144
145     ! Number of nodes
146     write(u, fmt_str) "Number of nodes", "=", pf%NNodes, " (" , &
147         & (pf%NNodes + 1) / 2, " nodes per semispan)"
148
149     ! Section Lift Slope
150     write(u, '(2x, a26, 1x, a1, f20.15)') &
151         & "Airfoil section lift slope", "=", pf%SectionLiftSlope
152
153     ! Aspect Ratio
154     write(u, '(2x, a12, 14x, 1x, a1, f20.15)') &
155         & "Aspect Ratio", "=", pf%AspectRatio
156
157     ! Taper Ratio
158     if (pf%WingType == Tapered) then
159         write(u, '(2x, a11, 15x, 1x, a1, f20.15)') &
160             & "Taper Ratio", "=", pf%TaperRatio
161     end if
162
163     ! Transition from tapered to elliptic
164     if (pf%WingType == Combination) then
165         write(u, '(2x, a20, 6x, 1x, a1, f20.15)') "Transition Point z/b", &
166             & "=", pf%TransitionPoint
167         write(u, '(2x, a20, 6x, 1x, a1, f20.15)') "Transition Point
c/croot", &
168             & "=", pf%TransitionChord
169     end if
170
171     ! Washout distribution type
172     if (pf%WingType /= Elliptic) then
173         write(u, '(2x, a20, 6x, 1x, a1, 3x, a)') "Washout Distribution", &
174             & "=", trim(GetWashoutDistributionType(pf))
175     end if
176
177     ! Location of aileron root, tip
178     write(u, '(2x, a19, 7x, 1x, a1, f20.15)') &
179         & "z/b at aileron root", "=", pf%AileronRoot
180     write(u, '(2x, a18, 8x, 1x, a1, f20.15)') &
181         & "z/b at aileron tip", "=", pf%AileronTip
182
183     ! Flap fraction at aileron root, tip
184     write(u, '(2x, a20, 6x, 1x, a1, f20.15)') &
185         & "cf/c at aileron root", "=", pf%FlapFractionRoot
186     write(u, '(2x, a19, 7x, 1x, a1, f20.15)') &
187         & "cf/c at aileron tip", "=", pf%FlapFractionTip
188
189     ! Hinge Efficiency Factor
190     write(u, '(2x, a16, 10x, 1x, a1, f20.15)') &
191         & "Hinge Efficiency", "=", pf%HingeEfficiency
192
193     ! Deflection efficiency factor

```

```

194     write(u, '(2x, a21, 5x, 1x, a1, f20.15)') &
195         & "Deflection Efficiency", "=", pf%DeflectionEfficiency
196
197     write(u, *)
198
199     call OutputLiftCoefficientParameters(u, pf)
200     call OutputDragCoefficientParameters(u, pf)
201     call OutputRollCoefficientParameters(u, pf)
202 end subroutine OutputPlanformSummary
203
204 subroutine OutputFourierCoefficients(u, pf)
205     integer, intent(in) :: u
206     type(Planform), intent(in) :: pf
207
208     integer :: i
209
210     write(u, '(a)') "Fourier Coefficients:"
211     write(u, '(a3, 4(2x, a20))') &
212         & "i", "a(i)", "b(i)", "c(i)", "d(i)"
213     do i = 1, pf%NNodes
214         write(u, '(i3, 4(2x, f20.15))') &
215             & i, pf%a(i), pf%b(i), pf%c(i), pf%d(i)
216     end do
217     write(u, *)
218 end subroutine OutputFourierCoefficients
219
220 subroutine OutputC(u, nnodes, c)
221     integer, intent(in) :: u
222     integer, intent(in) :: nnodes
223     real*8, intent(in) :: c(nnodes, nnodes)
224
225     write(u, *) "[C] Matrix:"
226     call printmat(u, nnodes, nnodes, c)
227     write(u, *)
228
229 end subroutine OutputC
230
231 subroutine OutputCInverse(u, nnodes, c_inv)
232     integer, intent(in) :: u
233     integer, intent(in) :: nnodes
234     real*8, intent(in) :: c_inv(nnodes, nnodes)
235
236     write(u, *) "[C]^-1 Matrix:"
237     call printmat(u, nnodes, nnodes, c_inv)
238     write(u, *)
239
240 end subroutine OutputCInverse
241
242 subroutine OutputHingeline(u, pf)
243     integer, intent(in) :: u
244     type(Planform), intent(in) :: pf
245
246     integer :: i
247
248     do i = 1, pf%NNodes
249         write(u, '(i3, 2x, f20.15, 2x, f20.15)') i, z_over_b_i(i,
pf%NNodes), y_i(pf, i)
250     end do
251 end subroutine OutputHingeline
252
253 subroutine PlotPlanform(pf)

```

```

254     type(Planform), intent(in) :: pf
255
256     integer :: i
257
258     ! Generate temporary text file for plotting
259     open(unit=11, file='.\\Output\\planform.dat')
260     write(11, '(a)') "$ Planform Geometry"
261
262     ! Write data points for planform
263     write(11, '(a)') "! Wing"
264     do i=1, pf%NNodes
265         write(11, '(f22.15, a, 2x, f22.15)') &
266             & z_over_b_i(i, pf%NNodes), ";", 0.25d0 * c_over_b_i(pf, i)
267         write(11, '(f22.15, a, 2x, f22.15)') &
268             & z_over_b_i(i, pf%NNodes), ";", -0.75d0 * c_over_b_i(pf, i)
269         write(11, '(f22.15, a, 2x, f22.15)') &
270             & z_over_b_i(i, pf%NNodes), ";", 0.25d0 * c_over_b_i(pf, i)
271     end do
272     do i=pf%NNodes, 1, -1
273         write(11, '(f22.15, a, 2x, f22.15)') &
274             & z_over_b_i(i, pf%NNodes), ";", -0.75d0 * c_over_b_i(pf, i)
275     end do
276     write(11, '(f22.15, a, 2x, f22.15)') &
277         & z_over_b_i(1, pf%NNodes), ";", 0.25d0 * c_over_b_i(pf, 1)
278
279     ! Write data points for right aileron
280     write(11, '(a)') "$"
281     write(11, '(a)') "! Right Aileron"
282     write(11, '(f22.15, a, 2x, f22.15)') pf%AileronRoot, ";", &
283         & -0.75d0 * c_over_b_zb(pf, pf%AileronRoot)
284     write(11, '(f22.15, a, 2x, f22.15)') pf%AileronRoot, ";", &
285         & (-0.75d0 + pf%FlapFractionRoot) * c_over_b_zb(pf, pf%AileronRoot)
286     write(11, '(f22.15, a, 2x, f22.15)') pf%AileronTip, ";", &
287         & (-0.75d0 + pf%FlapFractionTip) * c_over_b_zb(pf, pf%AileronTip)
288     write(11, '(f22.15, a, 2x, f22.15)') pf%AileronTip, ";", &
289         & -0.75d0 * c_over_b_zb(pf, pf%AileronTip)
290
291     ! Write data points for left aileron
292     write(11, '(a)') "$"
293     write(11, '(a)') "! Left Aileron"
294     write(11, '(f22.15, a, 2x, f22.15)') -pf%AileronRoot, ";", &
295         & -0.75d0 * c_over_b_zb(pf, pf%AileronRoot)
296     write(11, '(f22.15, a, 2x, f22.15)') -pf%AileronRoot, ";", &
297         & (-0.75d0 + pf%FlapFractionRoot) * c_over_b_zb(pf, pf%AileronRoot)
298     write(11, '(f22.15, a, 2x, f22.15)') -pf%AileronTip, ";", &
299         & (-0.75d0 + pf%FlapFractionTip) * c_over_b_zb(pf, pf%AileronTip)
300     write(11, '(f22.15, a, 2x, f22.15)') -pf%AileronTip, ";", &
301         & -0.75d0 * c_over_b_zb(pf, pf%AileronTip)
302
303     ! Close the geometry file
304     close(unit=11)
305
306     ! System call to plot planform
307     call system('C:\Program Files (x86)\ESPlot v1.3c\esplot.exe' ' &
308         & // '.\\Output\\planform.dat .\\Templates\\planform.qtp')
309 end subroutine PlotPlanform
310
311 subroutine PlotWashout(pf)
312     type(Planform), intent(in) :: pf
313
314     integer :: i

```

```

315
316     open(unit=11, file='.\\Output\\washout.dat')
317     write(11, '(a)') "$ Dimensionless Washout Distribution"
318
319     ! Write washout distribution
320     do i = 1, pf%NNodes
321         write(11, '(f22.15, a, 2x, f22.15)') &
322             & z_over_b_i(i, pf%NNodes), ";", pf%Omega(i)
323     end do
324
325     close(unit=11)
326
327     call system('C:\\Program Files (x86)\\ESPlot v1.3c\\esplot.exe" ' &
328         & // '.\\Output\\washout.dat .\\Templates\\washout.qtp')
329 end subroutine PlotWashout
330
331 subroutine WriteSectionLiftDistribution(pf)
332     type(Planform), intent(in) :: pf
333
334     integer :: i
335     real*8 :: zb, cl(pf%NNodes)
336
337     call GetLiftDistribution(pf, cl)
338
339     open(unit=11, file='liftdistribution.dat')
340     write(11, '(a)') "$ Section Lift Distribution"
341
342     do i = 1, pf%NNodes
343         zb = z_over_b_i(i, pf%NNodes)
344         write(11, '(f22.15, a, 2x, f22.15)') zb, ";", cl(i)
345     end do
346
347     close(unit=11)
348
349
350 end subroutine
351
352 subroutine PlotSectionLiftDistribution(pf)
353     type(Planform), intent(in) :: pf
354
355     call WriteSectionLiftDistribution(pf)
356     call system('C:\\Program Files (x86)\\ESPlot v1.3c\\esplot.exe" ' &
357         & // 'liftdistribution.dat .\\Templates\\liftdistribution.qtp')
358 end subroutine PlotSectionLiftDistribution
359
360 subroutine WriteNormalizedLiftCoefficient(pf)
361     type(Planform), intent(in) :: pf
362
363     integer :: i
364     real*8 :: zb, cb, cl1, cl_over_cl, cl(pf%NNodes)
365     ! Don't normalize if CL1 == 0
366     if (Compare(pf%CL1, 0.0d0, zero) == 0) then
367         cl1 = 1.0d0
368     else
369         cl1 = pf%CL1
370     end if
371
372     call GetLiftDistribution(pf, cl)
373
374     open(unit=11, file='liftcoefficient.dat')
375     write(11, '(a)') "$ Normalized Section Lift Coefficient"

```

```

376
377     do i = 1, pf%NNodes
378         zb = z_over_b_i(i, pf%NNodes)
379         cb = c_over_b_zb(pf, zb)
380         if (Compare(cb, 0.0d0, zero) == 0) then
381             if (Compare(cl(i), 0.0d0, zero) == 0) then
382                 if (pf%WingType == Elliptic) then
383                     cl_over_cl = NLC_ZeroChord_Elliptic(pf, zb, cb, cl1)
384                 else if (pf%WingType == Tapered) then
385                     cl_over_cl = NLC_ZeroChord_Tapered(pf, zb, cb, cl1)
386                 else if (pf%WingType == Combination) then
387                     cl_over_cl = NLC_ZeroChord_Tapered(pf, zb, cb, cl1)
388                 else
389                     stop "****Unknown Wing Type****"
390                 end if
391             else
392                 ! Finite lift from zero-chord section, should never happen
393                 cl_over_cl = 1.0d0 / zero
394             end if
395         else
396             cl_over_cl = cl(i) / cb / cl1
397         end if
398         write(11, '(f22.15, a, 2x, f22.15)') zb, ";", cl_over_cl
399     end do
400
401     close(unit=11)
402 end subroutine
403
404 subroutine PlotNormalizedLiftCoefficient(pf)
405     type(Planform), intent(in) :: pf
406
407     call WriteNormalizedLiftCoefficient(pf)
408     call system("C:\Program Files (x86)\ESPlot v1.3c\esplot.exe" ' &
409         & // 'liftcoefficient.dat .\Templates\liftcoefficient.qtp')
410 end subroutine PlotNormalizedLiftCoefficient
411
412 subroutine GetLiftDistribution(pf, cl)
413     type(Planform), intent(in) :: pf
414     real*8, intent(out) :: cl(pf%NNodes)
415
416     integer :: i, j
417     real*8 :: zb, theta
418
419     do i = 1, pf%NNodes
420         zb = z_over_b_i(i, pf%NNodes)
421         theta = theta_zb(zb)
422         cl(i) = 0.0d0
423         do j = 1, pf%NNodes
424             cl(i) = cl(i) + pf%BigA(j) * sin(real(j, 8) * theta)
425         end do
426         cl(i) = cl(i) * 4.0d0
427     end do
428 end subroutine GetLiftDistribution
429
430 real*8 function NLC_ZeroChord_Elliptic(pf, zb, cb, cl) result(cl_over_cl)
431     type(Planform), intent(in) :: pf
432     real*8, intent(in) :: zb
433     real*8, intent(in) :: cb
434     real*8, intent(in) :: cl
435
436     integer :: i

```



```

437     real*8 :: theta
438
439     theta = theta_zb(zb)
440     cl_over_cl = 0.0d0
441     do i = 1, pf%NNodes
442         cl_over_cl = cl_over_cl + real(i, 8) * pf%BigA(i) * &
443             & cos(real(i, 8) * theta) / cos(theta)
444     end do
445     cl_over_cl = cl_over_cl * pi * pf%AspectRatio / cl
446 end function NLC_ZeroChord_Elliptic
447
448 real*8 function NLC_ZeroChord_Tapered(pf, zb, cb, cl) result(cl_over_cl)
449     type(Planform), intent(in) :: pf
450     real*8, intent(in) :: zb
451     real*8, intent(in) :: cb
452     real*8, intent(in) :: cl
453
454     integer :: i
455     real*8 :: theta, cb2
456
457     if (zb < 0) then
458         theta = 1.0d-5
459     else
460         theta = pi - 1.0d-5
461     end if
462     cb2 = c_over_b(pf, theta)
463     cl_over_cl = 0.0d0
464     do i = 1, pf%NNodes
465         cl_over_cl = cl_over_cl + pf%BigA(i) * sin(real(i, 8) * theta)
466     end do
467     cl_over_cl = 4.0d0 * cl_over_cl / cb2 / cl
468 end function NLC_ZeroChord_Tapered
469 end module LiftingLineOutput

```

## K.7 Matrix Solver Module (matrix.f90)

```

1  module matrix
2      implicit none
3
4  contains
5      subroutine matinv_gauss(n, mat, mat_inv)
6          integer, intent(in) :: n
7          real*8, intent(in) :: mat(n,n)
8          real*8, intent(out) :: mat_inv(n,n)
9
10         real*8 :: b(n, n), c, d, temp(n)
11         integer :: i, j, k, m, imax(1), ipvt(n)
12
13         b = mat
14         ipvt = (/ (i, i=1, n) /)
15
16         do k = 1, n
17             imax = maxloc(abs(b(k:n, k)))
18             m = k - 1 + imax(1)
19
20             if (m /= k) then
21                 ipvt( (/m, k/) ) = ipvt( (/k, m/) )
22                 b( (/m, k/), :) = b( (/k, m/), :)
23             end if
24

```

```

25         d = 1.0d0 / b(k, k)
26
27         temp = b(:, k)
28         do j = 1, n
29             c = b(k, j) * d
30             b(:, j) = b(:, j) - temp * c
31             b(k, j) = c
32         end do
33         b(:, k) = temp * (-d)
34         b(k, k) = d
35     end do
36
37     mat_inv(:, ipvt) = b
38 end subroutine matinv_gauss
39
40
41 subroutine printmat(u, m, n, mat)
42     integer, intent(in) :: u
43     integer, intent(in) :: m
44     integer, intent(in) :: n
45     real*8, intent(in) :: mat(m, n)
46
47     integer :: i, j
48     character*80 :: format_string
49
50     if (u == 6) then
51         write(format_string, '(a, i10, a)') "(", n, "(F9.5, 2x))"
52     else
53         write(format_string, '(a, i10, a)') "(", n, "(F24.15, 2x))"
54     end if
55
56     do i = 1, m
57         write(u, format_string) (mat(i, j), j=1, n)
58     end do
59 end subroutine printmat
60
61 end module matrix

```

## K.8 Utilities Module (utilities.f90)

```

1  module Utilities
2      implicit none
3
4      real*8, parameter :: pi = acos(-1.0d0)
5      real*8, parameter :: zero = 1.0d-10
6
7  contains
8      integer function Compare(a, b, tol) result(eq)
9          ! Comparison function
10         ! Inputs:
11         !   a = First argument to compare
12         !   b = Second argument to compare
13         !   tol = Relative tolerance for comparison
14         ! Return Value (eq):
15         !   -1 = a < (b - tol)
16         !   0 = a == b (within tolerance)
17         !   1 = a > (b + tol)
18         real*8, intent(in) :: a, b, tol
19
20         if (abs(a) < tol .and. abs(b) < tol) then

```

```

21         eq = 0
22     else if (abs(a - b) / max(abs(a), abs(b)) < tol) then
23         eq = 0
24     else if (a < b) then
25         eq = -1
26     else
27         eq = 1
28     end if
29 end function Compare
30
31 real*8 function Residual(oldVal, newVal) result(res)
32     real*8, intent(in) :: oldVal
33     real*8, intent(in) :: newVal
34
35     res = dabs(oldVal - newVal) / max(dabs(oldVal), dabs(newVal), zero)
36 end function Residual
37
38 integer function CompareFiles(a, b) result(badline)
39     character*80, intent(in) :: a, b ! Filenames of files to compare
40
41     integer :: i, ios1, ios2
42     character*5000 :: results_line, work_line
43
44     open(unit=11, file=a)
45     open(unit=12, file=b)
46
47     badline = 0
48     ios1 = 0
49     i = 0
50     do while (badline == 0 .and. ios1 == 0)
51         i = i + 1
52
53         results_line(1:5000) = " "
54         read(11, '(A)', iostat=ios1, end=99) results_line
55
56         work_line(1:5000) = " "
57         read(12, '(A)', iostat=ios2, end=99) work_line
58
59         if (ios1 == 0) then
60             if (work_line /= results_line) then
61                 badline = i
62             end if
63         else if (len(trim(work_line)) /= 0) then
64             badline = i
65         end if
66     end do
67
68     close(unit=11)
69     close(unit=12)
70 99 continue
71 end function CompareFiles
72
73 character*2 function GetCharacterInput(def) result(inp)
74     character*2, intent(in) :: def ! Default value if invalid input
75
76     integer :: i
77     character :: a
78
79     read(5, '(a)') inp
80     if (len(inp) > 2 .or. len(inp) < 1) then
81         inp = def

```

```

82     else
83         do i = 1, 2
84             a = inp(i:i)
85             if(iachar(a) >= iachar('a') .and. iachar(a) <= iachar('z')) then
86                 inp(i:i) = char(iachar(a) - 32)
87             end if
88         end do
89     end if
90 end function GetCharacterInput
91
92 character*80 function GetStringInput(def) result(inp)
93     character*80, intent(in) :: def ! Default value if invalid input
94
95     integer :: i, ios
96     character :: a
97
98     read(5, '(a)', iostat=ios) inp
99     if (len(trim(inp)) < 1 .or. ios /= 0) then
100         inp = def
101     end if
102 end function GetStringInput
103
104 integer function GetIntInput(mn, mx, def) result(inp)
105     integer, intent(in) :: mn ! Minimum accepted value
106     integer, intent(in) :: mx ! Maximum accepted value
107     integer, intent(in) :: def ! Default value if invalid input
108
109     logical :: cont
110     character*80 :: inp_str
111     integer :: ios
112     integer :: len_mn, len_mx
113     character*80 :: msg_fmt
114
115     cont = .true.
116     do while (cont)
117         read(5, '(a)', iostat=ios) inp_str
118         if (ios == 0 .and. trim(inp_str) /= "") then
119             read(inp_str, *, iostat=ios) inp
120             if (ios /= 0 .or. inp < mn .or. inp > mx) then
121                 len_mn = int(log10(real(abs(mn)))) + 1
122                 if (mn < 0) len_mn = len_mn + 1
123
124                 len_mx = int(log10(real(abs(mx)))) + 1
125                 if (mx < 0) len_mx = len_mx + 1
126
127                 write(msg_fmt, '(a, i1, a, i1, a)') "(a, a, i", len_mn, &
128                     & ", a, i", len_mx, ", a)"
129
130                 write(6, *)
131                 write(6, msg_fmt) "Invalid input. Please ", &
132                     & "specify an integer between ", mn, " and ", mx, ","
133                 write(6, '(a)') "or press <ENTER> to accept the default
value."
134             else
135                 cont = .false.
136             end if
137         else
138             inp = def
139             cont = .false.
140         end if
141     end do

```

```

142     end function GetIntInput
143
144     real*8 function GetRealInput(mn_orig, mx_orig, dflt_orig) result(inp)
145         real*8, intent(in) :: mn_orig ! Minimum accepted value
146         real*8, intent(in) :: mx_orig ! Maximum accepted value
147         real*8, intent(in) :: dflt_orig ! Default value for input
148
149         logical :: cont
150         character*80 :: inp_str
151         integer :: ios
152         integer :: len_mn, ndec_mn
153         integer :: len_mx, ndec_mx
154         character*80 :: msg_fmt
155         real*8 :: mn, mx, dflt
156
157         if (Compare(mn_orig, 0.0d0, zero) == 0) then
158             mn = 0.0d0
159         else
160             mn = mn_orig
161         end if
162
163         if (Compare(mx_orig, 0.0d0, zero) == 0) then
164             mx = 0.0d0
165         else
166             mx = mx_orig
167         end if
168
169         if (Compare(dflt_orig, 0.0d0, zero) == 0) then
170             dflt = 0.0d0
171         else
172             dflt = dflt_orig
173         end if
174
175         cont = .true.
176         do while (cont)
177             read(5, '(a)', iostat=ios) inp_str
178             if (ios == 0 .and. trim(inp_str) /= "") then
179                 ios = ParseFormula(trim(inp_str), inp)
180                 write(*,*) ios, inp_str, inp
181                 if (ios /= 0 .or. inp < mn .or. inp > mx) then
182                     write(6, *)
183                     write(6, '(a, a, a, a, a, a)') "Invalid input. Please ", &
184                         & "enter a number between ", trim(FormatReal(mn, 5)), &
185                         & " and ", trim(FormatReal(mx, 5)), ", "
186                     write(6, '(a)') "or press <ENTER> to accept the default
value."
187                 else
188                     cont = .false.
189                 end if
190             else
191                 inp = dflt
192                 cont = .false.
193             end if
194         end do
195     end function GetRealInput
196
197     integer function ParseFormula(inp_str, num) result(estat)
198         character(len=*), intent(in) :: inp_str
199         real*8, intent(out) :: num
200
201         integer :: i, j, n_oper, last_ind, strlen, ios

```

```

202     character*40 :: operators, temp_num
203     real*8, Dimension(41) :: numbers
204
205     estat = 0
206     strlen = len(trim(inp_str))
207     n_oper = 0
208     last_ind = 0
209     do i = 2, strlen
210         if (inp_str(i:i) == '*' .or. inp_str(i:i) == '/') then
211             n_oper = n_oper + 1
212             operators(n_oper:n_oper) = inp_str(i:i)
213             temp_num = "
214             temp_num(1:i-last_ind-1) = inp_str(last_ind+1:i-1)
215             if ((temp_num(1:1) == 'P' .or. temp_num(1:1) == 'p') .and. &
216                 & (temp_num(2:2) == 'I' .or. temp_num(2:2) == 'i')) then
217                 numbers(n_oper) = pi
218             else
219                 read(temp_num, *, iostat=ios) numbers(n_oper)
220                 if (ios /= 0) then
221                     estat = 1
222                 end if
223             end if
224             last_ind = i
225         end if
226     end do
227
228     temp_num = "
229     temp_num(1:strlen-last_ind) = inp_str(last_ind+1:strlen)
230     if ((temp_num(1:1) == 'P' .or. temp_num(1:1) == 'p') .and. &
231         & (temp_num(2:2) == 'I' .or. temp_num(2:2) == 'i')) then
232         numbers(n_oper + 1) = pi
233     else
234         read(temp_num, *, iostat = ios) numbers(n_oper + 1)
235         if (ios /= 0) then
236             estat = 1
237         end if
238     end if
239
240     num = numbers(1)
241     do i = 1, n_oper
242         if (operators(i:i) == '*') then
243             num = num * numbers(i + 1)
244         else if (operators(i:i) == '/') then
245             num = num / numbers(i + 1)
246         else
247             estat = 2
248         end if
249     end do
250 end function ParseFormula
251
252 recursive character*80 function FormatReal(r, ndigits) result(real_str)
253     real*8, intent(in) :: r
254     integer, intent(in) :: ndigits
255
256     integer :: order, width, ndecimal
257     character*80 :: real_fmt
258     real*8 :: r_div_pi
259     integer :: num, denom
260
261     if (Compare(r, 0.0d0, zero) /= 0 .and. (IsFactorOfPi(r, ndigits) &
262         & .or. IsFractionOfPi(r, num, denom))) then

```

```

263     if (Compare(r, pi, zero) == 0) then
264         write(real_str, '(a)') "PI"
265     else if (IsFractionOfPi(r, num, denom)) then
266         if (denom == 1) then
267             write(real_str, '(a, a)') trim(FormatInteger(num)), "*PI"
268         else
269             write(real_str, '(a, a, a, a)') trim(FormatInteger(num)), &
270                 & "/", trim(FormatInteger(denom)), "*PI"
271         end if
272     else
273         r_div_pi = r / pi
274         write(real_str, '(a, a)') trim(FormatReal(r_div_pi, ndigits)), &
275             & "*PI )"
276     end if
277 else
278     if (Compare(r, 0.0d0, zero) == 0) then
279         order = 1
280     else
281         ! Determine the location of the first non-zero digit in the
number
282         order = int(log10(real(abs(r), 8))) + 1
283     end if
284
285     ! Check for sizes that should use exponential format
286     if (order <= -4 .or. order >= ndigits) then
287         if (r < 0.0d0) then
288             width = ndigits + 6 ! e.g. -1.2345E+67 - 5 digits + 6 other
289         else
290             width = ndigits + 5 ! e.g. 1.2345E-67 - 5 digits + 5 other
291         end if
292
293         write(real_fmt, '(a, i2, a, i2, a)') "(ES", width, ".", &
294             & ndigits - 1, ")"
295     else
296         if (r < 0.0d0) then
297             width = ndigits + 2 ! e.g. -12.345 - 5 digits + 2 other
298         else
299             width = ndigits + 1 ! e.g. 123.45 - 5 digits + 1 other
300         end if
301
302         if (order <= 0) then
303             width = width - order + 1 ! e.g. -0.012345 - additional for
leading 0
304         end if
305
306         write(real_fmt, '(a, i2, a, i2, a)') "(F", width, ".", &
307             & ndigits - order, ")"
308     end if
309     write(real_str, real_fmt) r
310 end if
311 end function FormatReal
312
313 character*80 function FormatInteger(i) result(int_str)
314     integer, intent(in) :: i
315
316     integer :: len_i
317     character*80 :: int_fmt
318
319     if (i == 0) then
320         len_i = 1
321     else

```

```

322         len_i = int(log10(real(abs(i)))) + 1
323         if (i < 0) then
324             len_i = len_i + 1
325         end if
326     end if
327
328     write(int_fmt, '(a, i2, a)') "(i", len_i, ")"
329     write(int_str, int_fmt) i
330 end function FormatInteger
331
332 logical function IsFactorOfPi(r, ndigits) result(isFactor)
333     real*8, intent(in) :: r
334     integer, intent(in) :: ndigits
335
336     real*8 :: rx, rx_trunc
337
338     rx = r / pi * 10**ndigits
339     rx_trunc = real(int(rx), 8)
340
341     if (Compare(rx, rx_trunc, zero) == 0) then
342         isFactor = .true.
343     else
344         isFactor = .false.
345     end if
346 end function IsFactorOfPi
347
348 logical function IsFractionOfPi(r, num, denom) result(isFraction)
349     real*8, intent(in) :: r
350     integer, intent(out) :: num
351     integer, intent(out) :: denom
352
353     integer :: i, num2, denom2
354     real*8 :: r_div_pi, r_div_pi_i
355
356     isFraction = .false.
357     r_div_pi = r / pi
358     do i = 1, 360
359         r_div_pi_i = r_div_pi * real(i, 8)
360         if (Compare(r_div_pi_i, real(int(r_div_pi_i), 8), zero) == 0) then
361             num = int(r_div_pi_i)
362             denom = i
363             isFraction = .true.
364             return
365         end if
366     end do
367 end function IsFractionOfPi
368
369 end module Utilities

```



## L PROOF OF EQUATION (5.2.5)

The derivation of the induced velocity at a point  $P$  due to a single straight vortex segment has been presented in Sec. 5.2. Eq. (5.2.5) gives the solution to the integral of the differential velocity over the vortex filament  $\overline{OR}$  (see Figure 5.2). Here we present the complete proof to this integral.

The first equality in Eq. (5.2.5) gives the integral to be solved, specifically

$$\mathbf{V} = \frac{\Gamma(\mathbf{l} \times \mathbf{r}_1)}{4\pi} \int_0^1 \frac{d\zeta}{\left(r_1^2 - 2\zeta \mathbf{r}_1 \cdot \mathbf{l} + \zeta^2 l^2\right)^{3/2}} \quad (\text{L.1})$$

To solve this integral we apply  $u$ -substitution, with

$$u = \left(r_1^2 - 2\zeta \mathbf{r}_1 \cdot \mathbf{l} + \zeta^2 l^2\right)^{1/2} \quad (\text{L.2})$$

$$du = \frac{-\mathbf{r}_1 \cdot \mathbf{l} + \zeta l^2}{u} d\zeta \quad (\text{L.3})$$

This gives for Eq. (L.1)

$$\mathbf{V} = \frac{\Gamma(\mathbf{l} \times \mathbf{r}_1)}{4\pi} \int_0^1 \frac{du}{u^2 (-\mathbf{r}_1 \cdot \mathbf{l} + \zeta l^2)} \quad (\text{L.4})$$

We now look for an appropriate expression  $v$  so that we can apply the quotient rule of differentiation, namely

$$\frac{v}{u} = \int \frac{u dv - v du}{u^2} \quad (\text{L.5})$$

where

$$u dv - v du = \frac{du}{(-\mathbf{r}_1 \cdot \mathbf{l} + \zeta l^2)} = \frac{d\zeta}{u} \quad (\text{L.6})$$

We try

$$v = c(-\mathbf{r}_1 \cdot \mathbf{l} + \zeta l^2) \quad (\text{L.7})$$

$$dv = cl^2 d\zeta \quad (\text{L.8})$$

where  $c$  is a constant found by substitution of Eqs. (L.2), (L.3), (L.7), and (L.8) into Eq. (L.6). This gives

$$c = \frac{1}{r_1^2 l^2 - (\mathbf{r}_1 \cdot \mathbf{l})^2} \quad (\text{L.9})$$

which suggests that our guess for  $v$  is valid since  $c$  is indeed constant with respect to  $\zeta$ . The indefinite integral of Eq. (L.1) is then

$$\frac{\Gamma(\mathbf{l} \times \mathbf{r}_1)}{4\pi} \int \frac{u dv - v du}{u^2} = \frac{\Gamma(\mathbf{l} \times \mathbf{r}_1)}{4\pi} \frac{v}{u} = \frac{\Gamma(\mathbf{l} \times \mathbf{r}_1)}{4\pi \left( r_1^2 l^2 - (\mathbf{r}_1 \cdot \mathbf{l})^2 \right)} \frac{-\mathbf{r}_1 \cdot \mathbf{l} + \zeta l^2}{\left( r_1^2 - 2\zeta \mathbf{r}_1 \cdot \mathbf{l} + \zeta^2 l^2 \right)^{1/2}} \quad (\text{L.10})$$

Applying the limits from Eq. (L.1) gives

$$\mathbf{V} = \frac{\Gamma(\mathbf{l} \times \mathbf{r}_1)}{4\pi \left( r_1^2 l^2 - (\mathbf{r}_1 \cdot \mathbf{l})^2 \right)} \left[ \frac{l^2 - \mathbf{r}_1 \cdot \mathbf{l}}{\left( r_1^2 - 2\mathbf{r}_1 \cdot \mathbf{l} + l^2 \right)^{1/2}} + \frac{\mathbf{r}_1 \cdot \mathbf{l}}{r_1} \right] \quad (\text{L.11})$$

We now wish to rewrite this equation in terms of  $\mathbf{r}_1$  and  $\mathbf{r}_2$  instead of  $\mathbf{r}_1$  and  $\mathbf{l}$ . We use the vector identities

$\mathbf{l} = \mathbf{r}_1 - \mathbf{r}_2$  and  $\mathbf{l} \times \mathbf{r}_1 = \mathbf{r}_1 \times \mathbf{r}_2$  to get

$$\mathbf{V} = \frac{\Gamma(\mathbf{r}_1 \times \mathbf{r}_2)}{4\pi \left( r_1^2 (\mathbf{r}_1 - \mathbf{r}_2) \cdot (\mathbf{r}_1 - \mathbf{r}_2) - [\mathbf{r}_1 \cdot (\mathbf{r}_1 - \mathbf{r}_2)]^2 \right)} \left[ \frac{l^2 - \mathbf{r}_1 \cdot (\mathbf{r}_1 - \mathbf{r}_2)}{r_2} + \frac{\mathbf{r}_1 \cdot (\mathbf{r}_1 - \mathbf{r}_2)}{r_1} \right] \quad (\text{L.12})$$

Further algebraic manipulation of Eq. (L.12) gives

$$\mathbf{V} = \frac{\Gamma(\mathbf{r}_1 \times \mathbf{r}_2)(r_1 + r_2)}{4\pi r_1 r_2 (r_1 r_2 + \mathbf{r}_1 \cdot \mathbf{r}_2)} \quad (\text{L.13})$$

which is the result given in Eq. (5.2.5).

# M TABULATED PROPERTIES OF THE NACA X410 FAMILY OF AIRFOILS

Tables M.1-M.4 present aerodynamic performance characteristics of the NACA X410 family of airfoils computed using XFOIL. The airfoil geometries were modeled using XFOIL's internal NACA airfoil modeler with a grid size of 200 nodes. Nodes were clustered near the leading and trailing edges to obtain higher resolution in areas of large curvature and flow gradients. The analyses were run assuming incompressible flow with a Reynolds number of  $Re = 2.4 \times 10^5$ . Turbulence in the boundary layer was modeled using XFOIL's turbulence transition model with a value of 2.6 for the  $N_{crit}$  input parameter. This value was estimated based on information provided in a wind tunnel survey of the AFRL Vertical Wind Tunnel (VWT). The data tabulated below were used in the numerical and experimental comparisons discussed in Sec. 5.4.

**Table M.1 Airfoil Coefficient Data for the NACA 2410 Airfoil**

$\alpha$ (deg)	$c_l$	$c_d$ (rad <sup>-1</sup> )
-20	-0.4578	0.19659
-19	-0.4441	0.18661
-17.95	-0.4185	0.17502
-16.95	-0.4196	0.16702
-15.95	-0.3829	0.15457
-14.95	-0.3734	0.14418
-13.95	-0.358	0.13471
-12.95	-0.3544	0.1246
-11.95	-0.3844	0.11457
-10.95	-0.3606	0.10158
-9.95	-0.4168	0.08026
-8.9	-0.6626	0.04901
-7.9	-0.6604	0.03277
-6.9	-0.6058	0.02358
-5.9	-0.5249	0.01891
-4.9	-0.4348	0.01624
-3.9	-0.2883	0.0137
-2.85	-0.1259	0.01164
-1.8	0.0218	0.00935
-0.8	0.1708	0.00856
0.15	0.3087	0.00816
1.15	0.4067	0.00817
2.15	0.5054	0.00858

3.2	0.6095	0.00929
4.2	0.7083	0.01014
5.25	0.8103	0.01121
6.25	0.8984	0.01317
7.25	0.9721	0.01722
8.25	1.0462	0.02107
9.25	1.1188	0.02536
10.25	1.1926	0.03082
11.25	1.2514	0.03812
12.25	1.2716	0.0481
13.25	1.214	0.06136
14.25	1.1301	0.08412

**Table M.2 Airfoil Coefficient Data for the NACA 4410 Airfoil**

$\alpha$ (deg)	$c_l$	$c_d$ (rad <sup>-1</sup> )
-10	-0.3503	0.11021
-9	-0.3582	0.09857
-8	-0.4013	0.08906
-7	-0.3943	0.07846
-6	-0.2827	0.02824
-5	-0.1411	0.01988
-4	0.0082	0.0158
-3	0.1372	0.01314
-2	0.2545	0.01145
-0.95	0.3644	0.00937
0	0.4777	0.00853
1	0.5842	0.00884
2	0.6907	0.00941
3	0.7966	0.01014
4	0.9022	0.01097
5	1.0061	0.01186
6	1.1027	0.0127
7	1.1945	0.01376
8	1.258	0.01667
9.05	1.2808	0.02292
10.05	1.304	0.0285
11.05	1.3313	0.03488
12.05	1.368	0.04179

13.05	1.4054	0.04913
14.05	1.4185	0.05986
15.05	1.3891	0.07539
16.05	1.317	0.09885
17.05	1.2122	0.13502

**Table M.3 Airfoil Coefficient Data for the NACA 6410 Airfoil**

$\alpha$ (deg)	$c_l$	$c_d$ (rad <sup>-1</sup> )
-10	-0.2956	0.12505
-9	-0.2606	0.11127
-8	-0.1966	0.09564
-7	-0.1127	0.07956
-6	-0.0078	0.06244
-5	0.1103	0.0435
-3.9	0.2533	0.01859
-2.9	0.3706	0.01451
-1.9	0.4829	0.01268
-0.9	0.5939	0.01163
0.05	0.6974	0.01096
1.1	0.8051	0.01
2.1	0.9118	0.01072
3.1	1.019	0.01159
4.1	1.1249	0.01253
5.1	1.2305	0.01356
6.1	1.3345	0.01469
7.2	1.4319	0.01557
8.2	1.5097	0.01661
9.2	1.5531	0.01862
10.2	1.4981	0.02819
11.2	1.4764	0.03854
12.2	1.4658	0.04972
13.2	1.4592	0.06147

**Table M.4 Airfoil Coefficient Data for the NACA 8410 Airfoil**

$\alpha$ (deg)	$c_l$	$c_d$ (rad <sup>-1</sup> )
-10	-0.0797	0.11796
-8.98	-0.0003	0.10197
-7.98	0.0609	0.09024
-6.98	0.1152	0.07774
-5.98	0.1736	0.06648
-4.97	0.2692	0.0537
-3.97	0.3837	0.04202
-2.96	0.5574	0.02251
-1.95	0.6862	0.01502
-0.95	0.7981	0.01335
0.04	0.9052	0.01285
1.05	1.0128	0.01285
2.06	1.1137	0.01225
3.06	1.2194	0.01322
4.06	1.325	0.01428
5.06	1.4289	0.01542
6.06	1.5333	0.01667
7.06	1.6341	0.01806
8.06	1.7177	0.0191
9.06	1.7757	0.02009
10.06	1.791	0.0221
11.06	1.7452	0.03019
12.07	1.6346	0.04922
13.07	1.5755	0.06769
14.07	1.5411	0.08482
15.07	1.5224	0.09989
16.07	1.5298	0.11027
17.07	1.565	0.11521
18.07	1.5887	0.12357
19.07	1.6011	0.13384

## CURRICULUM VITAE

Joshua D. Hodson

July 2019

## EDUCATION

**Ph.D. Mechanical Engineering**, *Utah State University*, Jun. 2019 (3.96 GPA)  
 Numerical Analysis and Spanwise Shape Optimization for Finite Wings of Arbitrary Aspect Ratio

**M.S. Mechanical Engineering**, *Utah State University*, Aug. 2007 (3.96 GPA)  
 RANS Modeling of Nuclear Reactor Lower Plenum Geometries

**B.S. Mechanical Engineering**, *Utah State University*, Aug. 2007 (3.77 GPA, *Cum Laude*)

## TEACHING AND PROFESSIONAL EXPERIENCE

03/18 – present	<b>Aerospace Research Engineer</b> , <i>Air Force Research Laboratory</i>
12/06 – 02/18	<b>Sr. Principle Mechanical Engineer (Analysis)</b> , <i>Orbital ATK Flight Systems</i>
05/17 – 08/17	<b>Graduate Research Assistant</b> , <i>Air Force Research Laboratory</i>
01/17 – 05/17	<b>Teaching Assistant (Computational Fluid Dynamics)</b> , <i>Utah State University</i>
08/16 – 12/16	<b>Instructor (Aerodynamics)</b> , <i>Utah State University</i>
08/13 – 12/13	<b>Teaching Assistant (Thermodynamics II)</b> , <i>Utah State University</i>
05/05 – 12/06	<b>Graduate Research Assistant</b> , <i>Utah State University</i>
05/04 – 04/05	<b>Mechanical Engineer Intern (Design)</b> , <i>Space Dynamics Laboratory</i>
01/04 – 05/04	<b>Math Tutor</b> , <i>Utah State University</i>

## JOURNAL PUBLICATIONS

- [1] D. Hunsaker, J. Taylor, J. Hodson, and O. Pope, “Aerodynamic Centers of Arbitrary Airfoils below Stall,” *J. Aircraft*, accepted for publication.
- [2] B. Limb, D. Work, J. Hodson, and B. Smith, “The Inefficacy of Chauvenet’s Criterion for Elimination of Data Points,” *J. Fluids Eng.*, Vol. 139, No. 5, Jun. 2016.
- [3] J. Hodson, R. Spall, and B. Smith, “Turbulence Model Assessment for Flow across a Row of Confined Cylinders,” *Nuclear Technology*, Vol. 161, pp. 268-276, 2008.

## CONFERENCE PRESENTATIONS AND PAPERS

- [1] J. Hodson, G. Reich, J. Deaton, A. Pankonien, P. Beran, “Aerostructure Design of a 2D Morphing Airfoil in Unsteady Supersonic Flow using Bio-Inspired Evolutionary Design Processes and Low-Fidelity Physics Models,” *ASME SMASIS*, Louisville, KY, Sep. 2019, accepted for presentation, SMASIS2019-5598.
- [2] B. Bielefeldt, D. Hartl, J. Hodson, G. Reich, P. Beran, A. Pankonien, J. Deaton, “Graph-Based Interpretation of L-System Encodings Toward Aeroelastic Topology Optimization of a Morphing Airfoil in Supersonic Flow,” *Proceedings of the ASME Conference on Smart Materials, Adaptive Structures and Intelligent Systems*, Louisville, KY, Sep. 2019, accepted for publication, SMASIS2019-5609.
- [3] J. Hodson, A. Christopherson, J. Deaton, A. Pankonien, G. Reich, and P. Beran, “Aeroelastic Topology Optimization of a Morphing Airfoil in Supersonic Flow using Evolutionary Design,” *Multidisciplinary Design Optimization, AIAA SciTech Forum*, San Diego, CA, Jan. 2019, AIAA-2019-1466.

- [4] D. Hunsaker, O. Pope, J. Hodson, and J. Rosqvist, "Aerodynamic Centers of Arbitrary Airfoils," *AIAA Aerospace Sciences Meeting, AIAA SciTech Forum*, Kissimmee, FL, Jan. 2018.
- [5] R. Spall and J. Hodson, "Educational Results obtained using an Improved Two-Dimensional Panel Method Code in Undergraduate Fluid Dynamics and Aerodynamics Courses," *ASME Fluids Engineering Division Summer Meeting*, Waikoloa, HI, Jul. 2017, FEDSM2017-69031.
- [6] J. Hodson, D. Hunsaker, B. Andrews, and J. Joo, "Experimental Results for a Variable Camber Compliant Wing," *35th AIAA Applied Aerodynamics Conference, AIAA Aviation Forum*, Denver, CO, Jun. 2017, AIAA-2017-4222.
- [7] J. Hodson, D. Hunsaker, and R. Spall, "Wing Optimization using Dual Number Automatic Differentiation in MachUp," *55th AIAA Aerospace Sciences Meeting, AIAA SciTech Forum*, Grapevine, TX, Jan. 2017, AIAA-2017-0033.
- [8] H. Dewey, J. Hodson, and K. Illum, "Asset Monitoring with the Internet of Things," *Orbital ATK Internal Conference*, Apr. 2016.
- [9] J. Hodson, H. Dewey, and D. DeVries, "Individual Motor Monitoring and Data Management Solutions to Solid Rocket Prognostic Health Management," *JANNAF 43<sup>rd</sup> Structures and Mechanical Behavior Subcommittee Meeting*, Salt Lake City, UT, Dec. 2015.
- [10] J. Hodson, J. Forsmann, and R. Spall, "Dual Number Automatic Differentiation in RELAP5-3D," *International RELAP5 User Group Meeting*, Idaho Falls, ID, Aug. 2015.
- [11] J. Hodson and H. Dewey, "IMLM DAAS Software Design and Implementation," *Orbital ATK Internal Conference*, Apr. 2015.
- [12] J. Hodson and R. Spall, "Dual Number Automatic Differentiation for CFD Optimization," *Utah Fluids Meeting*, Aug. 2014.
- [13] R. Monson and J. Hodson, "Real-Time Model Updates using Sensor Data in IMLM DAAS," *JANNAF 9<sup>th</sup> Modeling and Simulation Subcommittee Meeting*, Colorado Springs, CO, Apr. 2013.
- [14] J. Hodson, R. Spall, and B. Smith, "RANS Predictions in an Idealized Lower-Plenum Model," *14<sup>th</sup> International Conference on Nuclear Engineering*, Jul. 2006. ICONE14-89222.
- [15] J. Hodson, E. Thorston, R. Spall, and B. Smith, "CFD Validation of Flow Regimes in an Idealized Lower-Plenum Model," *ANS Winter Meeting and Technology Expo.*, Washington, D.C., Nov. 2005.